

**Hamilton
Standard**

**U
A.**
DIVISION OF UNITED AIRCRAFT CORPORATION

SVHSER 6285

CR-134159

**HYDROGEN DEPOLARIZED CARBON DIOXIDE CONCENTRATOR
PERFORMANCE IMPROVEMENTS AND CELL PAIR STRUCTURAL TESTS**

by

J. C. HUDDLESTON AND DR. J. R. AYLWARD

PREPARED UNDER CONTRACT NO. NAS 9-12920

by

HAMILTON STANDARD

DIVISION OF UNITED AIRCRAFT CORPORATION

WINDSOR LOCKS, CONNECTICUT

for

NATIONAL AERONAUTICS AND SPACE ADMINISTRATION

JOHNSON SPACE CENTER

HOUSTON, TEXAS

SEPTEMBER 1973

CR-134159
HYDROGEN DEPOLARIZED
CARBON DIOXIDE CONCENTRATOR PERFORMANCE
IMPROVEMENTS AND CELL PAIR STRUCTURAL
TESTS (Hamilton Standard) 301 P 400
\$17.25
CST 10A 03/ 3 23711



ABSTRACT

**HYDROGEN DEPOLARIZED CARBON DIOXIDE CONCENTRATOR
PERFORMANCE IMPROVEMENTS AND CELL PAIR STRUCTURAL TESTS**

by

J. C. HUDDLESTON and DR. J. R. AYLWARD

SEPTEMBER 1973

This report describes the investigations and testing associated with improving the CO₂ removal efficiency and voltage degradation of a Hydrogen Depolarized Carbon Dioxide Concentrator, and the vibration testing of a Water Vapor Electrolysis Cell Pair, under NASA Contract NAS 9-12920.

**Hamilton
Standard**

U
DIVISION OF UNITED AIRCRAFT CORPORATION
A

SVHSER 6285

**HYDROGEN DEPOLARIZED CARBON DIOXIDE CONCENTRATOR
PERFORMANCE IMPROVEMENTS AND CELL FAIR STRUCTURAL TESTS**

by

J. C. HUDDLESTON AND DR. J. R. AYLWARD

PREPARED UNDER CONTRACT NO. NAS 9-12920

by

HAMILTON STANDARD

DIVISION OF UNITED AIRCRAFT CORPORATION

WINDSOR LOCKS, CONNECTICUT

for

NATIONAL AERONAUTICS AND SPACE ADMINISTRATION

JOHNSON SPACE CENTER

HOUSTON, TEXAS

SEPTEMBER 1973

FOREWORD

This report was prepared by the Hamilton Standard Division of the United Aircraft Corporation for the National Aeronautics and Space Administration's Johnson Space Center, in accordance with Contract NAS 9-12920. This report describes the work accomplished during the period of 21 June 1972 through 28 September 1973, in improving the performance of the hydrogen depolarized carbon dioxide concentrator cell pair. This development effort consisted of detailed cell analysis, cell and cell pair testing, and a structural vibration test of a water vapor electrolysis cell pair.

Personnel responsible for the conduct of this program were Mr. F. H. Greenwood, Program Manager; Mr. J. C. Huddleston, Program Engineer; Dr. J. R. Aylward, Technical Consultant from Hamilton Standard; and Mr. A. Behrend, Technical Monitor and Mr. R. J. Gillen, Overall Program Supervisor for the NASA Johnson Space Center.

TABLE OF CONTENTS

	<u>Page No.</u>
<u>SUMMARY</u>	1
<u>INTRODUCTION</u>	3
<u>CONCLUSIONS</u>	7
<u>RECOMMENDATIONS</u>	9
<u>DISCUSSION</u>	11
SSP-HDC EVALUATION TESTING	13
<u>Analytical and Miscellaneous Tasks</u>	13
Objectives	13
Conclusions	13
<u>Cell Pair Test Program</u>	14
Objectives	14
Conclusions	14
HDC POWER DECAY INVESTIGATION	16
<u>Trace Impurities</u>	16
Ammonia	17
Hydrogen Sulfide and Sulfur Dioxide	24
Carbon Monoxide	26
Freon 113	26
Conclusions	26
<u>Experiments on Cell Pair S/N 017</u>	28
<u>Cell Pair S/N 019 Testing</u>	29
<u>Anode Examination</u>	31
<u>Anode Evaluation</u>	37
<u>Matrix Thickness and Cell Performance</u>	37
HDC ANALYTICAL TESTING	42
<u>Cesium Carbonate Electrolyte</u>	45
<u>TMAC Electrolyte</u>	47
<u>Conclusions</u>	51

TABLE OF CONTENTS (Concluded)

	<u>Page No.</u>
IMPROVED CO ₂ TRANSFER	52
<u>Electrolyte Catalyst</u>	52
<u>Cathode Improvement and Evaluation</u>	54
<u>Analytical Cell Test of DS 16-0 Cathode</u>	54
<u>Full Size Cell Test of DS 16-0 Type Cathode</u>	56
HDC ELECTROLYTE PROPERTIES	59
<u>Cesium Carbonate (Cs₂CO₃)</u>	59
<u>Cesium Bicarbonate (CsHCO₃)</u>	59
<u>Tetramethylammonium Carbonate (TMAC)</u>	59
MODIFIED ELECTROLYTES	83
SPECIAL TESTS	85
<u>Matrix Compression</u>	85
<u>Matrix Set</u>	92
HDC HYDROGEN FLOW IMPROVEMENT	99
HDC VERIFICATION TEST	99
<u>Cell Pair S/N 021 Testing</u>	103
<u>Cell Pair S/N 022 Testing</u>	112
WVE CELL PAIR VIBRATION TEST	114
WVE/HDC BREADBOARD FABRICATION	121
RELIABILITY/QUALITY ASSURANCE/SAFETY SUMMARY	124
<u>REFERENCES</u>	125
APPENDIX MASTER TEST PLAN	A-i

LIST OF FIGURES

<u>Figure No.</u>	<u>Title</u>	<u>Page No.</u>
1	WVE and HDC Cell Pairs	2
2	Baseline Potentiostatic Sweep on Platinum in Cs ₂ CO ₃ Solution	18
3	Oxidation of Ammonia (NH ₃) on Platinum Black Electrode	20
4	Reduction of Nitrite Ion (NO ₂ ⁻) on a Platinum Black Electrode	21
5	Effect of Ammonia on Cathode Performance	22
6	Oxidation of Sulfide Ion (S ⁻²) on a Platinum Black Electrode	23
7	Oxidation of Sulfur Dioxide (SO ₃ ⁻²) on a Platinum Black Electrode	25
8	Oxidation of Carbon Monoxide (CO) on a Platinum Black Electrode	27
9	HDC Cell Pair S/N 019 (Cs ₂ CO ₃) Performance vs Time	30
10	X-Ray Microprobe Line Scans of Cell Pair S/N 018 Anode	32
11	SEM Examination of Cell S/N 018 Anode (Mag. = 750X)	33
12	Characteristic X-Ray Distribution for Platinum and Fluorine (Teflon) of Cell S/N 018 Anode	34
13	X-Ray Microprobe Line Scan of Cell Pair S/N 019 Anode	36
14	Floating Electrode Cell Test Setup	38
15	Analytical Cell	43
16	HDC Analytical Test Unit Rig	44
17	Effect of Current Density and P _{CO₂} on CO ₂ Transfer Efficiency Using TMAC Electrolyte ²	48
18	Effect of Current Density and P _{CO₂} on the Absolute Amount of CO ₂ Transferred with TMAC Electrolyte	49

LIST OF FIGURES (Continued)

<u>Figure No.</u>	<u>Title</u>	<u>Page No.</u>
19	Modification to Center Housing to Reduce H ₂ Flow ΔP	58
20	Solubility Limit for Cs ₂ CO ₃ vs Temperature	63
21	Cs ₂ CO ₃ Density vs Concentration at 25°C	64
22	Cs ₂ CO ₃ Specific Volume vs Concentration	66
23	Cs ₂ CO ₃ Concentration vs Mole/Liter	67
24	Solubility of Cesium Bicarbonate vs Temperature	70
25	Density of Cesium Bicarbonate Solutions vs Concentration at 75°F	71
26	Specific Volume of Cesium Bicarbonate Solutions vs Concentration	73
27	Moles per Liter versus Percent Cesium Bicarbonate	74
28	TMAC Density versus Concentration	78
29	TMAC Specific Volume versus Concentration	80
30	TMAC Specific Volume versus Electrolyte Relative Humidity	81
31	Moles per Liter vs Weight Percent (TMAC)	82
32	Potential Sweep for Ethylene Carbonate	84
33	Matrix Conductivity Fixture	86
34	P&WA Asbestos - Electrolyte Resistance versus Thickness	88
35	Tissuquartz - Electrolyte Resistance versus Thickness	89
36	Neoprene Asbestos - Electrolyte Resistance versus Thickness	90
37	Tissuquartz - (Saturated KCl) Resistance versus Thickness	91

LIST OF FIGURES (Continued)

<u>Figure No.</u>	<u>Title</u>	<u>Page No.</u>
38	(WVE Matrix) Tissuquartz Neoprene Asbestos - Electrolyte Resistance versus Thickness	93
39	Matrix Compression versus Loading	94
40	Matrix Cyclic Compression versus Loading	95
41	Matrix Loading vs Time	96
42	Matrix Set Test	97
43	HDC Hydrogen Flow Test Results Percent CO ₂ versus Power and Efficiency	100
44	HDC Hydrogen Flow Test Results H ₂ /CO ₂ Removal versus Efficiency	101
45	HDC Hydrogen Flow Test Results H ₂ Stoichiometric Flow Versus Power and Efficiency	102
46	Electrochemical Test Facilities	104
47	System Rig Schematic	105
48	HDC Cell Pair S/N 021 (Cs ₂ CO ₃) Performance vs Time	106
49	Cell S/N 021 Anode	107
50	SEM Photographs of Normal (A) and Modified (B) Asbestos Matrix	109
51	Illustration of Cesium Ion Concentration Change with Electrode Separation	110
52	Relationship Between Cesium Ion Concentration, Anolyte pH and P _{CO₂}	111
53	HDC Cell Pair S/N 022 (TMAC) Performance vs Time	113
54	WVE Performance Data versus Operating Time	116

LIST OF FIGURES (Concluded)

<u>Figure No.</u>	<u>Title</u>	<u>Page No.</u>
55	Cell Pair Vibration Test Curve for X Axis	117
56	Cell Pair Vibration Test Curve for Y Axis	118
57	Cell Pair Vibration Test Curve for Z Axis	119
58	WVE Center Housing (Anode Side)	120
59	Integrated WVE/HDC Breadboard Schematic (SVSK 83513)	122
60	Integrated WVE/HDC Breadboard System	123

LIST OF TABLES

<u>Table No.</u>	<u>Title</u>	<u>Page No.</u>
I	Floating Electrode Evaluation of Anode Performance in Cesium Bicarbonate	39
II	Matrix Thickness Test Results	40
III	Effect of Air Velocity and CO ₂ Pressure at 18 ASF with Cs ₂ CO ₃ Electrolyte	46
IV	Effect of Current Density and CO ₂ Pressure at an Air Velocity of 7 Ft/Sec	46
V	Effect of Current Density	47
VI	Effect of P _{CO₂} and Relative Humidity at 18 ASF and at an Air Velocity of 10 Ft/Sec with TMAC Electrolyte	50
VII	Effect of Air Velocity with TMAC Electrolyte	50
VIII	Analytical Cell Parametric Data With DS 16-0 Type Cathode with Cs ₂ CO ₃ Electrolyte	55
IX	Effect of Hydrogen Back Pressure, Flow Rate and Air Temperature on CO ₂ Transfer	57
X	Vapor Pressure of H ₂ O (in mm Hg) for Cs ₂ CO ₃ at Various Concentrations and Temperatures	61
XI	Specific Conductance of Cs ₂ CO ₃ (OHM CM) ⁻¹ at Various Concentrations and Temperatures	62
XII	Viscosity of Cesium Carbonate Solution	65
XIII	Water Vapor Pressure (mm Hg) of Cesium Bicarbonate Solutions	68
XIV	Specific Conductivity of Cesium Bicarbonate	69
XV	Viscosity of Cesium Bicarbonate Solutions	72
XVI	Relative Humidity of Cesium Bicarbonate Solutions (Percent)	75

LIST OF TABLES (Concluded)

<u>Table No.</u>	<u>Title</u>	<u>Page No.</u>
XVII	Water Vapor Pressure of TMAC versus Concentration and Temperature	76
XVIII	Specific Conductivity of TMAC versus Concentration and Temperature	77
XIX	Viscosity of TMAC Solutions	79
XX	WVE Cell Pair History	115

ABBREVIATIONS AND SYMBOLS

A	Area
A-3R	Code Name for Experimental Electrode
A-10R	Code Name for Experimental Electrode
AA-2	Electrode Manufactured by American Cyanamid Company
AR	As Required
asf	Amps/Sq. Ft.
Avg.	Average
°C	Degrees Celsius (Centigrade)
cc	Cubic Centimeter
cfm	Cubic Feet per Minute
cm ²	Centimeter Squared
CO	Carbon Monoxide
CO ₂	Carbon Dioxide
CO ₃ ²⁻	Carbonate Ion
Cs+	Cesium Ion
Cs ₂ CO ₃	Cesium Carbonate
CsHCO ₃	Cesium Bicarbonate
Cs ₂ SO ₄	Cesium Sulfate
d	Electrode Separation
d'	Uncompressed Matrix Thickness
d ⁰	Maximum Compressed Matrix Thickness
dc	Direct Current
DP	Dew Point

ABBREVIATIONS AND SYMBOLS (Continued)

DS-16	Code Name for Improved HDC Cathode
E	Cell Voltage (IR Free)
f	Matrix Factor
°F	Degrees Fahrenheit
Ft	Foot
H ₂	Hydrogen
HCO ₃ ⁻	Bicarbonate Ion
HDC	Hydrogen Depolarized Carbon Dioxide Concentrator
Hsg	Housing
Hg	Mercury
hr.	Hour
H ₂ O	Water
H ₂ S	Hydrogen Sulfide
H ₂ SO ₄	Sulfuric Acid
Hz	Hertz (cycles per sec.)
I	Current
i	Current Density
in.	Inches
IR	Voltage Drop
KCl	Potassium Chloride
lb.	Pound
mg/cm ³	Milligrams per Cubic Meter
min.	Minute

ABBREVIATIONS AND SYMBOLS (Continued)

ml	Milliliter
mm	Millimeter
mV	Millivolt
N ₂	Nitrogen
N/A	Not Applicable
Nom.	Nominal
NH ₃	Ammonia
N ₂ O	Nitrous Oxide
NO	Nitric Oxide
NO ₂ ⁻	Nitrite Ion
NO ₃ ⁻	Nitrate Ion
O ₂	Oxygen
OH ⁻	Hydroxide Ion
P	Pressure
psi	Pounds per Square Inch
psia	Pounds per Square Inch Absolute
PH ₂ O	Partial Pressure of Water Vapor
PO ₂	Partial Pressure of Oxygen
PCO ₂	Partial Pressure of Carbon Dioxide
PPF	Code Name for Improved HDC Anode (Mfg. by P&WA)
PPM	Parts Per Million
PVC	Code Name for P&WA Experimental Electrode
P&WA	Pratt & Whitney Aircraft, Division of United Aircraft Corporation

ABBREVIATIONS AND SYMBOLS (Continued)

R	Resistance (ohms)
R.H.	Relative Humidity
SSP	Space Station Prototype
SEC	Code Name for Experimental Electrode
sec.	Second
SO ₃ ⁻²	Sulfite Ion
scc	Standard Cubic Centimeter
SO ₂	Sulfur Dioxide
SCFM	Standard Cubic Feet per Minute
SEM	Scanning Electron Microscope
T _{in}	Inlet Temperature
TMAC	Tetramethylammonium Carbonate
TMA	Tetramethylammonium
UAC	United Aircraft Corporation
VDC	Volts, Direct Current
WVE	Water Vapor Electrolysis
wt.	Weight
wt. %	Weight Percent
μ	Micro (10 ⁻⁶)
%	Percent
≈	Approximately Equals
=	Equals

ABBREVIATIONS AND SYMBOLS (Concluded)

<	Less Than
~	Approximate
Δ	Delta
ρ	Resistivity ($\text{ohm}^{-1} \text{cm}^{-1}$)
τ	Tortuosity

DEFINITIONS

<u>Anolyte</u>	Electrolyte in the immediate vicinity of the anode.
<u>Cell</u>	Electrochemical cell consisting of an anode, matrix with electrolyte, and cathode.
<u>Cell Pair</u>	Two cell packages with back to back hydrogen electrodes which share a common hydrogen chamber, housing and reservoir assemblies.
<u>Concentration Over - Voltage</u>	Voltage loss due to concentration differences between electrodes.
<u>Dry Out</u>	The condition of the cell, when the volume of the electrolyte is insufficient to completely fill the matrix due to loss of water.
<u>Electrokinetic Effects</u>	General phenomena associated with interaction of current with charged interfaces, i. e. , electroosmosis, electrophoresis, streaming potential, sedimentation potential.
<u>Electroosmosis</u>	Movement of a liquid through a porous solid via a voltage gradient.
<u>Electrophoresis</u>	Movement of a solid through a liquid via a voltage gradient.
<u>Flooding</u>	The condition of the cell when the electrolyte has absorbed an amount of water which results in an electrolyte volume exceeding the capacity of the cell matrix and electrodes.
<u>H₂ Crossover</u>	Occurs at dry out of the matrix and allows hydrogen and oxygen to pass through the matrix.
<u>IR Check</u>	Measurement of IR drop by current interruption.
<u>IR Drop</u>	Voltage loss due to pure ohmic resistance.
<u>Potential Sweeps</u>	A programmed potential change--usually a triangular wave.

DEFINITIONS (Concluded)

R. reservoir

A porous material which absorbs the excess electrolyte during cell flooding and returns it to the matrix during drying conditions.

Spreading Coefficient

The force which determines the wicking rate of a liquid into a porous solid--related to the interfacial tensions of the systems.

Steady State Operation

The operating condition when the cell voltage and current do not change significantly with time.

Tafel Slope

The slope of the Tafel curve.

Zeta Potential

Potential across the mobile part of the electrical double layer.

SUMMARY

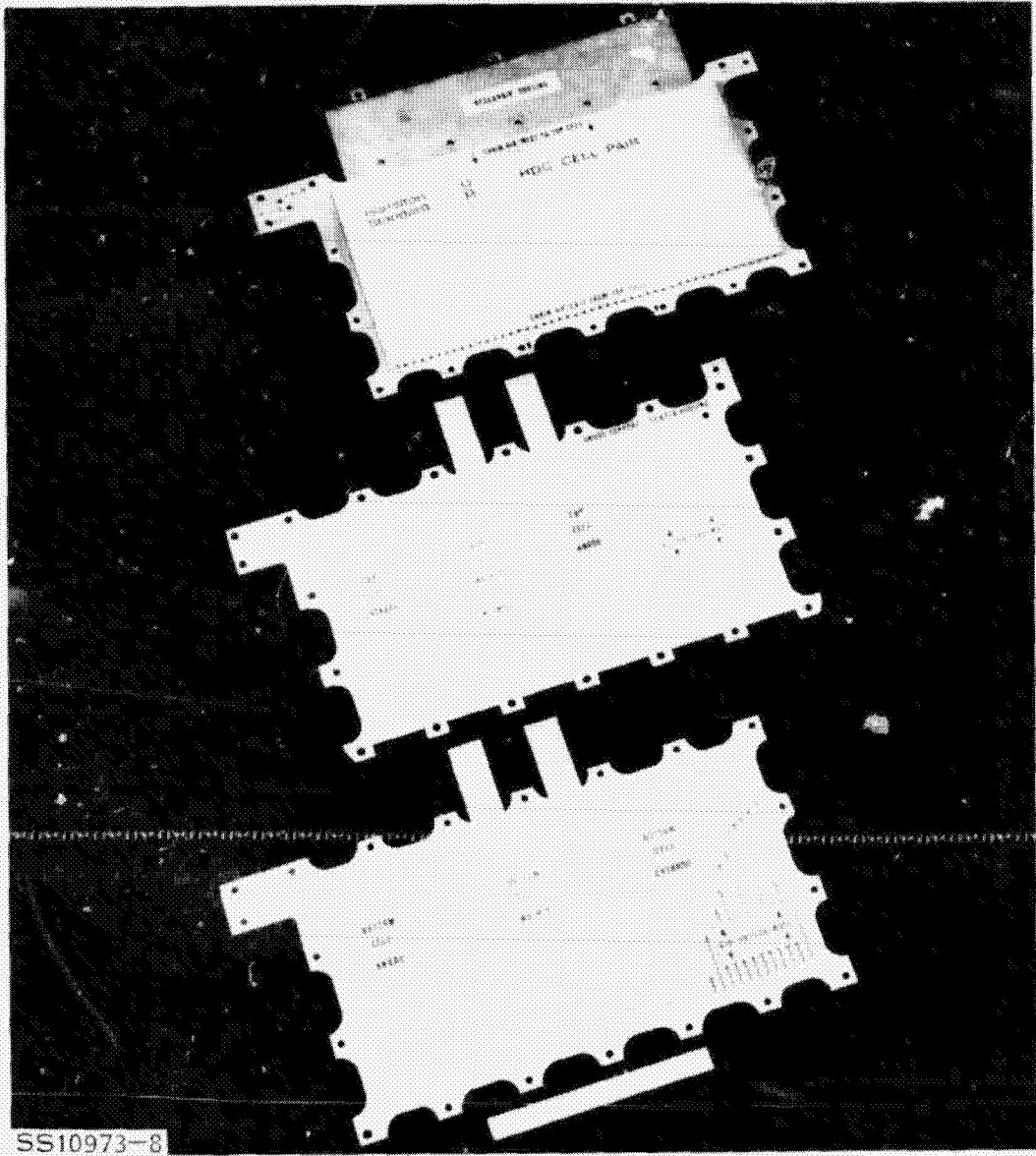
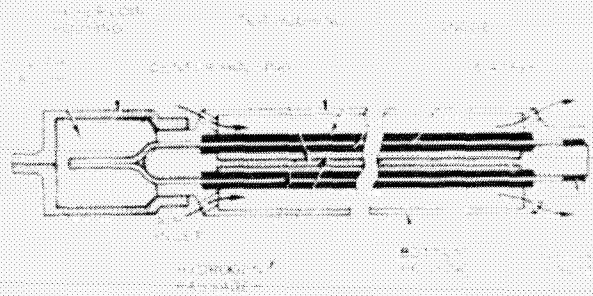
The objectives of this program, which were to reduce the voltage decay rate and improve the CO₂ transfer rate of the hydrogen depolarized CO₂ concentrator (HDC) cell pair (Figure 1), were accomplished. HDC endurance tests of two cell pairs verified that the improved electrodes reduced the voltage decay rate from approximately 200 μ v/hr to less than 50 μ v/hr and improved the CO₂ transfer efficiency from 60 percent to 86 percent for cesium carbonate (Cs₂CO₃) electrolyte and from 45 percent to 70 percent for tetramethylammonium carbonate (TMAC) electrolyte at a current density of 18 asf and a CO₂ partial pressure of 3 mm Hg. This was accomplished by a thorough analysis of cell and electrode performance behavior, effects of trace contaminants, matrix characteristics, and electrode structure examinations. Results of this effort revealed that the PPF electrode reduced the migration rate of the anode platinum catalyst and Teflon binder. Electrophoretic migration caused the anode to lose effective area. The DS 16-0 electrode used as a cathode increased the circulation rate of the catholyte, resulting in increased CO₂ removal.

An evaluation of various HDC matrix materials was made to determine the tortuosity, optimum compression for minimum IR drop, compression set characteristics, and the effect of thickness on the CO₂ removal rate and cell power.

Performance testing of the various HDC cell pairs with Cs₂CO₃ electrolyte provided sufficient parametric and endurance data to size the six-man Space Station Prototype (SSP) CO₂ removal system as having 36 HDC cell pairs, and to verify a life capability exceeding six months. Subsequent improvements in electrode structure, as noted above, increased cell life by a factor of four and allowed a reduction in the number of cell pairs to 20. Testing also demonstrated that TMAC is an acceptable HDC electrolyte for operating over the relative humidity range of 30 to 90 percent and over a temperature range of 50°F to 80°F.

The water vapor electrolysis (WVE) cell pair which was assembled and operated for 3940 hours under a preceding NASA contract (NAS 9-11830)⁽¹⁾ was successfully restarted, after three and one-half months of storage, was vibrated at Apollo launch levels, and was operated after vibration testing, providing a total running time of 5280 hours. The successful vibration test demonstrated that the Hamilton Standard electrochemical cell pair design, including an electrolyte reservoir, is structurally qualified for flight.

The integrated WVE/HDC breadboard unit designed under the previous NASA contract (NAS 9-11830) was fabricated and assembled during this program. The breadboard unit consisted of two HDC cell pairs and two WVE cell pairs integrated into a single package, which incorporated a blower, valving and instrumentation for operating the system. This unit was not tested, however, because the test requirement was deleted from the contract.



SS10973-8

FIGURE 1. WVE AND HDC CELL PAIRS

INTRODUCTION

This program was conducted in accordance with NASA Contract 9-12920 to improve the CO₂ removal rate and decrease the power decay of the HDC cell pair.

NASA Contract 9-12920 is a follow-on to NASA Contract NAS 9-11830 which resulted in the following accomplishments:

- Establishment of an HDC electrolyte (TMAC) for operation over a wide range in relative humidity.
- Initial testing of an integrated WVE/HDC.
- Design of a four cell pair integrated WVE/HDC breadboard unit.

The Improved Multi-Celled Breadboard Electrochemical Oxygen Generation and Carbon Dioxide Control System (NAS 9-12920) contract had as initial objectives:

- Investigation of various operating parameters of the HDC and WVE cell pairs.
- Fabrication and test of an integrated WVE/HDC breadboard unit.

The contract was revised twice to authorize the improvement of the HDC performance. As a result of the NASA's review of the HDC cell pair data, presented at the SSP Approval Design Review (ADR) meeting, this program was redirected to obtain additional HDC parametric test data and to demonstrate cell pair performance repeatability. This SSP oriented task established that:

- The required number of HDC cell pairs to maintain the P_{CO₂} level, for a six-man SSP cabin, below 3 mm Hg, would be 36.
- The degradation in cell voltage, which occurred over six months of testing, decreased with time and assured a six month cell life for a 36 cell pair unit.
- A CO₂ removal performance map was obtained for a range of P_{CO₂} from 1.2 to 3.0 mm Hg and current densities from 12 to 24 asf.

The evaluation of the HDC design and testing for this SSP oriented task are summarized in a separate report, SVHSER 6229, dated March 1973. (2)

Following completion of the above HDC testing, the NASA redirected this program in an attempt to improve the HDC CO₂ removal rate and to decrease the rate of cell voltage degradation. The final program consisted of the following tasks:

HDC Cell Pair Definition - Determine the HDC cell pair configuration for use on the SSP, as described in Report No. SVHSER 6229.

HDC Power Decay Investigation - Determine the cause for the degradation in HDC cell pair power which was experienced in units S/N 017 and S/N 018.

HDC Analytical Testing - Obtain a more detailed knowledge of the HDC cell operation and evaluate new concepts to improve its performance using Cs₂CO₃ and TMAC as the electrolytes in a small (1/24 sq. ft.) analytical cell.

Improved CO₂ Transfer - Improve the CO₂ removal efficiency of the HDC.

HDC Electrolyte Properties - Determine the various physical properties of the HDC electrolytes Cs₂CO₃ and TMAC.

Special Tests - HDC matrix and hydrogen flow tests.

HDC Verification Test - Demonstrate performance improvements with a 90-day verification test on two HDC cell pairs (one Cs₂CO₃ and one TMAC).

WVE Vibration - Evaluate the effects of vibration on performance and structural integrity of the WVE cell pair developed under the NAS 9-11830 contract.

WVE/HDC Breadboard - Fabricate and test a WVE/HDC breadboard unit. This task, however, was deleted after the basic cell pair rack assembly had been fabricated.

The successful completion of the previously described tasks provided:

- A more thorough understanding of the operation of an HDC cell.
- Detailed characteristics of the HDC electrolytes.
- A new HDC anode and cathode.

- An HDC which has an improved CO₂ transfer rate and a lower power degradation rate.
- Verification that the present HDC and WVE cell pair design is capable of withstanding launch vibration levels.

CONCLUSIONS

The results of this program effort to improve the performance of the HDC, vibrate the WVE cell pair, and perform various HDC oriented research type tasks lead to the following conclusions:

- The factors which contribute to the internal cell resistance and determine cell power output are electrode polarization, electrolyte concentration polarization, and matrix-electrolyte resistance.
- Anode concentration overvoltage is a major contributor to low HDC cell power output and is the only source of internal cell power loss which offers hope for significant improvement in the future.
- Power output is very sensitive to cell temperature because of the temperature effect on electrode polarization, and there is some drop-off in power when the hydrogen flow rate is reduced below three times stoichiometric (normal flow rate is five times stoichiometric).
- The main reason for HDC cell power decay was a change in the anode structure with time, caused by electrophoretic migration of the catalyst and Teflon binder.
- Some HDC cell power decay was attributed to matrix dissolution at the matrix-anode interface, because of the low anolyte pH.
- Trace impurities at the maximum allowable cabin level will have little effect on HDC cell power performance. In an environment typical of the present day urban terrestrial atmosphere, where impurity levels are much higher, some power loss could result from sulfur dioxide (SO₂) absorption. This power loss could be recovered by a closed circuit nitrogen purge of the HDC hydrogen chamber.
- The rate of CO₂ transfer is controlled mainly by the mass transport processes within the cathode structure. Thus, the cathode should be designed to obtain a high rate of electrolyte circulation within the electrode structure.
- The CO₂ transfer rate is essentially independent of cell temperature, hydrogen flow rate, and hydrogen pressure.

- For maximum CO₂ transfer efficiency the optimum catholyte pH is in the range of 12.3 to 13.0. Within limits, the catholyte pH can be controlled by proper choice of air flow rate and current density.
- The minimum electrolyte-matrix resistance is obtained when the matrix is compressed to a thickness which results in a 50 percent matrix void volume.
- A matrix thickness (electrode separation) of 20 to 30 mils provides optimum HDC performance based on a compromise between CO₂ transfer and cell power.
- Compressive relaxation of the asbestos matrix is complete after two weeks, and the final pressure is more than enough to maintain sufficient contact between the cell components (current collector-electrode-matrix).
- The HDC and WVE cell pair design can withstand launch vibration loads without structural damage or loss of performance.

RECOMMENDATIONS

Based on the various HDC and WVE test results of this program, the following recommendations are made:

- The recommended HDC electrodes which will provide increased CO₂ removal rates and reduced voltage decay rates are:

Anode - PPF Electrode

Cathode - DS 16-0 Electrode

- Continue investigation of HDC anode and anode-matrix interface behavior for possible ways to further improve the cell power and life.
- Change the HDC matrix material from fuel cell chrysotile asbestos to a more acid resistant material. A possible replacement material is Neoprene asbestos.
- Tetramethylammonium carbonate (TMAC) is recommended as the HDC electrolyte for units which are required to operate over a wide range of inlet air temperatures and dew points.
- Determine the physical properties of TMA bicarbonate and measure the decomposition rate of TMAC in an operating cell. This task was not accomplished during this program because of program redirection.
- Continue the search for new HDC electrolytes which will provide increased performance and life.
- To provide an improved product two design changes of detail parts should be made:
 - The outer housings of the cell pair should have a 0.050 to 0.60 inch concave bend in them. This will provide a more evenly loaded matrix when the housings are assembled.
 - The air outlet holes and outer edges of the housings should be coated with Teflon to prevent any possible electrolyte creep.

DISCUSSION

The discussion of the results obtained from this program is separated into eleven sections. These sections correspond to the ten major tasks of the program, which are defined in the INTRODUCTION of this report, plus a discussion of the program's reliability and safety aspects, and are titled:

- SSP-HDC EVALUATION TESTING
- HDC POWER DECAY INVESTIGATION
- HDC ANALYTICAL TESTING
- IMPROVED CO₂ TRANSFER
- HDC ELECTROLYTE PROPERTIES
- MODIFIED ELECTROLYTES
- SPECIAL TESTS
- HDC VERIFICATION TEST
- WVE VIBRATION
- WVE/HDC BREADBOARD
- RELIABILITY AND SAFETY

SSP-HDC EVALUATION TESTING

This task pertained to the evaluation testing of the HDC cell pair concept to determine whether the Hamilton Standard design could be considered ready for inclusion in the Space Station Prototype (SSP) system. As a result of this test program, the NASA concluded that further cell development was necessary before a full scale system is constructed and that the remaining funding of contract NAS9-12920 should be directed towards this HDC development. A formal report on the SSP test program, SVHSER 6229, was prepared for NASA-JSC and is summarized in the following paragraphs.

Various tests, analyses and miscellaneous tasks were performed in support of this task.

Analytical and Miscellaneous Tasks

Objectives

The objectives for the analytical and miscellaneous tasks were:

- Perform instrumentation error analysis on various test data parameters.
- Normalize test data of Hamilton Standard's cell pair S/N 010 to show CO₂ removal performance versus time (226 days).
- Define the N₂ purge technique (if any) to be employed during cell pair testing.
- Develop a computer mathematical model to determine the number of cell pairs required to satisfy the SSP requirements, based upon the CO₂ removal performance achieved during the test program.
- Perform various rig modifications to improve cell pair current control and test chamber ambient conditions.

Conclusions

The conclusions reached as a result of the analytical and miscellaneous tasks were:

- The RSS Measurement error for determining CO₂ transfer rate was $\pm 3.95\%$ on the reported tests.
- Normalization of cell pair S/N 010 data revealed that CO₂ removal performance remained constant throughout the test.

- A procedure for purging the cell with nitrogen once each day was developed and employed on each of the four tests of this test effort. This purge did not improve the CO₂ transfer efficiency, but it did decrease the rate of cell pair power degradation initially.
- An HDC system sizing computer program was developed based on actual cell pair performance. It established that 36 cell pairs would satisfy the SSP application.
- Modifications were made to the facility to enable constant current testing at selected current densities. Due to mechanical limitations, the test chamber to laboratory room air leakage rates were not improved. It was not established positively that the relatively high concentration of sulphur dioxide (20 ppm) which the test cells were consequently exposed to, contributed to the voltage degradation.

Cell Pair Test Program

Objectives

The objectives for all the cell pair test program were:

- Establish the adequacy of certain cell pair housings and electrodes.
- Evaluate the effects of varying matrix compression over a range compatible with cell assembly tolerances and matrix void volume variations.
- Determine the desirability of including Tissuquartz in the proposed SSP reservoir cell configuration to enable the cell to withstand a significant step change in inlet air temperature.
- Establish a map of cell performance at varying current density, inlet air temperature, inlet dew point, and carbon dioxide concentrations and evaluate the change in this performance versus cell operating time.

Conclusions

Conclusions reached from the cell pair testing were:

- Both the annealed and non-annealed housings were found acceptable; electroplated electrodes should be used in all tests.
- Short term testing, during which the matrix compression was varied from .022 to .030 inches revealed that cell voltage and CO₂ removal efficiency were independent from this change in matrix thickness.

- Tissuquartz assembled in strips within the matrix resulted in the reservoir cell being able to withstand a $\pm 4^{\circ}\text{F}$ air inlet step change...this configuration was subsequently employed.
- A map of CO_2 removal efficiency for different operating conditions was established over an extended test period. The originally planned test duration of six to eight weeks was extended. After five months of continuous testing, no permanent decrease in cell current efficiency (performance) occurred. Cell voltage decreased with time over five months, but remained sufficiently high to accommodate the necessary CO_2 transfer rate of 13.2 lbs/day for the SSP application.

HDC POWER DECAY INVESTIGATION

During HDC cell testing under the SSP program, cell power degradation was found to be associated mainly with the anode. Potential decay curves of the cell anode and cathode versus a reference probe showed that the effective anode surface area was decreasing with time, whereas the cathode area remained about the same.

Floating electrode tests on anodes from cells that had decayed in performance gave almost the same performance as an unused electrode.* This indicated that most of the initial performance capabilities of the anode were still available, but for some reason were not being utilized in the full cell. Several possible causes for the loss in anode performance were postulated.

- Anode Poisoning from oxidizable trace impurities.
- Electrolyte imbalance resulting in flooding or dry-out.
- Change in electrode structure due to electrophoretic migration, which would affect the electrolyte take-up capabilities of the anode.

To distinguish between the various possible causes of anode performance decay, a number of experiments was conducted on full size cells. In addition, the behavior of selected trace impurities in the electrolyte was investigated in half cells, and a micrographic examination of used and unused anodes was conducted to determine if the electrode structure had changed upon use. The effect of matrix thickness on cell performance also was investigated.

Trace Impurities

The effectiveness of a closed circuit nitrogen purge of the anode chamber in restoring a significant part of the cell voltage for a short period of time would indicate the presence of oxidizable or desorbable impurities in the electrolyte, the effects of which would not necessarily be detected in the floating electrode test because the electrode sample is exposed to air prior to the test.

The purpose of this study was to determine whether certain selected trace impurities and their oxidation or reduction products poison the HDC electrodes, and/or accumulate to significant levels in the electrolyte. It also was a goal of this study to define simple methods of recovering from any adverse effects due to trace impurities entering the HDC cell. The testing was conducted in accordance with the Master Test Plan, Section VI, included as the Appendix of this report.

*The anodic overvoltage at 20 asf for the used and unused electrode was 103 and 91 mV, respectively.

The trace impurities chosen for study and their maximum allowable levels in cabin air are given below. *

<u>Impurity</u>	<u>mg/m³</u>	<u>ppm</u>	<u>moles/m³</u>
CO	29	25	1 x 10 ⁻³
H ₂ S	1.5	1.3	5 x 10 ⁻⁵
SO ₂	2.6	1.0	4 x 10 ⁻⁵
NH ₃	3.5	5	2 x 10 ⁻⁴
Freon 113	700	100	4 x 10 ⁻³

* Numbers supplied by the NASA JSC, using SSP as a guideline.

In the cases where the impurity was added directly to the electrolyte for testing the poisoning effects, the amount added to 35 ml of electrolyte was equal to the number of moles in a cubic meter of air. All potentials are with respect to a hydrogen reference electrode in the same solution. Since the nature of the cation has little effect on the adsorption or electrochemical properties of a platinum electrode, cesium carbonate, rather than TMAC (tetramethyl ammonium carbonate) was used in this work for convenience in solution preparation and purification. Also, it would be difficult to prevent TMA ion decomposition with the test procedure employed and the presence of these decomposition products might have interfered with the test results.

Ammonia

Ammonia (NH₃) can be oxidized at the HDC cathode to a number of products; the most important are listed below along with their approximate standard potentials.

<u>NH₃ Oxidation Product</u>	<u>Standard Potential (Volts)</u>
N ₂	0.1
N ₂ O	0.5
NO	0.7
NO ₂ ⁻	0.8
NO ₃ ⁻	0.9

These numbers are only a guide, since the actual potential range where a significant oxidation rate occurs will depend on the kinetics of the various reactions. Potentiostatic sweeps were made to determine the actual potentials for ammonia oxidation and to help in identifying the major reaction products. A typical

potentiostatic sweep curve on platinum in Cs_2CO_3 solution is defined by the sketch below and is used as a baseline for comparison.

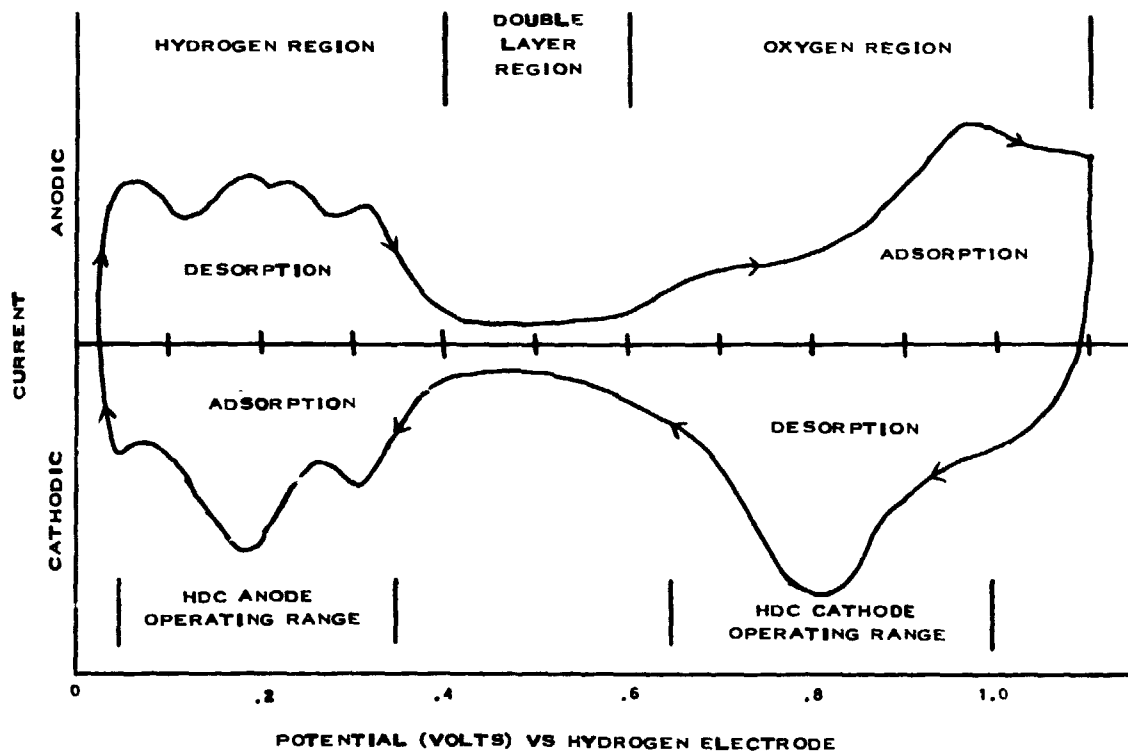


FIGURE 2. BASELINE POTENTIOSTATIC SWEEP ON PLATINUM IN Cs_2CO_3 SOLUTION

It is desirable that the reaction products be gaseous rather than ionic to avoid accumulation of foreign ions in the electrolyte. The maximum solubility of ammonia in the catholyte in equilibrium with 5 ppm NH_3 in air is approximately 2×10^{-4} per liter. The initial potential sweep tests using this concentration showed no change in the sweep curves. Ammonium carbonate then was added to the cesium carbonate electrolyte at a level corresponding to approximately 30 times this maximum allowable NH_3 level in order to identify the reactions more readily. Figure 3 shows the potential sweeps with and without the addition of ammonia. There is definite evidence of some ammonia oxidation to nitrogen in the hydrogen adsorption region (below 0.4 volts) as expected, and a large anodic peak starts at 0.5 volts, which can be attributed to the oxidation of ammonia to N_2O . The formation of higher oxidation products (NO , NO_2^-) is not evident from these data and the excess cathodic current observed on the down-sweep below 0.6 volts may be due to the reduction of any of these oxidation products formed during the upsweep. One interesting feature is the absence of an oxide reduction peak on the down-sweep (0.8 volts) and it must be concluded that ammonia or its oxidation products inhibits the oxidation of platinum.

It will be shown later that the HDC cathode operates near 0.8 volts with respect to a hydrogen electrode in the same solution. This being the case, ammonia as a trace contaminant in the air stream would be oxidized mainly to N_2O and possibly some small amount of NO and NO_2^- . To determine if a significant amount of NO_2^- , an electrolyte contaminant, is formed under cathode operating conditions, the electrode was held at 0.8 volts for one-half hour followed by an upsweep to 1.1 volts and then down (figure 4, Curve 1). No increase in cathodic current was observed on the down-sweep which could be attributed to NO_2^- reduction. To determine the potential range for NO_2^- reduction, 2×10^{-4} moles of sodium nitrite were added to the electrolyte and another sweep made (figure 4, Curve 2). A large reduction peak was observed in the hydrogen adsorption region (below 0.4 volts) so that even if some NO_2^- is formed at the HDC cathode it would be readily reduced to a gaseous product at the anode and therefore not accumulate in the cell electrolyte.

Since it was found that ammonia inhibits platinum oxidation, it was necessary to determine if trace amounts of ammonia would poison the cathodic reduction of oxygen by preventing oxygen adsorption on the platinum catalyst surface. For this test a floating SSP electrode was used with air, and 15 times the maximum amount of ammonia as ammonium carbonate was added to the cesium carbonate electrolyte. The results are shown in figure 5, where it can be seen that ammonia actually increases the cathode performance in the current density range of interest. This is reasonable because it was shown that ammonia inhibits platinum oxide formation and it is well known that bare platinum is a better catalyst for oxygen reduction than oxidized platinum. At low current densities ammonia oxidation results in a reduction of the net cathodic current.

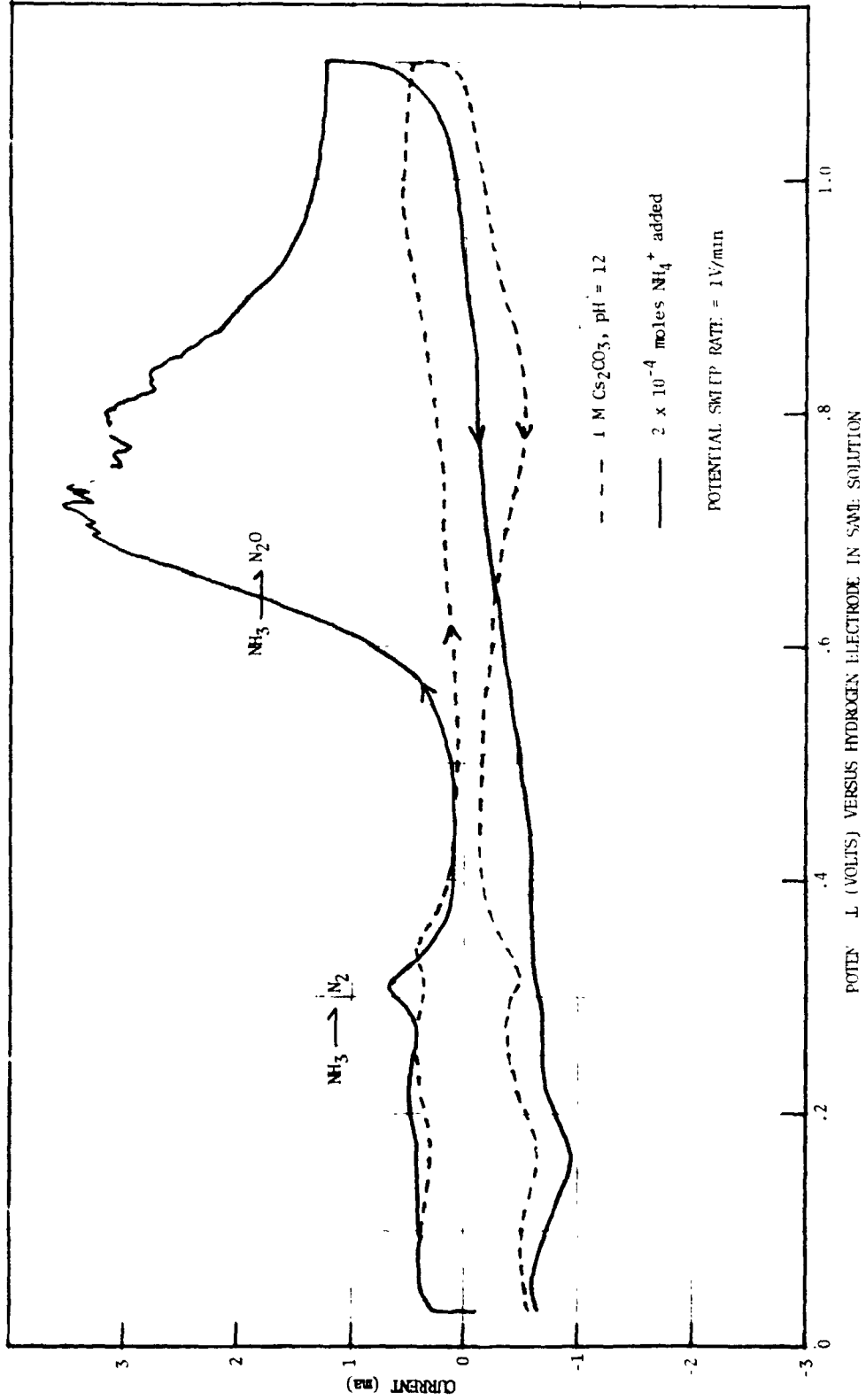


FIGURE 3. OXIDATION OF AMMONIA (NH₃) ON PLATINUM BLACK ELECTRODE

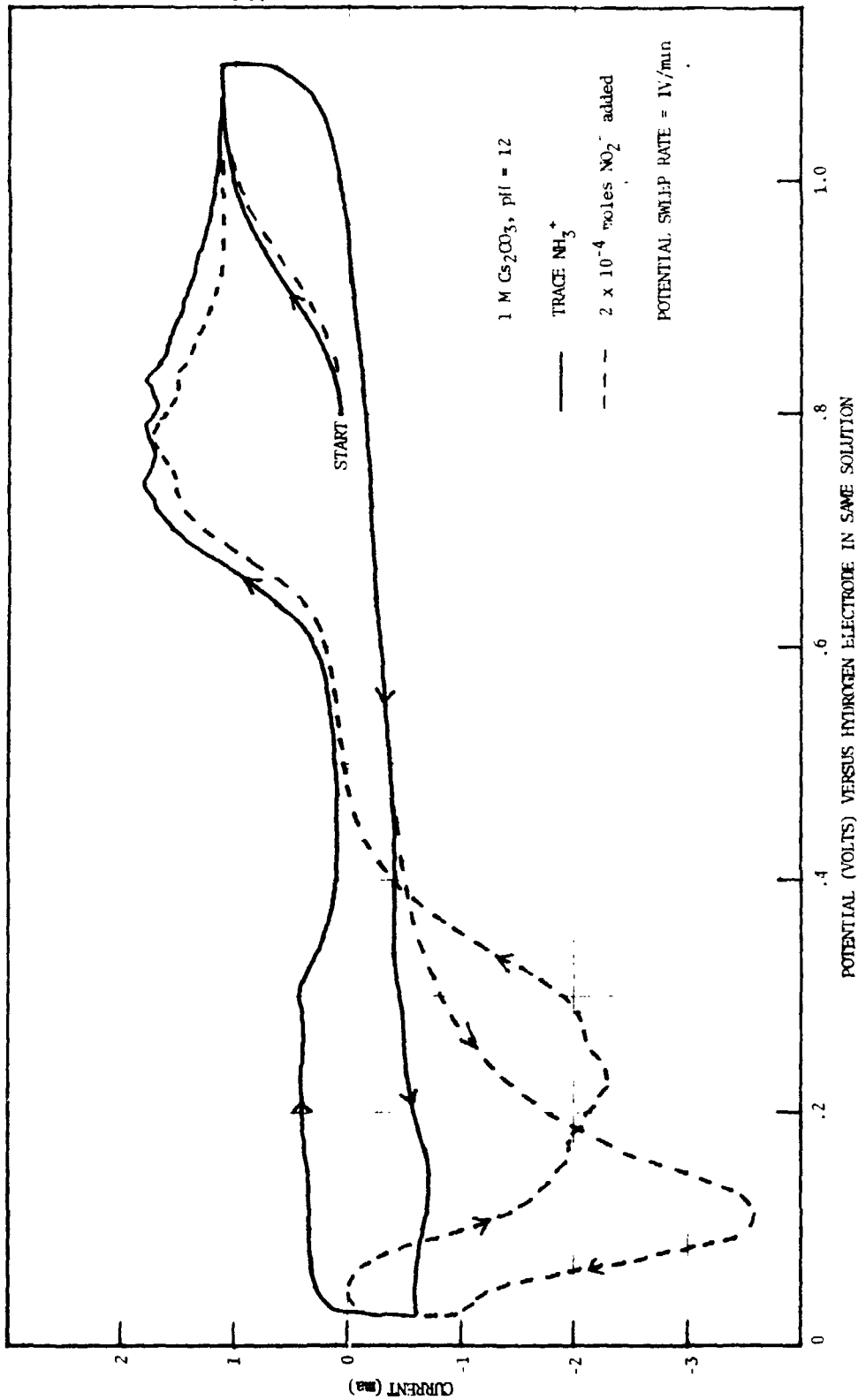


FIGURE 4. REDUCTION OF NITRITE ION (NO₂) ON A PLATINUM BLACK ELECTRODE

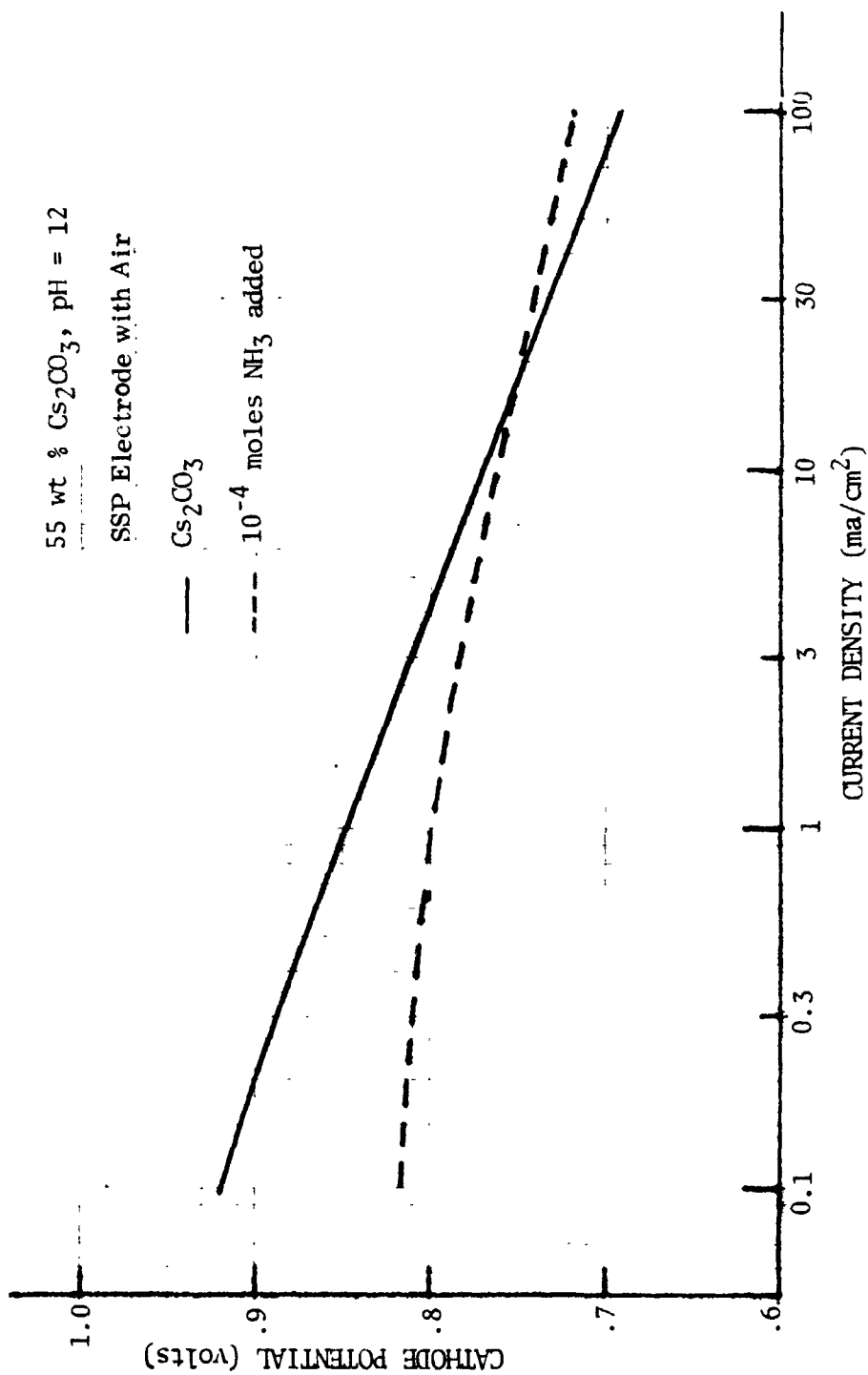


FIGURE 5. EFFECT OF AMMONIA ON CATHODE PERFORMANCE

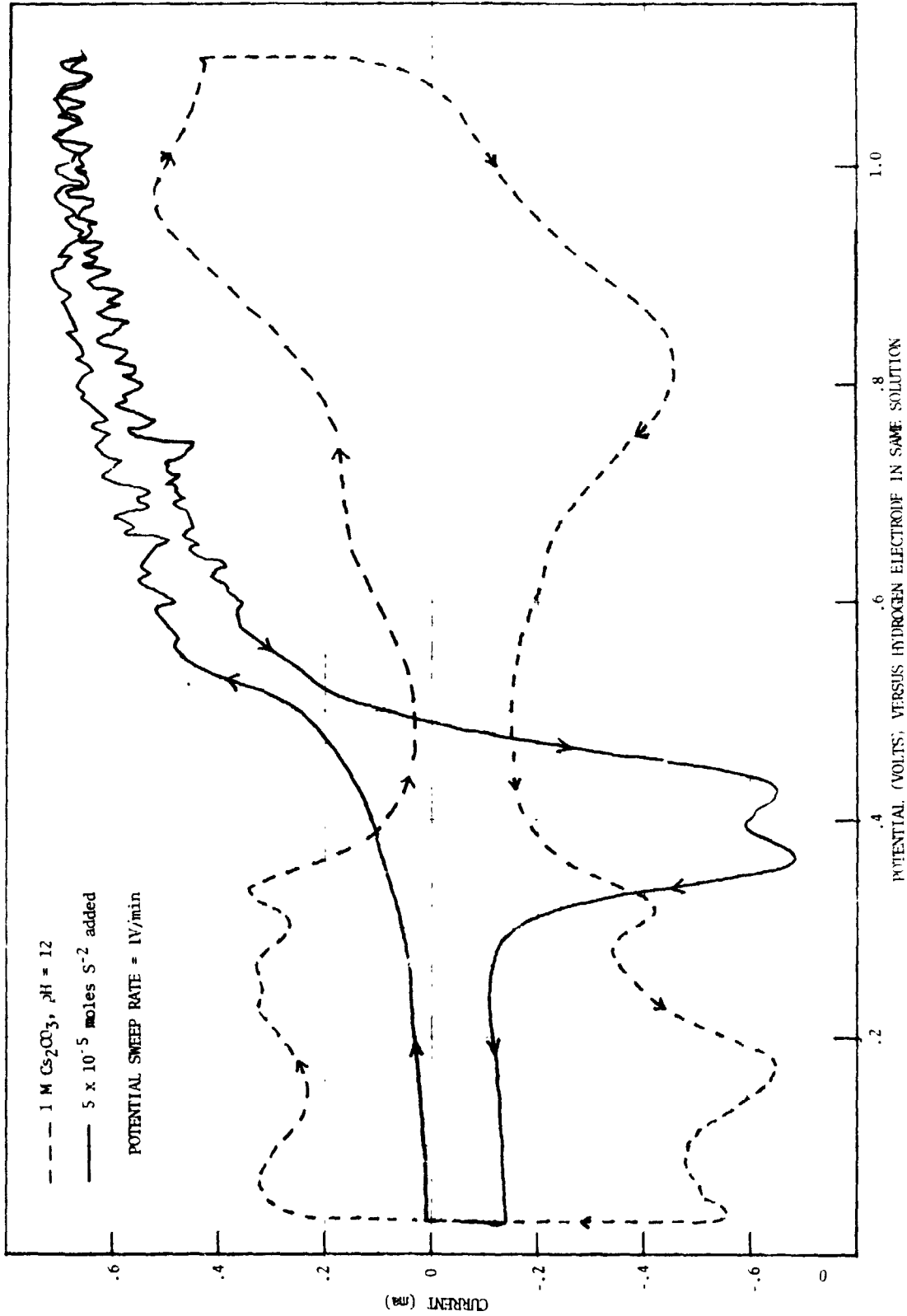


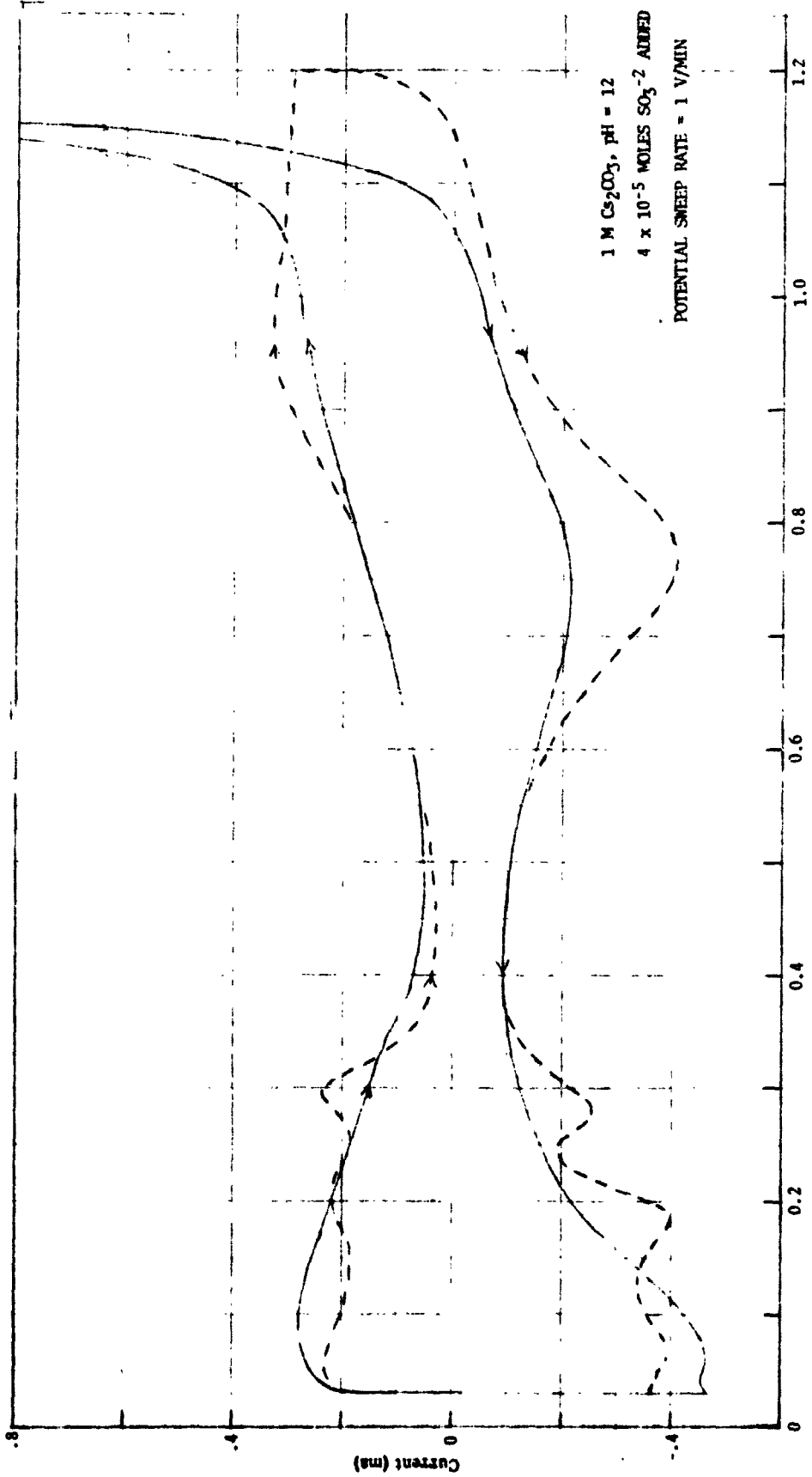
FIGURE 6. OXIDATION OF SULFIDE ION (S²⁻) ON A PLATINUM BLACK ELECTRODE.

Hydrogen Sulfide and Sulfur Dioxide

In addition to trace amounts of sulfur dioxide (SO_2) and hydrogen sulfide (H_2S) in the air stream, it is possible to get H_2S in the hydrogen gas from improper operation of the WVE. It is therefore necessary to consider the effect of H_2S on both the anode and cathode of the HDC. Both H_2S and SO_2 are acid gases and will react with the HDC electrolyte to form sulfide (S^{-2}) and sulfite (SO_3^{-2}) ions, respectively. Thus, these ions could accumulate in the electrolyte, reaching significant levels over a period of time. The only thermodynamically stable oxidation product of H_2S or SO_2 in the HDC electrolyte is the sulfate ion (SO_4^{-2}), although intermediate oxidation products such as sulfur and the various sulfur oxides will be produced at the HDC cathode during the oxidation of the sulfide or sulfite. The sulfate ion is not detrimental to the HDC electrolyte or electrodes; in fact, it was evaluated as an electrolyte additive to increase anolyte conductivity and lower anolyte pH under certain operating conditions. It can be calculated, considering mass transport limitations for H_2S and SO_2 in the air stream, that it would take about 10^5 hours for the sulfate concentration in the HDC electrolyte to reach a significant level (0.5 moles per liter).

A slow potential sweep, with and without the sulfide ion, is shown in figure 6. It can be seen that hydrogen absorption is strongly inhibited and sulfide oxidation becomes evident starting at ~ 0.15 volts and reaches a mass transport limiting current density at ~ 0.6 volts. On the downsweep, a reduction peak is seen at ~ 0.4 volts. In separate experiments it was determined that the number of coulombs corresponding to this reduction peak was $1/7$ that of the coulombs for oxidation at 0.8 volts. Oxidation at more positive potentials resulted in a decrease in the number of coulombs for the reduction peak. From these results it can be concluded that this peak corresponds to the reduction of an adsorbed intermediate reaction product formed during sulfide oxidation.

The behavior of SO_2 , which becomes SO_3^{-2} (sulfite) upon interaction with the electrolyte, is shown in figure 7. There is little effect on hydrogen adsorption and even after holding the potential at -0.16 volts for 10 minutes there was no evidence for the formation of SO_3^{-2} reduction products or a decrease in the amount of adsorbed hydrogen. Apparently the reduction of SO_3^{-2} is very slow under HDC anode conditions. Oxidation of SO_3^{-2} , presumably to sulfate, is obvious at 1.1 volts. Since the HDC cathode operates at 0.8 volts, it is expected that SO_2 would accumulate in the HDC electrolyte as SO_3^{-2} until the concentration reached a point where the rate of removal via oxidation, reduction and/or discharge in the hydrogen stream becomes equal to the rate of absorption. Over a relatively long period of time it is expected that sulfide would accumulate on the anode from sulfite reduction or H_2S adsorption, but this sulfide could be removed readily by increasing the anode potential to that of the air electrode (nitrogen purge, closed circuit) for a short period of time. The above reasoning is supported by gas analysis performed on the HDC cell. During normal operation it was found that approximately 1 percent of the SO_2 in the air stream (20 ppm) is transferred through the cell, but during a closed circuit nitrogen purge the amount of SO_2 in the HDC anode compartment increased by a factor of 100.



POTENTIAL (VOLTS) VS HYDROGEN ELECTRODE

FIGURE 7. OXIDATION OF SULFUR DIOXIDE (SO₃⁻²) ON A PLATINUM BLACK ELECTRODE

Carbon Monoxide

The only stable oxidation product of carbon monoxide (CO) under HDC cell conditions is carbon dioxide (CO₂). It is well known that carbon monoxide poisons the hydrogen anode reaction, but at the 22 ppm level only a slight reduction hydrogen adsorption was detected and no oxidation peak for CO could be found.

To determine the potential range for CO oxidation to CO₂ the cesium carbonate electrolyte was saturated with CO followed by a nitrogen purge for 20 minutes to remove the dissolved CO. Since the CO is strongly adsorbed on the electrode surface at +30 mV, little CO desorption would occur during the nitrogen purge.

Figure 8 shows the subsequent potential sweep compared to a sweep on a clean electrode surface. There is a significant reduction in the amount of adsorbed hydrogen, and the adsorbed CO gives an oxidation peak at ~0.7 volts. From these results it can be concluded that carbon monoxide would be readily oxidized at the HDC cathode and if a small amount eventually did get to the anode it could be easily removed by the nitrogen purge technique.

Freon 113

Freon 113 (CCl₂F-CF₂Cl) should be electrochemically inert under HDC cell conditions, since chemiadsorption is highly unlikely for such a stable chemical structure. Some physical adsorption may be possible in the double layer potential region (0.4 to 0.6 volts) but the Freon would be readily replaced by chemiadsorbed hydrogen or oxygen at the anode or cathode, respectively.

Potential sweeps with and without Freon 113 gave identical traces; therefore Freon 113 should have no detrimental effect on electrode performance. With HDC electrodes, which contain Teflon, the Freon may adsorb on the Teflon surface but the electrode wetting characteristics should not change significantly.

Conclusions

In view of these results it can be concluded that the above trace impurities at the levels normally present in cabin air will have little effect on HDC cell power performance. At much higher levels some poisoning could occur from H₂S, CO and SO₂, but an open circuit nitrogen purge of the hydrogen chamber would oxidize these materials off the electrodes and restore power. Sulfur dioxide (SO₂) would be the most difficult of the above impurities to remove, since it accumulates in the electrolyte as the sulfite ion (SO₃⁻²). Fortunately, it does not poison the electrodes directly and its rate of reduction to sulfur or sulfide (both poisons) is very slow.

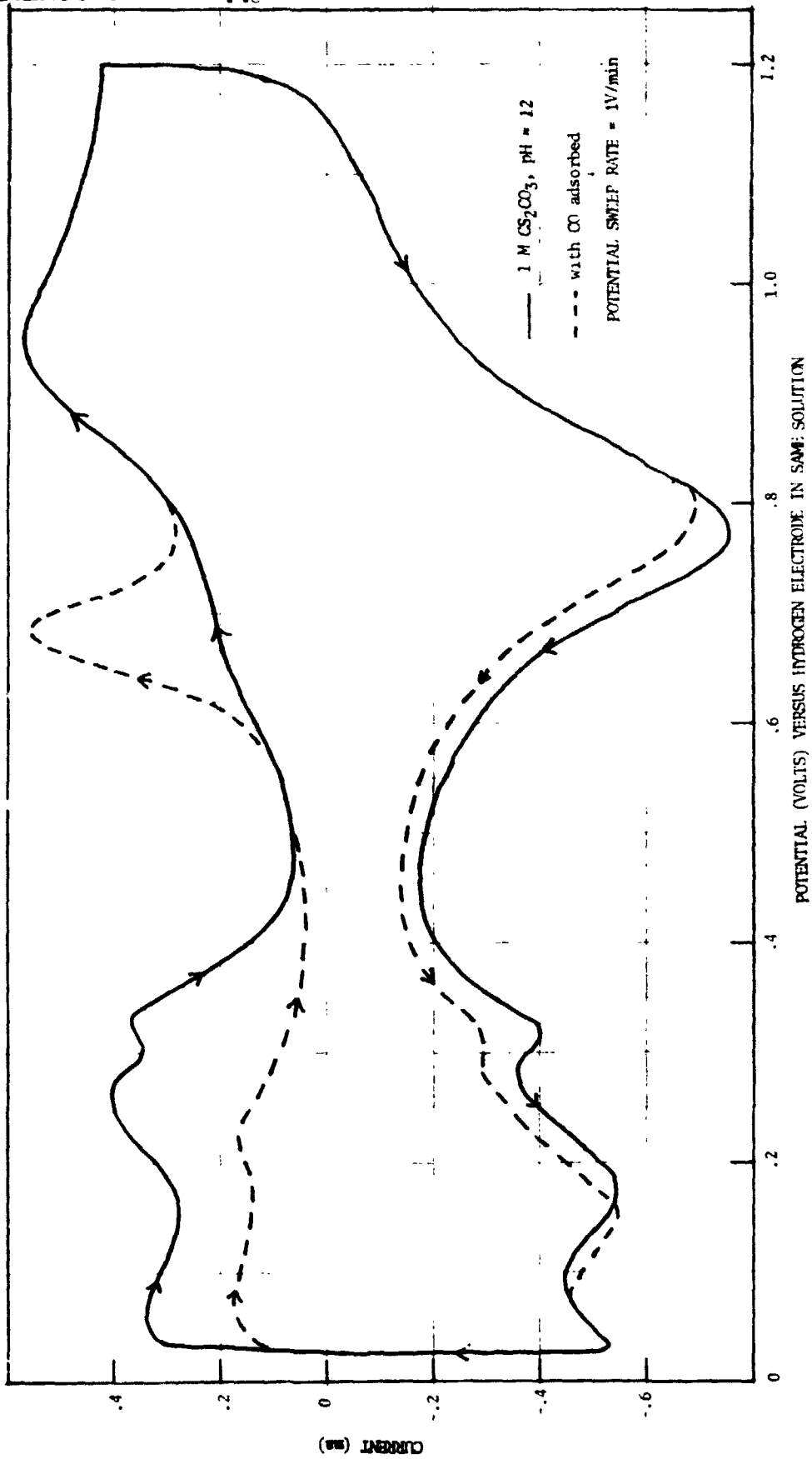


FIGURE 8. OXIDATION OF CARBON MONOXIDE (CO) ON A PLATINUM BLACK ELECTRODE

From our experience with the electrochemical behavior of organic materials it is predicted that their rate of oxidation to CO_2 and H_2O in the HDC or WVE cell would exceed their rate of adsorption from the air stream. Thus, no significant poisoning from organic impurities is expected for the normal cabin concentrations.

Experiments on Cell Pair S/N 017

Experiments were conducted on cell pair S/N 017 (per the Master Test Plan, Section X, reference Appendix) in an attempt to isolate the cause of the degradation in cell power ($\sim 200 \mu$ volts/hr at 18 asf) experienced over a six month period.

The first approach was to establish whether electrolyte imbalance was a problem, although this is unlikely with the reservoir type cell unless the capacity of the reservoir is exceeded. A wet condition causing electrode flooding results in very little loss in cell power and would not persist because the relatively high air flow rate would remove the excess electrolyte from the cell. In order to be absolutely sure that excess electrolyte was not the problem, the air and hydrogen passageways were flushed with nitrogen at a high flow rate. The amount of electrolyte removed from the cell by this procedure was less than 1.0 ml, and there was no change in cell power. To determine if the cell was too dry, 20 ml of electrolyte were added to the reservoir, and after two days there still was no effect on cell power. To eliminate the possibility that the reservoir was not feeding electrolyte to the cell matrix, 5 ml of electrolyte were then added to the top cathode via the air passages. This resulted in a slight decrease (0.2 watts) in cell power, and potential decay measurements showed a small loss in effective cathode area, as might be expected, but no change in anode area. At this point there was more than sufficient electrolyte in the cell and a vacuum was applied to the hydrogen side for four hours in order to force electrolyte into and through the anode. This procedure resulted in a substantial increase (1.8 watts) in cell power, which decayed slowly back to the original level after three days. Potential decay measurements after the vacuum treatment showed a large increase in effective anode surface area and a small increase in cathode surface area. The slow decay of cell power during the next three days was found to be associated with a gradual loss in effective anode surface area as determined by potential decay measurements. The results of this experiment definitely indicate that the anode gradually loses its ability to take up electrolyte from the matrix.

Since the vacuum treatment did not result in complete recovery to the original power level, it was reasoned that other factors could be contributing to the power decay. The accumulation of trace impurities in the electrolyte still was a possibility. If a closed circuit nitrogen purge of the anode resulted in the desorption rather than the oxidation of a given impurity, a temporary power recovery would be expected as observed.

A temporary power recovery from a closed circuit nitrogen purge also would be expected if a relatively large amount of impurity, such as SO_2 (SO_3^{-2}) had accumulated in the electrolyte. To establish if either of these possibilities had contributed to the power decay of cell pair S/N 017, the anode was cleaned electrochemically (closed circuit nitrogen purge followed by an oxygen purge) and maintained in the oxidized state while the electrolyte was replaced by clean electrolyte. This was accomplished by flushing distilled water through the cell via the hydrogen passageways, through the anode, matrix, cathode and then out of the air passageways. This flushing was continued until the water pH and conductivity indicated all the electrolyte had been removed. The cell then was purged with nitrogen to remove most of the water and then filled with clean electrolyte by the above flushing technique.

Cell pair S/N 017 was operating at 1.3 watts (15 amps) before anode cleaning and electrolyte replacement. The initial power after electrolyte replacement was above 4 watts and had decayed to 2.3 watts after six days. Also, the voltage decay rate ($630 \mu\text{v/hr}$) at 15 asf decreased with time. This behavior would not be expected for power degradation caused by trace impurity pickup. Unfortunately, due to scheduling, the test could not be continued long enough to establish if there would be a leveling off of the power above the previous 1.3 watt value to give a net gain which might be attributed to the elimination of an anode poison. In any case the difference would have been less than 0.5 watts, which is small compared to the total power loss experienced with this cell pair.

Upon disassembly of cell pair S/N 017 everything seemed normal except for a slight embrittlement of the anode current collector screen. This embrittlement of the anode screen was observed also in the first analytical cell test. In both cases it was found that these particular screens had been coated with platinum by sputtering rather than the standard electroplating process. Apparently, something associated with the sputtering process or the characteristics of the resulting coating makes the tantalum screens susceptible to hydrogen embrittlement. It is believed that this screen embrittlement did not contribute significantly to cell pair S/N 017 decay because cell pair S/N 018, which had an electroplated screen not affected by embrittlement, showed the same power decay characteristics ($\sim 200 \mu\text{ volts/hr}$ at 18 asf).

Cell Pair S/N 019 Testing

Late in the SSP HDC program it was realized that one of the causes for HDC cell power decay might be associated with a change in the anode structure due to electrophoretic platinum migration. Therefore, a modified catalyst with reduced electrokinetic effects was used for the cell pair S/N 019 anode (P&WA PPF electrode). These anodes were run for a total of 3700 hours with Cs_2CO_3 electrolyte and showed a voltage decay at 18 asf of only 20 microvolts per hour (figure 9). The average CO_2 transfer efficiency, at 18 asf and 3 mm Hg PCO_2 was a low 52 percent because of the modified cathode structure used in this cell. After development of the improved DS 16-0 cathode, cell pair S/N 019 was rebuilt with the same PPF anodes and the CO_2 transfer efficiency increased to 86 percent. These results are discussed in more detail on page 52.

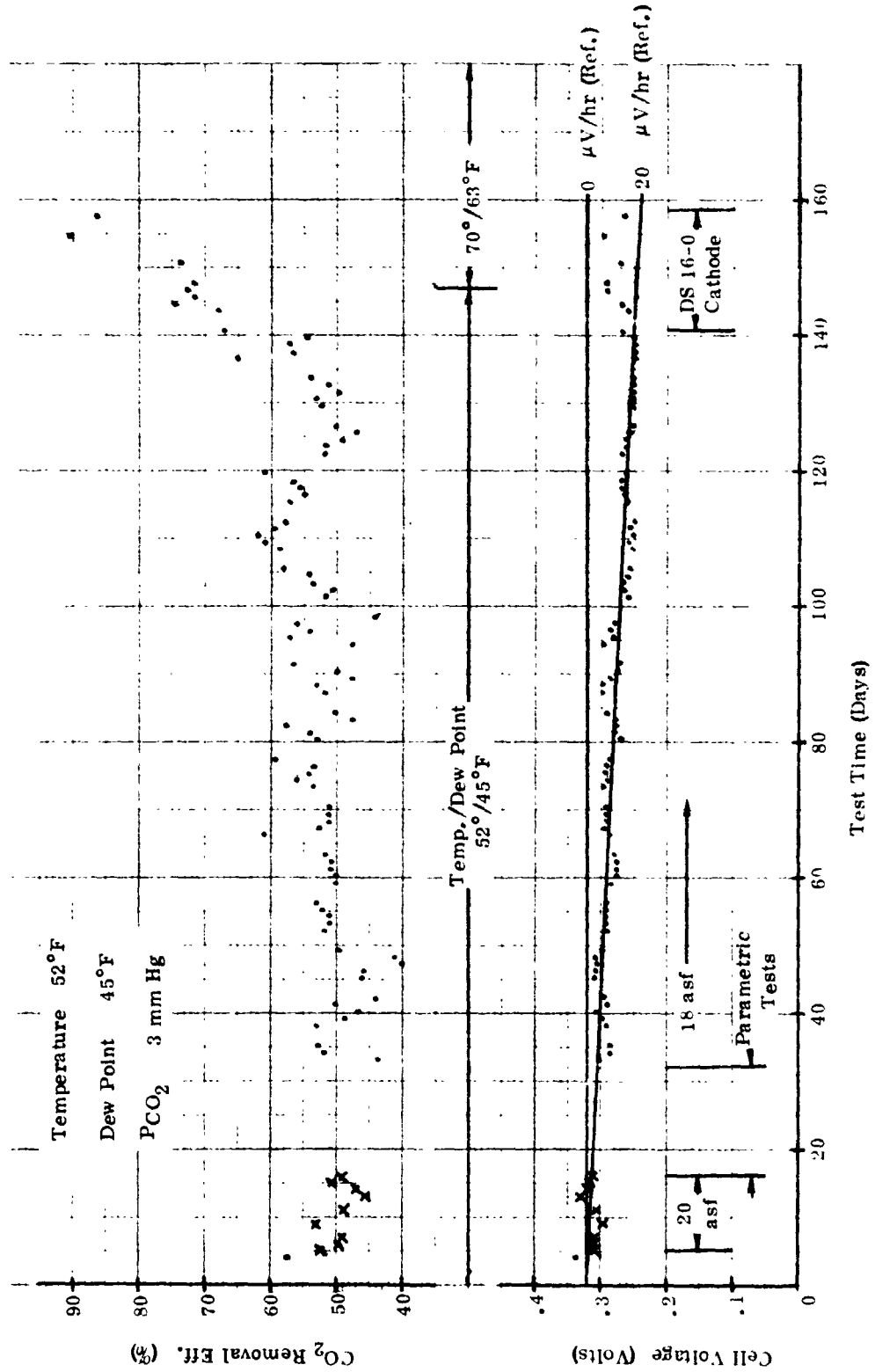


FIGURE 9. HDC CELL PAIR S/N 019 (C₅₂CO₂) PERFORMANCE VS TIME

Since the voltage decay rate of cell pair S/N 019 ($20 \mu\text{v/hr}$) was such a large improvement over that of previous cells ($\sim 200 \mu\text{v/hr}$) it was deemed worthwhile to examine the anodes of cell pairs S/N 018 and S/N 019 to see if any structural differences could be detected. The anode of cell pair S/N 018 rather than S/N 017 was chosen as more representative of previous cells because of the screen embrittlement problem encountered with the cell pair S/N 017 anode.

Anode Examination

Micrographic examination of the anodes from cell pairs S/N 018 and S/N 019 included the use of optical, scanning electron microscope (SEM), X-ray microprobe, and replica electron microscope analyses. The SEM and X-ray microprobe results were the most informative and only these pictures are shown here, in figures 10, 11 and 12. Both unused and used samples of the electrodes were examined in cross section.

The unused electrode (cell pair S/N 018) showed a fairly even platinum distribution (figure 10a) with a tight structure of low void volume (figure 11a). The outer surfaces of the electrode contained a slightly higher Teflon concentration than the interior (figures 10a and 12a).

The used anode (7 months of operation in cell pair S/N 018) had increased in thickness by almost a factor of two as can be seen from a comparison of figures 10b and 11b with figures 10a and 11a. In the expanded or "puffed out" area on the gas side, the platinum-Teflon ratio is essentially the same as the original; however, the catalyst density is about one-half that of the original electrode. This resulted in a large increase in void volume at the gas side and to a lesser extent on the electrolyte side of the anode, as can be most clearly seen from the platinum distribution scan of figure 10b compared to figure 10a. It is also obvious from a comparison of the Teflon distribution scans shown in figure 10 that the Teflon has migrated in the opposite direction; i. e., toward the matrix. This Teflon migration is even more dramatically evident from the characteristic X-ray distribution for platinum and fluorine (Teflon) shown in figure 12.

Since both the platinum and the Teflon are in the colloidal state, it is not surprising that they would tend to migrate in the electrical field (electrophoresis) of the cell. The platinum, having a negative charge, would be forced away from the cell cathode which is opposite to the direction of electrolyte pumping (electroosmosis). The Teflon, with a positive charge, would migrate toward the cell cathode. The migration of the Teflon in the anode toward the matrix would result in a large increase in the hydrophobicity at the electrode - matrix interface. This, combined with the increase in void volume, would greatly reduce the electrode capillarity and therefore its ability to pull back electrolyte from the matrix. The result is a reduction in the utilized catalyst area with time and therefore a decrease in anode electrochemical

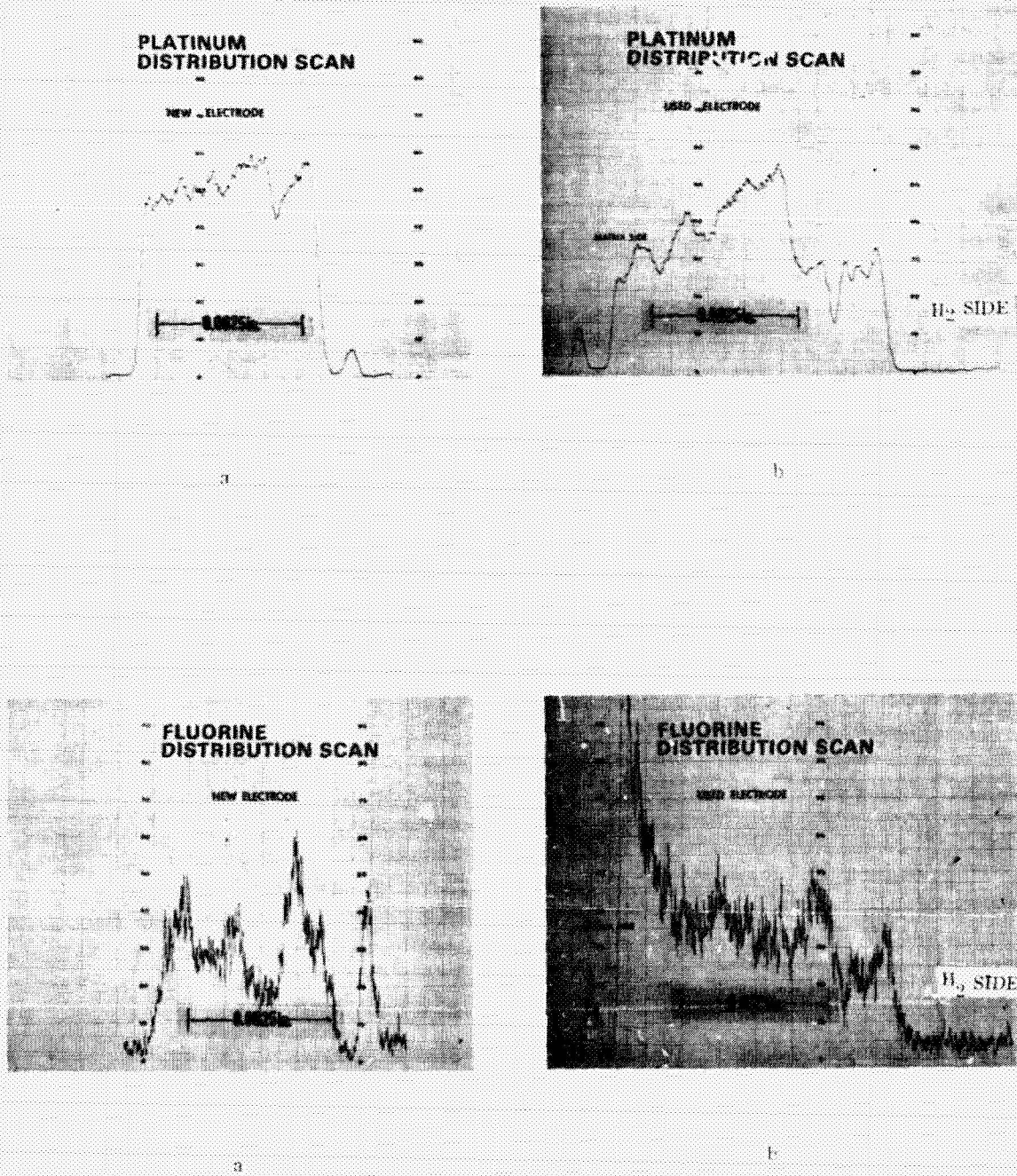


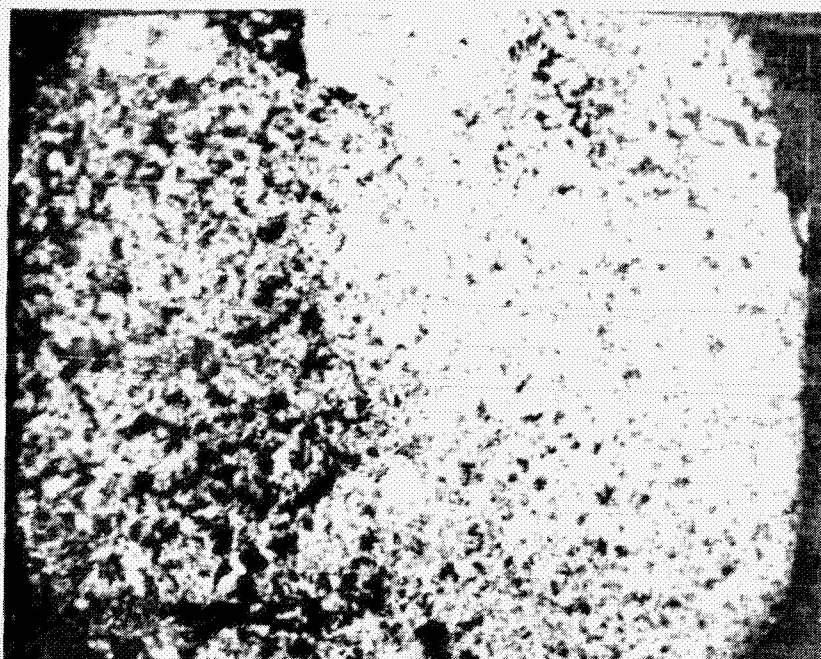
FIGURE 10. X-RAY MICROPROBE LINE SCANS OF CELL P-IR S/N 018 ANODE

HAMILTON
STANDARD

U
A.

SWISER 6285

GAS SIDE



MATRIX SIDE



b

a

FIGURE 11. SEM EXAMINATION OF CELL S/N 018 ANODE ($\times 1000$, $V = 750$ N)

REPRODUCIBILITY OF THE ORIGINAL PAGE IS POOR.

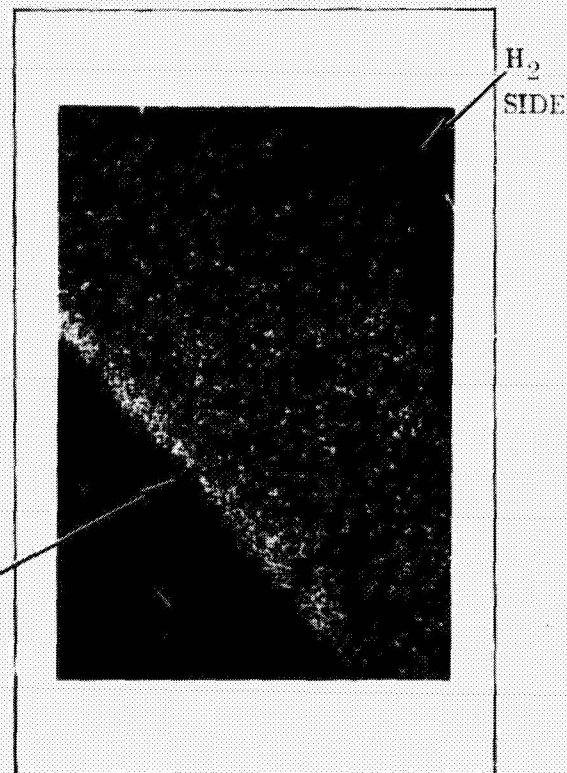
Hamilton
Standard

U
A.

SVHSR 6285



a. UNUSED



b. USED

COLOR CODE: GREEN - PLATINUM
RED - TEFLON
YELLOW - PLATINUM AND TEFLON

FIGURE 12. CHARACTERISTIC X-RAY DISTRIBUTION FOR PLATINUM AND FLUORINE (TEFLON) OF CELL S/N 018 ANODE

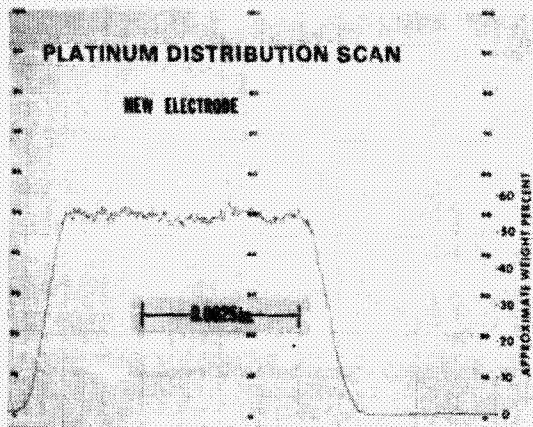
performance. The performance can be increased temporarily by forcing electrolyte into the anode structure, e.g. by pulling vacuum on the hydrogen side. This has been demonstrated many times, but after a short interval of time the electroosmotic pumping restores the amount of electrolyte in the anode to its equilibrium level.

Most of the catalyst in the expanded area (gas side) is probably no longer effective because of the high void volume. This may account for the fact that complete recovery of the cell power to the original level was not obtained after the vacuum treatment or the electrolyte replacement.

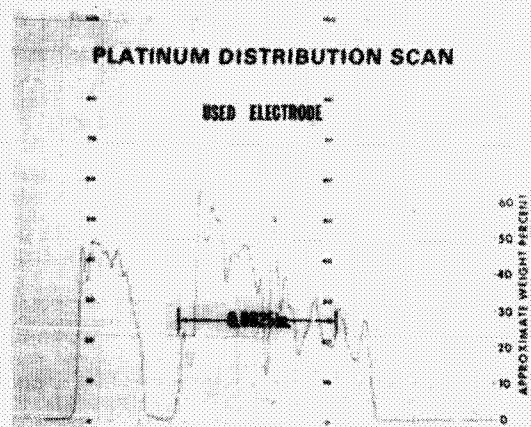
The observation that the cell power decay rate after electrolyte replacement was slower than after a vacuum treatment can be explained by the difference in electrolyte availability in the two cases. After electrolyte replacement, there was initially an excess of electrolyte at a higher than equilibrium concentration so that the cell to anode electrolyte pressure differential was small. In contrast, the vacuum treatment decreased the amount of available electrolyte, thereby increasing the capillary pressure differential between anode and reservoir which would reduce the anode electrolyte take-up rate.

In view of the observed changes in electrode structure the mechanism by which either an open circuit treatment or a nitrogen purge causes temporary cell power increase can be explained. Reducing the cell current to zero via open circuit or a closed circuit nitrogen purge would stop electroosmotic pumping of electrolyte out of the anode structure and allow electrolyte replenishment into the anode structure via capillarity. The fact that a nitrogen purge is more effective than an open circuit treatment in increasing cell power may be related to the difference in anode potential in the two cases. At open circuit the anode potential goes to zero with respect to a hydrogen reference electrode in the same solution but during a closed circuit nitrogen purge the anode potential increases to ~1.1 volts with respect to the same reference. Since the electrocapillary maximum for platinum in aqueous solution is nearer to zero volts, a nitrogen purge would affect a greater reduction in the platinum-solution interfacial tension, thus making the spreading coefficient more positive which results in an increased anode wicking rate for electrolyte take-up.

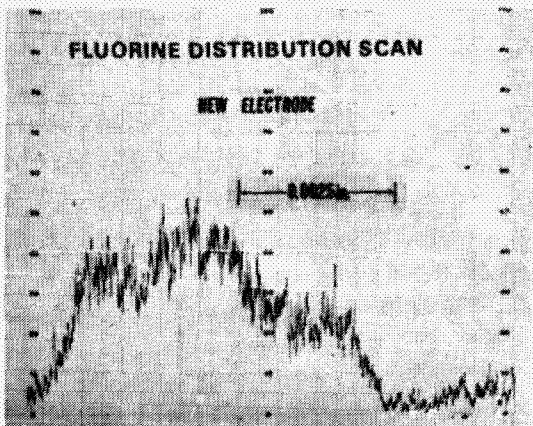
The PPF anode from cell pair S/N 019 showed no evidence of any structural changes by optical or SEM examination. The X-ray microprobe line scan (figure 13) showed no evidence of Teflon migration and, at most, only a slight migration of platinum toward the hydrogen side. The gap near the matrix side in the scan of figure 13 b is due to a crack in the electrode which developed during the sample mounting process.



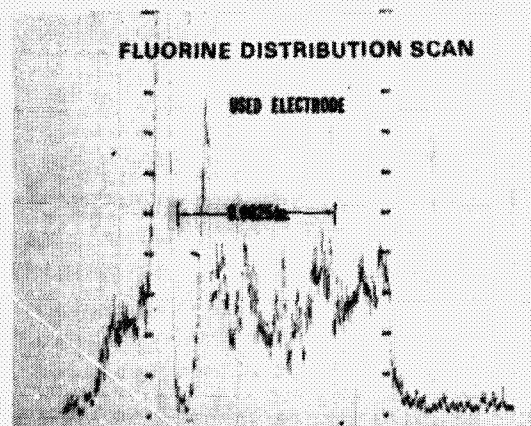
a



b



a



b

FIGURE 13. X-RAY MICROPROBE LINE SCAN OF CELL PAIR S/N 019 ANODE

Anode Evaluation

Four other electrodes (A-3R, A-10R, SEC and PVC) were screened for initial power performance as HDC anodes via floating electrode tests⁽³⁾ (test set up. Reference figure 14). The A-3R and A-10R electrodes are intended to be more CO and possibly "reduced CO₂" tolerant, whereas the SEC and PVC electrodes represent a considerable reduction in catalyst loading and cost without a sacrifice in power performance at high temperatures. Table I gives the anode performance of these electrodes in addition to the SSP, PPF, and American Cyanamide AA-2 electrodes. The SEC electrode (4 mg cm⁻²) gave the best power performance, but it was found that the catalyst was unstable in the CsHCO₃ electrolyte. The PPF electrode at a catalyst loading of 15 mg cm⁻² had essentially the same power performance as the SEC and, from cell pair S/N 019R experience, the PPF performance degradation with time is very small.

If the data in Table I is normalized per mg cm⁻² of catalyst, the PVC electrode containing only 1 mg cm⁻² of active supported catalyst looks promising. Unfortunately, the catalyst-to-support ratio is at its maximum level and increasing the loading by a factor of three, to match PPF performance, would result in an electrode of unreasonable thickness.

From these results and from cell pair S/N 019 power performance, the PPF electrode was chosen for use as the anode in future cell tests.

Matrix Thickness and Cell Performance

The matrix thickness test was run under the following conditions: P_{CO₂} = 3 mm Hg, air velocity = 15 ft/sec, current density = 18 asf, air inlet temperature/dew point = 70°/63°F, ambient pressure = 14.7 psia.

One, two, and four layers of asbestos were used at the optimum compression thickness of 12.5, 25, and 50 mils, respectively. The electrolyte was Cs₂CO₃ (Reference Appendix, Master Test Plan, Section IX).

The results given in Table II show the expected trend in CO₂ processing efficiency; however, the high IR drop for one asbestos layer (compressed to 12.5 mils) is difficult to explain.* Also, in view of the anode and cathode pH values, the high cell voltage obtained with one asbestos layer seems peculiar.

* It is possible that a calculation error was made in the IR drop measurement such that the actual value should be 1/2 of that recorded, i.e. 25 mV. Unfortunately, the abnormally high value was not noticed until after the experimental series had been completed and time did not permit a rerun.

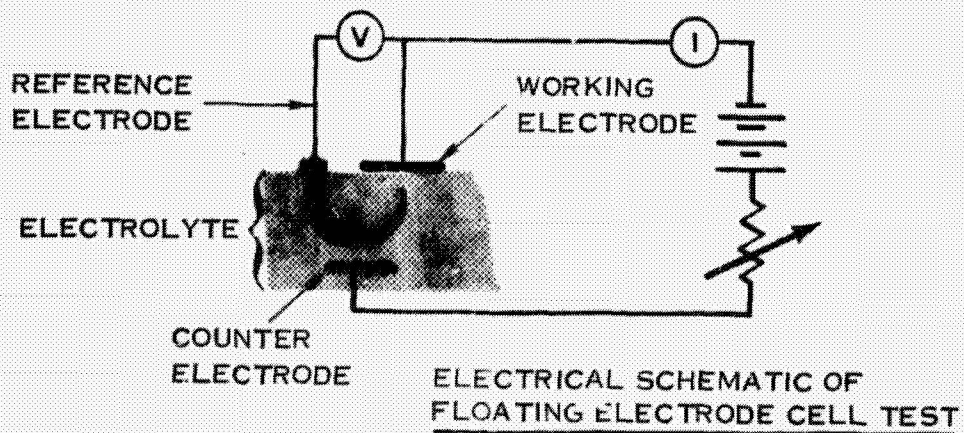
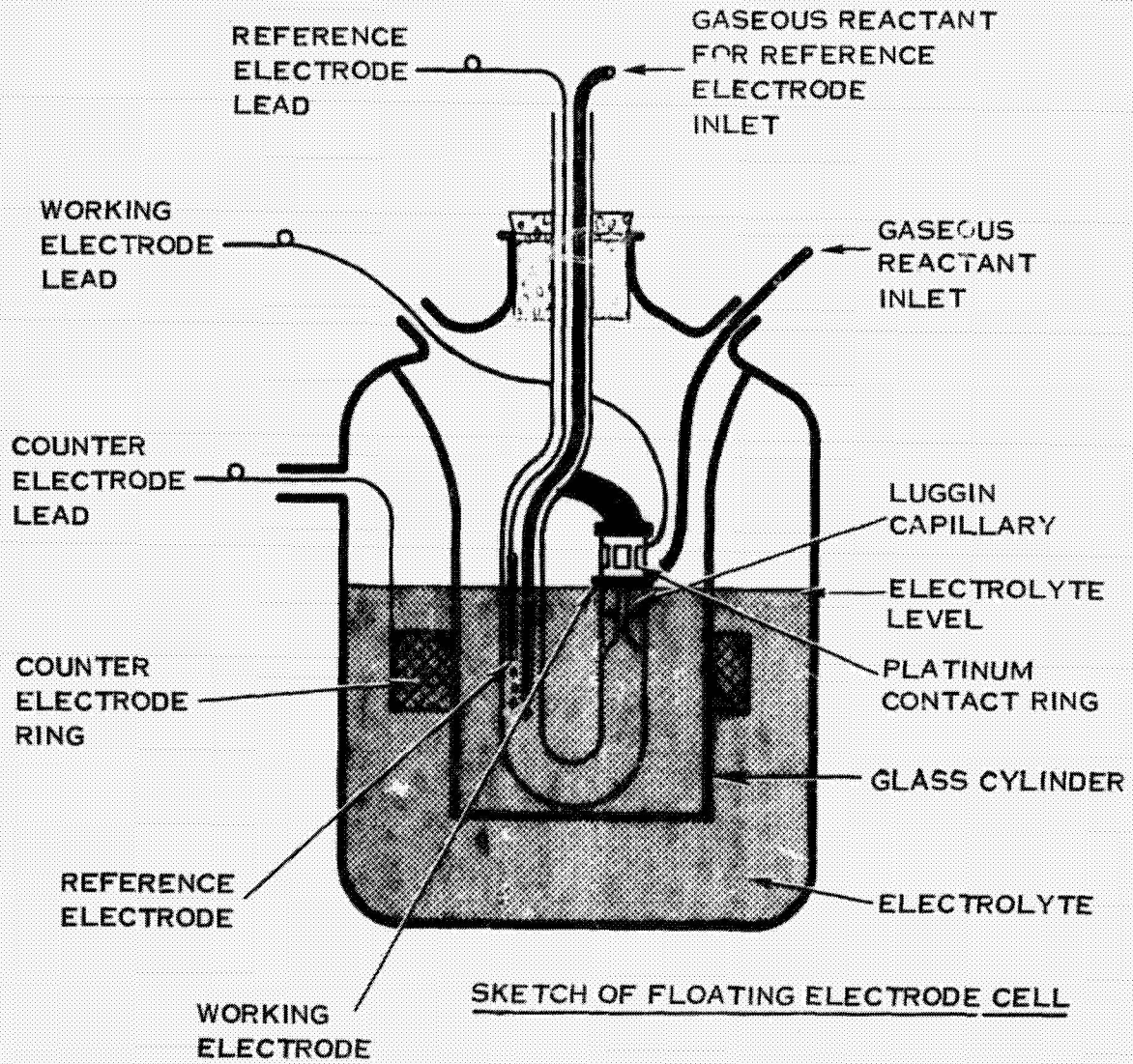


FIGURE 14. FLOATING ELECTRODE CELL TEST SETUP

TABLE I
FLOATING ELECTRODE EVALUATION OF ANODE
PERFORMANCE IN CESIUM BICARBONATE

Electrode	PPF	SEC	A-3R	A-10R	PVC	AA-2	SSP
Catalyst Loading (mg cm ⁻²)	15	4	20	13	1	10	10
Current Density (asf)	Overvoltage (mV)						
10	40	40	65	75	123	75	70
15	82	82	113	113	164	106	104
20	100	98	160	152	196	134	130
30	145	137	225	205	252	180	166
50	210	190	330	275	--	240	210

TABLE II
MATRIX THICKNESS TEST RESULTS

Thickness	CO ₂ Efficiency	Voltage	IR Drop	Cathode	Anode
mils	Percent	Volts	mV	pH	pH
12.5	66.4	0.452	50	12.0	8.5
25	98	0.385	38	12.3	8.2
50	106	0.364	70	12.5	8.0

With the four layers of asbestos compressed to 50 mils it took about 30 hours to reach steady state conditions. The initial cell voltage was low and the pH high. Operation at 30 asf with the four layers resulted in a gradual increase in IR drop with time which increased the cell temperature. This test was discontinued when the ΔT between air inlet and outlet, normally 3.5°F, approached 8°F. At this time the IR drop was approaching 2 volts. The obvious cause of this behavior was that the electrolyte concentration at the anode was approaching zero under these conditions. Apparently, even under normal operating conditions with a matrix thickness of 25 mils the cesium ion concentration at the anode is significantly lower than had been anticipated. This information helps to explain two factors which were previously difficult to rationalize: the abnormally high anode polarization and the large anode electrokinetic effects.

The anode polarization measured in the analytical cell is typically one to two hundred millivolts greater than that measured in the floating electrode test even though the pH is the same (8.0) in each case. This discrepancy can be explained if the electrolyte concentration at the anode of a full cell is considerably lower than that in the floating electrode cell. This would result in additional intra-anode IR drop and concentration polarization for a full cell anode.

To determine the effect of electrolyte dilution on anode performance an electrode was tested in 9 weight percent cesium bicarbonate (58 weight percent diluted 10:1 by volume) and compared to the performance in 58 weight percent,* both solutions having a pH of 8. The dilute bicarbonate electrolyte gave 130 mv more anode polarization at 20 asf (corrected for IR drop) than the concentrated electrolyte. Thus, the unusually high cell voltage observed with one layer of matrix (12.5 mils) can be explained by a decrease in anode overvoltage due to the higher anolyte concentration obtained with

* Evaluation of anode performance via the floating electrode test was done in 58 weight percent CsHCO₃ with a pH of 8.0.

the smaller inter-electrode distance. If a higher anolyte concentration could be maintained with a 25 or 30 mil electrode spacing, the cell voltage could be significantly improved without sacrificing the CO₂ transfer efficiency.

Two factors contribute to the overall anode polarization: intra anode IR drop, and intra anode concentration polarization.* The addition of an inert electrolyte such as cesium sulfate would decrease the intra anode IR drop but increase the concentration polarization so that the net effect on overall anode polarization is difficult to predict.

To determine the net effect of inert electrolyte addition, anode polarization was measured on a floating electrode in two electrolyte solutions: 0.5 mole CsHCO₃ and 0.5 mole CsHCO₃ + 1 mole Cs₂SO₄. With the inert electrolyte, the solution resistance was reduced by a factor of two and presumably there was a corresponding decrease in intra anode IR drop. However, the total anode polarization at 20 asf was about 30 mv greater. From this result it seems that concentration polarization is the major factor limiting anode performance and the addition of an inert electrolyte would be expected to give a slightly lower cell power output.

The fact that electrokinetic phenomena seem to be more pronounced at the anode than at the cathode was difficult to understand, since it is well known that these effects on platinum are greatly enhanced by high solution pH, yet there has been no indication of cathode electrochemical degradation with time, as observed with the anode where the pH is low. In view of the evidence for a low electrolyte concentration at the anode it is now clear that the large anode electrokinetic effects must be related to the much greater zeta potential associated with the more dilute anolyte. Increasing the anolyte concentration by the addition of an inert electrolyte should suppress the zeta potential and thereby promote anode life by reducing the platinum and Teflon migration rates; however, some sacrifice in power would result due to the increase in intra anode concentration polarization.

* Activation overvoltage would not normally be affected by electrolyte concentration changes when the major ions do not take part in the electrode reaction. Also, the activation overvoltage for hydrogen oxidation at normal HDC current densities should be negligible.

HDC ANALYTICAL TESTING

The purpose of the HDC analytical tests, described in Sections V and VII of the Master Test Plan, (reference Appendix) was to obtain more detailed information on the HDC cell to gain a better understanding of its operation. Such data are useful in the development of an HDC cell math model and in defining areas where improvements could be made to give better performance.

The analytical test cell illustrated by figure 15 was constructed from full cell pair hardware to give an electrode area of only $1/24 \text{ ft}^2$ while keeping the full scale airflow path length of six inches. Reference electrodes were incorporated on both the anode and the cathode sides, and access ports were added to allow pH measurements at the anode or cathode during cell operation. The matrix consisted of one layer of Tissuquartz (18 mils) between two layers of fuel cell asbestos (20 mils each) compressed to 25 mils. All testing was done on the analytical test rig (figure 16) at an air temperature of 70°F . The current density, air velocity, CO_2 partial pressure and air dew point were controlled at a given level. The more unusual parameters which were determined are listed below.

- Open circuit voltage
- IR drop
- Cathode overvoltage = cathode potential - cathode reference potential
- Anode overvoltage = anode potential - anode reference potential
- Anolyte and catholyte pH
- Concentration overvoltage and pH

The concentration overvoltage is equal to (open circuit voltage) - [(Cathode ref. - anode ref.) - (IR drop)]. The ΔpH is equal to concentration overvoltage divided by 0.06 volts.

The ΔpH value determined in this manner can be compared to the difference between the measured catholyte and anolyte pH values, and in most cases the correlation is good. (See Tables III and IV for Cs_2CO_3 electrolyte).

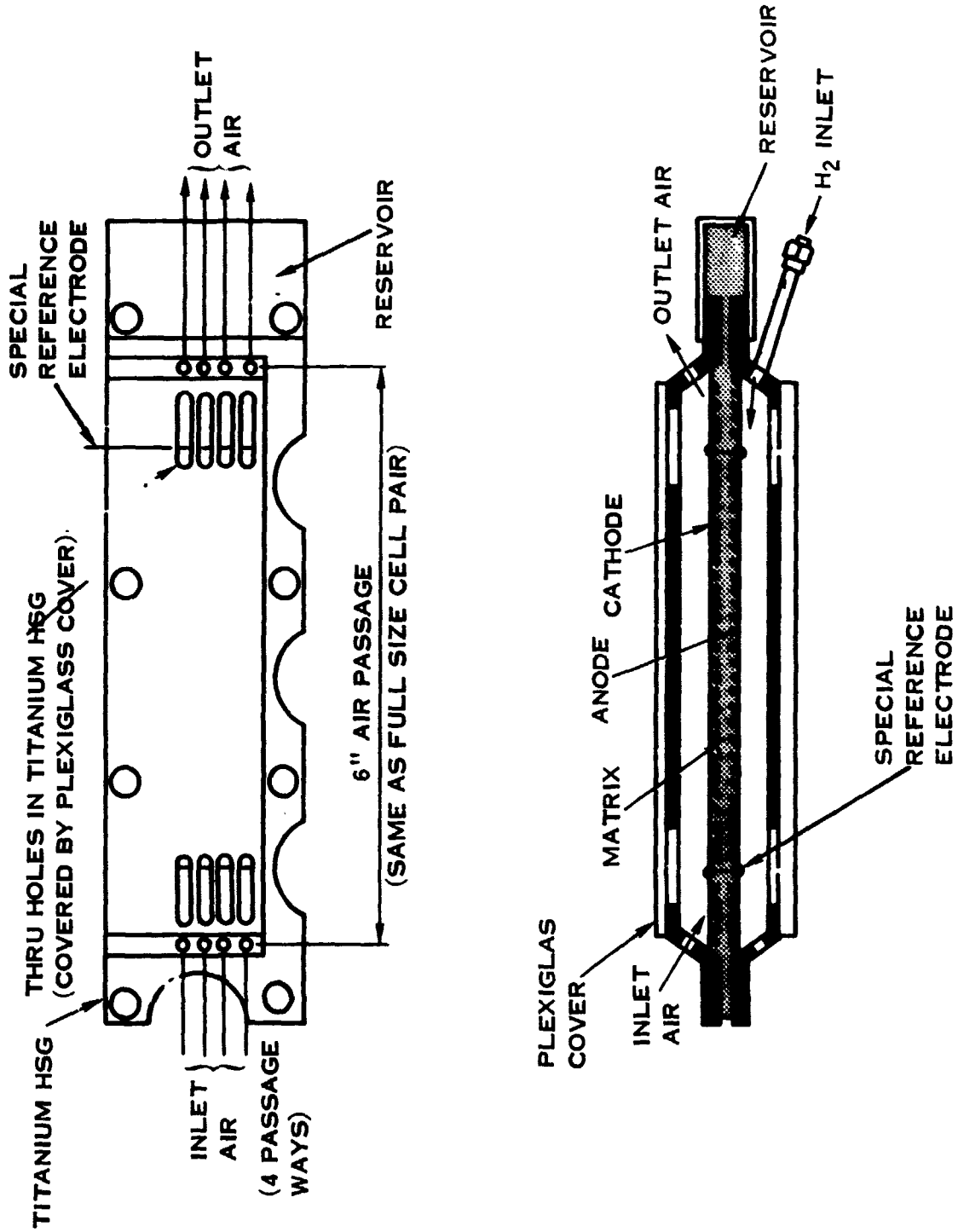


FIGURE 15. ANALYTICAL CELL

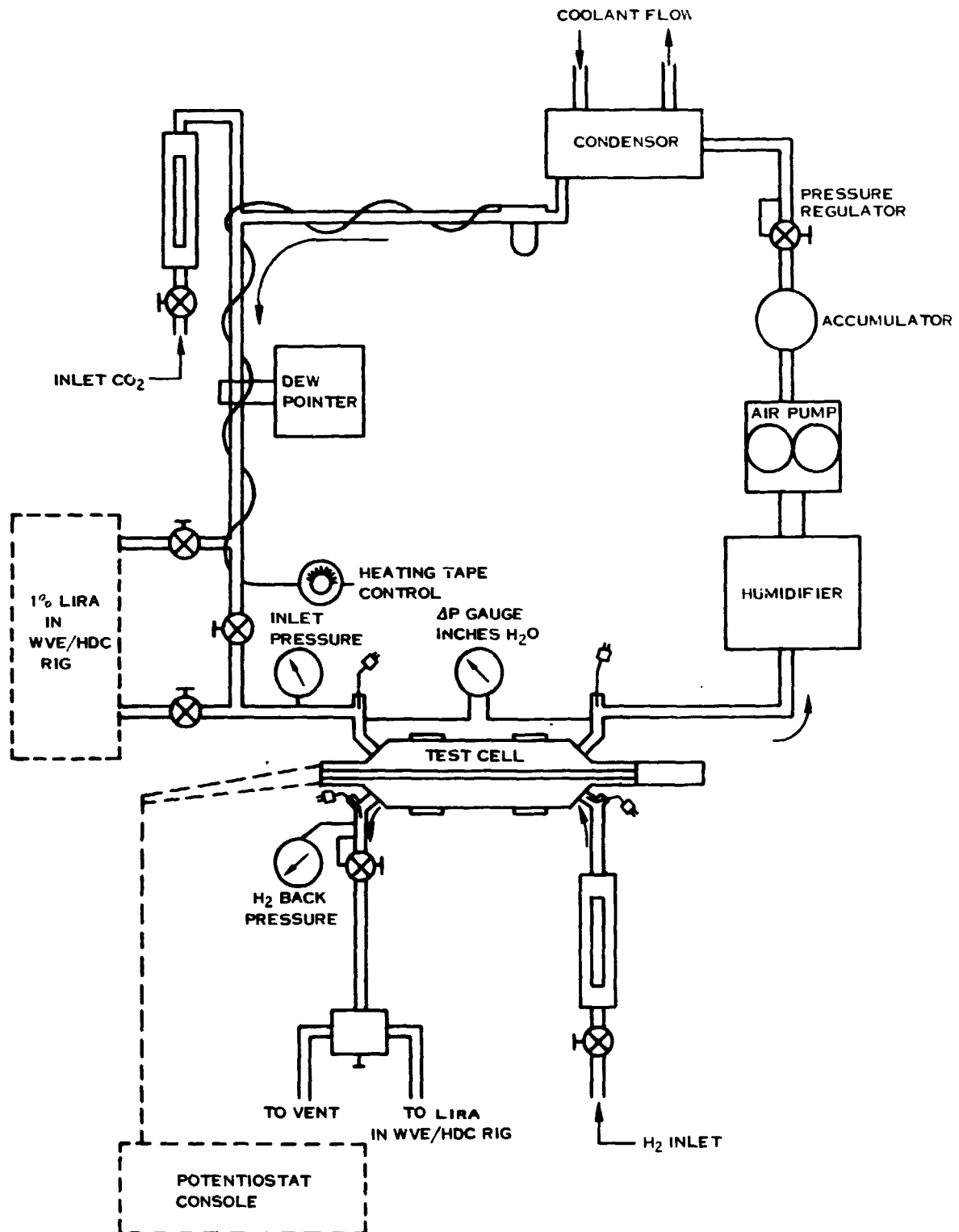


FIGURE 16. HDC ANALYTICAL TEST UNIT RIG

Cesium Carbonate Electrolyte

The analytical cell testing with Cs_2CO_3 electrolyte used the standard SSP electrodes as requested by the NASA-JSC and the air dew point was controlled at 63°F. The open circuit voltage was 1.122 volts and the electrolyte-matrix resistance, as calculated from the IR drop, was constant at 2.0 ± 0.1 milli ohms ft^2 .

The anode overvoltage and cell voltage are not reported because, after a few weeks of operation, the anode performance decayed rapidly with time making these readings meaningless for the purpose at hand. The reported pH values were measured near the cell air exit. At low air flow velocities and low PCO_2 the pH values near the air inlet were somewhat lower due to significantly different gas phase mass transport rates at the extremes of the cell.

Table III shows the effect of CO_2 partial pressure and air velocity in the region where gas phase mass transport rates are important in determining the CO_2 processing efficiency. In this case increasing either the CO_2 partial pressure or the air velocity results in an increase in CO_2 processing efficiency, increased cathode polarization and a decrease in electrolyte pH. The increase in cathode polarization is a result of the decrease in catholyte pH. The results given in table IV also show this pH effect on cathode polarization and it is obvious that the pH effect predominates over the current density in determining the magnitude of the cathode overvoltage in this operating range.

TABLE III

**EFFECT OF AIR VELOCITY AND CO₂ PRESSURE AT 18 ASF
WITH Cs₂CO₃ ELECTROLYTE**

Air Vel. (ft/sec)	P _{CO₂} (mm Hg)	Efficiency %	Cathode pH	Anode pH	ΔpH	Cathode Overvoltage (mV)
5	0.25	12	14	11	3.1	-144
10	0.25	17	14	11.5	3.2	-153
20	0.25	18	13.8	11	3.0	-166
5	0.5	19	14	11	3.0	-160
10	0.5	22	13.5	10	3.0	-170
20	0.5	29	13.5	10	3.3	-185
5	1.0	33	13.5	11	2.5	-163
10	1.0	44	13.5	10	3.1	-172
20	1.0	51	13.5	9	4.5	-200

NOTE: Air Temperature 70°F, Dew Point 63°F.

**TABLE IV
EFFECT OF CURRENT DENSITY AND CO₂ PRESSURE
AT AN AIR VELOCITY OF 7 FT/SEC**

P _{CO₂} (mm Hg)	Current Density (asf)	Efficiency %	Cathode pH	Anode pH	ΔpH	Cathode Overvoltage (mV)
0.25	24	12	14	11.5	3.2	-152
0.25	12	20	13.3	11.3	2.1	-174
1.0	24	30	13.5	9.5	4.1	-169
1.0	12	42	13	9.5	3.3	-217
4.0	24	65	13	8.0	5.1	-195
4.0	12	75	12.3	7.5	4.8	-246
3.0	6	71	12.3	8.5	3.9	-245

NOTE: Air Temperature 70°F, Dew Point 63°F.

TMAC Electrolyte

The purpose of the TMAC electrolyte tests was to obtain more detailed information on cell operation with TMAC and to compare these results to those obtained with cesium carbonate electrolyte. Cell construction was identical to the Cs_2CO_3 analytical cell testing except for the electrodes which were PPF anode and DS 16-0 cathode.

Table V shows the effect of current density on cell performance. The decrease in cell voltage with increasing current density is due to an increase in the anode overvoltage (related to ΔpH) and IR drop. The cathode overvoltage decreases with increasing current density because of the increase in catholyte pH. Additional data on CO_2 transfer versus current density is given in figures 17 and 18. Although the CO_2 transfer efficiency decreases with increasing current density over the range studied (figure 17), the absolute amount of CO_2 processed increases as shown in figure 18.

TABLE V
EFFECT OF CURRENT DENSITY
($\text{P}_{\text{CO}_2} = 1 \text{ mm Hg}$, $\text{RH} = 49.3\%$, Air Velocity = 10 ft/sec)

Current Density (asf)	Cell Voltage (Volts)	Cathode pH	Anode pH	Overvoltage mV		Efficiency %	IR drop (mV)
				Cathode	Anode		
12	0.380	12.6	9.2	-226	249	80	60
18	0.348	12.6	9.2	-91	358	55.6	100
30	0.284	13.0	9.2	-49	430	36	110

Table VI shows the effect of air CO_2 partial pressure and relative humidity on cell performance. Increasing CO_2 partial pressures reduces cell voltage because of increased cathode overvoltage and IR drop which over-compensate the reduction in anode overvoltage. The decrease in anode overvoltage with increasing P_{CO_2} is not understood, since there seems to be no change in anolyte pH and the electrolyte resistance increase would indicate a decrease in anolyte concentration which has been shown to result in greater, not less, anode polarization. Admittedly the pH measurements are somewhat crude for this purpose and are that of the bulk anolyte rather than that at the catalyst surface which would determine the degree of anode polarization.

Increasing the air relative humidity increases the cell voltage because the reduction in cathode overvoltage and IR drop is greater than the increase in anode overvoltage and concentration polarization. With the more dilute electrolyte solution one would expect an increase in anode overvoltage, and a decrease in electrolyte resistance and anolyte pH as obtained. The lower cathode overvoltage observed with the more

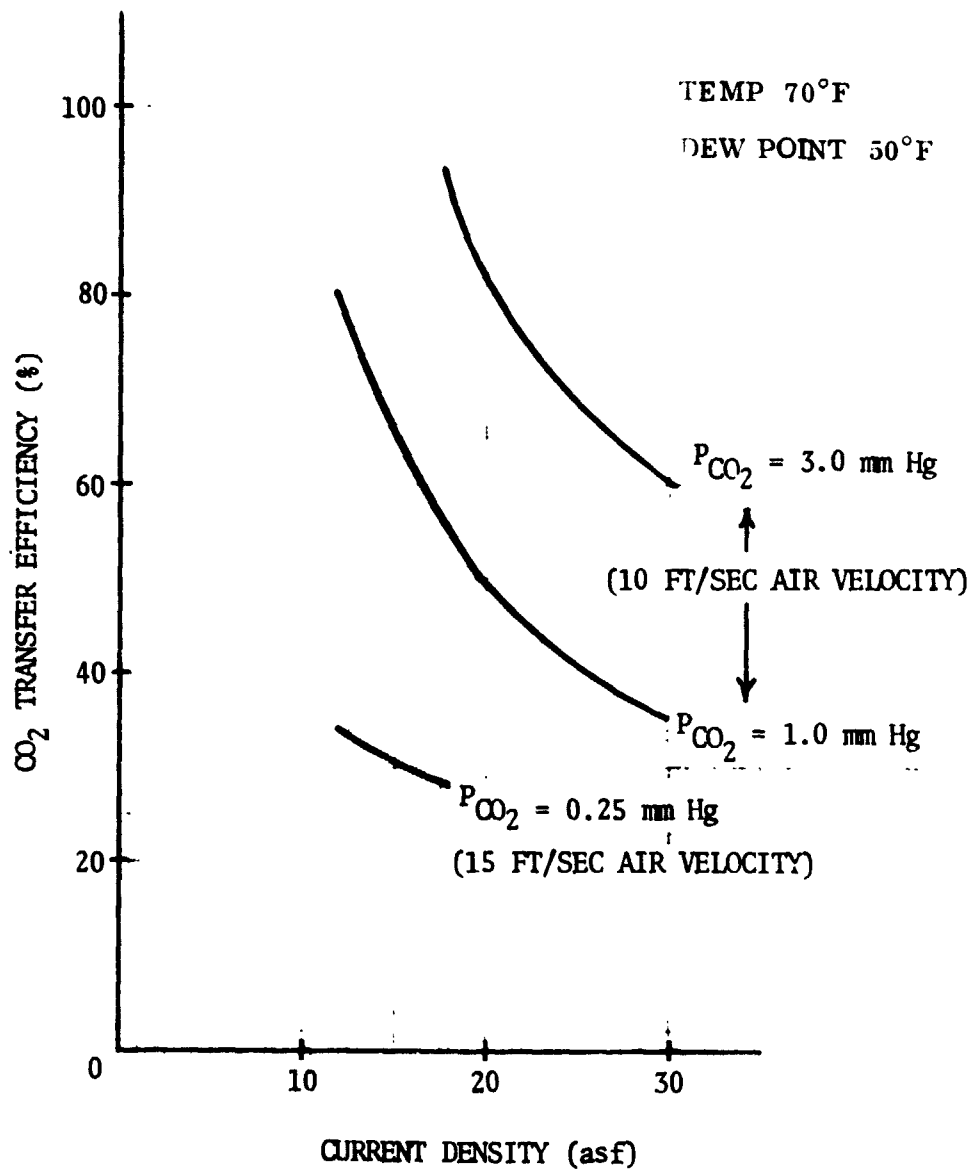


FIGURE 17. EFFECT OF CURRENT DENSITY AND P_{CO_2} ON CO₂ TRANSFER EFFICIENCY USING TMAC ELECTROLYTE

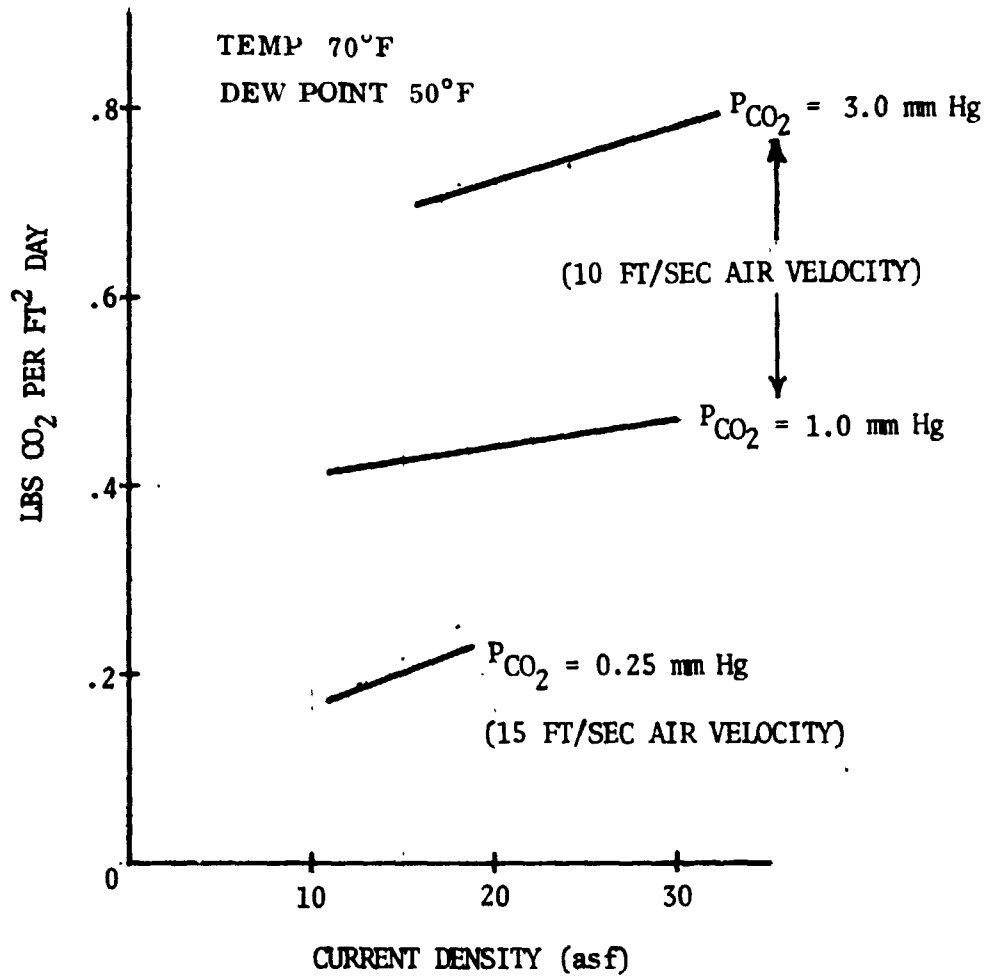


FIGURE 18. EFFECT OF CURRENT DENSITY AND P_{CO_2} ON THE ABSOLUTE AMOUNT OF CO₂ TRANSFERRED WITH TMAC ELECTROLYTE

TABLE VI

EFFECT OF P_{CO_2} AND RELATIVE HUMIDITY
AT 18 ASF AND AT AN AIR VELOCITY OF 10 FT/SEC
WITH TMAC ELECTROLYTE (Air Temp = 70°F)

P_{CO_2} (mm Hg)	% R H (D. P.)	Cell Voltage (volts)	Cathode pH	Anode pH	Overvoltage (mV)		Efficiency (%)	IR drop (mV)
					Cathode	Anode		
0.25	33.6 (40°F)	0.354	13.5	10.5	- 46	415	19.0	100
1.0	33.6 (40°F)	0.246	13.3	10	-166	381	55.7	110
4.0	33.6 (40°F)	0.192	13.0	11	-294	368	92.4	120
0.25	71.2 (60°F)	0.387	13.5	9.2	-	-	19.6	65
1.0	71.2 (60°F)	0.274	13.3	9.2	-104	398	55.8	80
4.0	71.2 (60°F)	2.42	13.0	9.0	-150	383	97.8	90

TABLE VII

EFFECT OF AIR VELOCITY WITH TMAC ELECTROLYTE

(P_{CO_2} = 0.25 mm Hg, asf = 18, Relative Humidity = 49.3%, Temp 70°F)

Air Velocity (ft/sec)	Cell Voltage (volts)	Cathode pH	Anode pH	Overvoltage (mV)		Efficiency (%)	IR Drop (mV)
				Cathode	Anode		
5	0.423	13.5	10.5	- 36	375	18.0	80
10	0.370	13.5	10	-	-	19.3	100
15	0.364	13.0	10.5	- 98	395	28.8	90

dilute electrolyte (high air R. H.) is probably associated with a decrease in catholyte viscosity, since there is no change in catholyte pH. Air relative humidity (or electrolyte concentration) has little effect on CO₂ transfer efficiency.

Table VII shows the effect of air velocity, at ambient CO₂ levels, on cell performance. The decrease in cell voltage with increasing air velocity is caused by the lower cell temperature and the change in catholyte pH which is affected by the rate of CO₂ mass transport. At air velocities of 5 and 10 ft/sec, convective mass transport of CO₂ is definitely limiting as evidenced by the low CO₂ transfer efficiency.

Conclusions

The general conclusions from the results of the analytical cell testing are:

1. The cathodic overvoltage with both electrolytes is strongly affected by the catholyte pH.
2. For maximum CO₂ transfer efficiency the optimum catholyte pH for both electrolytes is in the range of 12.3 to 13.0. Within limits the optimum catholyte pH can be obtained by proper choice of air flow rate and current density.
3. The TMAC electrolyte results in a higher electrolyte resistance and anode polarization than Cs₂CO₃, and this accounts for the lower cell power output obtained with TMAC.
4. The anode overvoltage is a major contributor to low HDC cell power output and is the only source of cell power loss which offers hope for significant improvement in the future.

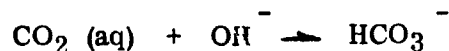
IMPROVED CO₂ TRANSFER

Past experience has indicated that the overall CO₂ transfer process is controlled mainly by the reactions and mass transport processes at the cathode. The CO₂ must first be transported from the air stream to the gas-electrolyte interface within the cathode structure. Relatively high air velocities, approaching turbulent, are used to minimize the gas phase mass transport resistance. The next step is the absorption of the gaseous CO₂ into the catholyte as aqueous CO₂ followed by its reaction with hydroxide ions to form the bicarbonate ion. The subsequent, purely ionic, reaction to form the carbonate ion from hydroxide and bicarbonate ions is very rapid compared to the CO₂ (aq), OH⁻ reaction. One can see from this sequence that the cathode structure should play an important role in determining the rate of these intra-cathode processes. The rate of gaseous CO₂ mass transport within the cathode structure would be determined by the hydrophobic gas pore geometry of the cathode. The absorption rate of gaseous CO₂ would be a function of the total available gas-catholyte interfacial area, and the CO₂, OH⁻ reaction would be dependent on mass transport rates within the hydrophilic catalyst-matrix of the cathode.

To improve the overall CO₂ processing rate a catalyst for the CO₂ (aq), OH⁻ reaction was investigated and modifications of the cathode structure were made to increase the intra-cathode mass transport rates. The effect of electrolyte-matrix thickness (electrode spacing) on the overall CO₂ transfer rate also was determined.

Electrolyte Catalyst

Under certain conditions of cell operation it is possible for the reaction



to be rate determining in the overall CO₂ transfer process, and under these conditions a catalyst for the above reaction would be beneficial. The most active known catalyst for this reaction is the enzyme carbonic anhydrase and it has been demonstrated qualitatively at Hamilton Standard that carbonic anhydrase at very low levels is effective in speeding up the absorption of CO₂ in both cesium carbonate and TMAC to form the respective bicarbonates. Also, potential sweeps showed no evidence of electrode poisoning or carbonic anhydrase instability over the potential range of 0 to 1200 m volts. However, long term stability and effectiveness in the HDC environment had not been evaluated.

Carbonic anhydrase was tested in the analytical test cell with Cs₂CO₃ electrolyte under the following conditions:

P_{CO_2} = 2.5 mm Hg
Air velocity = 7 ft/sec
Current density = 12, 18 and 24 asf
Ambient pressure = 14.7 psia

During a five day test with an SSP type cathode, there was no evidence of electrode poisoning from the carbonic anhydrase, however, there was no detectable improvement in the CO_2 transfer rate either. A repeat of this test using an American Cyanamide AA2 cathode, which gives a higher CO_2 transfer rate also gave a negative result. From this it can be concluded that either the CO_2 , OH^- reaction is not rate controlling under normal operating conditions or that the carbonic anhydrase is not effective in the HDC environment. However, the fact that the CO_2 transfer rate varies with different cathode structures would indicate that intra-electrode mass transport, not the CO_2 , OH^- reaction rate, is the controlling factor.

Cathode Improvement and Evaluation

Since CO₂ is absorbed by the catholyte, an increase in catholyte volume and circulation rate would be expected to increase the CO₂ processing rate. Circulation of the catholyte within the cathode structure is determined by the local electroosmotic and capillarity pressure differentials. In the cathode, electrolyte tends to be pumped toward the air side in regions of high current density. In order for the capillary pressure differential to exceed the electroosmotic pressure, thus causing the electrolyte to be returned into the electrode structure, regions of low current density are required. It was reasoned that decreasing the density of the catalyst structure should increase its electronic resistance resulting in a significant drop-off in current density remote from the current collector screen. Thus, there would be a corresponding decrease in the electroosmotic pumping force while the capillary force would be independent of position from the current collector screen. Also microscopic examination and comparison of the SSP cathode with the American Cyanamid AA2 electrode, which gives a much higher CO₂ processing rate, showed that the AA2 electrode had a much less dense catalyst structure. The less dense electrode structure should also increase the intra-cathode CO₂ gas mass transport rate.

Analytical Cell Test of DS 16-0 Cathode

The first approach was to modify the standard fuel cell electrode manufacturing process to achieve a less dense structure; however, the extent of this modification was limited and the CO₂ processing efficiency could only be increased from 50 percent to 60 percent. In discussion of our requirements with the Electrode Development Group at P&WA a different experimental electrode, was recommended. This electrode (DS 16-0), when used in the analytical cell with Cs₂CO₃ electrolyte gave a CO₂ processing efficiency of 98 percent at 18 asf and 3 mm Hg compared to an efficiency of 90 percent for the American Cyanamide AA2. Some parametric data for the DS 16-0 cathode obtained in the analytical cell is given in table VIII. The anode was a 15 mg/cm² PPF. Three additional Type DS 16-0 cathodes made for the analytical cell gave the same performance as the first DS 16-0 cathode. One of these cathodes was made with twice the platinum loading but showed no increase in CO₂ processing rate. Also, in an earlier test doubling the loading of the SSP type cathode did not affect the CO₂ processing rate. From these results it can be concluded that the catholyte volume is of minor importance compared to the catholyte circulation rate, assuming all the catalyst is being utilized.

Floating electrode tests of all the cathodes showed only small differences in electrochemical performance. The overvoltage at 20 asf was -250 ± 25 mV and there was a general trend toward increased overvoltage with decreasing catalyst density as would be expected.

**TABLE VIII ANALYTICAL CELL PARAMETRIC DATA WITH DS 16-0 TYPE CATHODE
WITH CS₂CO₃ ELECTROLYTE**

Current Density (asf)	Efficiency (%)	Cell Voltage (Volts)	PCO ₂ (mm Hg)	Air Velocity (ft/sec)	Air Dew Point(°F)	Cathode pH	Anode pH
12	82	0.416	3	10	64	12.3	8.0
18	98	0.400	3	10	62	12.5	8.2
24	92	0.290	3	10	63	12.7	8.3
30	84	0.231	3	15	65	12.5	8.2
36	75	0.183	3	15	65	12.3	8.2
42	68	0.110	3	15	65	12.5	8.2
54	53	0.050	3	15	63	-	-
18	97	0.374	3	10	62	12.2	8.2
18	63.4	0.364	1	10	65	13	8.2
18	24	0.365	0.25	15	63	> 13.5	8.7

Note: Air inlet temperature was 70°F for all tests.

Full Size Cell Test of DS 16-0 Type Cathode

HDC cell pair S/N 019 operated for 3360 hours using Cs_2CO_3 electrolyte prior to its disassembly to incorporate DS 16-0 cathodes. During this time the degradation in cell power was approximately 20 micro volts per hour. The average CO_2 removal rate for the unit at 18 asf was 70 scc/min or a 52 percent current efficiency. After the reassembly, which incorporated the same PPF anodes, a new matrix and DS 16-0 cathodes, this cell pair (now S/N 019-2) was placed on test at an air inlet condition of 3 mm Hg PCO_2 , 52°F/45°F temperature/dew point and operated at 18 asf. The current efficiency was approximately 74 percent. Since the full size cell pair performance did not agree with the analytical cell performance (74 percent vs 98 percent), cell pair S/N 019-2 was disassembled and a section of the top cathode was removed and tested in the analytical cell. This testing revealed a current efficiency of 92 percent, which indicated a loss of 6 percent in current efficiency when scaling up to a large size electrode. Cell pair S/N 019-2 was reassembled with new matrix, the same electrodes and with new "O"-Seals on the hydrogen manifold block because it was suspected that the original seals may have leaked. Test results revealed a current efficiency of 86 percent after three days of testing* (figure 9).

The difference in CO_2 transfer efficiency between the full size cell pair and the analytical cell was investigated. It was established that differences in hydrogen back pressure, temperature, hydrogen velocity (Table IX), and housing resistance have little effect on the CO_2 transfer efficiency. Also the possibility of a hydrogen maldistribution in the full size cell pair was eliminated by reducing the hydrogen pressure drop and sealing the crossover points as shown in figure 19. The only apparent difference between the two cells is the partial pressure of CO_2 in the hydrogen gas coming out of the cells. The analytical cell has typically less than 1 percent CO_2 whereas the full size cell has greater than 5 percent CO_2 . Changing the hydrogen flow rate in the full size cell to vary the percentage of CO_2 from 5 to 20 had no effect on CO_2 transfer efficiency (figure 43), and likewise the hydrogen flow rate in the analytical cell was varied from 0.1 to 1 percent CO_2 without affecting the CO_2 transfer efficiency (Table IX). A cell pair operated with a modified center housing to allow sampling of the hydrogen - carbon dioxide gas at various points showed no variation in the CO_2 transfer efficiency across the cell.

The discrepancy in CO_2 transfer efficiency between the full size cell pair and the analytical cell still has not been resolved.

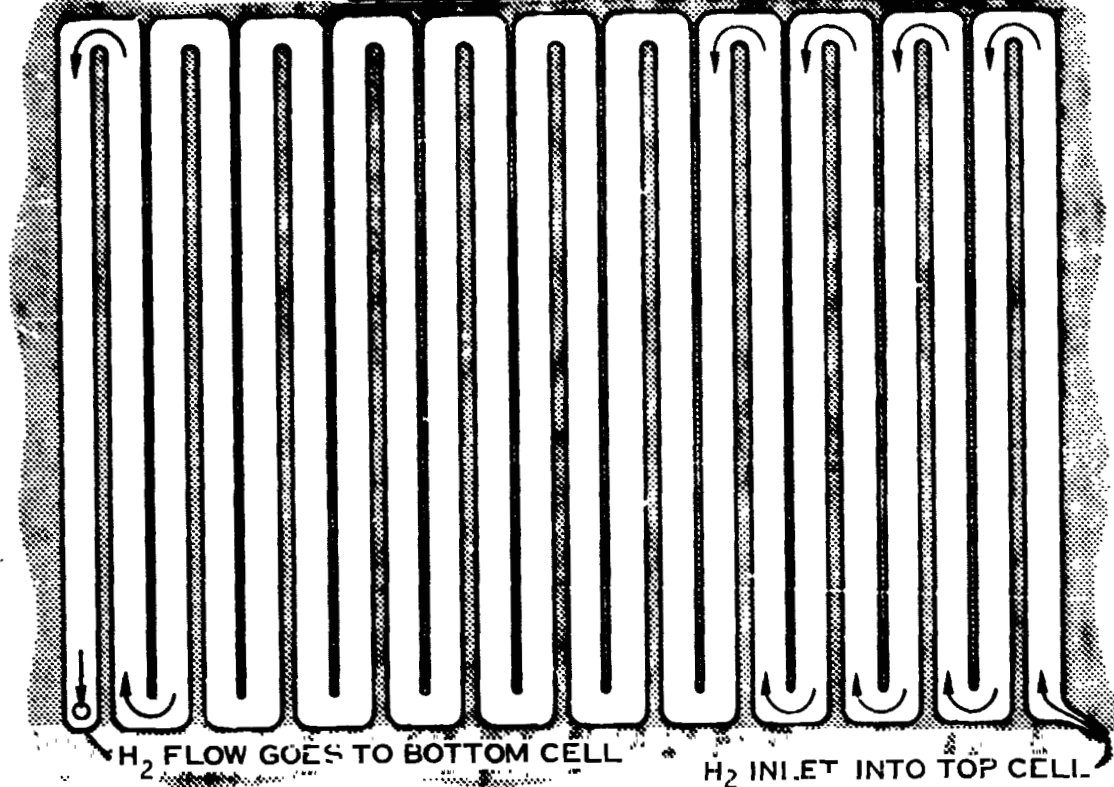
* Other full size cell pairs with Cs_2CO_3 electrolyte subsequently tested with DS 16-0 cathodes under the same conditions gave CO_2 transfer efficiencies varying from 82 to 92 percent.

**TABLE IX EFFECT OF HYDROGEN BACK PRESSURE, FLOW RATE
AND AIR TEMPERATURE ON CO₂ TRANSFER**

H ₂ Back Pressure (psia)	14.7	19.7	Cell S/N 019 Data
CO ₂ Transfer (scc/min)	59.7	59.0	
Air Temperature	52°F	70°F	
CO ₂ Transfer (scc/min)	96.5	96.5	
CO ₂ /H ₂ Ratio Out * (x 10 ³)	1.1	3	Analytical Cell Data
CO ₂ Transfer (scc/min)	5.2	5.41	

* Varied by changing H₂ flow rate.

A. BEFORE MODIFICATION TO CENTER HOUSING



AFTER MODIFICATION TO CENTER HOUSING

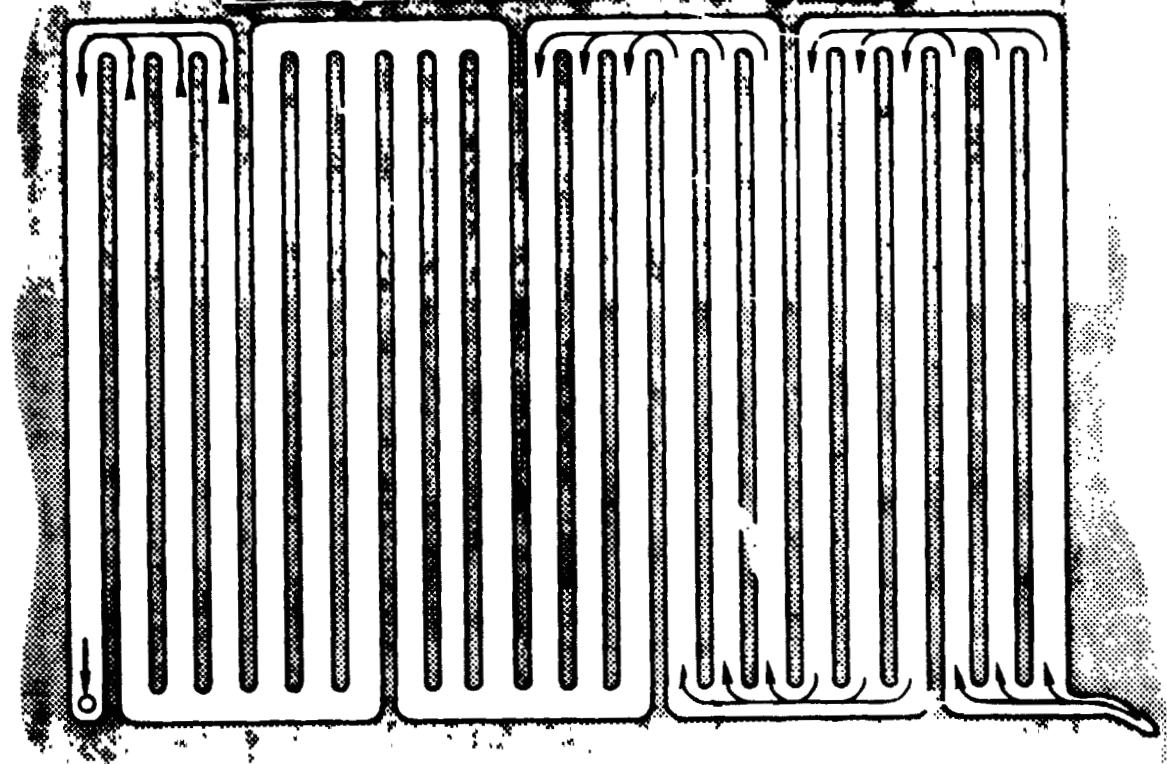


FIGURE 19. MODIFICATION TO CENTER HOUSING TO REDUCE H_2 FLOW ΔP

HDC ELECTROLYTE PROPERTIES

The physical properties of cesium bicarbonate and tetramethylammonium carbonate (TMAC) electrolyte were determined in order to provide the necessary design data for the HDC cell. The properties of cesium carbonate, except for viscosity, were determined under the previous contract (NAS 9-11830) but are included here for convenience. The viscosity data for TMAC, measured by Dr. C. H. Lin at the NASA-JSC, also is included. The data is presented in the following order:

Cesium Carbonate (Cs_2CO_3)

Table X	Vapor pressure versus concentration and temperature
Table XI	Specific conductivity versus concentration and temperature
Figure 20	Solubility versus temperature
Figure 21	Density versus concentration
Table XII	Viscosity versus concentration
Figure 22	Specific volume versus concentration
Figure 23	Moles per liter versus weight percent

Cesium Bicarbonate (CsHCO_3)

Table XIII	Vapor pressure versus concentration and temperature
Table XIV	Specific conductivity versus concentration and temperature
Figure 24	Solubility versus temperature
Figure 25	Density versus concentration
Table XV	Viscosity versus concentration
Figure 26	Specific volume versus concentration
Figure 27	Moles per liter versus weight percent
Table XVI	Relative humidity versus concentration and temperature

Tetramethylammonium Carbonate (TMAC)

Table XVII	Vapor pressure versus concentration and temperature
Table XVIII	Specific conductivity versus concentration and temperature
Figure 28	Density versus concentration

Table XIX	Viscosity versus concentration
Figure 29	Specific volume versus concentration
Figure 30	Specific volume versus relative humidity
Figure 31	Moles per liter versus weight percent

TABLE X
VAPOR PRESSURE OF H₂O (in mm Hg) FOR C₂H₂CO₃
AT VARIOUS CONCENTRATIONS AND TEMPERATURES

C ₂ H ₂ CO ₃ CONCENTRATION (WT - %)	C ₂ H ₂ CO ₃ TEMPERATURE -(°F)											
	45	50	55	60	65	70	75	80	85	90	95	100
0	7.7	9.22	11.1	13.25	15.77	18.76	22.2	26.1	30.8	36.2	42.2	49.8
40	7.1	8.5	10.2	12.3	14.4	17.3	20.6	24.2	28.8	33.7	39.3	46.0
50	6.4	7.7	9.25	11.2	13.3	15.7	18.7	22.2	26.1	30.6	35.7	41.8
60	5.52	6.65	7.95	9.55	11.3	13.5	16.2	19.0	22.2	26.2	30.7	36.0
65	4.93	5.8	6.95	8.36	10.0	11.7	14.0	16.5	19.5	23.0	27.0	31.5
70	4.02	4.82	5.75	6.88	8.22	9.8	11.5	13.6	16.2	19.0	22.1	25.8
73	3.42	4.11	4.9	5.88	7.0	8.3	9.84	11.5	13.5	16.0	18.6	21.8
75	2.83	3.39	4.02	4.82	5.75	6.82	8.03	9.45	11.1	13.0	15.2	17.7
77	2.38	2.84	3.37	4.02	4.8	5.7	6.68	7.85	9.23	10.7	12.6	14.6
78.5	2.03	2.43	2.88	3.46	4.12	4.88	5.72	6.74	7.92	9.25	10.7	12.5
80	1.75	2.09	2.49	2.97	3.56	4.16	4.87	5.72	6.73	7.9	9.2	10.6

TABLE XI
SPECIFIC CONDUCTANCE OF Cs₂CO₃ (OHM CM)⁻¹
AT VARIOUS CONCENTRATIONS AND TEMPERATURES

Cs ₂ CO ₃ Concentration (Wt-%)	Cs ₂ CO ₃ Temperature (°F)																							
	45	50	55	60	65	70	75	80	85	90	95	100	45	50	55	60	65	70	75	80	85	90	95	100
40	0.144	0.154	0.163	0.173	0.183	0.192	0.202	0.211	0.221	0.230	0.240	0.249	0.144	0.154	0.163	0.173	0.183	0.192	0.202	0.211	0.221	0.230	0.240	0.249
45	0.161	0.172	0.182	0.192	0.202	0.213	0.223	0.233	0.243	0.253	0.263	0.274	0.161	0.172	0.182	0.192	0.202	0.213	0.223	0.233	0.243	0.253	0.263	0.274
50	0.170	0.180	0.191	0.201	0.212	0.222	0.233	0.243	0.253	0.264	0.274	0.285	0.170	0.180	0.191	0.201	0.212	0.222	0.233	0.243	0.253	0.264	0.274	0.285
55	0.171	0.181	0.192	0.203	0.213	0.224	0.234	0.245	0.255	0.266	0.276	0.287	0.171	0.181	0.192	0.203	0.213	0.224	0.234	0.245	0.255	0.266	0.276	0.287
60	0.165	0.175	0.185	0.196	0.206	0.217	0.227	0.238	0.248	0.258	0.269	0.279	0.165	0.175	0.185	0.196	0.206	0.217	0.227	0.238	0.248	0.258	0.269	0.279
62.5	0.158	0.168	0.178	0.189	0.199	0.210	0.219	0.230	0.241	0.250	0.261	0.270	0.158	0.168	0.178	0.189	0.199	0.210	0.219	0.230	0.241	0.250	0.261	0.270
65	0.148	0.158	0.168	0.178	0.188	0.198	0.208	0.218	0.229	0.239	0.249	0.258	0.148	0.158	0.168	0.178	0.188	0.198	0.208	0.218	0.229	0.239	0.249	0.258
68	0.130	0.137	0.149	0.159	0.169	0.178	0.191	0.200	0.211	0.221	0.231	0.241	0.130	0.137	0.149	0.159	0.169	0.178	0.191	0.200	0.211	0.221	0.231	0.241
70	0.113	0.123	0.134	0.144	0.154	0.164	0.175	0.185	0.195	0.205	0.215	0.226	0.113	0.123	0.134	0.144	0.154	0.164	0.175	0.185	0.195	0.205	0.215	0.226
71	0.104	0.115	0.126	0.136	0.146	0.156	0.167	0.177	0.187	0.197	0.207	0.217	0.104	0.115	0.126	0.136	0.146	0.156	0.167	0.177	0.187	0.197	0.207	0.217
72		0.118	0.128	0.138		0.148	0.157	0.166	0.177	0.186	0.196	0.207		0.118	0.128	0.138		0.148	0.157	0.166	0.177	0.186	0.196	0.207
73						0.138	0.147	0.156	0.166	0.175	0.185	0.194						0.138	0.147	0.156	0.166	0.175	0.185	0.194
74	Cs ₂ CO ₃ SOLUBILITY LIMIT																							
75	USE LAST NUMBER IF LIMIT IS EXCEEDED																							
76																								

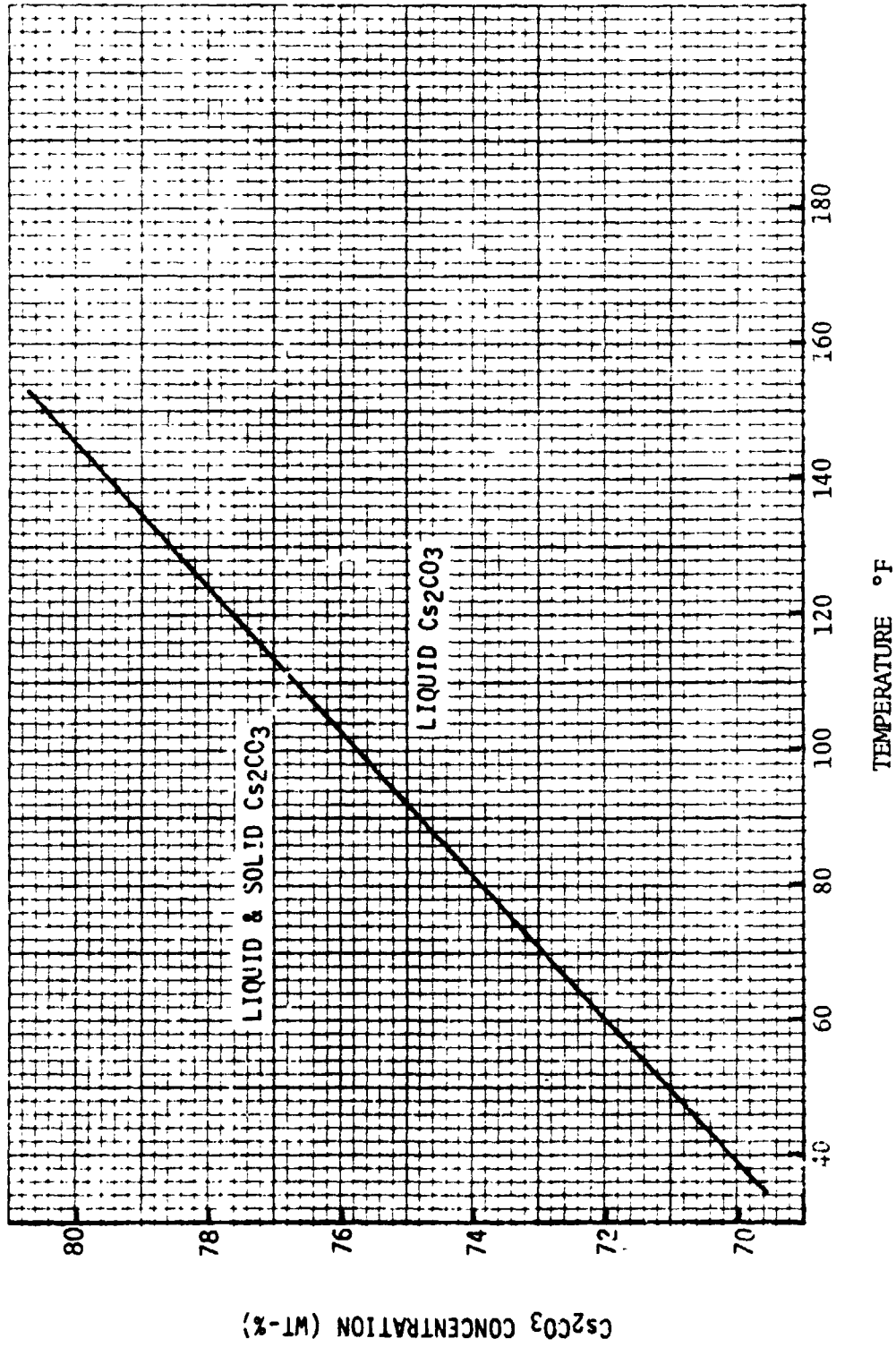


FIGURE 20. SOLUBILITY LIMIT FOR Cs_2CO_3 VS TEMPERATURE

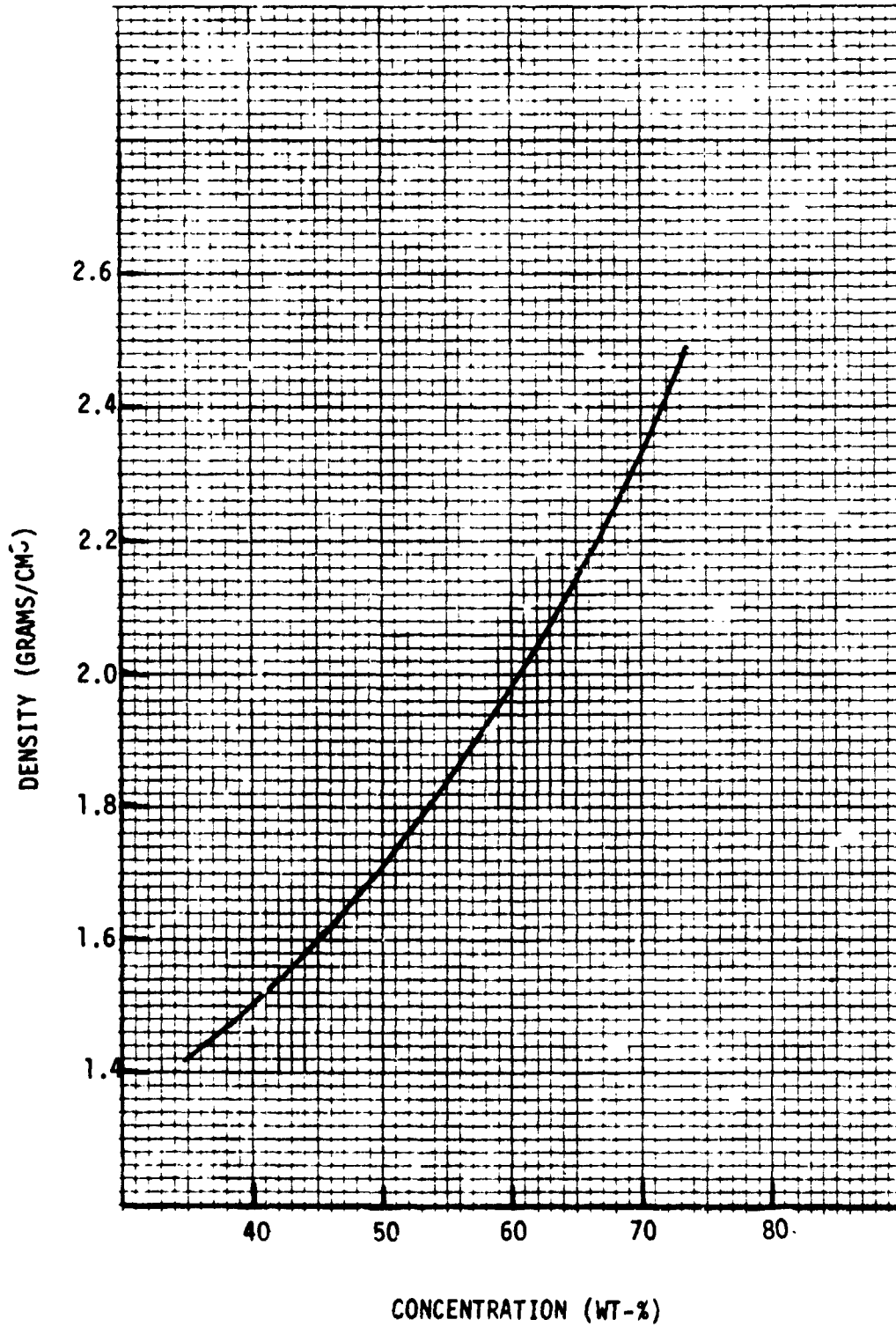


FIGURE 21. Cs_2CO_3 DENSITY VS CONCENTRATION AT 25°C

TABLE XII VISCOSITY OF CESIUM CARBONATE SOLUTION

CESIUM CARBONATE SOLUTION			
CONCENTRATION	DENSITY	ABS. VISCOSITY	KIN. VISCOSITY
Wt. %	Grams/cc	Centipoise	Centistokes
70	2.194	5.68	2.59
65	2.034	3.87	1.90
60	1.897	2.97	1.56
55	1.772	2.38	1.34
50	1.663	2.00	1.20
40	1.476	1.56	1.06

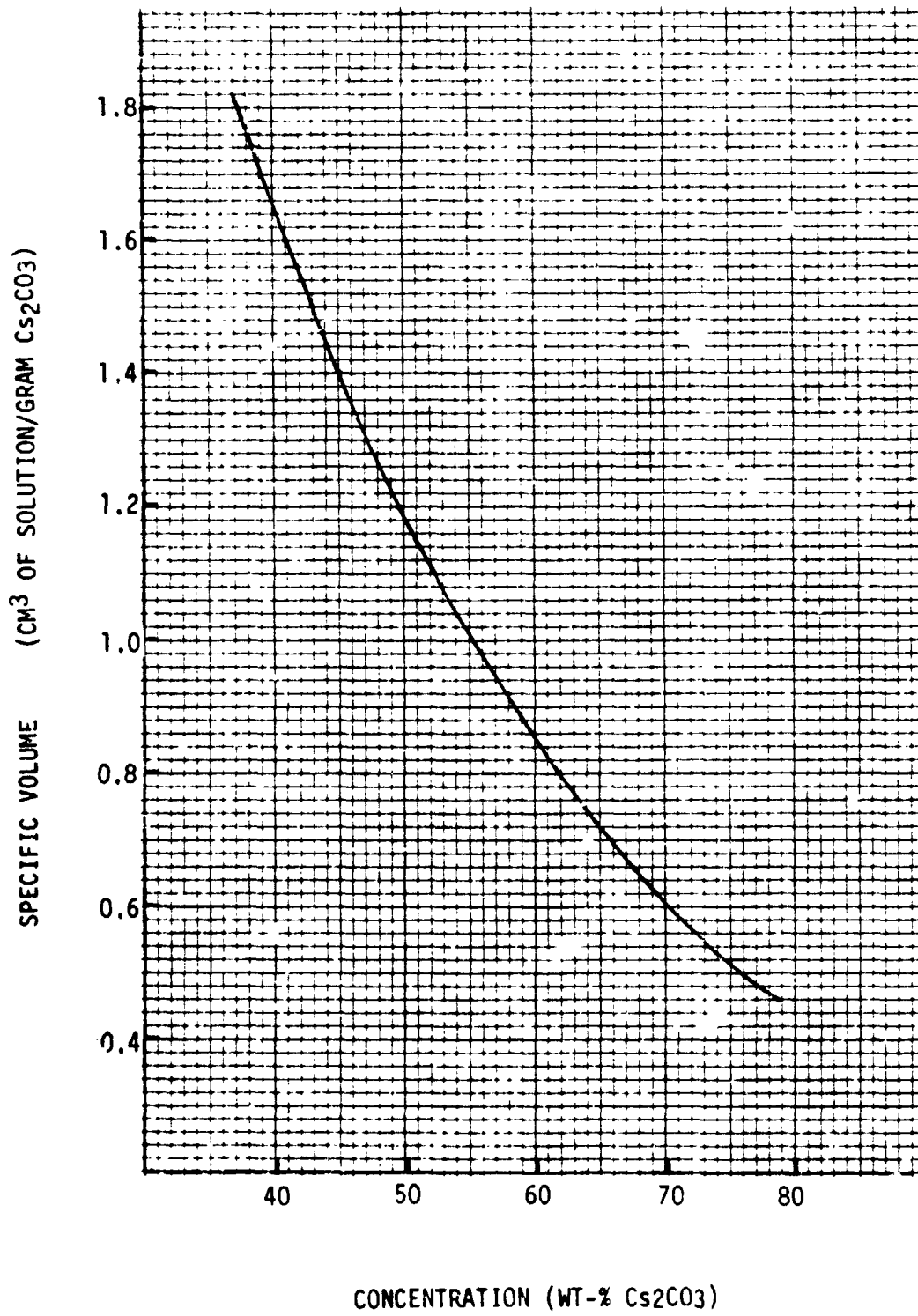


FIGURE 22. Cs₂CO₃ SPECIFIC VOLUME VS CONCENTRATION

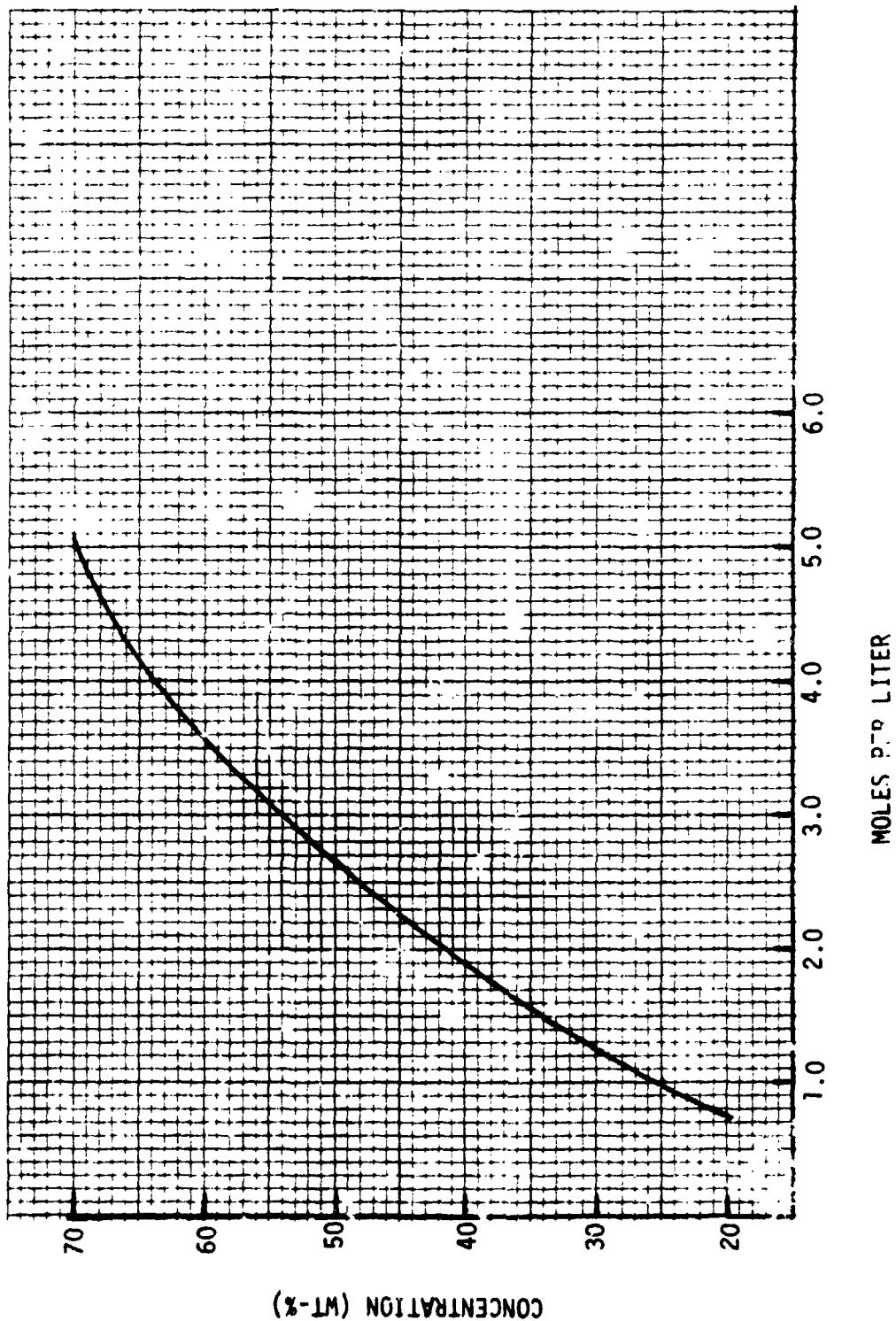


FIGURE 26. Cs_2CO_3 CONCENTRATION VS MOLE/LITER

TABLE XIII WATER VAPOR PRESSURE (mm Hg) OF CESIUM BICARBONATE SOLUTIONS
(pH = 8.0, P_{CO2} = 1 atm.)

°F t	°C													
	40	45	50	55	60	65	70	75	80	85				
0	6.29	7.63	9.21	11.07	13.25	15.80	18.78	22.23	26.21	30.81				
5	6.24	7.48	8.96	10.64	12.62	14.98	17.52	20.51	23.96	27.92				
25	6.22	7.44	8.88	10.52	12.43	14.65	17.24	20.20	23.59	27.46				
30	6.17	7.38	8.78	10.38	12.25	14.44	16.97	19.89	23.22	26.90				
35	6.12	7.29	8.68	10.25	12.06	14.22	16.69	19.56	22.83	26.56				
40	6.07	7.22	8.57	10.11	11.87	13.97	16.41	19.20	22.44	26.10				
45	5.99	7.11	8.44	9.95	11.70	13.75	16.11	18.82	21.99	25.54				
50	5.87	6.97	8.26	9.75	11.46	13.46	15.75	18.38	22.42	24.87				
55	5.68	6.75	8.01	9.45	11.12	13.05	15.26	17.80	20.76	24.07				
60	5.43	6.46	7.69	9.07	10.67	12.55	14.65	17.09	19.89	23.05				
65	5.11	6.09	7.25	8.56	10.07	11.84	13.84	16.14	18.77	21.72				
70	4.69	5.60	6.66	7.87	9.29	10.89	12.77	14.87	17.30	20.04				

TABLE XIV SPECIFIC CONDUCTIVITY OF CESIUM BICARBONATE
(ohm cm^{-1}) at pH = 8

°F Wt %	40	45	50	55	60	65	70	75	80	85
20	.0613	.0658	.0700	.0745	.0788	.0830	.0874	.0918	.0960	.1004
25	.0975	.0825	.0873	.0923	.0972	.1024	.1073	.1123	.1172	.1226
30	.0934	.0990	.1050	.1140	.1160	.1220	.1275	.1332	.1390	.1446
35	.1086	.1150	.1213	.1280	.1345	.1408	.1470	.1530	.1595	.1660
40	.1205	.1280	.1350	.1425	.1500	.1570	.1642	.1714	.1788	.1860
45	.1320	.1400	.1478	.1557	.1635	.1715	.1794	.1872	.1952	.2030
50	.1410	.1496	.1583	.1670	.1757	.1843	.1930	.2018	.2105	.2193
55	.1490	.1576	.1663	.1750	.1840	.1925	.2012	.2100	.2188	.2275
60	.1490	.1576	.1663	.1750	.1840	.1925	.2012	.2100	.2188	.2275
65	.1322	.1420	.1510	.1598	.1685	.1771	.1860	.1946	.2035	.2122
70	.1170	.1258	.1344	.1432	.1520	.1606	.1694	.1780	.1868	.1954

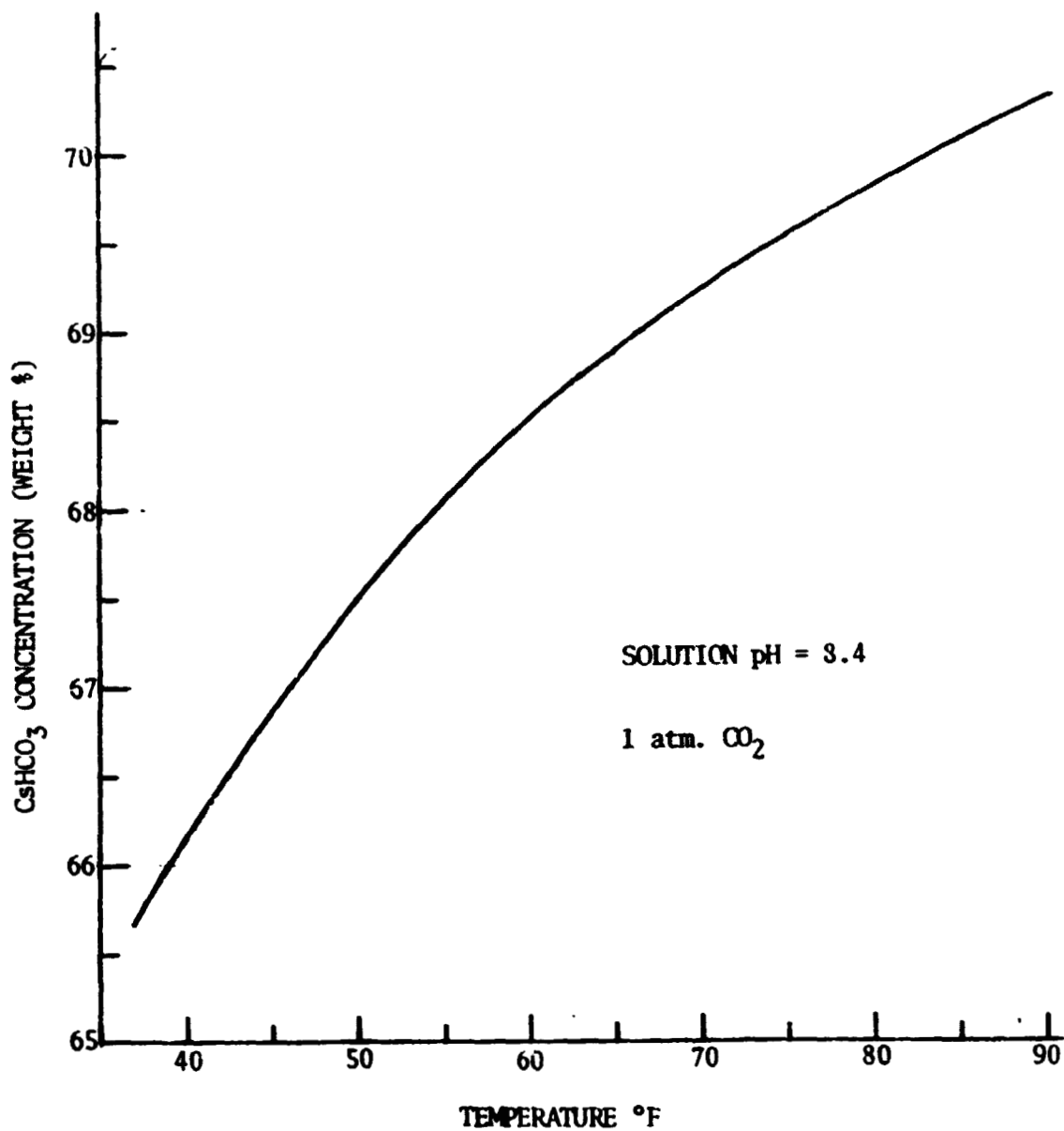


FIGURE 24. SOLUBILITY OF CESIUM BICARBONATE VS TEMPERATURE

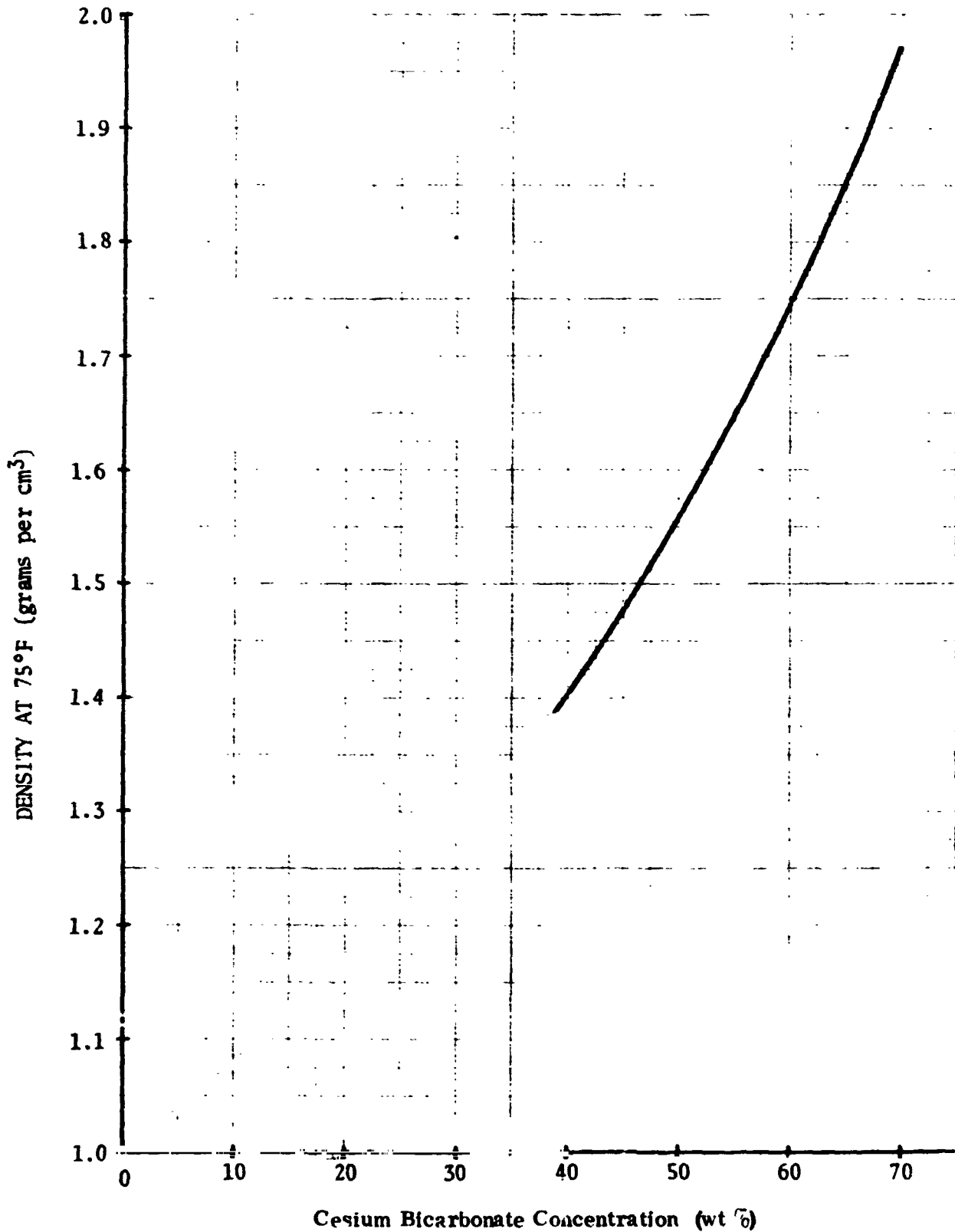


FIGURE 25. DENSITY OF CESIUM BICARBONATE SOLUTIONS VS CONCENTRATION AT 75°F

TABLE XV VISCOSITY OF CESIUM BICARBONATE SOLUTIONS

CESIUM BICARBONATE SOLUTION*			
CONCENTRATION	DENSITY	ABS. VISCOSITY	KIN. VISCOSITY
Wt %	Grams/cc	Centipoise	Centistokes
69.4	2.006	3.92	1.955
65	1.892	3.00	1.59
60	1.774	2.38	1.34
55	1.672	1.99	1.19
50	1.580	1.77	1.12
40	1.421	1.44	1.01

* 1 atm. CO₂, 73°F

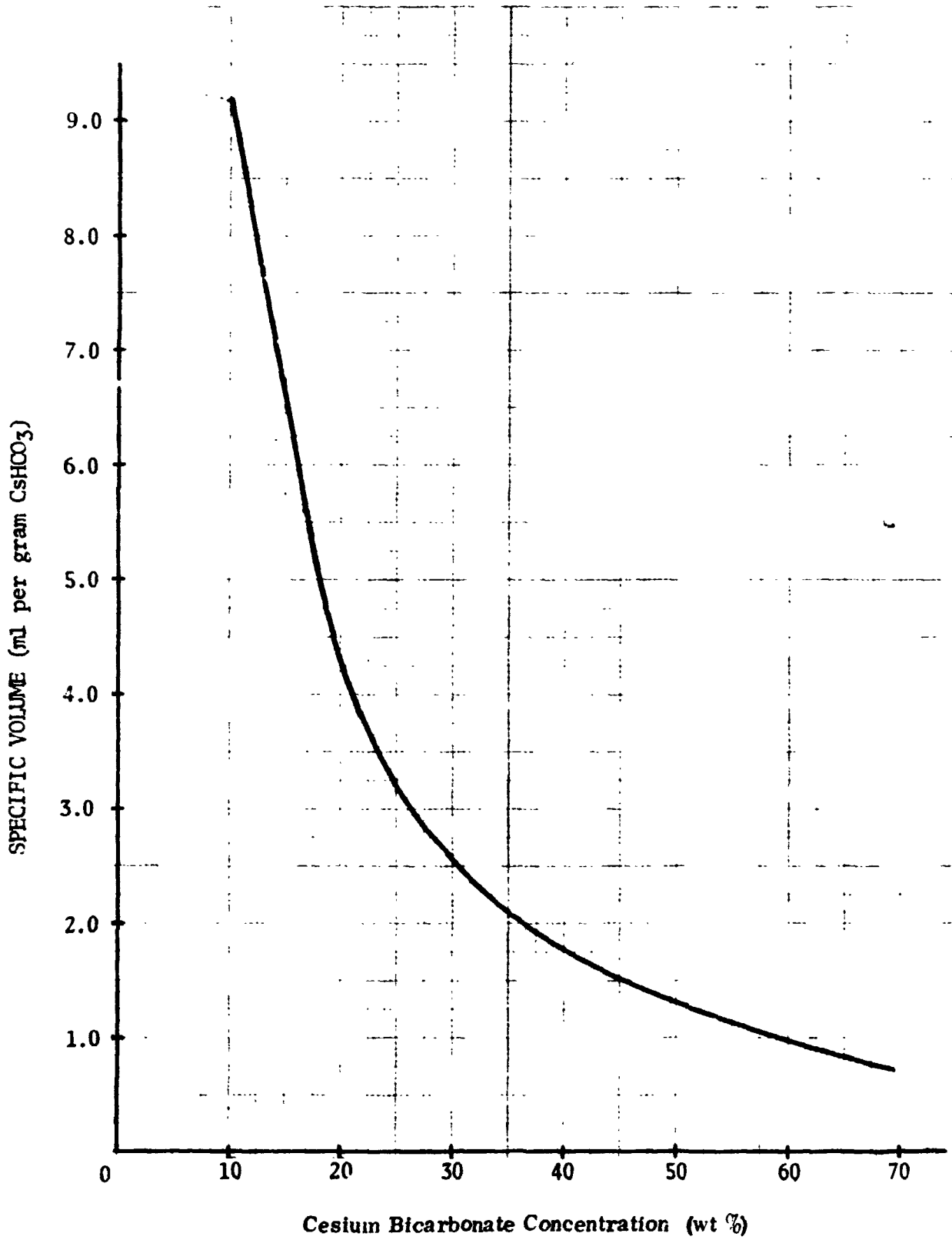


FIGURE 26. SPECIFIC VOLUME OF CESIUM BICARBONATE SOLUTIONS VS CONCENTRATION

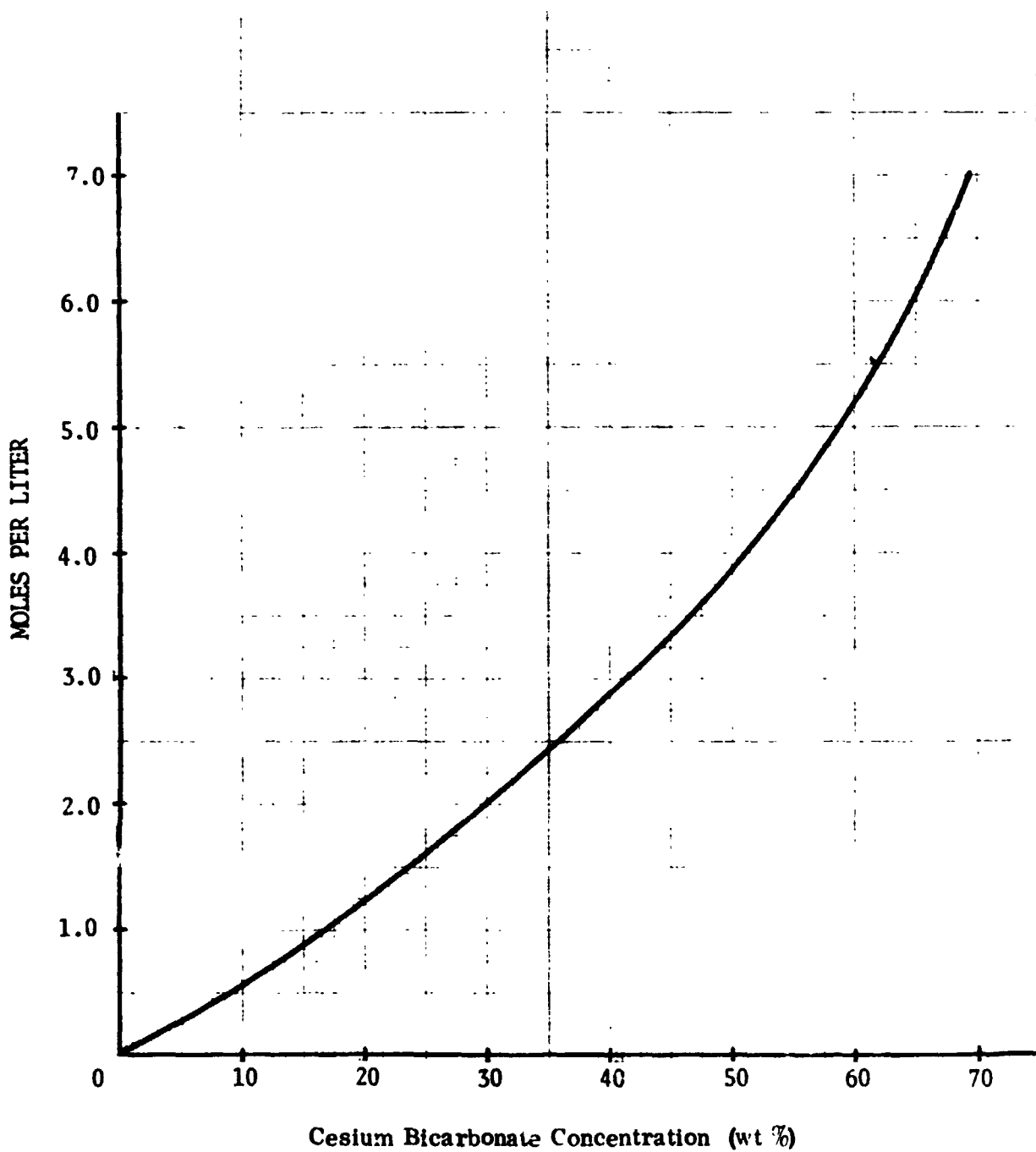


FIGURE 27. MOLES PER LITER VERSUS PERCENT CESIUM BICARBONATE

TABLE XVI RELATIVE HUMIDITY OF CESIUM BICARBONATE SOLUTIONS (PERCENT) (pH = 8.0, P_{CO₂} = 1 atm.)

°F Wt %	40	45	50	55	60	65	70	75	80	85
20	99.2	98.1	97.5	96.1	95.2	94.2	93.3	92.3	91.4	90.6
25	98.8	97.7	96.4	95.0	93.8	92.8	91.8	90.9	90.0	89.1
30	98.1	96.7	95.3	93.8	92.4	91.35	90.4	89.5	88.6	87.3
35	97.3	95.6	94.2	92.6	91.0	90.0	88.9	88.0	87.1	86.2
40	96.4	94.6	93.0	91.3	89.6	88.4	87.4	86.4	85.6	84.7
45	95.2	93.2	91.6	89.9	88.3	87.0	85.8	84.7	83.9	82.9
50	93.2	91.4	89.7	88.1	86.5	85.16	83.9	82.7	81.7	80.7
55	90.2	88.5	87.0	85.4	83.9	82.6	81.3	80.1	79.2	78.1
60	86.3	84.7	83.5	81.95	80.5	79.4	78.0	76.9	75.9	74.8
65	81.2	79.8	78.7	77.3	76.0	74.9	73.7	72.6	71.6	70.5
70	74.6	73.4	72.3	71.1	70.1	68.9	68.0	66.9	66.0	65.06

**TABLE XVII WATER VAPOR PRESSURE OF TMAC VERSUS
CONCENTRATION AND TEMPERATURE**

Wt %	°F		60	65	70	75	80	85	90	% RH
	WATER VAPOR PRESSURE (mmHg) OF TMAC pH - 12.5									
0	11.09	13.29	15.77	18.76	22.24	26.27	30.75	36.07	100	
10	10.77	12.91	15.32	18.23	21.61	25.55	29.87	35.02	97.1	
15	10.54	12.62	14.98	17.83	21.13	24.98	29.20	34.27	95.0	
20	10.14	12.14	14.41	17.15	20.33	24.02	28.10	32.97	91.4	
25	9.44	11.31	13.42	15.96	18.93	22.37	26.18	30.70	85.1	
30	8.47	10.14	12.04	14.33	16.99	20.07	23.48	27.56	76.4	
35	7.32	8.76	10.41	12.38	14.68	17.36	20.28	23.81	66.0	
40	6.11	7.34	8.71	10.36	12.27	14.52	16.98	19.87	55.1	
45	4.71	5.65	6.70	7.98	9.45	11.17	13.07	15.33	42.5	
50	3.60	4.32	5.13	6.09	7.23	8.55	9.99	11.72	32.5	

TABLE XVIII SPECIFIC CONDUCTIVITY OF TMAC VERSUS
CONCENTRATION AND TEMPERATURE

Wt% OF	10	15	20	25	30	35	40	45	50	55
55	.404	.508	.561	.548	.491	.410	.305	.196	.104	.048
60	.440	.553	.609	.594	.538	.454	.345	.233	.132	.064
65	.475	.597	.656	.640	.585	.498	.386	.270	.159	.077
70	.512	.642	.703	.686	.630	.542	.427	.307	.187	.092
75	.547	.687	.750	.731	.675	.585	.467	.343	.215	.109
80	.583	.730	.797	.776	.721	.628	.508	.379	.243	.122
85	.624	.775	.844	.822	.767	.672	.548	.416	.270	.138
90	.655	.819	.891	.867	.813	.716	.589	.452	.298	.158

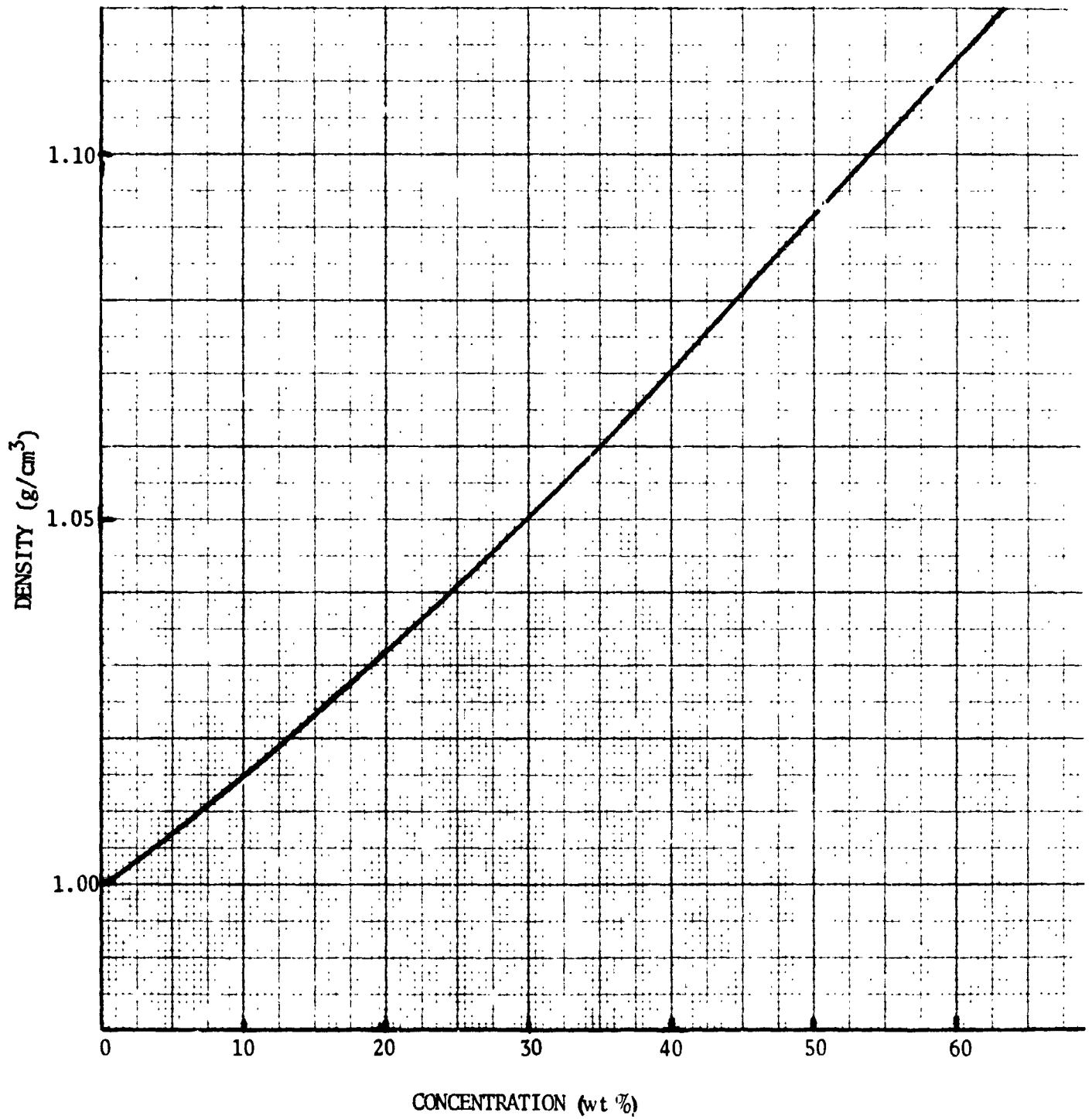


FIGURE 28. TMAC DENSITY VERSUS CONCENTRATION

TABLE XIX VISCOSITY OF TMAC SOLUTIONS

TMAC SOLUTION*			
CONCENTRATION	DENSITY	ABS. VISCOSITY	KIN. VISCOSITY
Wt. %	Grams/cc	Centipoise	Centistokes
51.5	1.092	32.8	30.04
39.9	1.07	7.67	7.17
30.0	1.05	3.09	2.94
20.0	1.032	1.86	1.80
10.0	1.015	1.31	1.29
5.0	1.008	1.034	1.046

* pH \approx 10.9, Data from NASA JSC

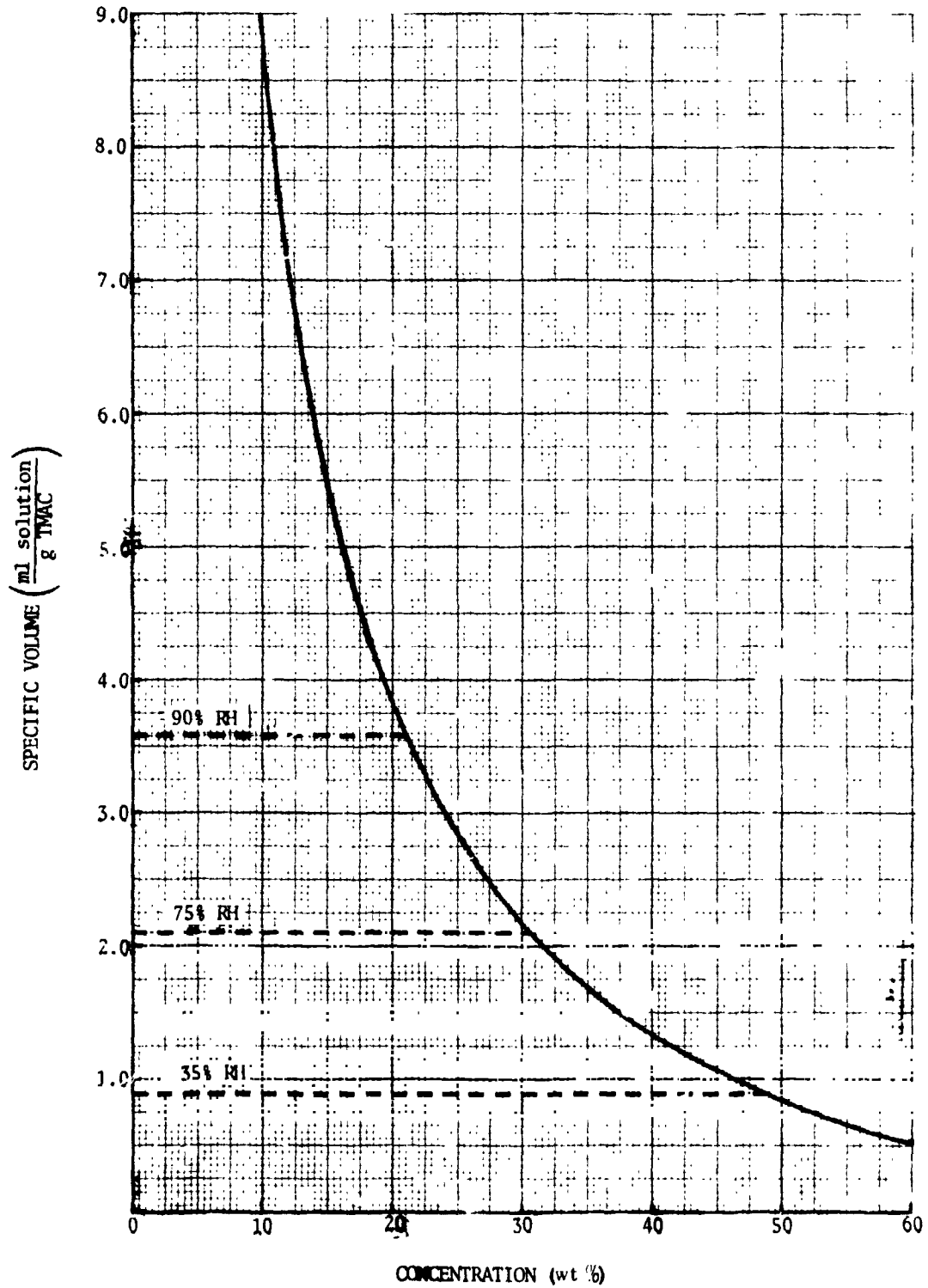


FIGURE 29. TMAC SPECIFIC VOLUME VERSUS CONCENTRATION

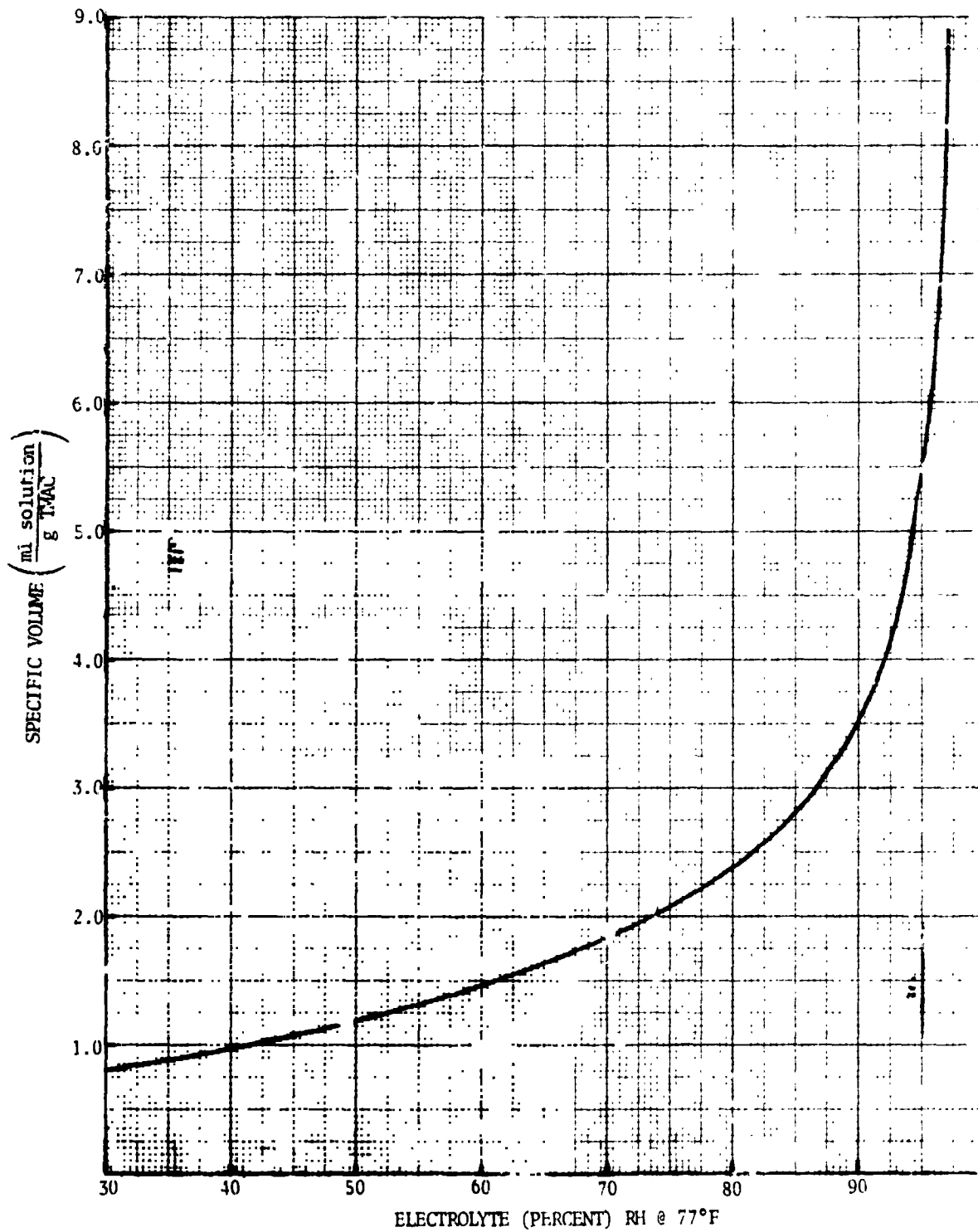


FIGURE 30. TMAC SPECIFIC VOLUME VERSUS ELECTROLYTE RELATIVE HUMIDITY

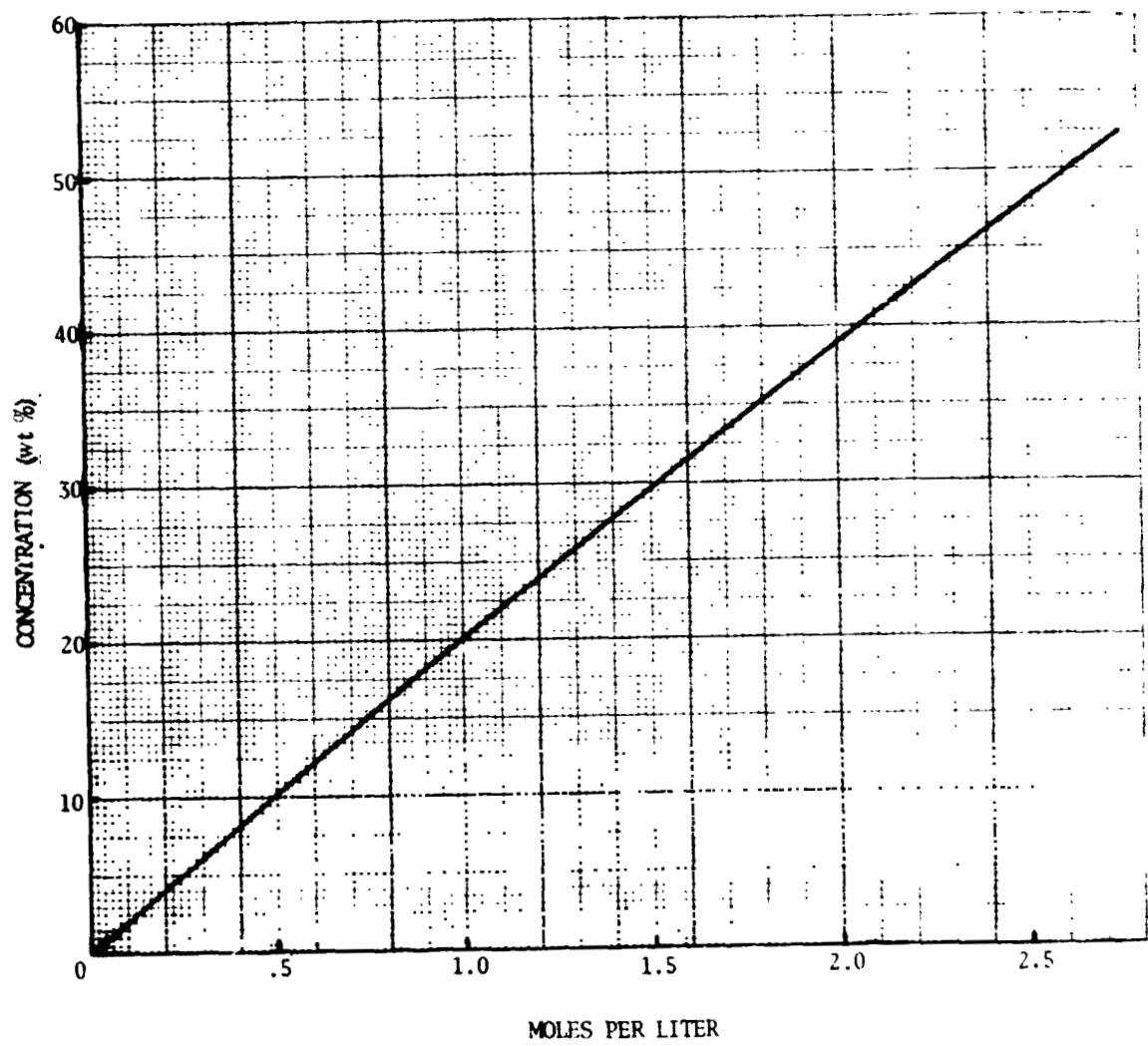


FIGURE 31. MOLES PER LITER VS WEIGHT PERCENT (TMAC)

CS

MODIFIED ELECTROLYTES

A search and evaluation of mixed (aqueous-nonaqueous) solvents to develop another electrolyte with low relative humidity capabilities was conducted.

One of the methods for obtaining an electrolyte with a low water vapor pressure is to replace a significant part of the water with a non-electrolyte solvent. The necessary properties for a non-electrolyte additive are:

- Negligible vapor pressure at cell operating temperature.
- Miscible with water.
- Resulting solution must dissolve a sufficient amount of electrolyte salt to give good electrical conductivity.
- Stable under cell conditions.

The initial literature search for materials with suitable properties was reported under the previous contract, NAS 9-11830. Only two materials, propylene carbonate and ethylene carbonate, were found which looked promising.

The solubility of propylene carbonate was found to be 3 ml per 10 ml of water* and this would result in a limited dew point depression. Ethylene carbonate has a melting point of 40°C (104°F) but a fifty-fifty volume mixture with water is soluble above 65°F where the HDC cell would operate.

The literature search revealed that propylene and ethylene carbonate had been employed as electrolyte solvents (anhydrous) and were relatively stable over a wide potential range. However, the stability should depend on the nature of the electrode material (catalyst) and probably the availability of water, which could induce hydrolysis of these cyclic esters to alcohol and acid or carbon dioxide.

A potential sweep with and without ethylene carbonate (three drops in 35 ml of 1 M Cs₂CO₃) is shown in figure 32 from which it is obvious that these materials are readily oxidized on a platinum black electrode in the presence of water. The relatively large anodic peak at ~0.75 volts on both the up and down sweeps cannot be due to the direct oxidation of ethylene carbonate. It is more reasonable to assume that the ethylene carbonate is rapidly hydrolyzed by base and platinum catalyst to alcohol followed by oxidation of the alcohol.

To date the only materials found that have sufficient solubility in water contain amine, hydroxy or ester groups, and all of these are readily oxidized under HDC conditions.

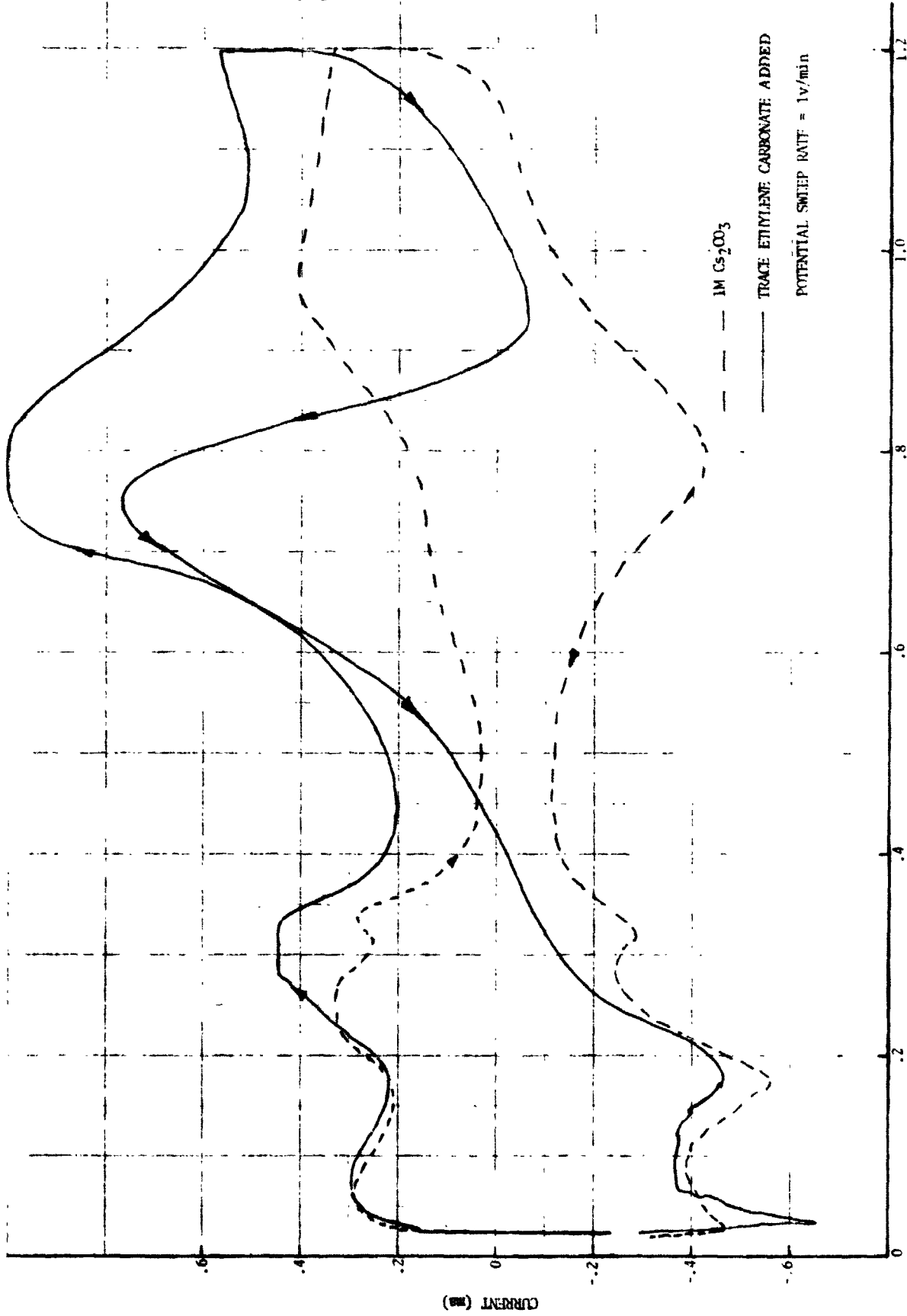
* The literature shows propylene carbonate as very soluble in water.

Hamilton
Standard

DIVISION OF UNITED AIRCRAFT CORPORATION

U
A₆

SVHSER 6285



POTENTIAL (VOLTS) VERSUS HYDROGEN ELECTRODE IN SAME SOLUTION

FIGURE 32. POTENTIAL SWEEP FOR ETHYLENE CARBONATE

SPECIAL TESTS

In addition to the HDC tests discussed in the previous sections, three special investigations were made involving the HDC matrix compression, matrix set, and the hydrogen flow rate through the cell.

Matrix Compression

The purpose of the matrix compression tests was to determine the tortuosity and optimum matrix compression for asbestos, Neoprene asbestos, and Tissuquartz. The general procedure (reference Appendix) Master Test Plan, Section IV) was to measure electrolyte resistance (R) with and without matrix as a function of electrode distance (d) using the special micrometer cell shown in figure 33.

The resistance should be given by

$$R = \rho \frac{d}{A} \cdot \frac{d \tau}{d - d' (1 - m)} = \frac{\rho d f \tau}{A}$$

where ρ is the electrolyte resistivity, A the electrode geometric area, τ the tortuosity, d' the uncompressed matrix thickness (dry) and m is the matrix void volume. The dry uncompressed matrix thickness and the maximum compressed thickness, $d^0 = d' (1 - m)$, were measured with a micrometer to ± 2 mils and ± 0.5 mils, respectively. Without matrix, the tortuosity and matrix factor ($f = d/d-d^0$) are both equal to one and the above equation reduces to $R = \rho d/A$. For a given electrolyte ρ/A is found by plotting R versus d and extrapolating to $d = 0$ to correct for the cell electronic resistance. The tortuosity is found from a plot of R versus $fd \rho/A$ and if f is not a function of d the optimum compression should be at $d = 2d^0$.

To determine the resistance a constant voltage (± 50 mV, 1 K Hz) square wave was applied to the cell and the resulting current was extrapolated to "zero" time ($\pm 2 \mu$ sec) to eliminate capacitance and polarization effects. The electrolyte was 1 gram KCl per liter to give a resistance (~ 50 ohms at 25 mils) compatible with the instrumentation. To obtain reproducible results it was necessary to keep the cell in a 100 percent relative humidity chamber to prevent water evaporation from the electrolyte. Also, as the electrode spacing was decreased, the excess electrolyte was removed by blotting with electrolyte dampened paper tissue. It was found that the use of dry tissue had a tendency to remove too much electrolyte from the matrix material.

For each matrix material studied, a plot of R versus d (figure-a) and R versus $fd\rho/A$ (figure-b) is given. The R versus d plot also shows the electrolyte resistance without matrix and the calculated resistance for a tortuosity value of one. The values for the dry uncompressed matrix thickness and the thickness at a maximum compression are shown as d' and d^0 , respectively. Except where noted, two layers of matrix were used.

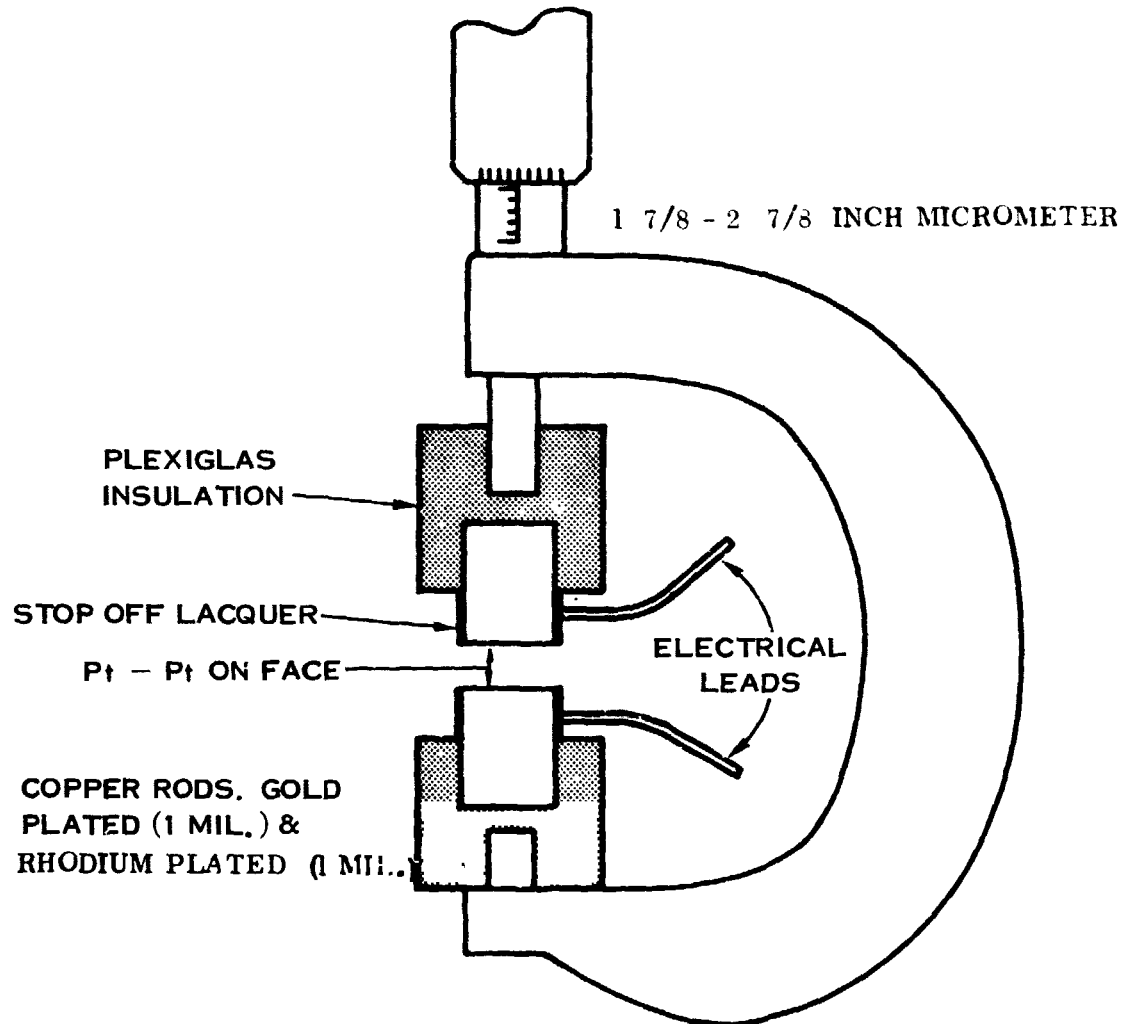


FIGURE 33. MATRIX CONDUCTIVITY FIXTURE

The data for fuel cell asbestos are shown in figures 34a and 34b. The tortuosity factor is 1.53 for $d > 35$ mils but decreases for d values less than 35 mils. This behavior may be due to edge effects where a small fraction of the matrix remains uncompressed resulting in a constant (with d) parallel resistance so that the measured value is less than the true resistance between the electrode faces at low values of d as reflected in figure 32. The minimum resistance occurs at close to the calculated value of $2d^0 = 24$ mils.

The data for Tissuquartz and Neoprene asbestos are given in figures 35 and 36 respectively. Both of these materials, having an uncompressed void volume greater than 90 percent, gave unexpected results. As can be seen from figures 35 and 36, the R versus ρ/A plot is a straight line with a slope of one ($\tau = 1$) but does not extrapolate to zero. Unless it is assumed that the tortuosity increases continuously with increasing matrix compression, it appears that the equation for resistance should contain an added factor which is independent of d .

In view of the very high void volume, a tortuosity factor of one would be expected for all but very small values of d so that an additional term to the resistance equation seems more reasonable, although it is somewhat difficult to justify a priori. A possible explanation could be attributed to double layer effects associated with the large matrix - solution interfacial area. This interfacial area would be independent of the compressed matrix thickness d . Also, from microscopic examination of the three matrix materials it appears that the P&WA fuel cell asbestos has a much smaller surface area than the other two materials so that double layer effects would be much less pronounced with the fuel cell asbestos.

To minimize any electroosmotic effect a saturated solution of KCl was used as the electrolyte in one experiment with Tissuquartz. This experiment required special instrumentation because the measured resistance was in the order of 1/2 ohm. A Hewlett Packard model 606B signal generator supplied a 98μ amp rms 100K Hz sine wave and the voltage was fed into a Tektonix 1A7A amplifier with a Fluke model 873A AC/DC differential voltmeter as readout. With this equipment the measurements could be made to 0.1 micro volt. The results corrected for an electronic resistance of 0.345 ohms are shown in figure 37. The line for Tissuquartz is parallel to the plain electrolyte line but displaced by 0.075 ohms which would indicate again that the resistance equation should contain an additional term independent of d but probably a function of ρ .

An equation of the form $R = \rho/A [df\tau + \alpha]$, where α is a constant for a given matrix material and electrolyte, allows a fit of the data. The dilute and saturated KCl solutions with Tissuquartz gave the same α value which would indicate that α is independent of electrolyte concentration, however, additional experiments would be necessary to definitely establish this as fact. Data obtained with Neoprene asbestos and dilute TMAC electrolyte also required the addition of the α term but its value was different than that for the KCl electrolyte.

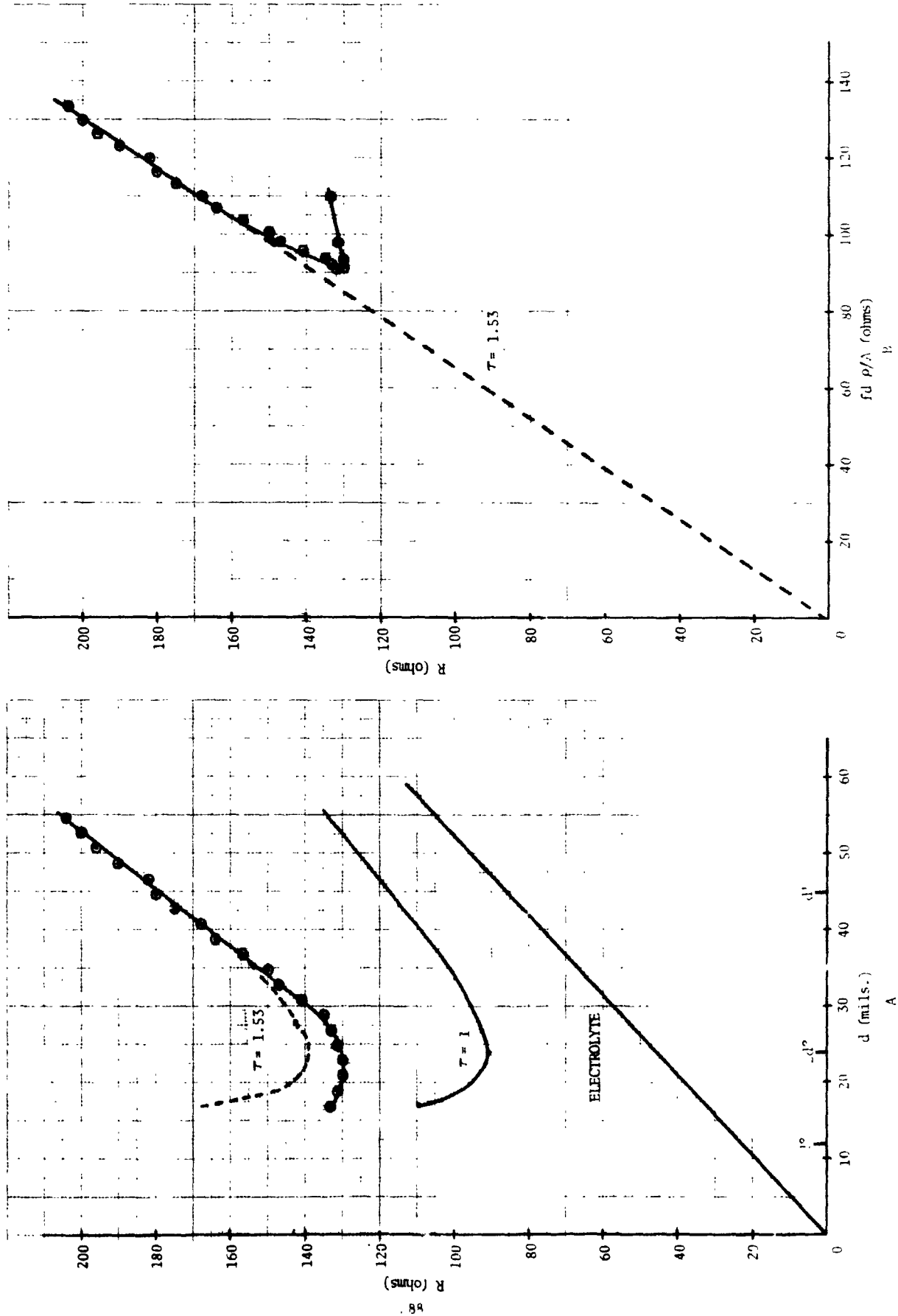


FIGURE 14. PAWA ASBESTOS - ELECTROLYTE RESISTANCE VERSUS THICKNESS

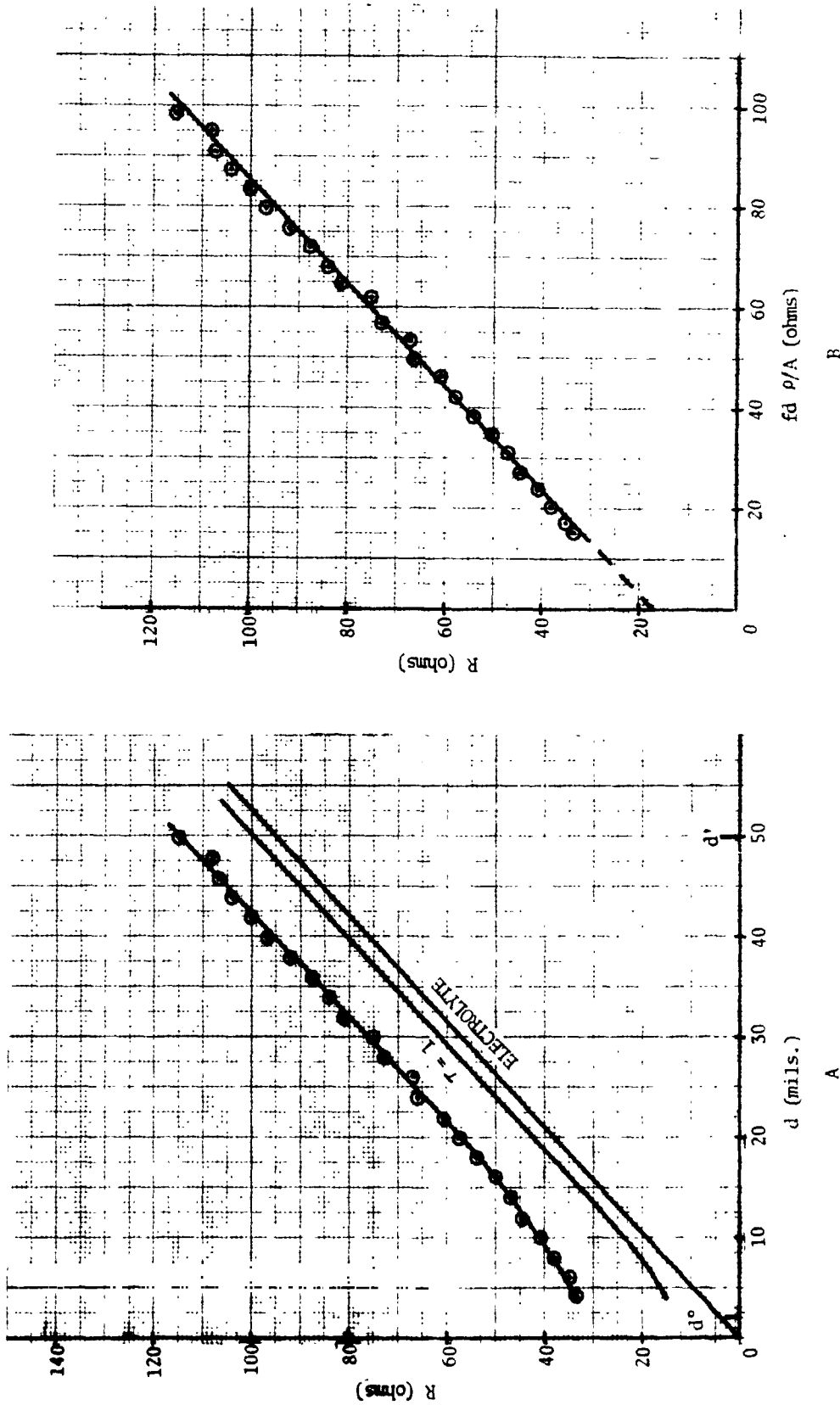


FIGURE 35. TISSUQUARTZ - ELECTROLYTE RESISTANCE VERSUS THICKNESS

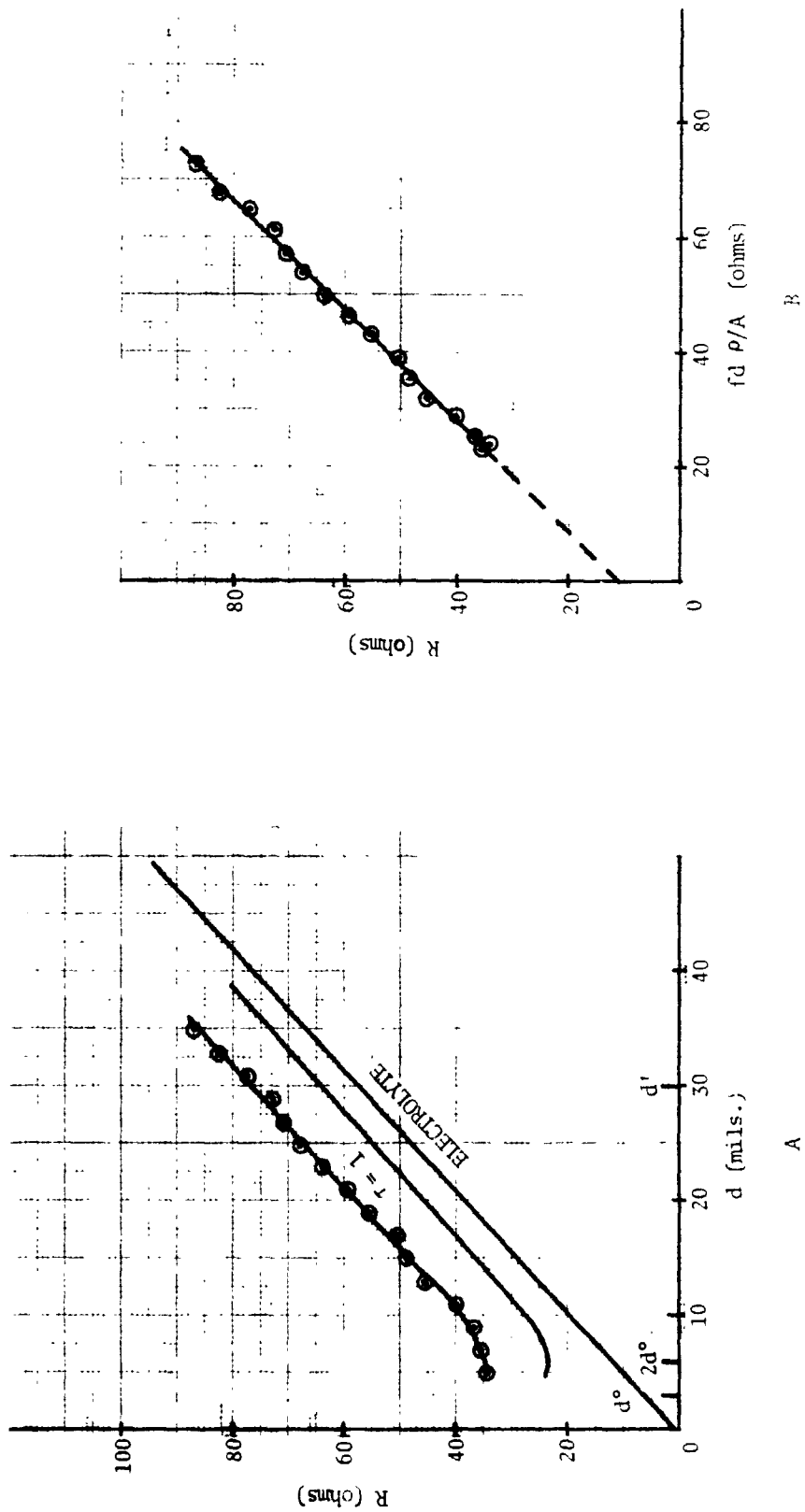


FIGURE 36. NEOPRENE ASBESTOS - ELECTROLYTE RESISTANCE VERSUS THICKNESS.

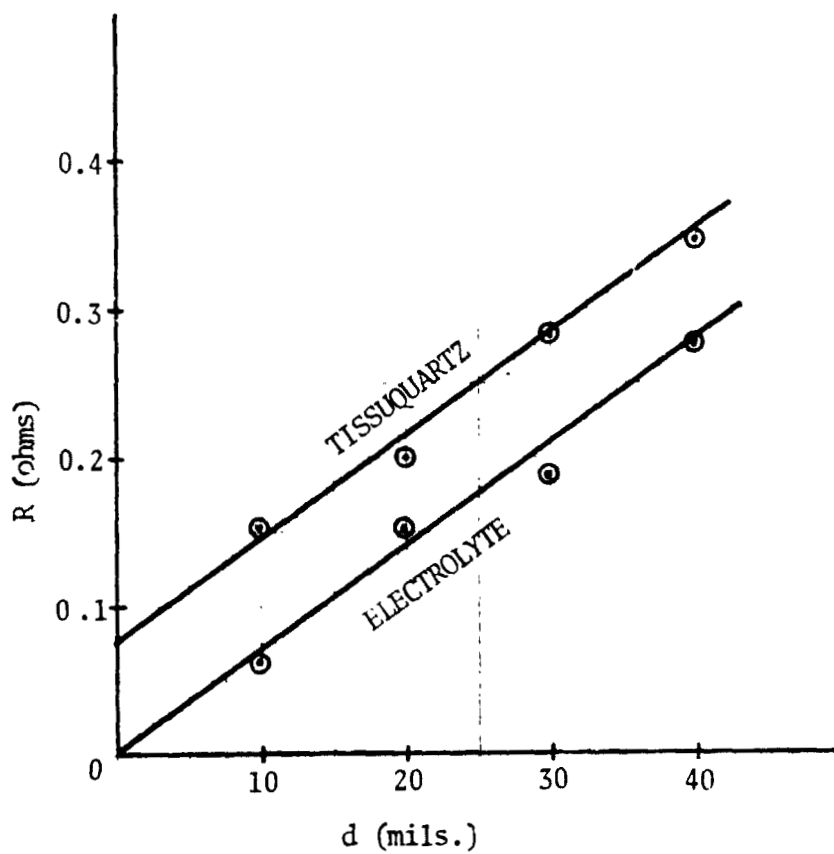


FIGURE 37. TISSUQUARTZ - (SATURATED KCl) RESISTANCE VERSUS THICKNESS

It is conceivable that the various interactions between the ion solution and those immobilized in the double layer at the matrix - solution interface would result in retardation of the mobile ions in solution. Such a decrease in ion mobility would increase the matrix - electrolyte resistance by an additional factor.

Since the matrix for the WVE cell consists of one layer of Neoprene asbestos and two layers of Tissuquartz, data for this combination is shown in figure 38. The optimum compression is approximately 7 mils which corresponds to the value for $2d^0$. The simple equation would not apply to a combination of matrix material so an R versus $d \rho/A$ plot was not made.

Matrix Set

Part of the task of investigating the HDC matrix characteristics required a compression relaxation and set test to be performed. The objective of this task was to determine if the final set of the matrix provided sufficient compression resistance (10 psi minimum) to maintain good contact between current collector, electrodes, and matrix. The testing established the pressure load versus matrix compression for various matrix configurations and for various durations up to six months. Tests were performed in accordance with the Master Test Plan, Section VIII, reference Appendix.

The comparison of loading versus deflection of three typical matrix configurations is presented in figure 39. This data shows that the addition of one sheet of Tissuquartz increases the loading very little, but one additional sheet of asbestos increases the loading by a factor of approximately 1.5. The slope of these curves, loading pressure per inch of deflection, is about the same.

The effects of compression cycling the matrix are shown in figure 40, which reveals the largest change in loading between the first and second cycles and very little change in the loading between the second through the fifth cycles.

The change in loading at a set matrix compression (0.022") is presented in figure 41, which shows about a 14 percent decrease in the matrix loading during the initial two hours of assembly.

Six samples were tested for the endurance portion of the matrix set investigation. Each sample, consisted of two sheets of 0.020 inch thick asbestos, separated by a 0.018 inch thick Tissuquartz, saturated with Cs_2CO_3 and compressed to 0.024 inch thickness and held. The test fixtures holding the compressed samples, were placed in a test chamber where a 52°F/45°F temperature/dew point and 2.5 mm Hg PCO_2 condition was maintained. After one, two, six, fifteen and twenty-five week durations, the samples were removed and compressed using a loading of 0 to 200 psi. The one and two week samples required a 70 psig loading before any indication of additional matrix compression was noted. Both of these samples, as shown in figure 42 had the same

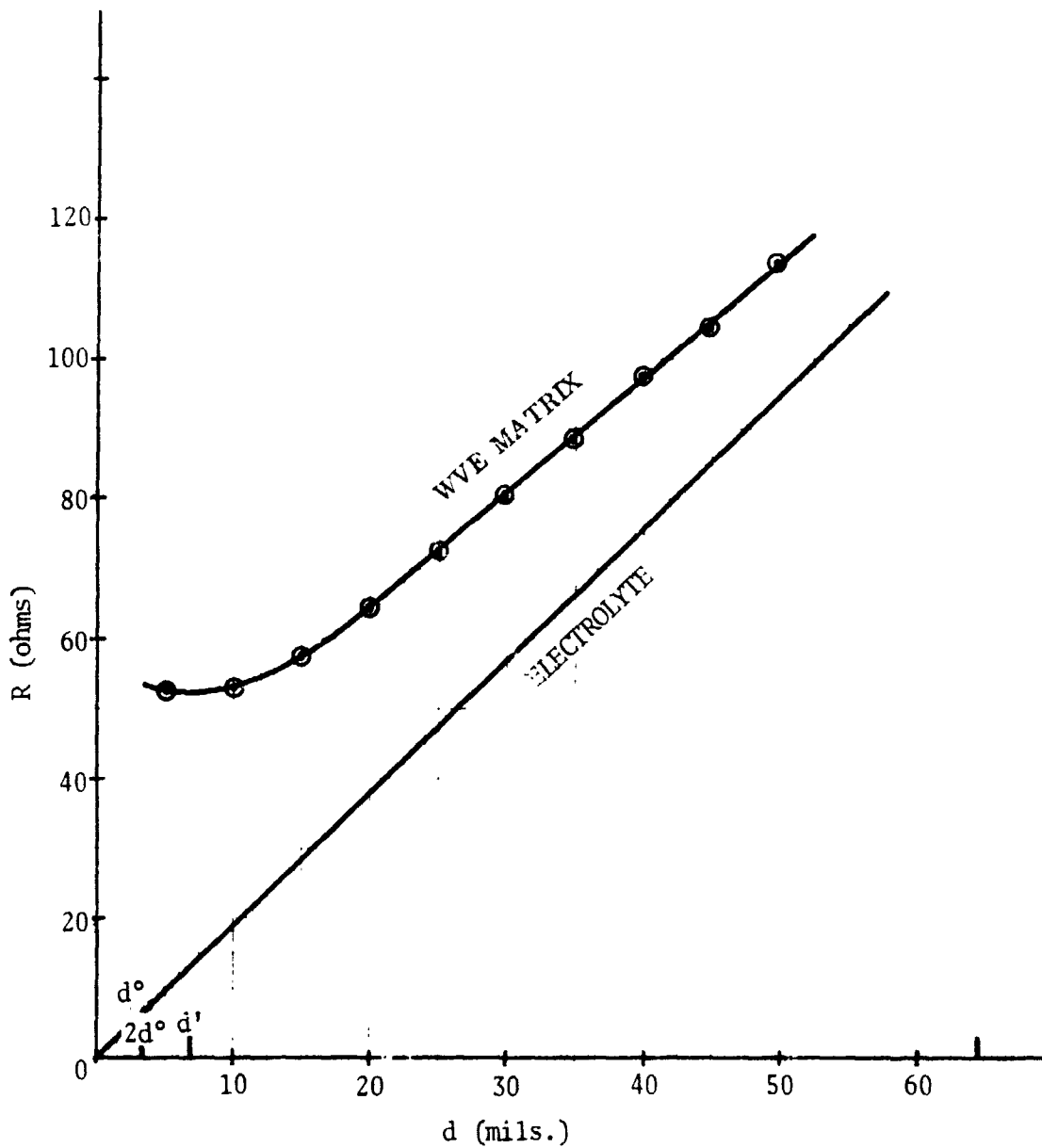


FIGURE 38. (WVE MATRIX) TISSUQUARTZ NEOPRENE ASBESTOS - ELECTROLYTE RESISTANCE VERSUS THICKNESS

MATRIX SET TEST
NAS 9-12920 MASTER TEST PLAN
SECTION VIII PARA. 4.0
0.020" PEMA SUPER CLEAN ASBESTOS

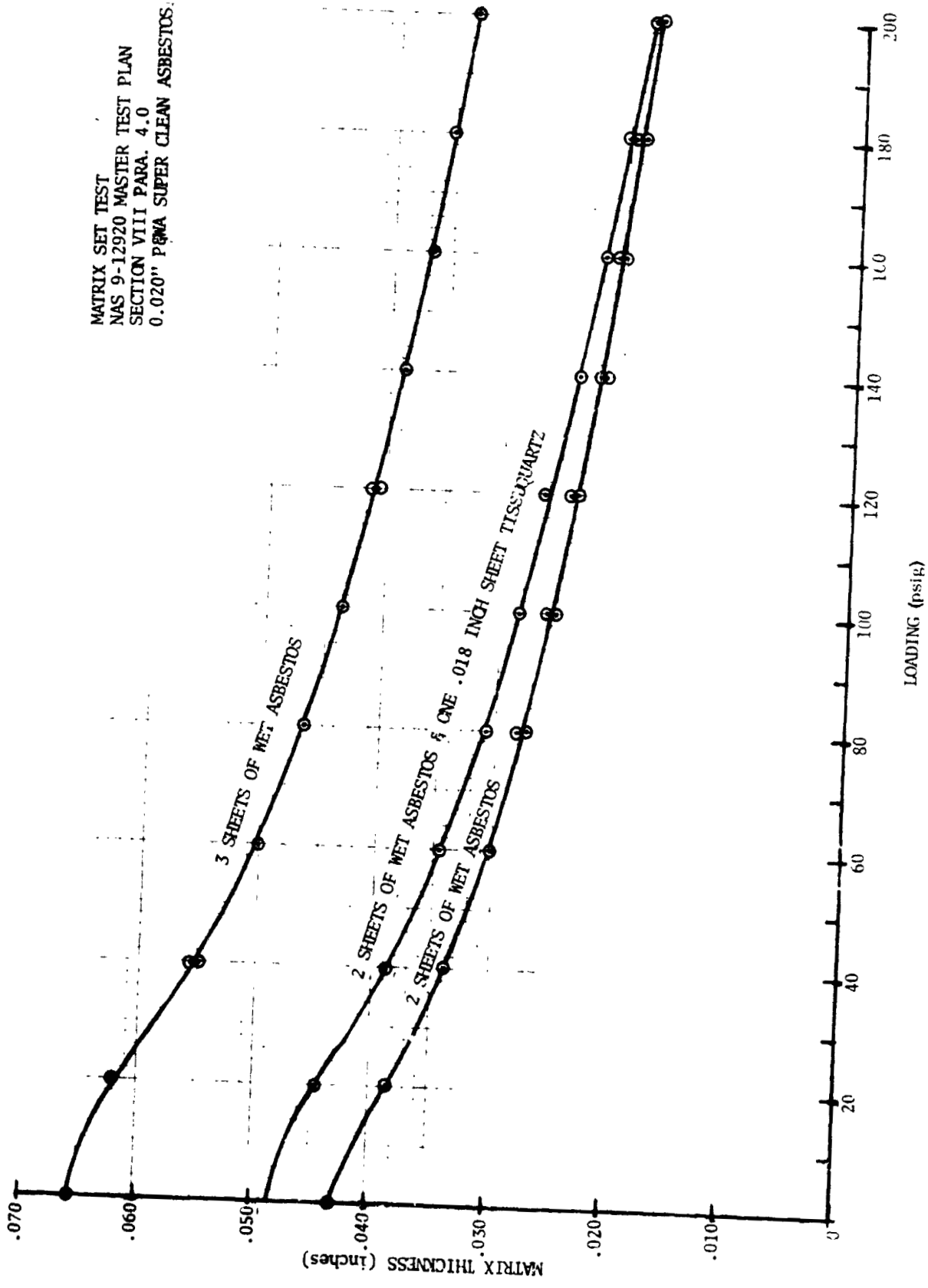


FIGURE 39. MATRIX COMPRESSION VERSUS LOADING

MATRIX SET TEST
NAS 9-12920 MASTER TEST PLAN
SECTION VII PARA. 4.0
2 SHEETS OF 0.020" P&WA
SUPER CLEAN ASBESTOS (WET)

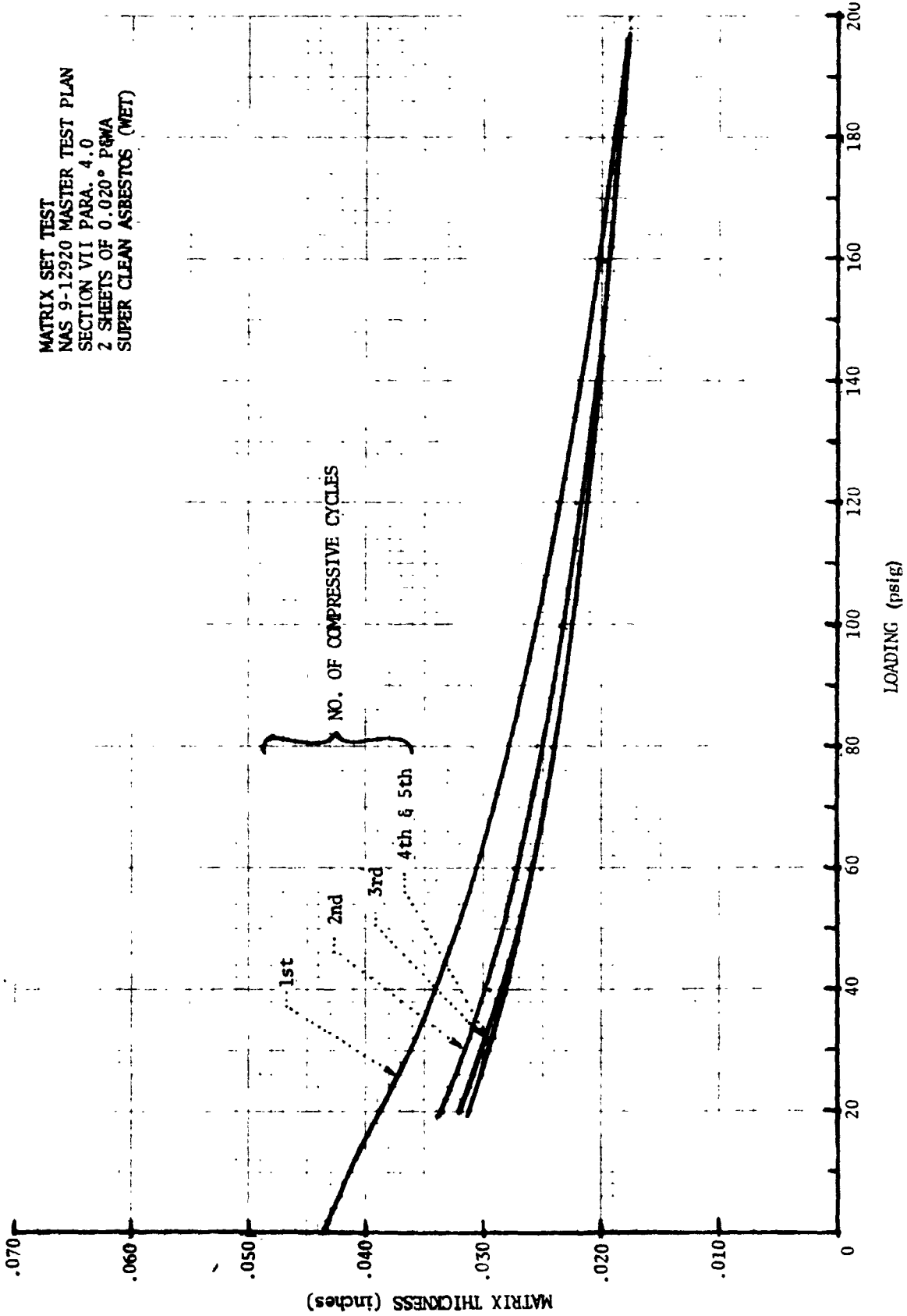


FIGURE 40. MATRIX CYCLIC COMPRESSION VERSUS LOADING

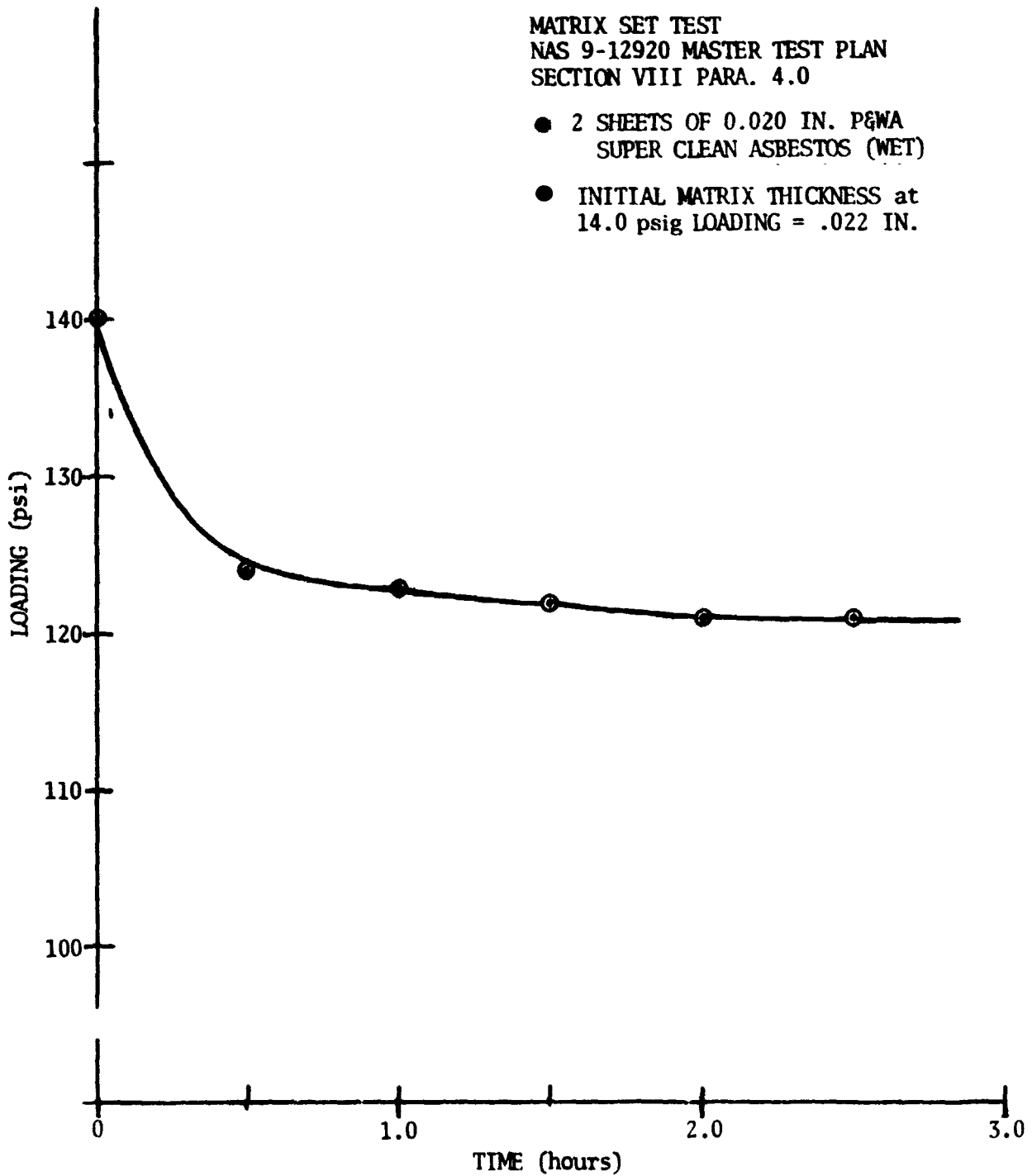


FIGURE 41. MATREX LOADING VS TIME

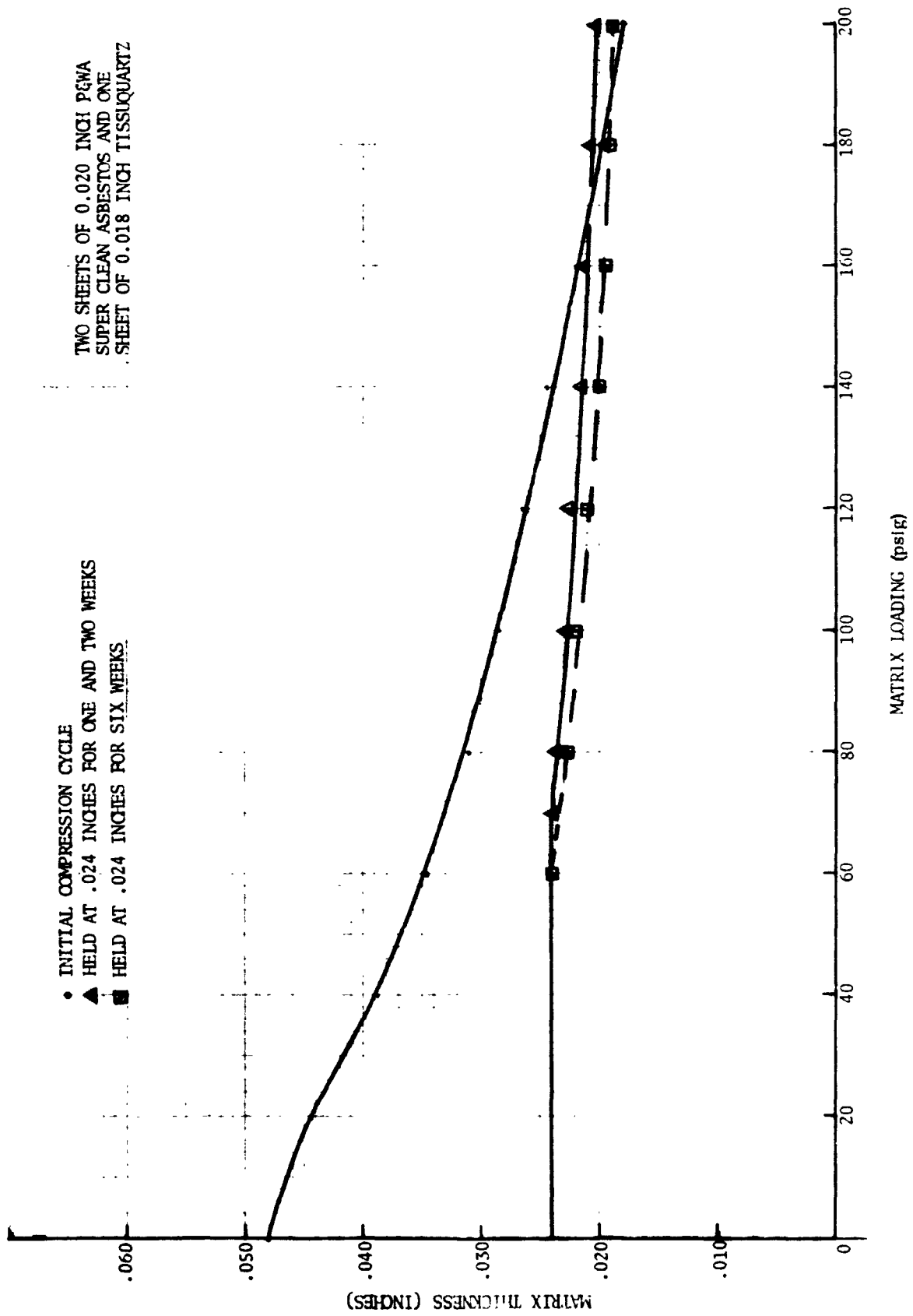


FIGURE 42. MATRIX SET TEST

compression versus loading values. The six, fifteen and twenty-five week samples required a 60 psig loading before deflection was observed, but the slope of the compression/loading curve is the same as the earlier samples.

The six month endurance data reveals that the matrix maintains sufficient compression resistance (60 psig) to provide good interface contact between the matrix, electrodes and housings which should not cause any change in the cell's IR value.

HDC HYDROGEN FLOW IMPROVEMENT

The objective of testing the HDC at various inlet hydrogen flow rates was to determine the effect of this variation on cell performance. Testing was done per Master Test Plan, Section III, reference Appendix. The HDC cell pair which was used for this testing was cell pair S/N 011-3 which is a non-reservoir type cell using Cs_2CO_3 for the electrolyte. This cell pair previously had been used under the SSP HDC test program for approximately four months and was restarted for this test program on 8 September 1972. The inlet conditions to the cell were maintained at 68°F dew point, 74°F dry bulb, 3.00 mm Hg CO_2 partial pressure and 21 percent oxygen. The cell was operated at a constant current of 16 asf, except at the very low inlet H_2 flow rates where the current dropped off to a low of 14.2 asf. Nitrogen purging of the cell was done daily for approximately 5 minutes duration. The test data presented on figures 43 through 45 show that current efficiency (normalized) is not significantly affected by hydrogen flow rate. However, the power output of the HDC is reduced at the lower H_2 inflow rates below a stoichiometric flow of 3.0. This drop off in power below a stoichiometric flow of 3.0 will not present a problem to the WVE/HDC system since the WVE at 50 asf will produce sufficient H_2 to maintain a stoichiometric flow about 3.0.

HDC VERIFICATION TEST

The objective of this 90 day test program was to verify that the HDC cell pair modifications derived during the development phase of this program, would decrease the voltage decay rate and improve the CO_2 removal rate of the cell pair.

The cell pairs, reference figure 1, were of the following configuration:*

<u>Item</u>	<u>Cell Pair S/N 021</u>	<u>Cell Pair S/N 022</u>
Anode	PPF	Same
Cathode	DS 16-0	Same
Matrix	2 Sheets of (0.020 inches each) Fuel cell asbestos with 1 sheet of (0.018 inches Tissuquartz in the center	Same
Compressed Thickness Matrix	0.025 inches	Same
Electrolyte	Cs_2CO_3	TMAC
Outer Housings	Titanium Housings Platinum Plated (SVSK 83638 B) rolled to provide 0.060 inches concave curvature	Same

* Detail cell pair description and drawings are defined in reference (1).

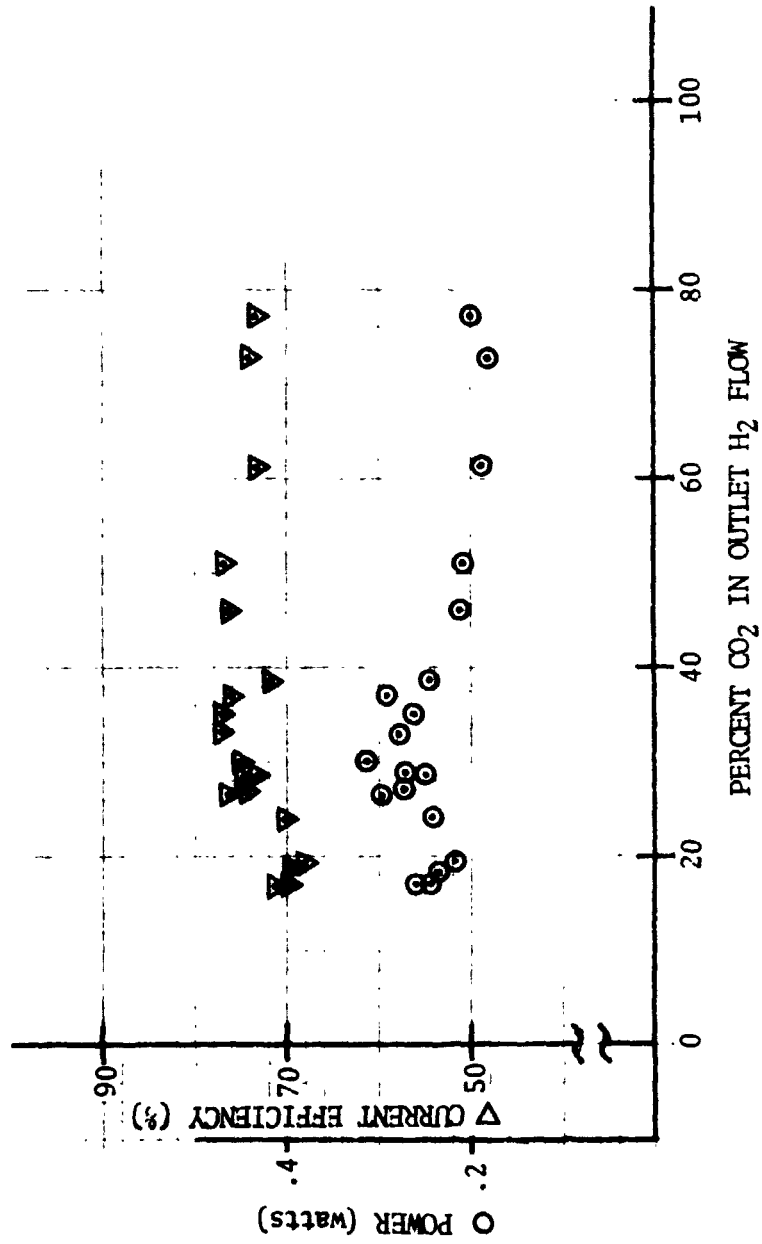


FIGURE 43. HDC HYDROGEN FLOW TEST RESULTS PERCENT CO₂ VERSUS POWER AND EFFICIENCY

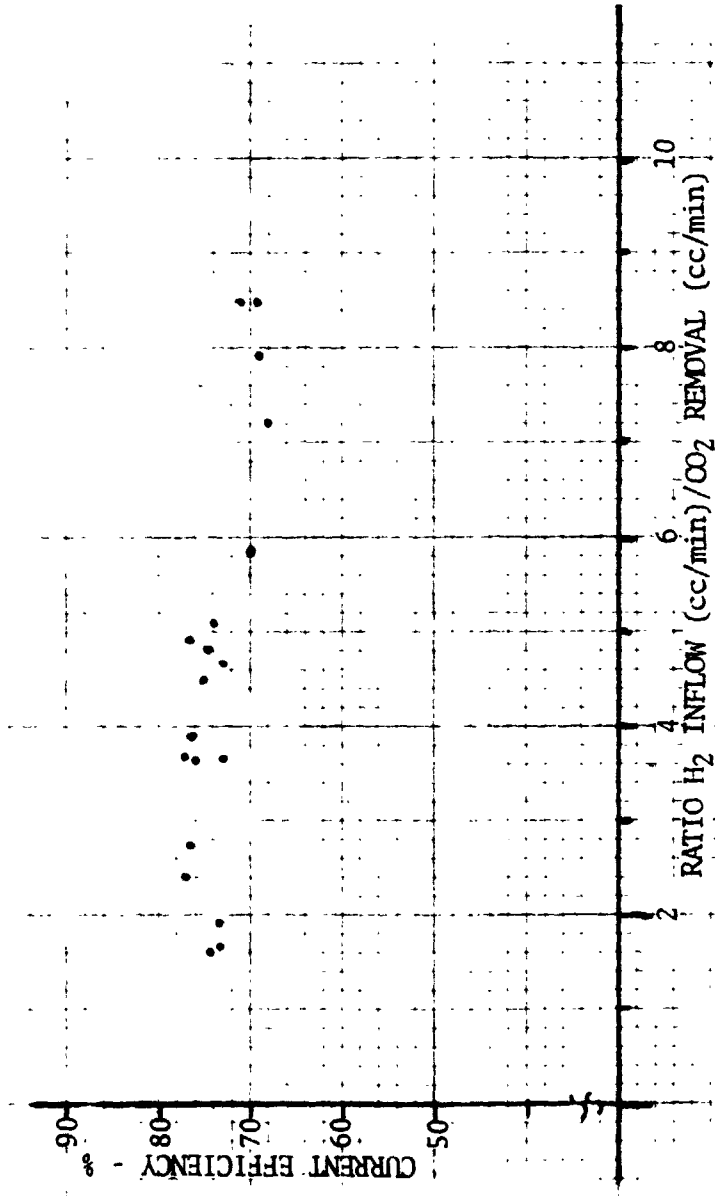


FIGURE 44. HDC HYDROGEN FLOW TEST RESULTS H₂/CO₂ REMOVAL VERSUS EFFICIENCY

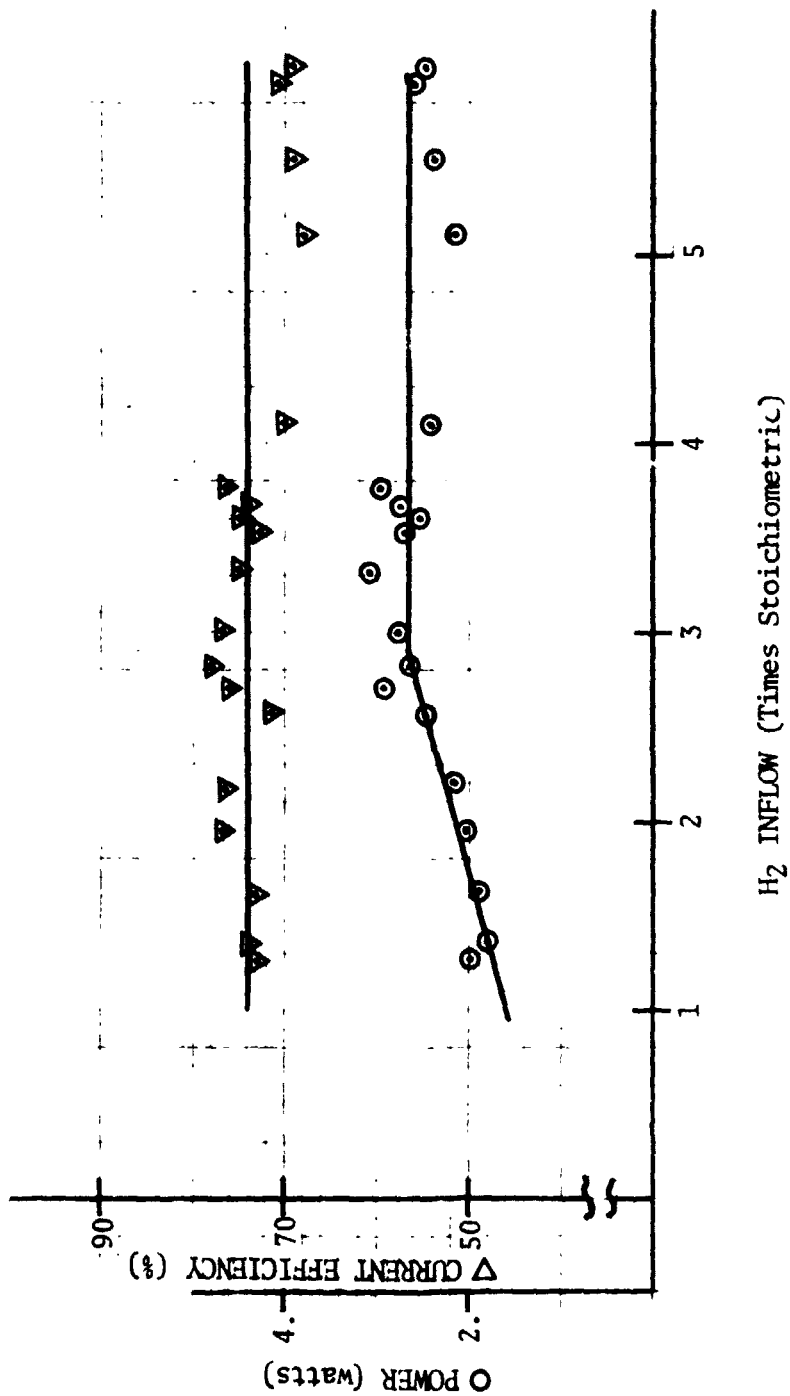


FIGURE 45. HDC HYDROGEN FLOW TEST RESULTS H₂ STOICHIOMETRIC FLOW VERSUS POWER AND EFFICIENCY

<u>Item</u>	<u>Cell Pair S/N 021</u>	<u>Cell Pair S/N 022</u>
Center Housing	Titanium Housing Gold Plated (SVSK 83639 B) with a H ₂ serpentine path of 0.060 inches width	Same

Testing of these cell pairs was done in individual test chambers as defined by figure 46 and schematically by figure 47. The facility consisted of separate plexi-glass chambers, automatic data recorder, facility support equipment which maintained the chamber environment (P_{CO_2} , P_{O_2} , temperature and dew point) and cell pair current, and instrumentation for monitoring all the desired rig and cell parameters.

Verification testing of the two HDC cell pairs was conducted in accordance with the approved Master Test Plan, Test Number X (Appendix). The scope of the test plan was to establish parametric and endurance test data on the two types of HDC electrolytes at various levels of P_{CO_2} and temperatures.

Cell Pair S/N 021 Testing

Cell pair S/N 021 operated satisfactorily for 40 days with an average CO_2 removal of 84% and an average voltage decay rate of $58 \mu v/hr$ until a malfunction in the test facility caused the unit to flood with the loss of considerable electrolyte. During reconditioning at $52^\circ/45^\circ F$ a hydrogen leak developed and the cell was rebuilt with the same electrodes. At this time the electrode spacing was increased from the normal 25 mils to 35 mils in an attempt to increase the CO_2 transfer efficiency.

After this rebuild (test period 42nd-58th day) the cell power decayed rapidly as shown in figure 48. Potential decay curves of the anode and cathode of Cell Pair S/N 021 revealed a loss of active anode surface area but little change in the cathode. Just prior to shutdown for disassembly, attempts were made to restore cell power via the methods of open circuit, nitrogen purge, and vacuum on the hydrogen side, but the cell was not respondent to any of these treatments. Upon disassembly of the cell pair all components looked normal except the anode. Approximately 40 percent of the anode area contained a white precipitate, predominant on the hydrogen side but extending into the electrode structure as shown in figures 49a and 49b. This precipitate was found to be quite insoluble in water compared to cesium bicarbonate. Spectrographic analysis of the precipitate revealed silica as the major component with trace amounts of magnesium and calcium.

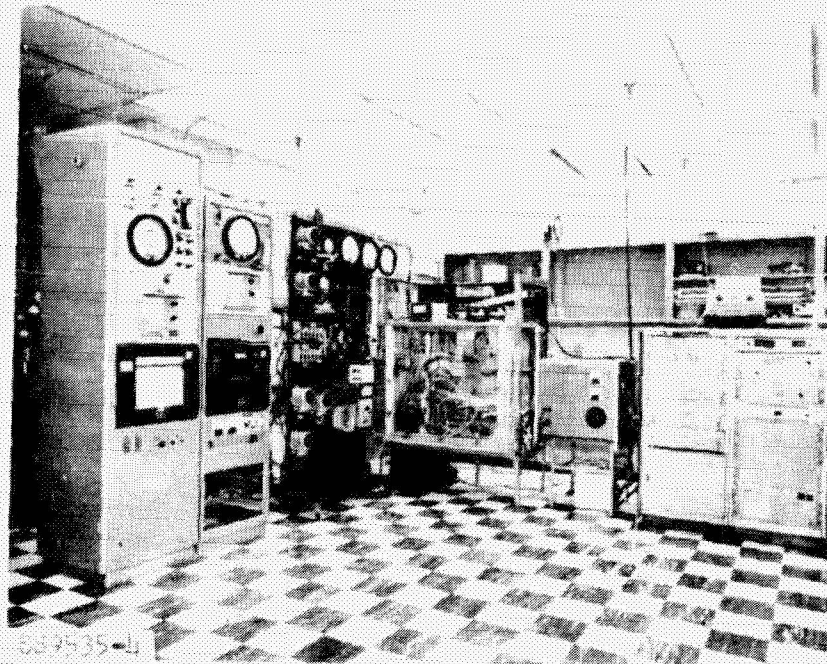
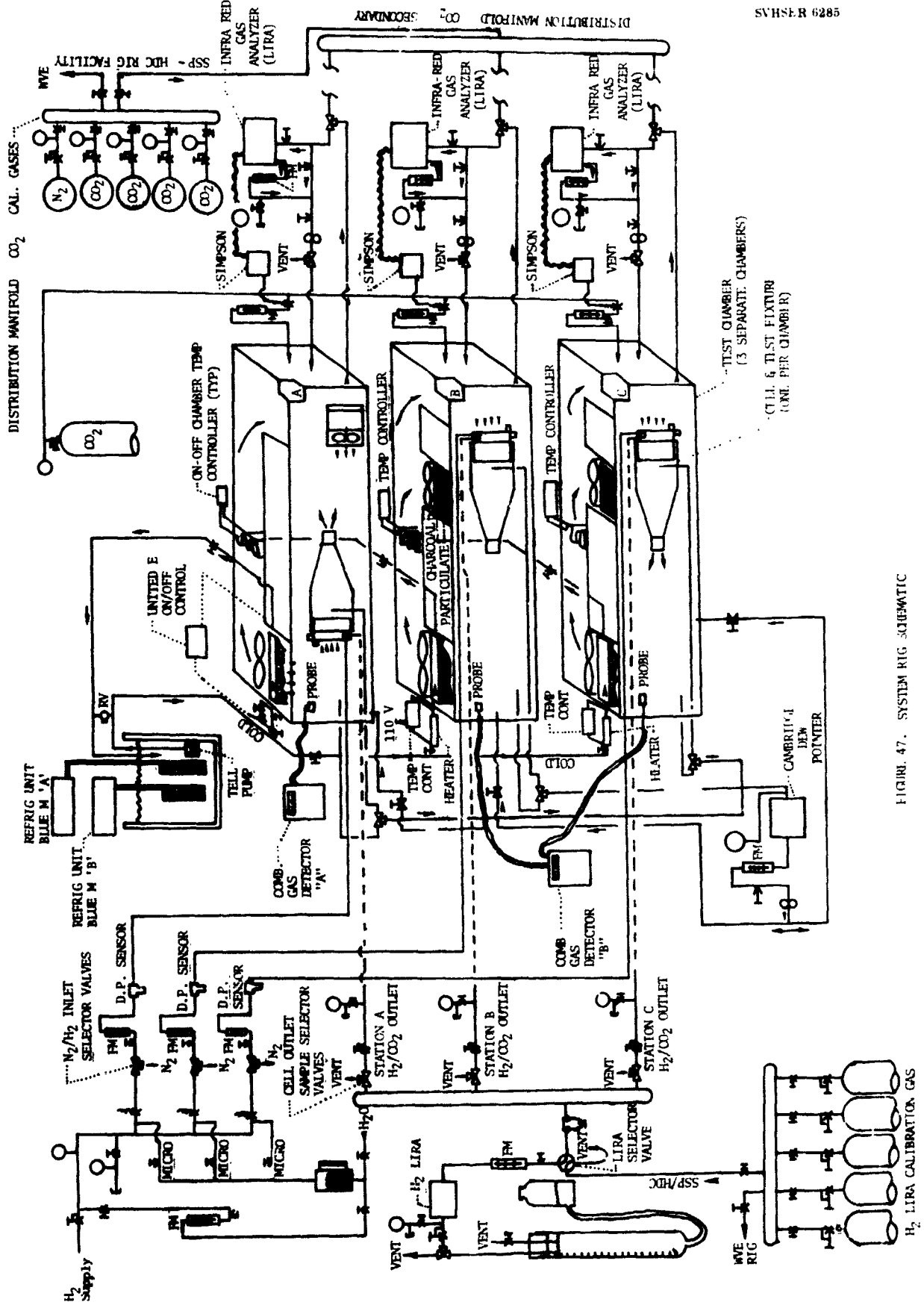


FIGURE 46. ELECTROCHEMICAL TEST FACILITIES



989 R 585A

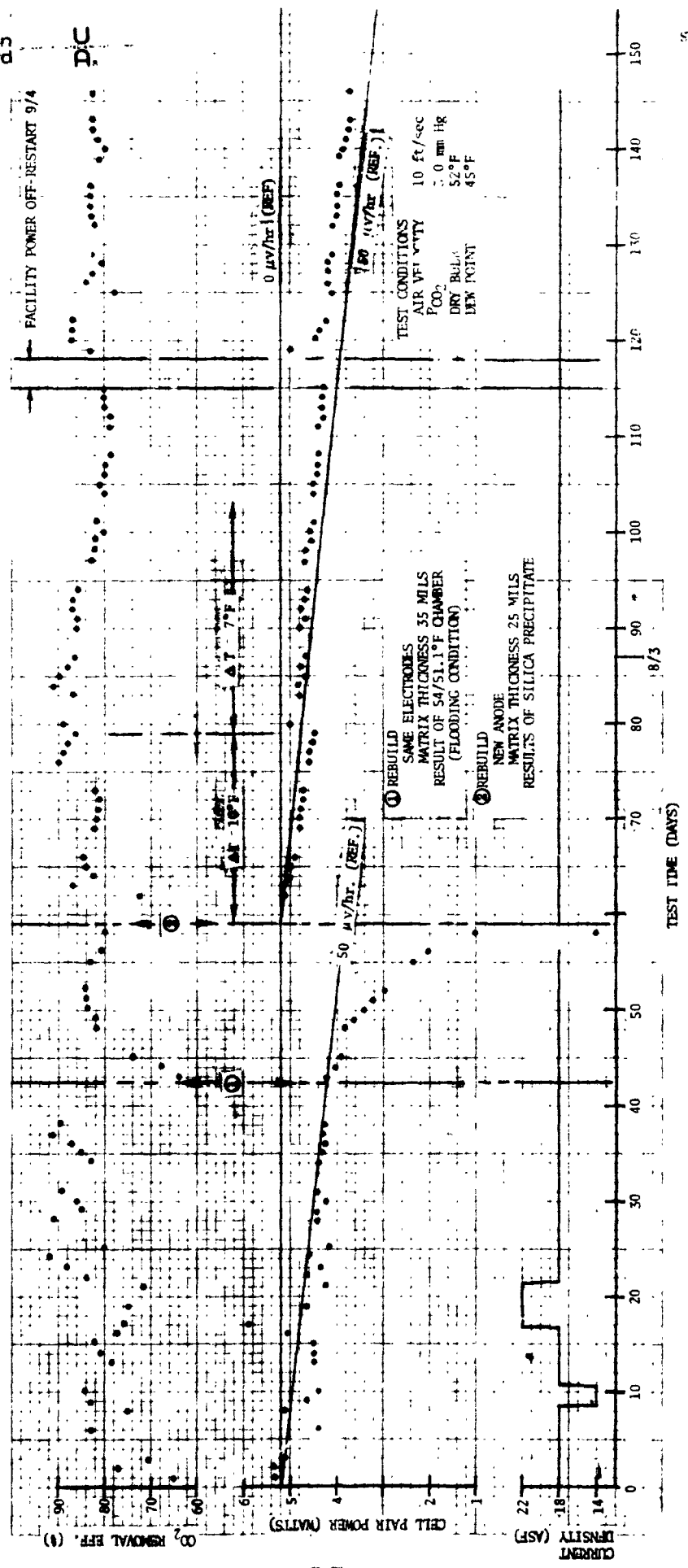
FIGURE 47. SYSTEM RIG SCHEMATIC

Hamilton
Standard

10 V. DISTENSION GRAPH PAPER
D.S. 7.5 IN. X 10 IN.

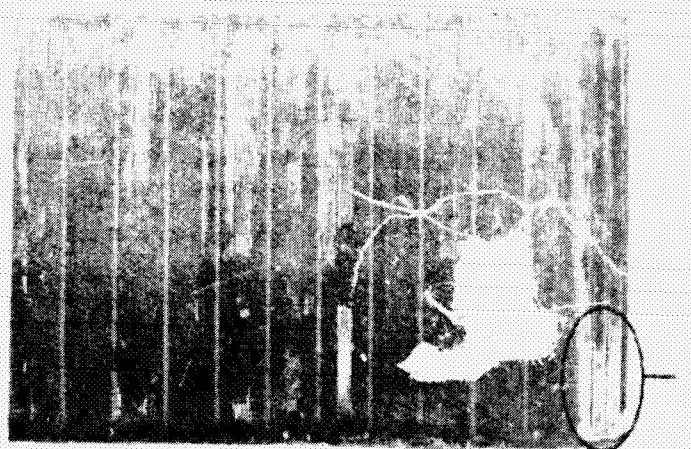
ELREK DIFFEREN. CO
MADISON, WIS.

10 X 10 PER INCH
DISTENSION GRAPH PAPER



SVHSER 0255

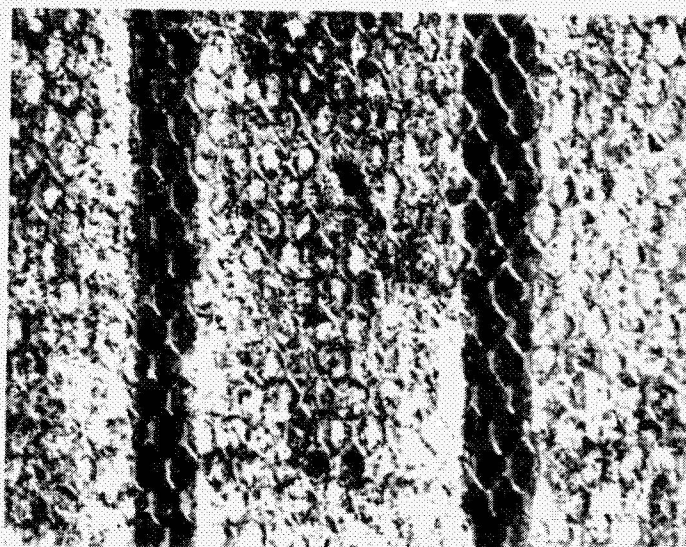
FIGURE 48. HDC CELL PAIR S/N 021 (C₅₂CO₃) PERFORMANCE VS. TIME



49 a

Mag = 0.4 x

MAGNIFIED VIEW OF SECTION A



49 b

Mag = 6 x

FIGURE 49. CELL S/N 021 ANODE

This was the first time an insoluble precipitate had been found in the anode structure although some modification of the asbestos structure from fibrous to amorphous at the anode-matrix interface had been noted in the past. SEM photographs of a normal and a modified matrix from Cell Pair S/N 018 are shown in figures 50a and 50b, respectively. Figure 50a shows the normal fibrous structure from near the center of the cell matrix and figure 50b the modified structure at the anode-matrix interface. Apparently the anolyte pH is low enough to cause some attack of the asbestos at the interface, and this appears to be the reason for the matrix sticking to the anode.

The asbestos matrix is chrysotile ($Mg_6(OH)_8Si_4O_{10}$), a basic magnesium silicate. Acid attack of chrysotile dissolves the magnesium leaving a silica structure. Apparently the anolyte pH of Cell Pair S/N 021 was low enough to dissolve the matrix, at a relatively rapid rate, and the silica with a negative charge migrated toward the hydrogen side of the anode.

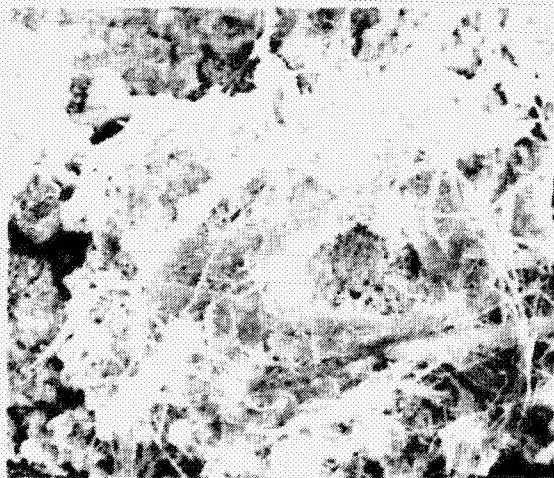
The only difference in the Cell Pair S/N 021 build-up which could enhance matrix attack was the increase in matrix thickness from 25 to 35 mils which would result in a lower anolyte pH. The reason for the lower anolyte pH is that the cesium ion concentration decreases from cathode to anode because of the potential gradient, and at a fixed catholyte concentration the anolyte concentration would be significantly reduced in going to a 35 mil electrode separation (see figure 51). From thermodynamics it is known that the anolyte pH is a function of the cesium ion concentration and the equilibrium CO_2 partial pressure. As shown in figure 52 a reduction in the cesium ion concentration at constant P_{CO_2} results in a decrease in anolyte pH.* It is reasonable to assume that the dissolution rate of chrysotile is directly proportional to the hydrogen ion concentration, which would be equivalent to an exponential function of pH. Therefore a one unit decrease in pH would increase the dissolution rate by a factor of ten.

It can be rationalized that the increase in matrix thickness to 35 mils reduced the anolyte pH sufficiently to result in a relatively rapid matrix dissolution and subsequent blockage of the anode pores with silica. With TMAC electrolyte the problem of matrix attack is greatly reduced because the anolyte pH is higher as found from analytical cell testing. This also is supported by the fact that there is much less tendency for the asbestos matrix to bond to the anode surface in TMAC cells.

* The equilibrium partial pressure of CO_2 also has a large effect on anolyte pH; however, there is some evidence that the CO_2 evolution reaction is not at equilibrium, and if this is the case the CO_2 partial pressure in the hydrogen would have a much smaller effect on anolyte pH.



A



B

FIGURE 50. SEM PHOTOGRAPH OF UNMODIFIED (A) AND MODIFIED (B) ASBESTOS MATRIX

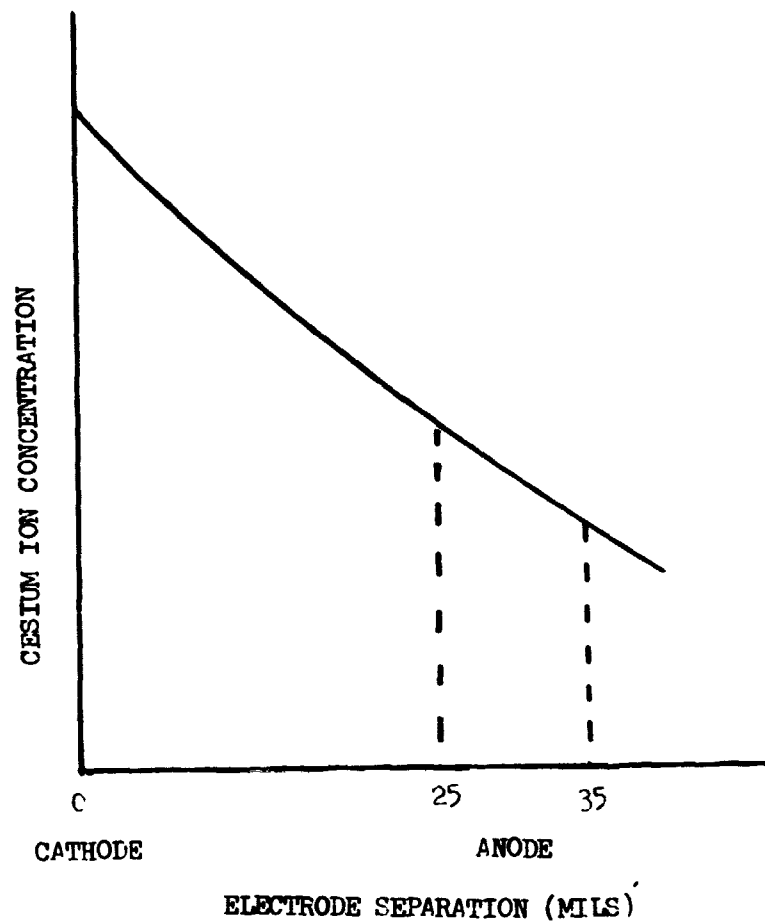


FIGURE 51. ILLUSTRATION OF CESIUM ION CONCENTRATION CHANGE WITH ELECTRODE SEPARATION

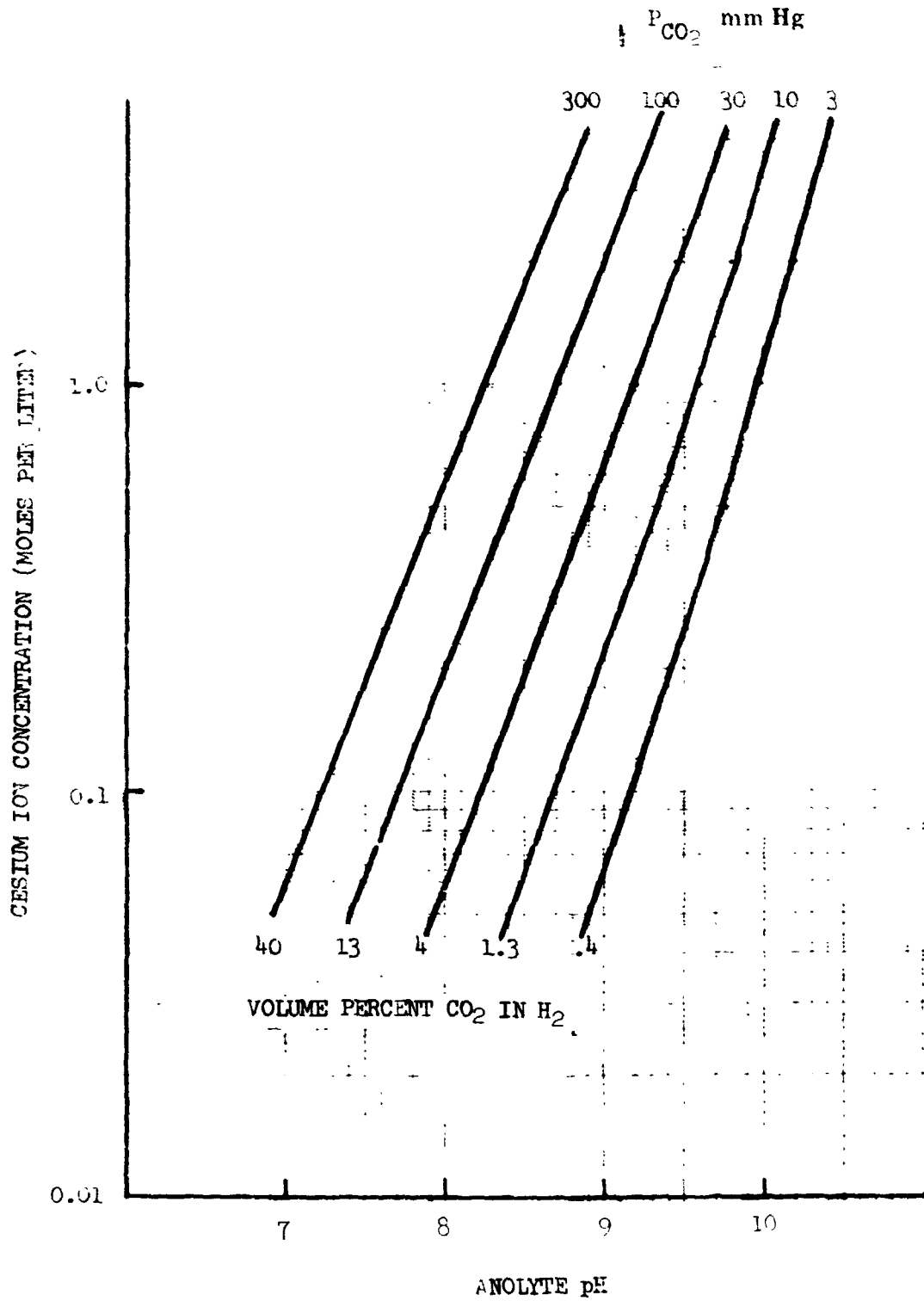


FIGURE 52. RELATIONSHIP BETWEEN CESIUM ION CONCENTRATION, ANOLYTE pH AND P_{CO_2}

A number of possibilities exist for preventing or minimizing the matrix dissolution problem in the future to achieve long term cell life.

- The electrode spacing could be reduced to 20 mils with a small sacrifice ($\approx 3\%$) in CO_2 transfer efficiency.
- A more acid resistant matrix material could be used (Neoprene asbestos).
- A dual-porosity sinter-type anode could be used to isolate the matrix from the low pH anolyte region.

The only one of these suggested changes which would eliminate the dissolution of the matrix would be the second one, a more acid resistant matrix. The suggested matrix material of Neoprene asbestos has been used in the WVE cell pair (H_2SO_4 electrolyte) very successfully and should be suitable for the HDC cell pair.

Cell Pair S/N 021 was reassembled on the 59th day using new electrodes and a matrix thickness of 0.025 inches. The performance of the rebuilt cell pair, at 18 asf during the remainder of the test program was a CO_2 removal efficiency of 83 percent (average) and power voltage decay of less than $50 \mu\text{v}/\text{hour}$. The noticeable decrease in power followed by a step increase during the 74th to 80th day test period resulted from first, a low chamber dew point (ΔT of 10°F), which is on the borderline condition for forming cesium bicarbonate precipitate that caused a low cell power, and second, an increase in chamber dew point to obtain a temperature - dew point difference of 7°F , causing an increase in power output (5.0 watt). The unit was removed from test after successfully completing 90 days of testing.

Cell Pair S/N 022 Testing

During the initial parametric testing (figure 53) of Cell Pair S/N 022 (TMAC unit) the test fixture fan failed causing the unit to operate without any cooling air which caused flooding of the unit and a permanent loss of electrolyte. For the next fifteen days of operation, after replacement of the fixture fan and addition of concentrated electrolyte to the cell pair reservoir, the unit slowly increased its output power, but not sufficiently to warrant continuation of the test. The unit was rebuilt, using the same electrodes but fresh matrix and electrolyte, and resumed testing. After the parametric testing at $52/45^\circ\text{F}$ (61st day) the inlet air conditions were changed to room air (temperature $\approx 74^\circ\text{F}$, dew point $\approx 60^\circ\text{F}$ and $\text{PCO}_2 \approx 1/4$ mm Hg). The warmer inlet air and the low PCO_2 caused an initial increase in power, to a peak of 5 watts. After several days at this condition the cell power stabilized at 2.5 watts. The following 40 days of the testing was done at room air temperature and dew point but at 3.0 mm Hg PCO_2 . The average voltage decay rate of this unit for the entire test period was less than $50 \mu\text{v}/\text{hour}$ and provided an average CO_2 removal efficiency of ≈ 72 percent. The last portion of the test was conducted at room air conditions, including PCO_2 , which caused the power to increase and the CO_2 removal to decrease ($\approx 16\%$).

NO 343 D. DIETZEM DRAWING PAPER
13 X 10 PER INCH

LUDWIG DIETZEM CO
MADE IN U.S.A.

NO 343 D. DIETZEM DRAWING PAPER
13 X 10 PER INCH

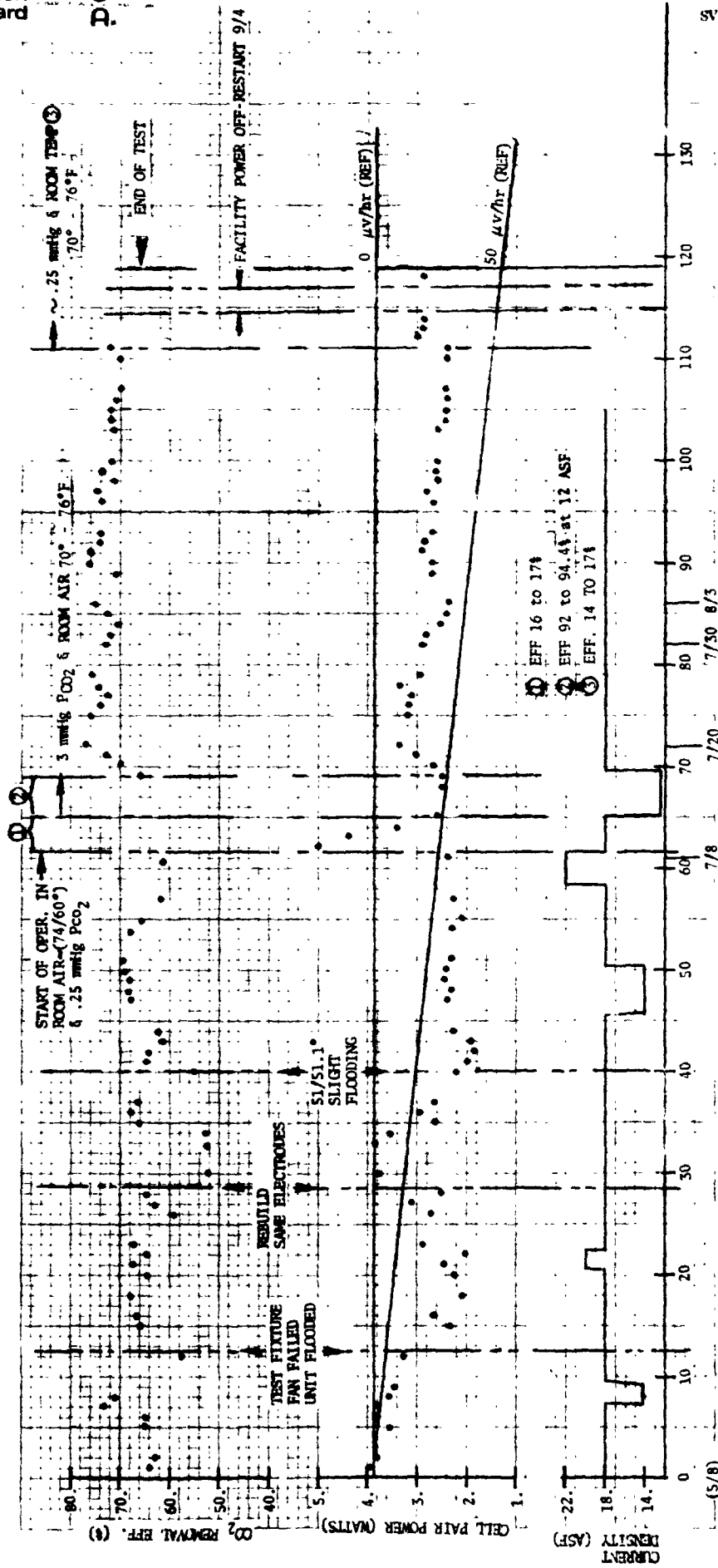


FIGURE 53. HDC CELL PAIR S/N 022 (MAC) PERFORMANCE VS TIME

WVE CELL PAIR VIBRATION TEST

The WVE cell pair which had been assembled and tested for 3940 hours under the previous contract, NAS 9-11830, was restarted on August 30, 1972 to obtain a performance base line prior to vibration tests. The complete history of this WVE cell pair is given in Table XX. The performance prior to vibration, (figure 54) was 53 asf at 1.7 vdc for an inlet air condition of 68°F dew point and 75°F dry bulb. The unit was removed from test and vibrated in all three axes to the Apollo launch levels indicated in figures 55-57. The unit was not damaged structurally or electrochemically, did not leak, and did not release any free electrolyte from the cell. A very small amount of electrolyte (2-3 drops) was released from the reservoir area. This loss of electrolyte would not be expected in a flight type unit, with reservoir housings made of metal instead of plexiglass.

The initial performance of the WVE after vibration and 145 hours of non-operation was slightly lower than previous performance; approximately 47 asf at 1.7 v, however, the performance slowly increased as the cell pair continued to operate (figure 52). At the completion of the post vibration test, 5279 hours total operation time, the performance was 49 asf at 1.7 volts and the post vibration test was completed. This slight change in performance from the pre-vibration testing is considered acceptable.

Upon shutdown of the WVE, it was determined that the inlet to the cells hydrogen passage was blocked because the nitrogen purge gas was not purging out the hydrogen.

Visual examination of the WVE after vibration revealed some flaking of the gold plating on the outside surfaces of the center housing. The disassembly of the WVE cell pair, after the post vibration base line test, revealed that the gold plate of the titanium center housing internal to the cell also was flaking in certain areas (figure 58), and there was evidence of a slight titanium corrosion in these areas. A detail examination of the center plate by the Hamilton Standard Material Engineering group revealed that the gold plate was somewhat porous allowing gradual attack of the titanium by the sulfuric acid electrolyte which caused a weakening of the gold-titanium bond. The vibration may have contributed to the flaking in the weakened bond areas, making the problem more evident, but it certainly was not the original cause. A different type of plating procedure will be used in the future. This will provide a better gold-titanium bond and a less porous gold plate.

**TABLE XX
WVE CELL PAIR HISTORY**

Date	Event	NASA/MSC Contract
10/71	Hardware Manufacture	NAS 9-11830
11/18/71	Initial Assembly	NAS 9-11830
11/18-71- 12/2/71	Cell Was Operated (181 Hours)	NAS 9-11830
12/2/71	Final Assembly	NAS 9-11830
12/2/71- 5/12/72	Cell Was Operated (3940 Hours)	NAS 9-11830
5/12/72	Cell Was Removed From Test and Put In Storage	No Contract
8/30/72	Restart of Cell	NAS 9-12920
8/30/72- 10/12/72	Cell Was Operated (1028 Hours)	NAS 9-12920
10/12/72	Removed From Test For Vibration Test	NAS 9-12920
10/17/72	Cell Vibrated	NAS 9-12920
10/18/72- 10/31/72	Cell Operated (311 Hours) Post Vibration Baseline	NAS 9-12920
10/31/72	Cell Removed From Test and Disassembled	NAS 9-12920
Total Operating Time		5460 Hours
Total Time Assembled		11.5 Months

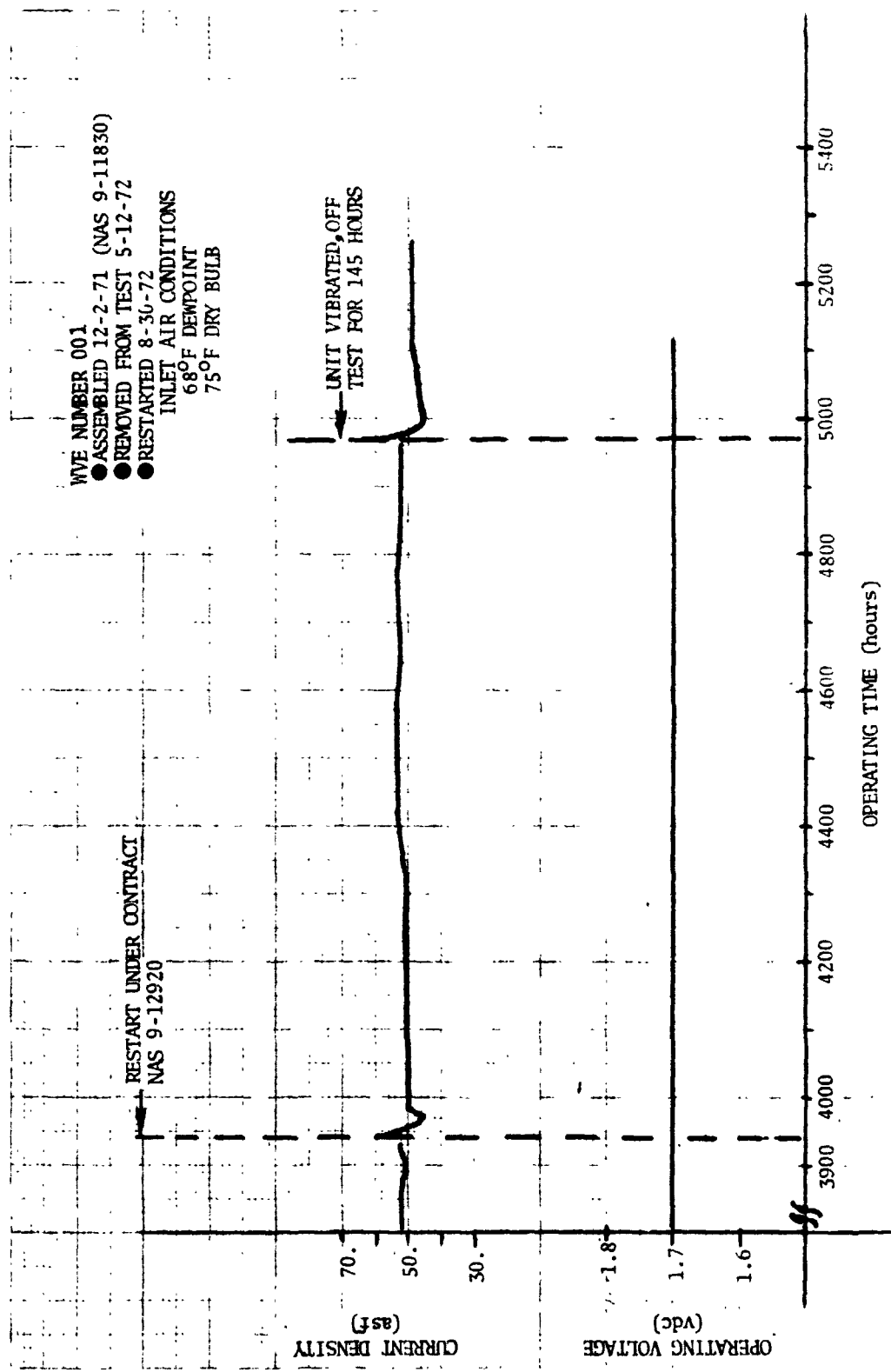


FIGURE 54. WVE PERFORMANCE DATA VERSUS OPERATING TIME

**RANDOM VIBRATION TEST
 ANALYSIS METHOD A**

MSF-1634A	TEST ENGINEER	WITNESS
PLOTTED BY <i>M. J. A.</i>	BRADFORD	
PROJECT Ms 9-12930	SERIAL NO. 03	TYPE OF TEST DKT
SPEC. ECS-2128-1-031	ATA NO.	DATE 19/17/73
ITEM RESERVOIR CELL PAIR	ACTION SHEET NO.	TEST NO. 7
PHASE RANDOM		

EXCITATION ALONG X	AXIS
GRMS INPUT 11.25	
NON-OPERATING	
TEMP. 75	°F
PERIOD OF TEST	START <input checked="" type="checkbox"/> END <input type="checkbox"/>
DURATION OF TEST 2.5	MIN.
ACCEL. SERIAL NO. WRI	
ACCEL. SENSITIVITY	MV RMS / GP
2.996	COL. / GP
ACCEL. SENSING	AXIS
X	
ACCEL. LOCATION Ax	
TAPER REEL NO. 612 3Y0	
SPECIAL CONDITIONS	
REPORT NO. SVHSER 6285 5	

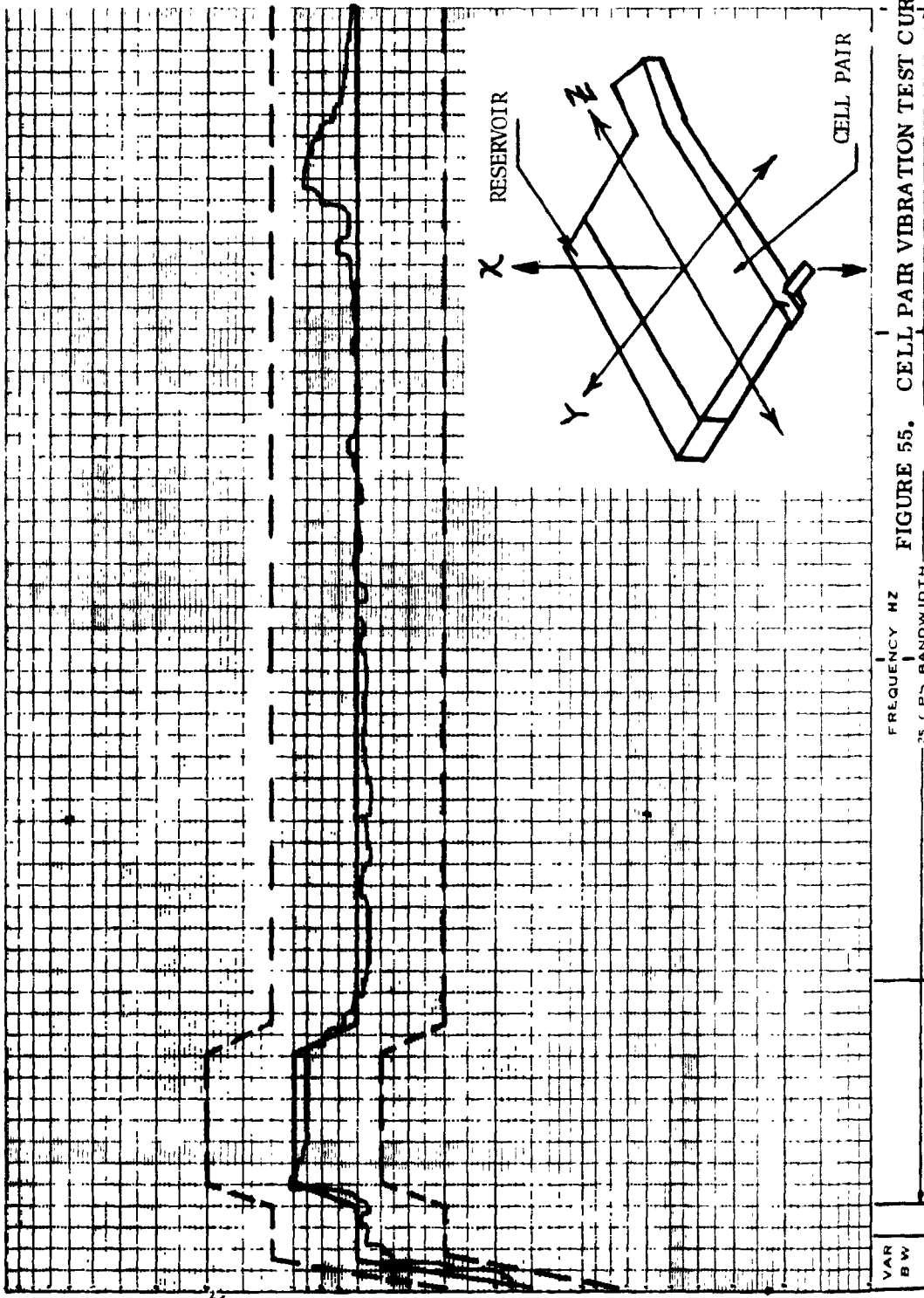
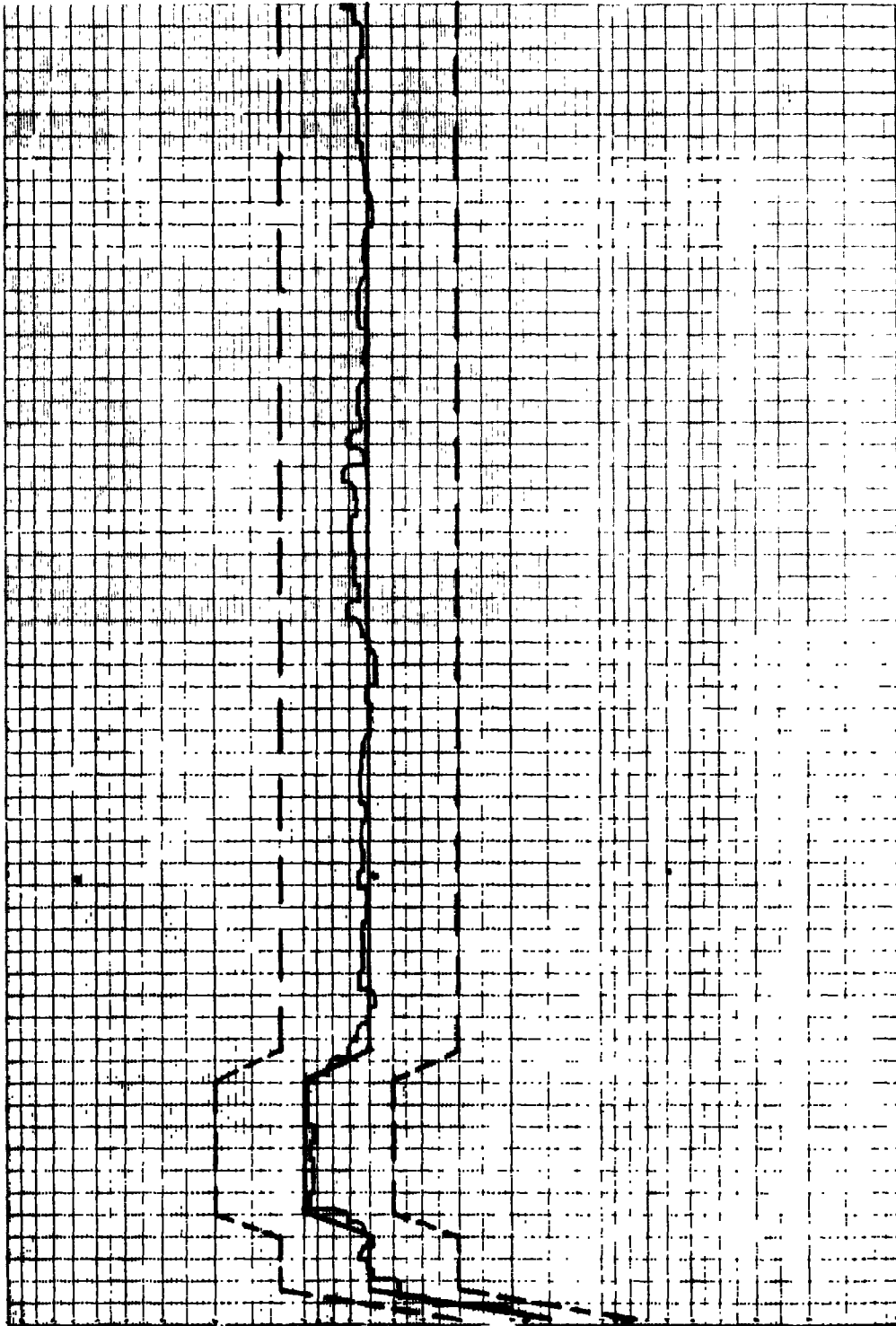


FIGURE 55. CELL PAIR VIBRATION TEST CURVE FOR X AXIS

RANDOM VIBRATION TEST ANALYSIS METHOD A

MSF-1634A	TEST ENGINEER	WITNESS
PLotted BY <i>MARLET</i>	<i>MARLET</i>	
PROJECT NAS 9-12930	SERIAL NO. 03	TYPE OF TEST DVT
SPEC. EGS-2128-1-035	ATA NO.	DATE 10/17/72
CHECKED BY <i>D. J. F.</i>	ACTION SHEET NO.	TEST NO. 6
ITEM RESERVOIR CELL PAIR		
PARA. -		
PHASE RANDOM		

EXCITATION ALONG AXIS <i>Y</i>	GRMS INPUT <i>11.05</i>
NON-OPERATING	TEMP. <i>75</i> °F
PERIOD OF TEST <input checked="" type="checkbox"/> START <input type="checkbox"/> END	DURATION OF TEST <i>2.5</i> MIN.
ACCEL. SENSITIVITY <i>1629</i>	ACCEL. SERIAL NO.
MV RMS <i>2.677</i>	GP
COL <i>GP</i>	GP
ACCEL. SENSING <i>Y</i>	ACCEL. LOCATION <i>AY</i>
TAPER REEL NO. <i>012340</i>	SPECIAL CONDITIONS



REPORT NO. SVHSER 6285
 FIGURE 56. CELL PAIR VIBRATION TEST CURVE FOR Y AXIS

RANDOM VIBRATION TEST ANALYSIS METHOD A

MSF-1634A	PLOTTED BY MICKET	CHECKED BY SJA	TEST ENGINEER BRADFORD	RIG NO. 26	WITNESS ---
PROJECT NAS 9-12920	ITEM WAVE RESERVOIR CELL PAIR	ATA NO. ---	ATA NO. ---	SERIAL NO. 03	TYPE OF TEST DVT
SPEC. CC-2128-4-035	PARA. RANDOM	DATE 10-18-72	DATE 10-18-72	ACT ION SHEET NO. ---	TEST NO. 5

EXCITATION ALONG Z	AXIS Z
GRMS INPUT 11.25	NON-OPERATING
TEMP. 75	°F
PERIOD OF TEST <input checked="" type="checkbox"/> START <input type="checkbox"/> END	
DURATION OF TEST 2.5	MIN.
ACCEL. SERIAL NO. VL31	
ACCEL. SENSITIVITY 2.628	MV RMS / GP
ACCEL. SENSING Z	AXIS
ACCEL. LOCATION Az	
TAPER REEL NO. 012340	
SPECIAL CONDITIONS	

REPORT NO.
SVHSER 6285

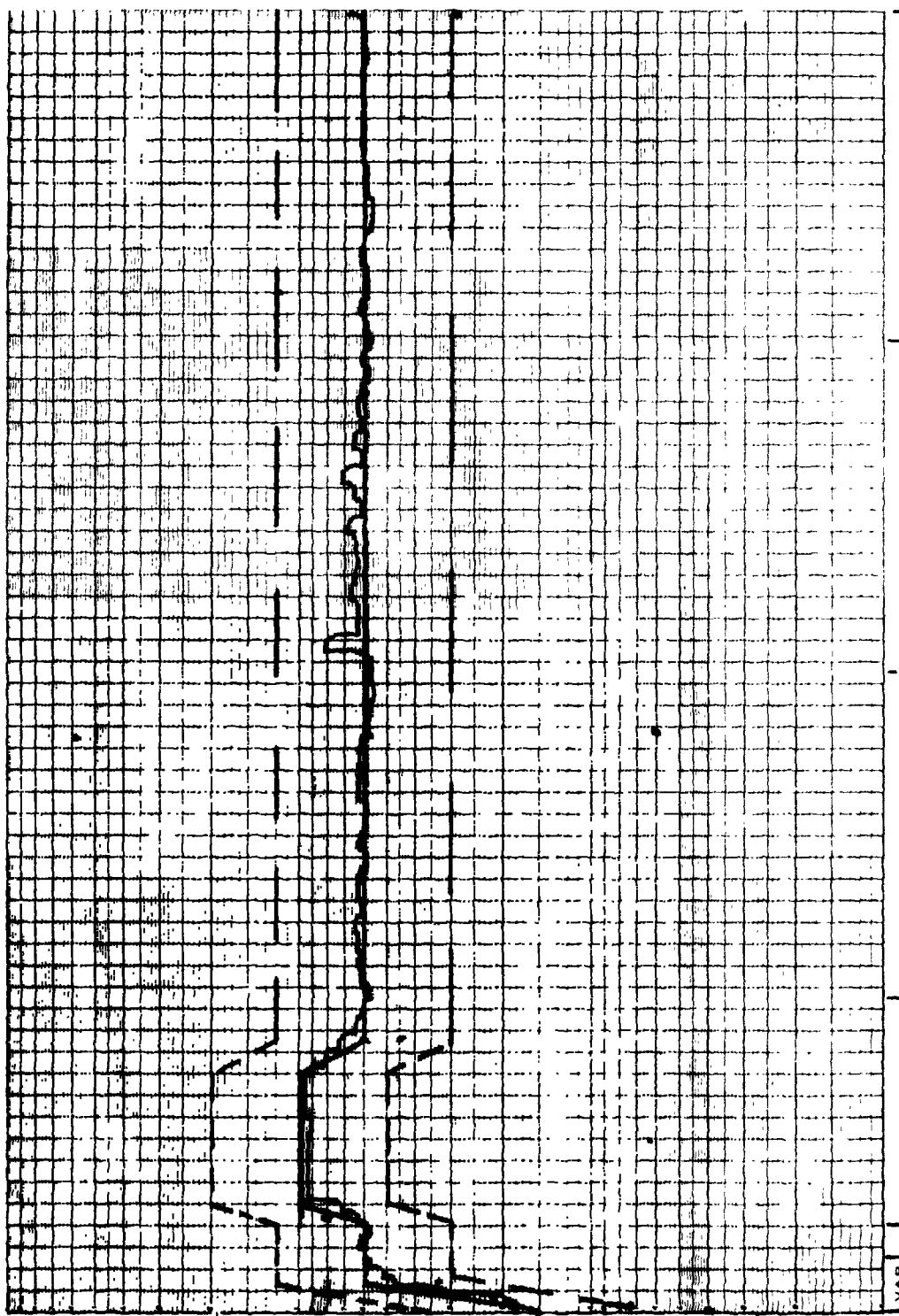


FIGURE 57. CELL PAIR VIBRATION TEST CURVE FOR Z AXIS

REPRODUCIBILITY OF THE ORIGINAL PAGE IS POOR.

Hamilton
Standard

U
A.

SVHSER 6285

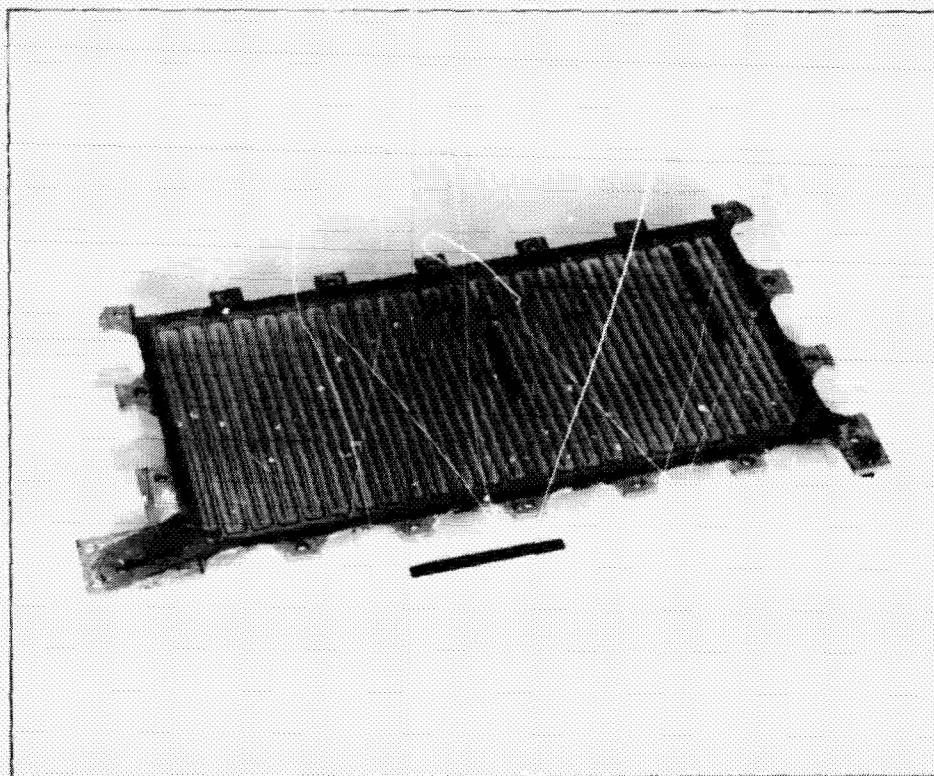
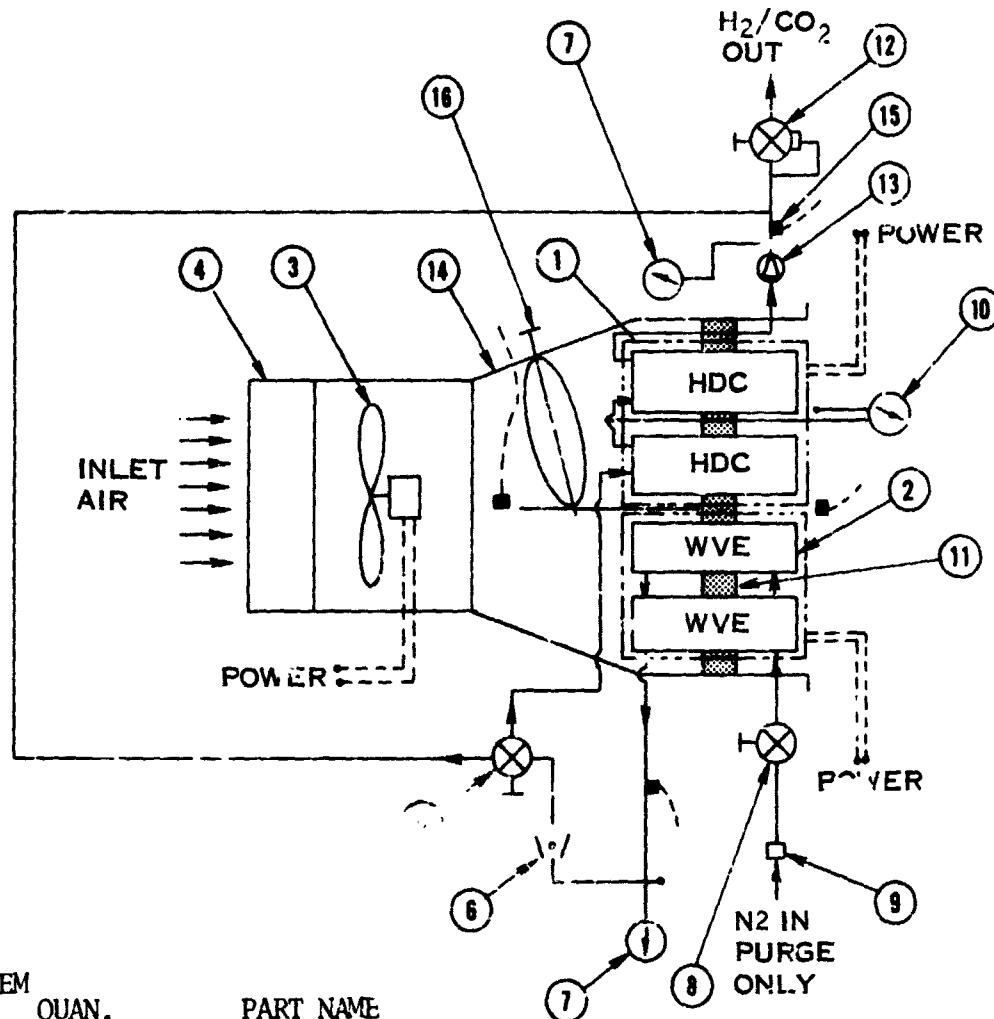


FIGURE 58. WVE CENTER HOUSING (ANODE SIDE)

WVE/HDC BREADBOARD FABRICATION

The Integrated WVE/HDC Breadboard unit illustrated schematically by figure 59, was designed under the previous WVE/HDC contract, NAS 9-11830, and manufactured and assembled during this program. The Integrated WVE/HDC Breadboard unit consisted of four cell pairs (2 WVE and 2 HDC), an air blower, miscellaneous valving and instrumentation incorporated into one package as shown by figure 60. This packaging provided parallel air flow through the cells, hydrogen gas manifolding between the cell pairs (HDC's in series and WVE's in parallel), provisions for isolating the HDC cell pairs, and means to monitor cell pair performance.

Testing of this unit was not conducted because of program redirection. The four cell pairs (2 WVE and 2 HDC) that were used for assembly and air flow checkout were not electrochemically functional.



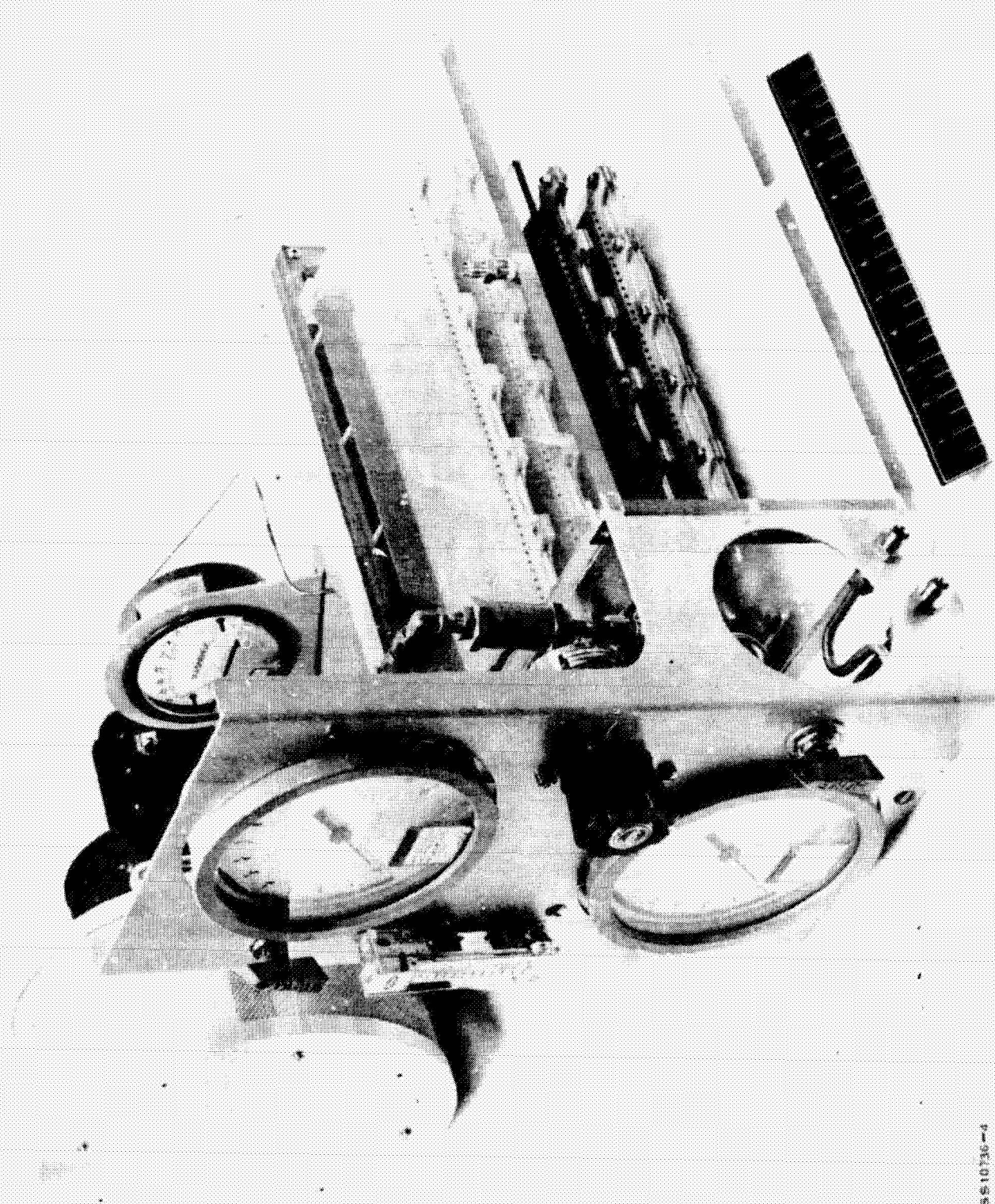
ITEM NO.	QUAN.	PART NAME
16	1	DUCT CONTROL VALVE
15	4	TEMPERATURE SENSOR
14	1	HOUSING
13	1	CHECK VALVE
12	1	BACK PRESSURE REGULATOR
11	AR	SPONGE RUBBER
10	1	DIFFERENTIAL PRESSURE GAGE
9	1	SWAGELock FITTING
8	1	SHUT-OFF VALVE
7	2	PRESSURE GAGE
6	1	FLOW METER
5		MANUAL VALVE 3 WAY
4	1	CHARCOAL FILTER
3	1	FAN
2	2	WATER VAPOR ELECTROLYSIS CELL
1	2	HYDROGEN DEPOLARIZED CELL

FIGURE 59. INTEGRATED WVE/HDC BREADBOARD SCHEMATIC (SVSK 83513)

Hamilton
Standard

U
DIVISION OF UNITED AIRCRAFT CORPORATION
A_®

SVHSER 6285



561030-4

FIGURE 60. INTEGRATED WVE/HDC BREADBOARD SYSTEM

RELIABILITY/QUALITY ASSURANCE/SAFETY SUMMARY

The following is a summary of the effort performed during the various tasks of this program in the areas of Quality Assurance, Reliability and Safety.

- The successful demonstration of the WVE cell pair to withstand launch vibration loads verified that the cell pair design for both HDC and WVE systems is safe for flight use and will not release free electrolyte.
- The disassembly of the WVE cell pair (after approximately one year of assembly) revealed a poor gold plating of the center housing. Future plating of the cell pair housing will be done at Hamilton Standard where improved control can be applied to the various steps of the plating operation.
- In order to assure consistently high quality of electrodes for future cell pairs, Hamilton Standard will prepare electrode fabrication operation sheets and will use quality control surveillance during the fabrication of electrodes.
- All HDC cell pair malfunctions which occurred during testing were resolved and corrective action instituted to prevent the recurrence of each malfunction. As a result of this positive type failure analysis, the HDC has become a more reliable unit during this program.

REFERENCES

1. "Development of an Integrated Water Vapor Electrolysis Oxygen Generator and Hydrogen Depolarized Carbon Dioxide Concentrator" by J. C. Huddleston and Dr. J. R. Aylward, NASA-JSC Report No. CR-115575, Hamilton Standard, Division of United Aircraft Corporation, Windsor Locks, Connecticut, May 1972. (NASA Contract NAS9-11830)
2. "Hydrogen Depolarized Cell Pair Definition for Space Station Application" by C. R. Russell, Hamilton Standard, Division of United Aircraft Corporation, Windsor Locks, Connecticut, March 1973. (NASA Contract NAS 9-12920)
3. "A Simple Method for Measuring the Overvoltage of Hydrophobic Gas Diffusion Electrodes" by J. Giner and S. Smith, Electrochem. Tec. 5, 59 (1967).

APPENDIX

MASTER TEST PLAN

MASTER TEST PLAN

IMPROVED MULTI-CELLED BREADBOARD
ELECTROCHEMICAL OXYGEN-GENERATION
AND CARBON DIOXIDE CONTROL SYSTEM

PREPARED UNDER CONTRACT NAS 9-12920

by

HAMILTON STANDARD

DIVISION OF UNITED AIRCRAFT CORPORATION

WINDSOR LOCKS, CONNECTICUT

for


NATIONAL AERONAUTICS AND SPACE ADMINISTRATION

MANNED SPACECRAFT CENTER

HOUSTON, TEXAS

AUGUST 1972

Prepared by:


J. C. Huddleston
Program Engineer

Approved by:

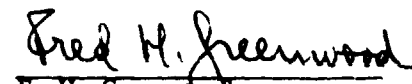

F. H. Greenwood
Program Manager

TABLE OF CONTENTS

	<u>Page</u>	
GENERAL INFORMATION	1	
TEST PLAN AND PROCEDURES	3	
Section I WVE/HBC Breadboard Test Plan	6	B
Section II WVE Vibration Test Plan	21	
Section III HDC Flow Improvement Test Plan	25	
Section IV Matrix Compression Test Plan	27	
Section V TMAC Electrolyte Analytical Test Cell	31	
Section VI Trace Impurities Test Plan	38	
Section VII Cs ₂ CO ₃ Electrolyte Analytical Test Cell	40	
Section VIII HDC Matrix Compression Set	46	
Section IX HDC Analytical Cell Tests	52	B
Section X HDC Cell Pair Tests	54	

1.0 GENERAL INFORMATION

1.1 Scope

The purpose of this Master Test Plan is to define the test methods and equipment which will be utilized to perform the various Water Vapor Electrolysis (WVE) and Hydrogen Depolarized CO₂ Concentration (HDC) cell pair, ~~breadboard~~ and electrolyte tests required under NASA/MSC contract NAS 9-12920. This test program will be conducted at Hamilton Standard, Space Systems Department, test facilities.

| B

1.2 Applicable Documents

NASA/MSC contract NAS 9-12920
Hamilton Standard Program Operating Plan for contract NAS 9-12920
~~WVE/HDC Cell Pair Breadboard Unit, SVSK 83513~~

| B

1.3 Functional Requirements

Unless otherwise specified, the following operating conditions* and requirements will apply to the testing of the WVE and HDC cell pairs.

| B

Standard operating conditions:

Air flow through cell pair	10 SCFM
Inlet air dry bulb temperature	70°F
Inlet air dew point temperature	53°F
Inlet Air CO ₂ partial pressure	3 mmHg
Oxygen concentration	20-21%

WVE operating requirements:

Nominal current density	60 asf (min at 2.0 VDC)
Maximum voltage	2.0 VDC
H ₂ production	Current x 7.48 scc/min
O ₂ production	Current x 3.74 scc/min

HDC operating requirements:

Nominal current density	16 asf
Min H ₂ inflow	350 scc/min
Current efficiency (design goal) @ 16 asf and 2.5 mmHg	75% = $\frac{\text{CO}_2 \text{ Removed (scc/min)}}{7.5 \times \text{current (asf)}}$

| B

* With exception to Table I of Test Number X, page 56.

| B

1.4 Test Condition Tolerances

Unless otherwise specified, the following tolerances will apply to the referenced test parameters:

Temperature	± 1°F
Pressure	± .1 psia
	± .02 inches of water
Dew Point	± 1°F
Voltage	± 0.01 volts
Current	± 0.10 amps
CO ₂ Level	± 2%
Flow Measurement	± 2.8%

2.0 TEST PLAN AND PROCEDURES

The test plans and procedures for the following tests are detailed in the corresponding sections as noted:

<u>TEST</u>	<u>SECTION</u>
WVE/HDC Breadboard (WBS 1.0)	I
WVE Vibration Test (WBS 5.0)	II
HDC Flow Test (WBS 6.0)	III
Matrix Compression Test (WBS 3.3)	IV
TMAC Electrolyte Analytical Tests (WBS 3.4)	V
Trace Impurities (WBS 3.5)	VI
Cs ₂ CO ₃ Electrolyte Analytical Tests (WBS 3.6)	VII
HDC Matrix Compression Set (WBS 9A)	VIII
HDC Analytical Cell Tests (WBS 9A)	IX
HDC Cell Pair Testing (WBS 9B)	X

2.1 Test Facility and Instrumentation Readings

The schematic of the test set-up for the various electrolyte, cell, and cell pair tests, is defined in the detail test procedure for each test. The general data acquisition for all the testing is presented in Table I.

<u>Data Point</u>	<u>Instrument</u>	<u>Range & Readout</u>
Inlet & Outlet Air Temperature of Cell Pair (°F)	Thermocouple and Bristol Recorder	0° to 250°F (1°F inc.)
Inlet & Outlet Air Dew Point of Cell Pair (°F)	Cambridge 880 Dew Pointer	-40° to 120°F (2°F inc.)
WVE Hydrogen Outlet Temperature (°F)	Thermocouple & Bristol	0° to 250°F (1°F inc.)
WVE Hydrogen Outlet Dew Point (°F)	Cambridge 880 Dew Pointer	-40°F to 120°F (2°F inc.)
HDC H ₂ & CO ₂ Outlet Temperature (°F)	Thermocouple & Bristol	-30°F to 250°F (1°F inc.)
HDC CO ₂ Inlet Temperature (°F)	Thermocouple & Bristol	-30°F to 250°F (1°F inc.)
HDC Hydrogen Inlet Temperature (°F)	Thermocouple & Bristol	-30°F to 250°F (1°F inc.)
Chamber Pressure (inches of H ₂ O)	Slant Water Manometer	0 to 2 in. of H ₂ O (0.02 inc.)
Item Fan Δ P (inches of H ₂ O)	Slant Water Manometer	0 to 4 in. of H ₂ O (0.01 inc.)
WVE Hydrogen Outlet Pressure (psia)	HISE Pressure Gauge	0 to 30 psia (0.1 psia inc.)
HDC Hydrogen Inlet Pressure (psia)	HISE Pressure Gauge	0 to 30 psia (0.1 psia inc.)
HDC CO ₂ Inlet Pressure (psia)	HISE Pressure Gauge	0 to 50 psia (0.1 psia inc.)
HDC H ₂ /CO ₂ Outlet Pressure (psia)	HISE Pressure Gauge	0 to 30 psia (0.1 psia inc.)
Cell Pair Voltage (Volts)	Digital Meter	0 to 4.0 volts (.0005 volts inc.)
Cell Pair Current (amps)	Digital Meter	0 to 100 amps (0.05 amp inc.)
HDC CO ₂ Inlet Concentration (%)	Lira Gas Analyzer	0% to 1% (0.02% inc.)

DATA ACQUISITION

TABLE I

<u>Data Point</u>	<u>Instrument</u>	<u>Range & Readout</u>
HDC - CO ₂ Outlet Concentration in H ₂ stream (%)	Lira Gas Analyzer	0% to 100% (2% inc.)
WVE Outlet Hydrogen Flow (cc/min.)	Water Displacement Measurement	1.0 cc inc. and 0.001 min. inc.
HDC - H ₂ /CO ₂ Outlet Flow (cc/min.)	Water Displacement Measurement	1.0 cc inc. and 0.001 min. inc.
HDC - Inlet CO ₂ Flow (%)	Flowmeter	0 to 16% (.2 inc.)
HDC - Hydrogen Inlet Flow (%)	Flowmeter	0 to 20% (0.2 inc.)
Chamber Gas O ₂ Concentration (%)	Beckman O ₂ Analyzer	0 to 100% (2% inc.)

TABLE I (Continued)

~~SECTION I~~

(DELETED)

~~WVE/HDC BREADBOARD~~

TEST PLAN

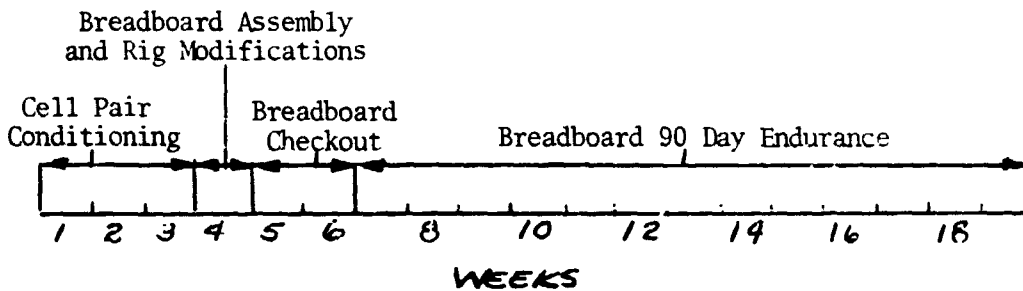
~~(WBS 1.2)~~

(Pages 6-20 deleted with Revision B)

WVE/HDC BREADBOARD TESTS (WBS 1.2)

The test plan for the WVE/HDC Breadboard Unit is presented in two parts, the conditioning of the cell pairs, and the actual operation of the WVE/HDC breadboard.

SCHEDULE

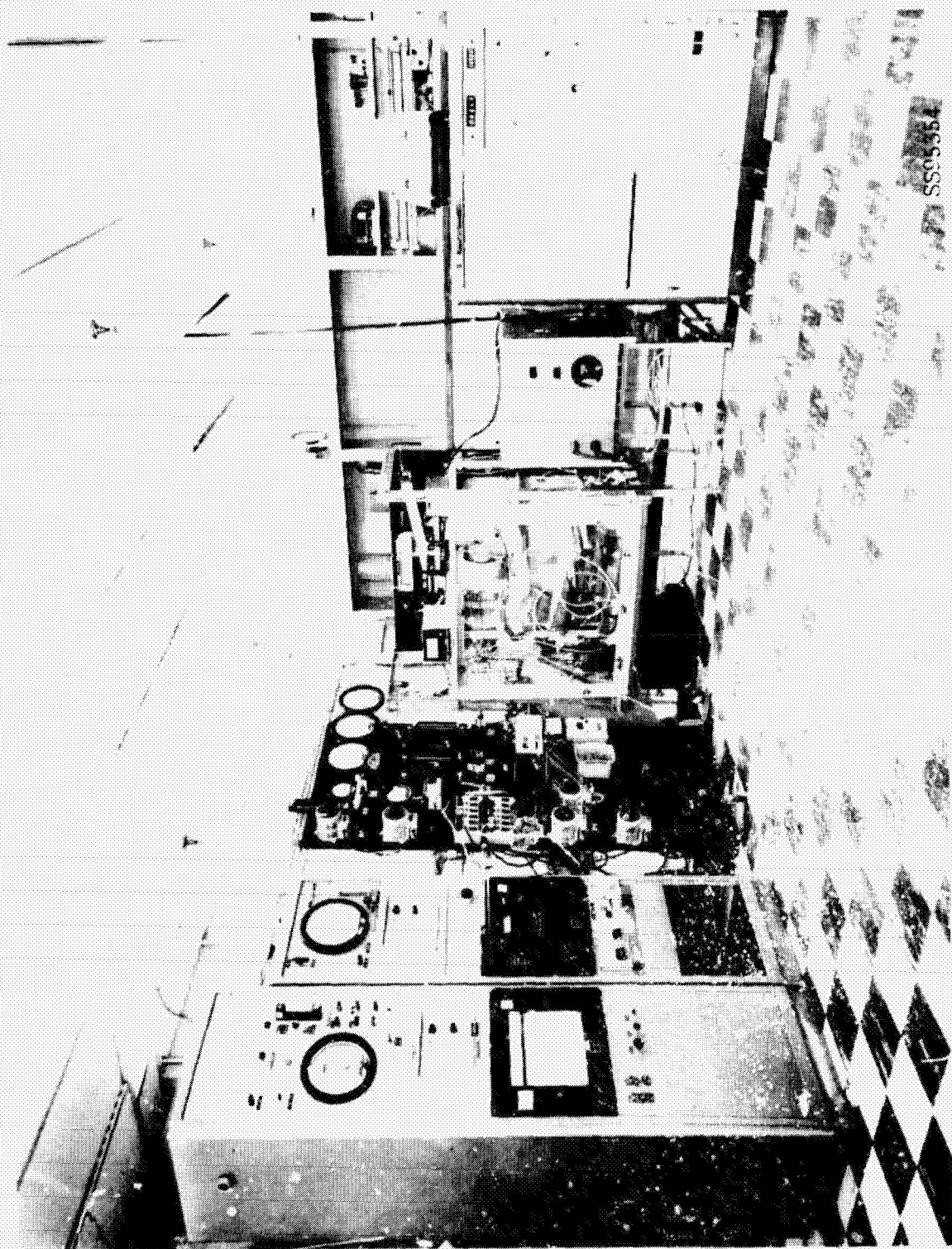


TEST FACILITIES

The test rig, as illustrated in figures 1 and 2, will be used for the cell pair and breadboard testing. The lira instrumentation of this test rig will be calibrated daily during the HDC cell pair and breadboard tests.

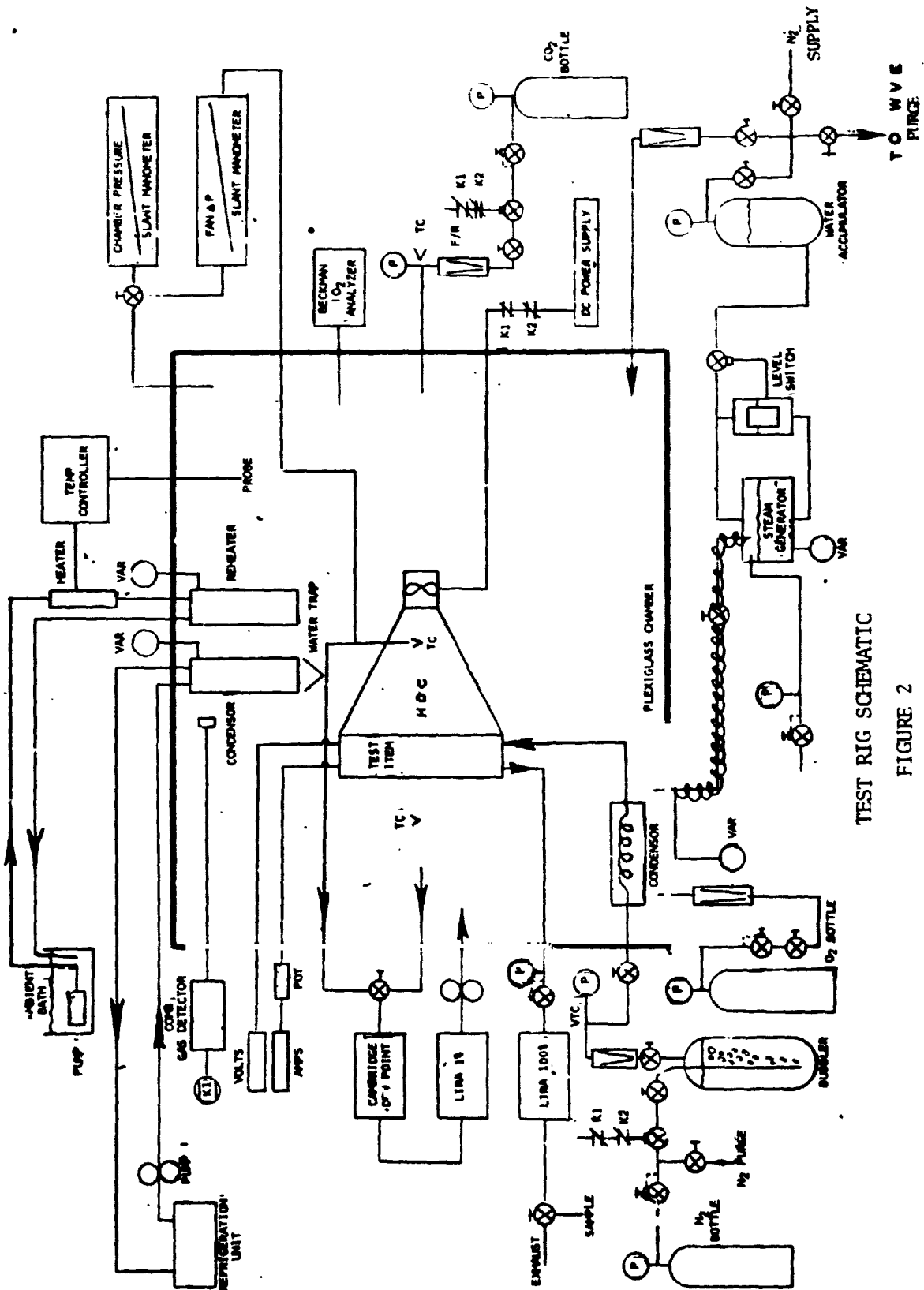
OVERALL TEST PHILOSOPHY

Any changes in the cell pair or breadboard configuration, and in the testing procedures or parameters will be reviewed with NASA/MSD prior to the change. In emergencies where changes must be made to protect the test unit, corrective action can be made without prior review with NASA/MSD. However, a full review of the incident will be made within 24 hours.



TEST FACILITY

FIGURE 1



TEST RIG SCHEMATIC

FIGURE 2

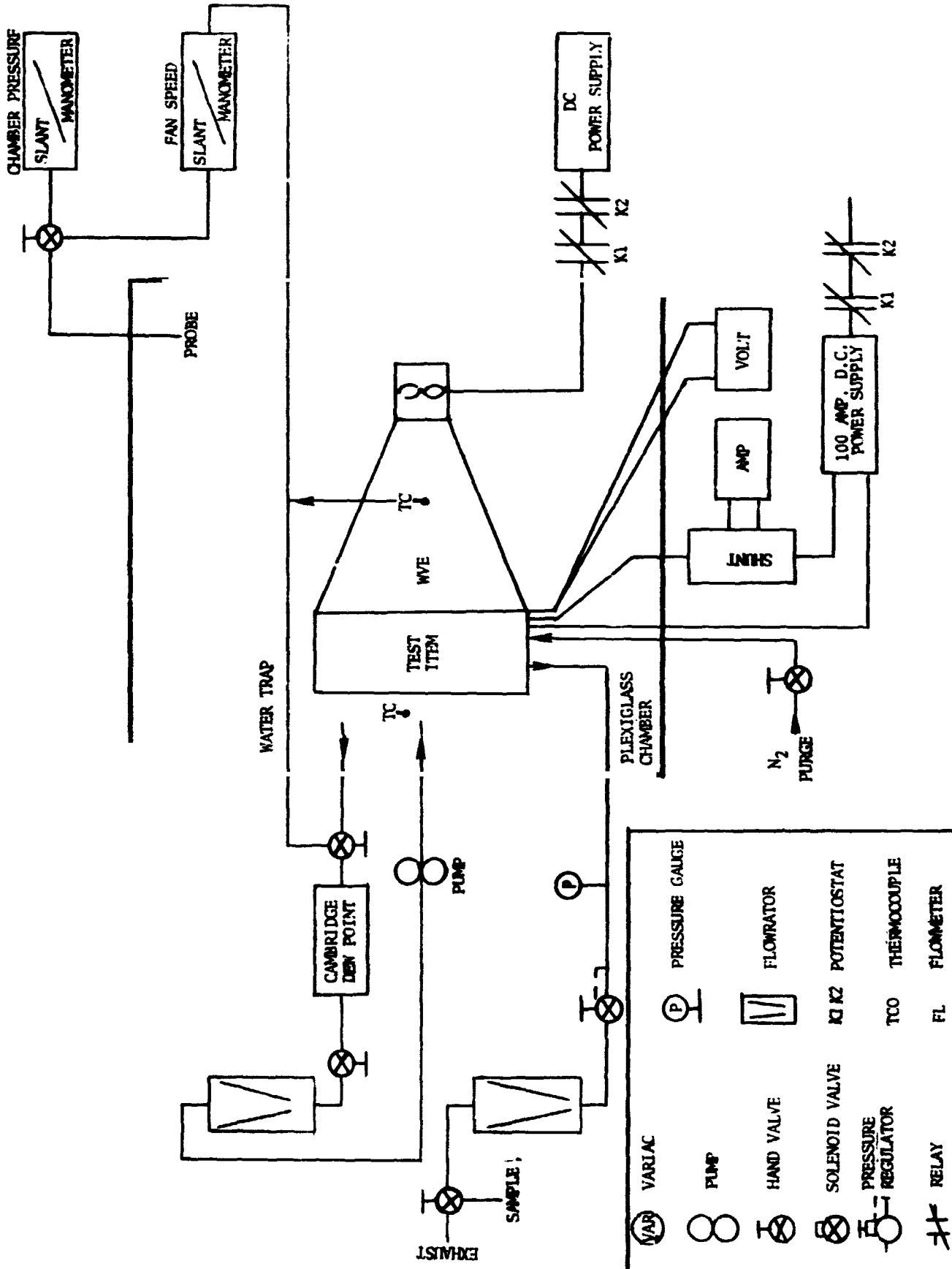


FIGURE 2 (Continued)

MS F-927 6/56

TEST NO. I-A

HAMILTON STANDARD

PAGE 1 OF _____

PLAN OF TEST

JOB: WVE and HDC Cell Pair Conditioning Tests

PLAN PREPARED BY: J. Huddleston

PROJECT & ORDER: NAS 9-12920

APPROVED BY: _____

INSTRUCTION: _____

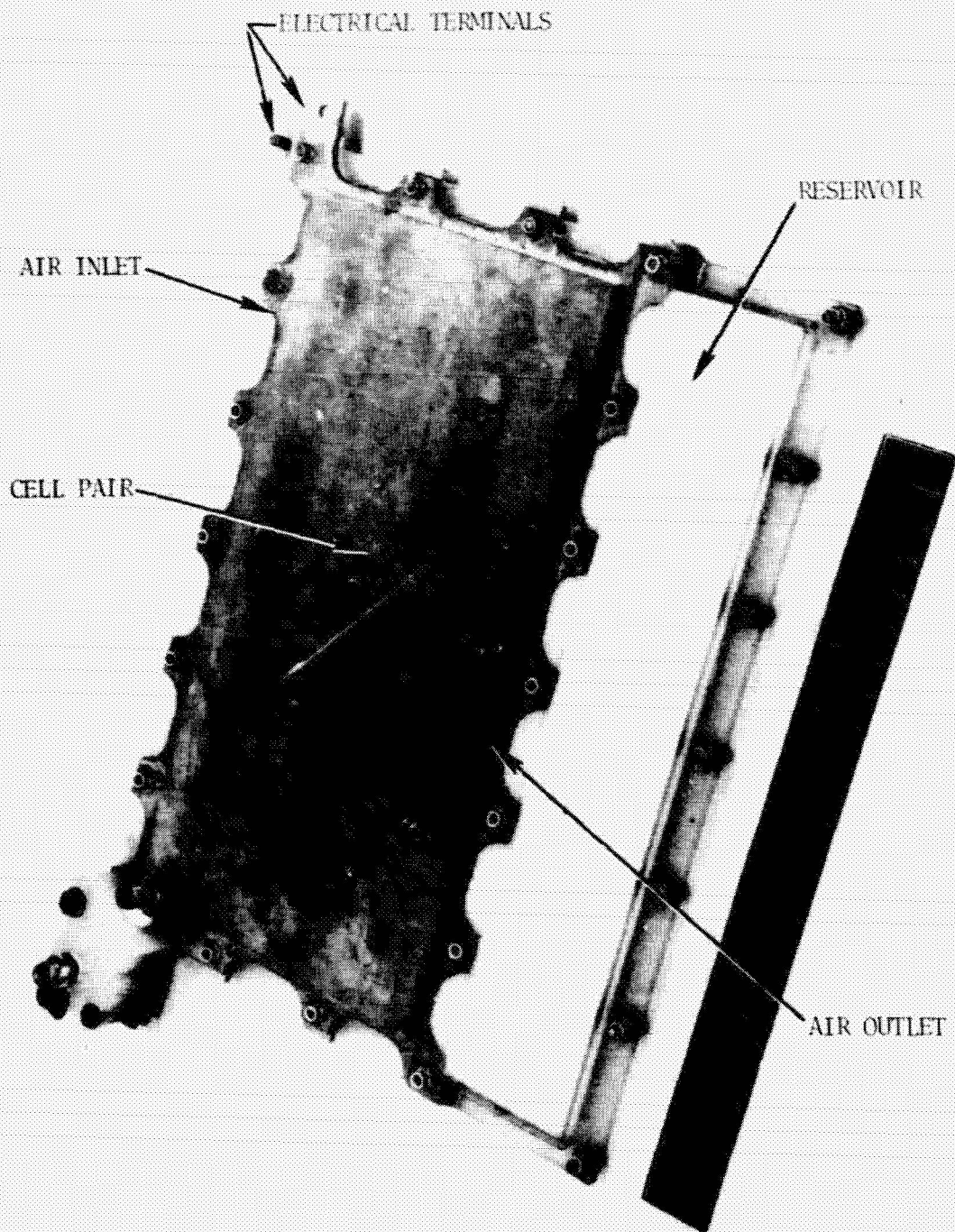
TEST ENGINEER: _____

TIME PERIOD: _____ TO _____

1. WHAT IS ITEM BEING TESTED?
2. WHY IS TEST BEING RUN? WHAT WILL RESULTS SHOW OR BE USED FOR?
3. DESCRIBE TEST SET UP INCLUDING INSTRUMENTATION. ATTACH SKETCH OF INSTALLATION.
4. ITEMIZE RUNS TO BE MADE GIVING LENGTH OF EACH AND READINGS TO BE TAKEN.
5. SPECIAL INSTRUCTIONS: SAFETY PRECAUTIONS FOR OPERATORS AND HANDLING EQUIPMENT. OBSERVATIONS BY SIGHT, FEEL, OR HEARING. LIST POINTS OF OBSERVATION WHICH MIGHT CONTRIBUTE TO ANALYSIS OF (A) PERFORMANCE OF UNITS, (B) INCIDENT TROUBLE BEFORE IT OCCURS, AND (C) CAUSE OF FAILURE.
6. HOW WILL DATA BE USED OR FINALLY PRESENTED? GIVE SAMPLE PLOT, CURVE, OR TABULATION AS IT WILL BE FINALLY PRESENTED.

NUMBER ENTRY AS LISTED ABOVE AND DESCRIBE BELOW

1. ITEM BEING TESTED: The WVE and HDC cell pairs including the electrolyte reservoir (reference figure 1). This testing will be done on each cell pair.	A
2. PURPOSE OF TEST: The conditioning testing of the cell pairs establishes the maximum relative humidity which the unit can operate under. The excess electrolyte is also removed from the air passageways of the cell during this period.	
3. TEST PROCEDURE: The tests will be conducted in the WVE/HDC test rig, using the cell pair test fixture (reference figure 2) under nominal cell operating mode and inlet air conditions as presented in Table I. Data will be taken three times daily and presented on log sheets per figures 3 and 4.	
4. TEST RUNS: The duration of this test will be approximately one week or until the unit shows that it has stabilized. N ₂ purging of the H ₂ passages will be investigated during the cell pair testing.	A
5. SPECIAL INSTRUCTIONS: None.	
6. PRESENTATION OF DATA: The performance will be graphically presented vs. time.	



SS10110-4

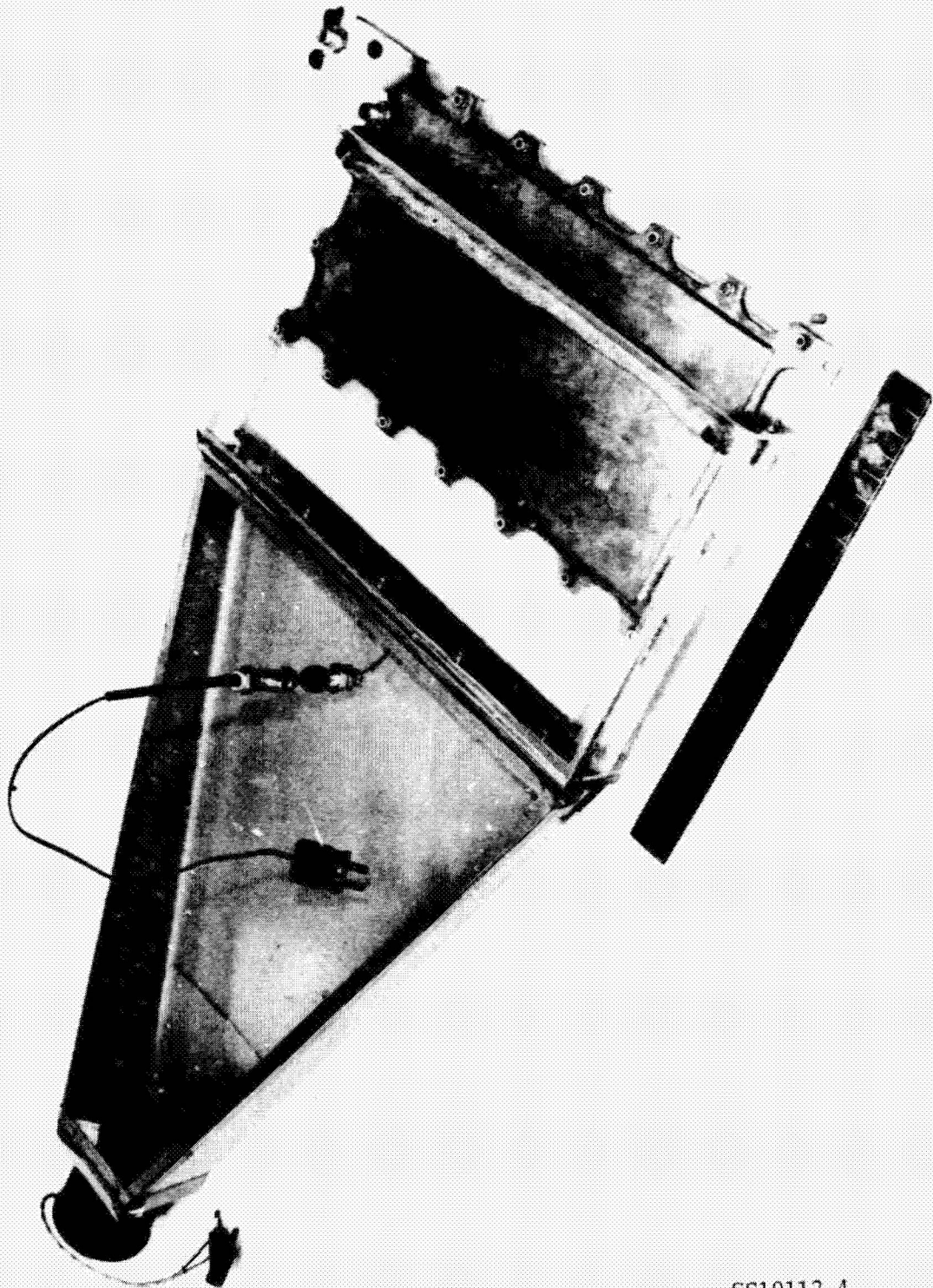
TYPICAL WE OR HDC CELL PAIR

FIGURE 1

Hamilton
Standard

U
A.

ECS-2128-L-035



SS10112-4

CELL PAIR AND TEST FIXTURE

FIGURE 2

A-13

No.	Test Conditions	WVE Cell Pair	HDC Cell Pair
Set Conditions			
1	Inlet Air Temperature	70°F	70°F
2	Inlet Air Dewpoint	65°F	65°F
3	Inlet Air CO ₂ Partial Pressure	---	3mmHg
4	Inlet Air O ₂ Concentration	20-21%	20-21%
5	Air Flow Through Cell	10 scfm	10 scfm
6	ΔP Across Matrix	1.0 psi	1.0 psi
7	Voltage	1.7 VDC	---
8	Current	---	16 ASF
9	H ₂ Inflow	---	320 cc/min
Monitored Parameters			
	All of the Set Conditions	X	X
	H ₂ Out Flow	X	-
	H ₂ + CO ₂ Out Flow	-	X
	CO ₂ Removal Rate	-	X
	Current Efficiency	-	X
	Current	X	X
	Voltage	X	X
	Chamber Pressure	X	X
	N ₂ Inflow (Diluent)	X	-
	H ₂ Temperature (out)	X	-

A

TEST CONDITIONS

TABLE I

TEST NO. I-B

HAMILTON STANDARD

PAGE 1 OF _____

PLAN OF TESTJOB: WVE/HDC Integrated Breadboard Testing PLAN PREPARED BY: J. HuddlestonPROJECT & ORDER: NAS 9-12920 APPROVED BY: _____

INSTRUCTION: _____ TEST ENGINEER: _____

TIME PERIOD: _____ TO _____

1. WHAT IS ITEM BEING TESTED?
2. WHY IS TEST BEING RUN? WHAT WILL RESULTS SHOW OR BE USED FOR?
3. DESCRIBE TEST SET UP INCLUDING INSTRUMENTATION. ATTACH SKETCH OF INSTALLATION.
4. ITEMIZE RUNS TO BE MADE GIVING LENGTH OF EACH AND READINGS TO BE TAKEN.
5. SPECIAL INSTRUCTIONS: SAFETY PRECAUTIONS FOR OPERATORS AND HANDLING EQUIPMENT. OBSERVATIONS BY SIGHT, FEEL, OR HEARING. LIST POINTS OF OBSERVATION WHICH MIGHT CONTRIBUTE TO ANALYSIS OF (A) PERFORMANCE OF UNITS, (B) INCIPIENT TROUBLE BEFORE IT OCCURS, AND (C) CAUSE OF FAILURE.
6. HOW WILL DATA BE USED OR FINALLY PRESENTED? GIVE SAMPLE PLOT, CURVE, OR TABULATION AS IT WILL BE FINALLY PRESENTED.

NUMBER ENTRY AS LISTED ABOVE AND DESCRIBE BELOW

1. ITEM BEING TESTED: Integrated WVE/HDC Breadboard Assembly, SVSK 83513
(reference schematic figure 1).

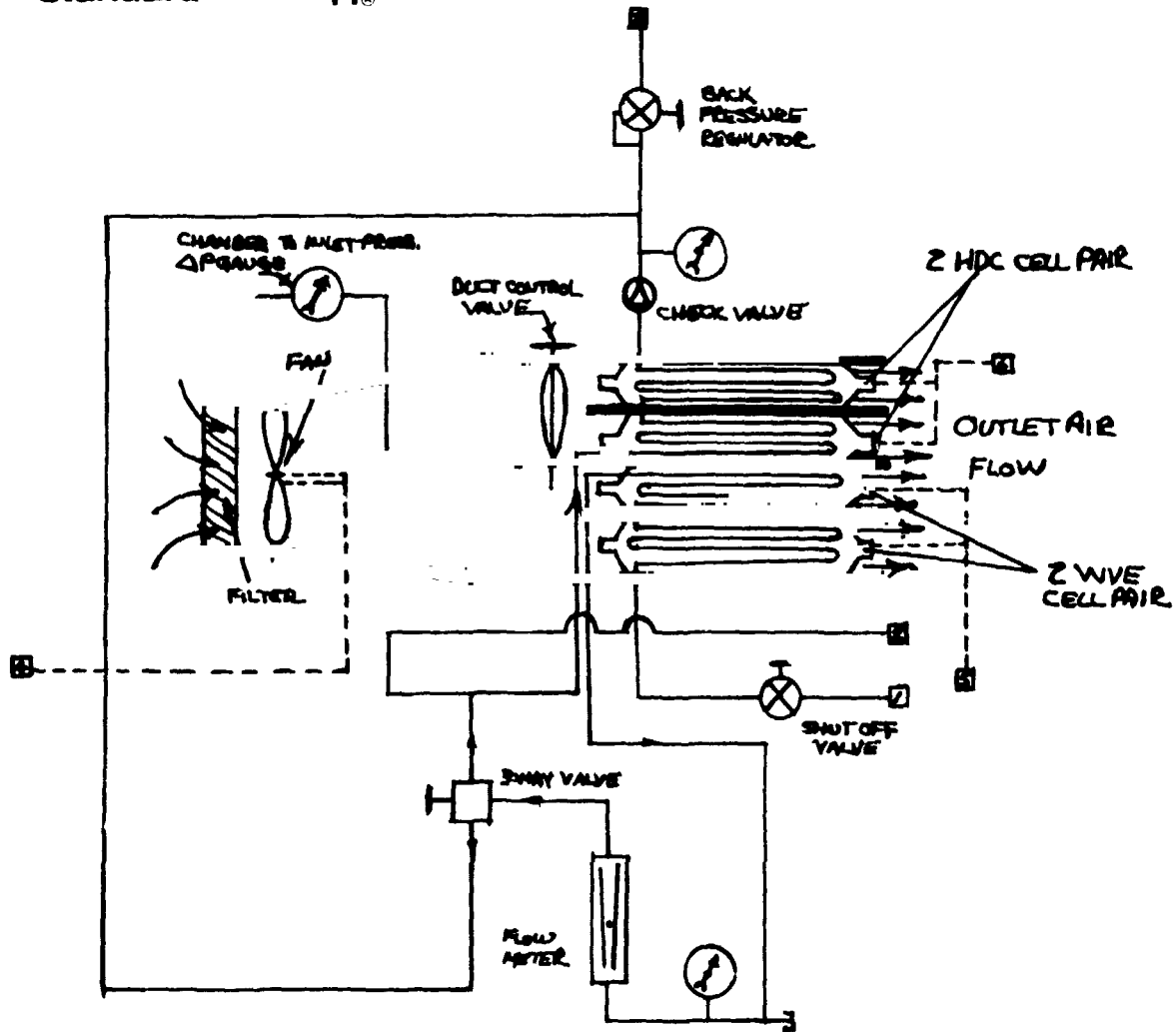
2. PURPOSE OF TEST: To obtain design data of an Integrated WVE/HDC Multi-
Celled Unit which will be used in the design of large multi-celled
assemblies.

3. TEST PROCEDURES: The breadboard unit will be tested in the WVE/HDC test
rig. Testing will consist of a two week checkout followed by a 90 day
endurance test. The test parameters for these two test periods are out-
lined in Table I. The procedure for nitrogen purge of the HDC cell pairs,
established during cell pair conditioning, will be incorporated into this
test program. Data will be taken three times daily and presented on log
sheets per figure 2.

4. TEST RUNS: The duration of each test is specified on Table 1.

5. SPECIAL INSTRUCTIONS: None.

6. PRESENTATION OF DATA: The performance of the WVE and HDC units will be
graphically presented.



- Rig to Breadboard Interface:
- 1 N₂ Purge Control Pressure Supply
 - 2 N₂ Purge Control Pressure Supply
 - 3 To Lira and Total Flow Measuring
 - 4 Controlled AC Power to Fan
 - 5 DC Power Input to WVE Cell Pairs
 - 6 DC Power Output from HDC to Control Source in Rig

MULTI-CELLED WVE/HDC BREADBOARD UNIT

FIGURE 1

NOMINAL CELL PAIR OPERATING CONDITIONS:

<u>WVE</u>	Constant Voltage	1.7 VDC
	Air Flow	10 scfm
	H ₂ Back Pressure	1.0 psig
<u>HDC</u>	Constant Current	16 ASF
	Air Flow	10 scfm
	P Across Matrix	1.0 psi
	H ₂ Inflow	320 cc/min
	CO ₂ Partial Pressure	3mmHg

Test No.	Inlet Temp. °F	Inlet Dew Point °F	Change to nominal cell pair operation		Duration of Test
			HDC	WVE	
Checkout	70	53	Basically nominal operation - however all adjustable parameters will be checked out during this test period.		
Endurance					
A	70	41	Nominal	Nominal	1 wk.
B ₁	70	61	Nominal	Nominal	1 wk.
B ₂	↓	↓	PCO ₂ = 2.0 mmHg	↓	}
B ₃			PCO ₂ = 1.0		
B ₄			PCO ₂ = 0.5		
B ₅			PCO ₂ = 0.2		
B ₆			PCO ₂ = 1.0		
B ₇			PCO ₂ = 2.0		
B ₈			PCO ₂ = 3.0		
C ₁					
C ₂			5.0 psi		
C ₃			2.5 psi		
C ₄			1.0 psi		
D ₁	70	41	Nominal	Nominal	1 wk.
D ₂	↓	↓	PCO ₂ = 2.0 mmHg	↓	2 days
E	70	61	PCO ₂ = 1.0 mmHg	↓	2 days
F	70	61	Nominal	Nominal	1 wk.
G	70	61	Nominal/Cyclic*	Nominal/Cyclic*	1 wk.
H	70	61	Nominal	Nominal	3 days
	(Conditions TBD after review of data through test F.)				2 1/2 wks.

* Cyclic operation: during this mode, the power to the WVE will be removed and the WVE cells closed circuited. The air flow through the cells will be left on and the HDC left closed circuited. If the H₂ back pressure decays, nitrogen will be used to maintain the back pressure. Cycle time will be 60 min on, 30 min off.

TEST CONDITIONS

TABLE I

SECTION II

WVE VIBRATION

TEST PLAN

(WBS 5.1 and 5.2)

TEST NO. II

HAMILTON STANDARD

PAGE 1 OF _____

PLAN OF TEST

JOB: WVE Vibration Test (WBS 5.1) PLAN PREPARED BY: J. Huddleston

PROJECT & ORDER: NAS 9-12920 APPROVED BY: _____

INSTRUCTION: _____ TEST ENGINEER: _____

TIME PERIOD: _____ TO _____

1. WHAT IS ITEM BEING TESTED?
2. WHY IS TEST BEING RUN? WHAT WILL RESULTS SHOW OR BE USED FOR?
3. DESCRIBE TEST SET UP INCLUDING INSTRUMENTATION. ATTACH SKETCH OF INSTALLATION.
4. ITEMIZE RUNS TO BE MADE GIVING LENGTH OF EACH AND READINGS TO BE TAKEN.
5. SPECIAL INSTRUCTIONS: SAFETY PRECAUTIONS FOR OPERATORS AND HANDLING EQUIPMENT. OBSERVATIONS BY SIGHT, FEEL, OR HEARING. LIST POINTS OF OBSERVATION WHICH MIGHT CONTRIBUTE TO ANALYSIS OF (A) PERFORMANCE OF UNITS, (B) INCIPIENT TROUBLE BEFORE IT OCCURS, AND (C) CAUSE OF FAILURE.
6. HOW WILL DATA BE USED OR FINALLY PRESENTED? GIVE SAMPLE PLOT, CURVE, OR TABULATION AS IT WILL BE FINALLY PRESENTED.

NUMBER ENTRY AS LISTED ABOVE AND DESCRIBE BELOW

1. Test Item:	<u>WVE Reservoir Cell Pair</u>
2. Purpose of Test:	<u>To determine the effect of vibration on the Reservoir Cell Pair Design (SVSK 81239 Concept).</u>
3. Test Procedure:	<u>Testing will consist of one week of WVE baseline testing per Section I (WVE Conditioning Test), random vibration per Table I and a Post Baseline Test of one week.</u> <u>Setup for Vibration Test: The cell pair will be mounted in a test fixture to simulate a rack mount. This fixture will provide additional protection to the Plexiglas Reservoir Housing.</u>
	<u>The cell pair will be bagged to prevent any contamination of the cells and to protect the vibration equipment in case electrolyte (H₂SO₄) is vibrated loose from the matrix.</u>
4. Test Runs:	<u>baseline test 1 week; vibration in each of three mutually perpendicular planes; examination of cell after each plane of vibration; and one week of post baseline test.</u>
5. Special Instructions:	<u>If the unit has been structurally damaged during vibration testing Hamilton Standard and NASA/MSD will determine the remaining</u>

WE Vibration Test (WSS 5.1) (Continued)

program activity for this task.

6. Test Data: Performance and vibration test data will be presented graphically.

Random Vibration Levels - 2.5 minutes duration in each of the three (3) mutually perpendicular axes (x, y, z).

20 to 30 Hz at +3 db/octave

30 to 180 Hz at 0.06 g²/Hz

180 to 200 Hz at +12 db/octave

200 to 400 Hz at 0.10 g²/Hz

400 to 450 Hz at -12 db/octave

450 to 2000 Hz at 0.06 g²/Hz

A minimum of six (6) accelerometers will be mounted, observed and recorded during this test, three (3) will be mounted on the fixture at the item/fixture interface as close to the mounting point as possible, sensing the vibration in each of the orthogonal directions of the item; and three (3) accelerometers located on the item to sense the vibration motion in the same direction as those accelerometers on the fixture.

Each of the accelerometers on the fixture will be used to control the vibration level during that portion of the test when it is primary sensor.

During the random testing all the accelerometers signals will be continuously recorded on magnetic tape. This tape will be retained for the remainder of the NAS 9-12920 program.

RANDOM VIBRATION

TABLE I

SECTION III

HDC FLOW IMPROVEMENT

TEST PLAN

(NBS 6.1)

SECTION IV

MATRIX COMPRESSION

TEST PLAN

(WBS 3.3)

NS F-027 6/90

TEST NO. IV

HAMILTON STANDARD

PAGE 1 OF _____

PLAN OF TEST

JOB: Matrix Compression (WBS 3.3) PLAN PREPARED BY: J. R. Aylward

PROJECT & ORDER: NASA Contract - NAS 9-12920 APPROVED BY: _____

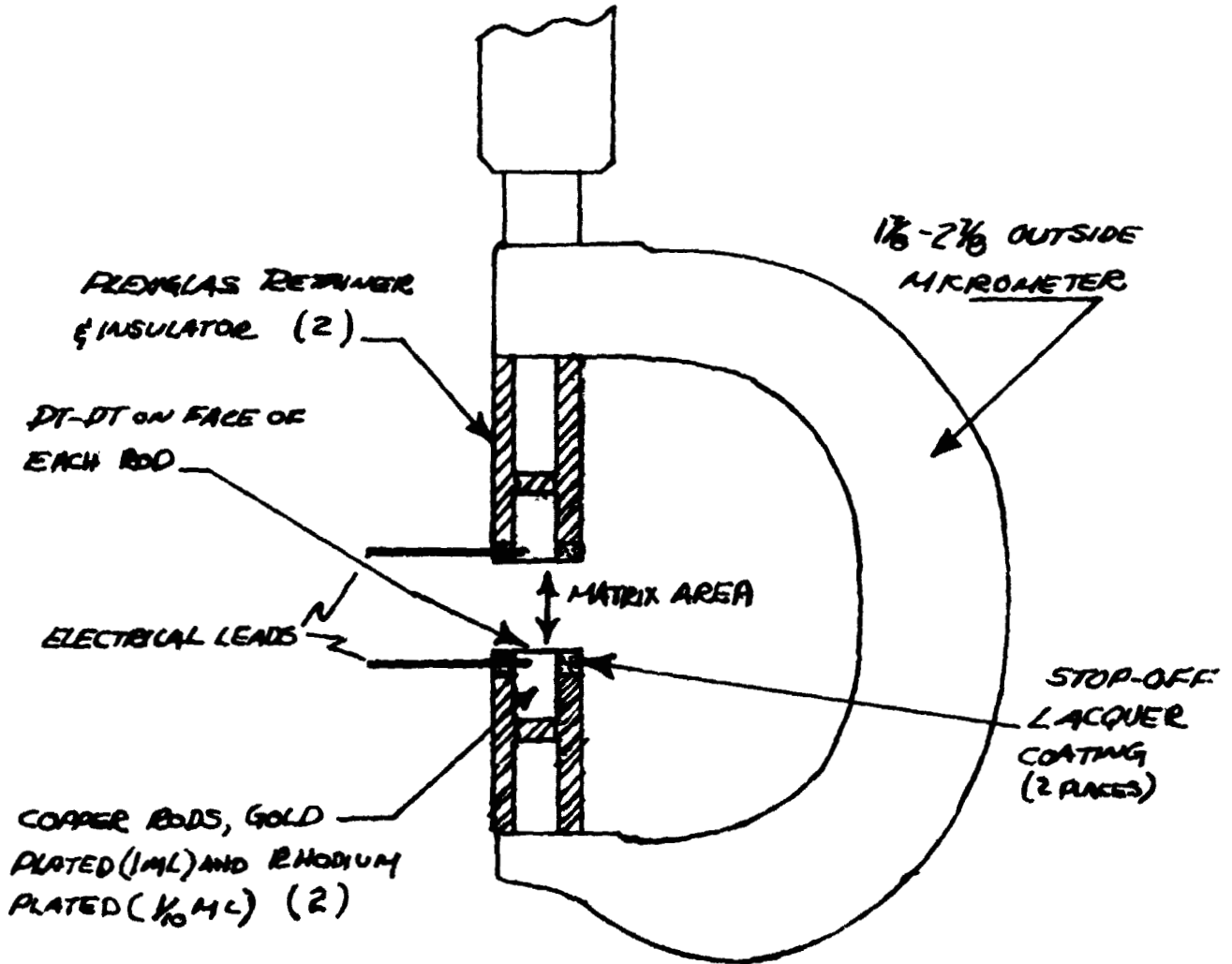
INSTRUCTION: _____ TEST ENGINEER: _____

TIME PERIOD: _____ TO _____

1. WHAT IS ITEM BEING TESTED?
2. WHY IS TEST BEING RUN? WHAT WILL RESULTS SHOW OR BE USED FOR?
3. DESCRIBE TEST SET UP INCLUDING INSTRUMENTATION. ATTACH SKETCH OF INSTALLATION.
4. ITEMIZE RUNS TO BE MADE GIVING LENGTH OF EACH AND READINGS TO BE TAKEN.
5. SPECIAL INSTRUCTIONS: SAFETY PRECAUTIONS FOR OPERATORS AND HANDLING EQUIPMENT. OBSERVATIONS BY SIGHT, FEEL, OR HEARING. LIST POINTS OF OBSERVATION WHICH MIGHT CONTRIBUTE TO ANALYSIS OF (A) PERFORMANCE OF UNITS, (B) INCIPIENT TROUBLE BEFORE IT OCCURS, AND (C) CAUSE OF FAILURE.
6. HOW WILL DATA BE USED OR FINALLY PRESENTED? GIVE SAMPLE PLOT, CURVE, OR TABULATION AS IT WILL BE FINALLY PRESENTED.

NUMBER ENTRY AS LISTED ABOVE AND DESCRIBE BELOW

1. Test Item: <u>Asbestos, Neoprene asbestos, Tissuquartz</u>
2. Purpose of Test: <u>To determine the matrix factor, tortuosity and optimum matrix compression for use in HDC computer program.</u>
3. Test Procedure: <u>Measure electrolyte resistance (R) with and without matrix as a function of electrode distance (d) using special micrometer cell (Figure 1) and suitable electrolyte. Determine uncompressed matrix thickness (d') and matrix void volume (m) with micrometer.</u>
$R = \frac{\rho d}{A} \times \frac{d \tau}{d - d' (1-m)} = \frac{\rho d}{A} \times f \tau$
<p>(A = Area and ρ = Resistivity)</p> <p>Without matrix, tortuosity ($\tau = 1$) and $m = 1$ so $R = \rho/A \times d$. Find ρ/A from plot of R vs d and correct for electronic resistance by extrapolation to $d = 0$. Find τ from plot of R vs d if ρ/A data with matrix ($f =$ matrix factor). Determine if τ is function of d. If $\tau = f(d)$ optimum compression is at $d = 2d' (1 = m)$.</p>
4. Number of Runs: <u>As required.</u>



MATRIX CONDUCTIVITY FIXTURE

FIGURE 1

Matrix Compression (WVS 3.3) (Continued)

5. Special Instructions: None.
6. Test Results: The matrix factor, tortuosity and optimum compression for each matrix material will be tabulated.

SECTION V

TMAC ELECTROLYTE ANALYTICAL TEST CELL

TEST PLAN

(WBS 3.4)

TEST NO. V

HAMILTON STANDARD

PAGE 1 OF

PLAN OF TEST

JOB: TMAC Analytical Cell Tests (WBS 3.4) PLAN PREPARED BY: J. R. Aylward

PROJECT & ORDER: NASA Contract - NAS 9-12920 APPROVED BY:

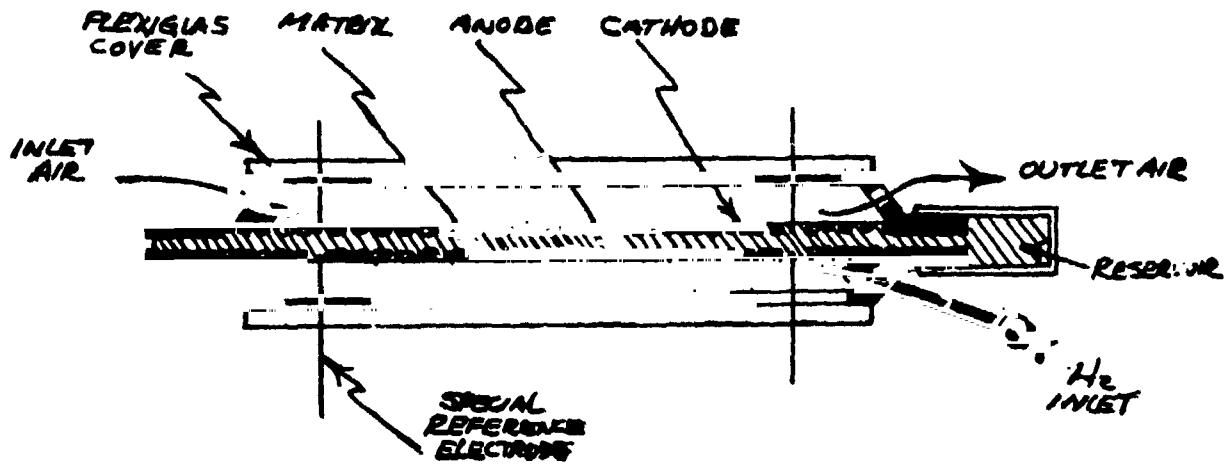
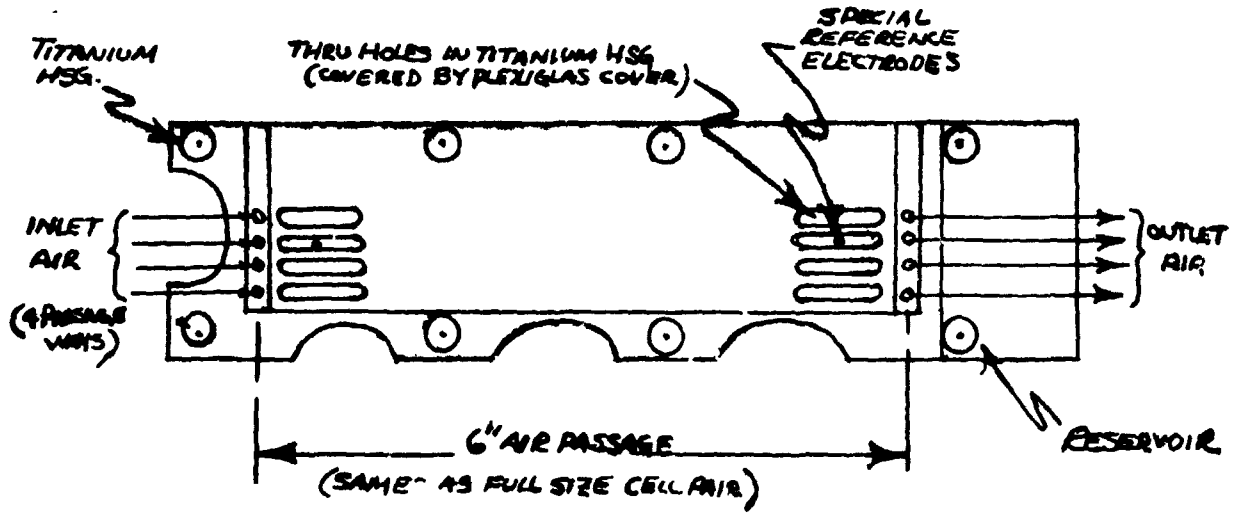
INSTRUCTION: TEST ENGINEER:

TIME PERIOD: TO

1. WHAT IS ITEM BEING TESTED?
2. WHY IS TEST BEING RUN? WHAT WILL RESULTS SHOW OR BE USED FOR?
3. DESCRIBE TEST SET UP INCLUDING INSTRUMENTATION. ATTACH SKETCH OF INSTALLATION.
4. ITEMIZE RUNS TO BE MADE GIVING LENGTH OF EACH AND READINGS TO BE TAKEN.
5. SPECIAL INSTRUCTIONS: SAFETY PRECAUTIONS FOR OPERATORS AND HANDLING EQUIPMENT. OBSERVATIONS BY SIGHT, FEEL, OR HEARING. LIST POINTS OF OBSERVATION WHICH MIGHT CONTRIBUTE TO ANALYSIS OF (A) PERFORMANCE OF UNITS, (B) INCIPIENT TROUBLE BEFORE IT OCCURS, AND (C) CAUSE OF FAILURE.
6. HOW WILL DATA BE USED OR FINALLY PRESENTED? GIVE SAMPLE PLOT, CURVE, OR TABULATION AS IT WILL BE FINALLY PRESENTED.

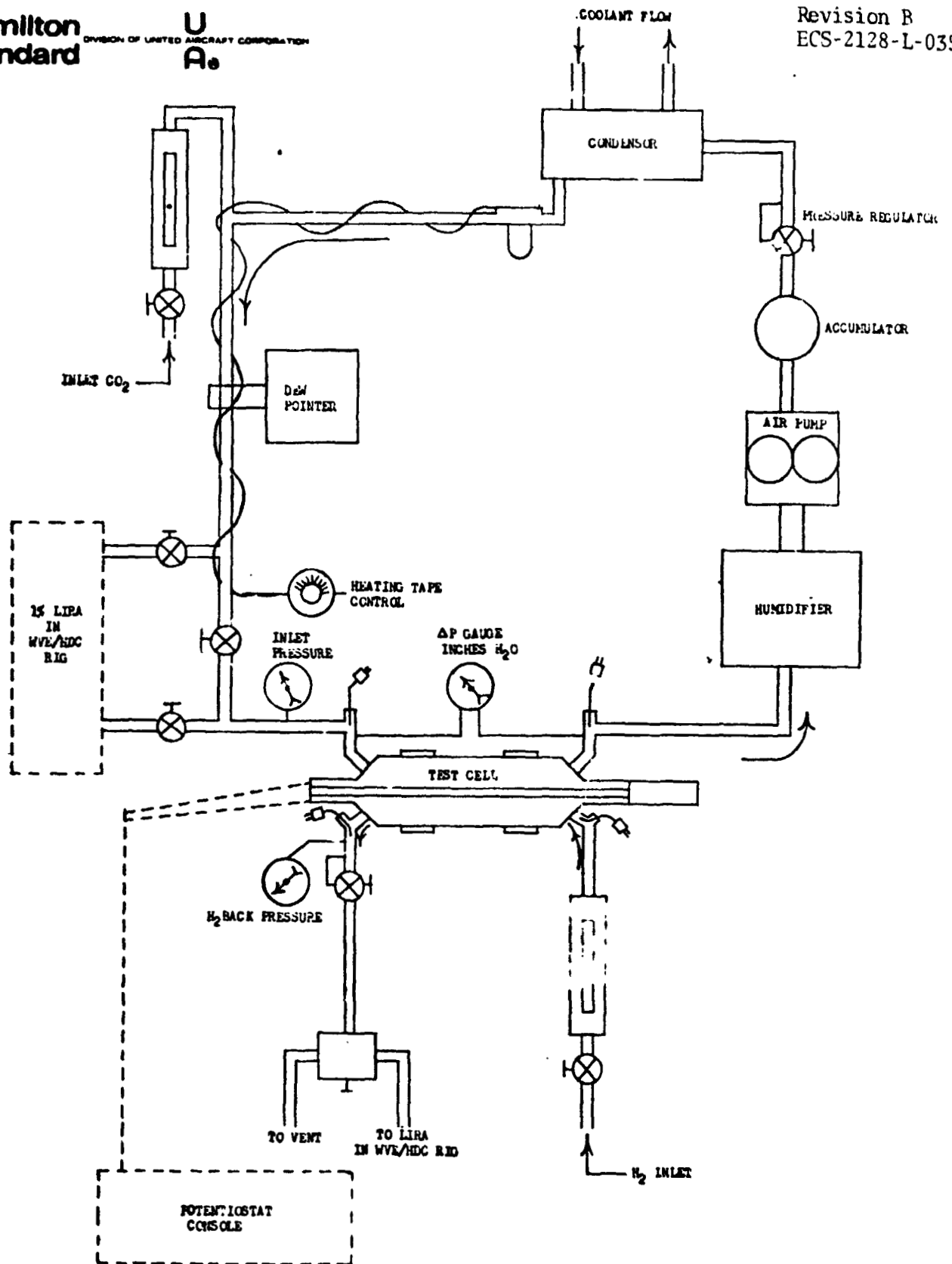
NUMBER ENTRY AS LISTED ABOVE AND DESCRIBE BELOW

1.	Test Item: Analytical HDC test cell using TMAC Electrolyte (Figure 1)
2.	Purpose of Test: To obtain a more detailed knowledge of HDC cell operation and evaluate new concepts to improve its performance.
3.	Test Procedure: The analytical test cell will be operated in an environment provided by the test rig as illustrated in Figure 2. The electrical operation of the cell will be controlled and monitored by a potentiostat console pictured in Figure 3.
	Each test condition will be run for approximately two days with at least three data readings taken each day. The data and calculations which will be made during each test condition are listed in Table I.
4.	Itemized Runs: See Table II
5.	Special Instructions: None
6.	Test Results: Test data will be summarized in tabular form.



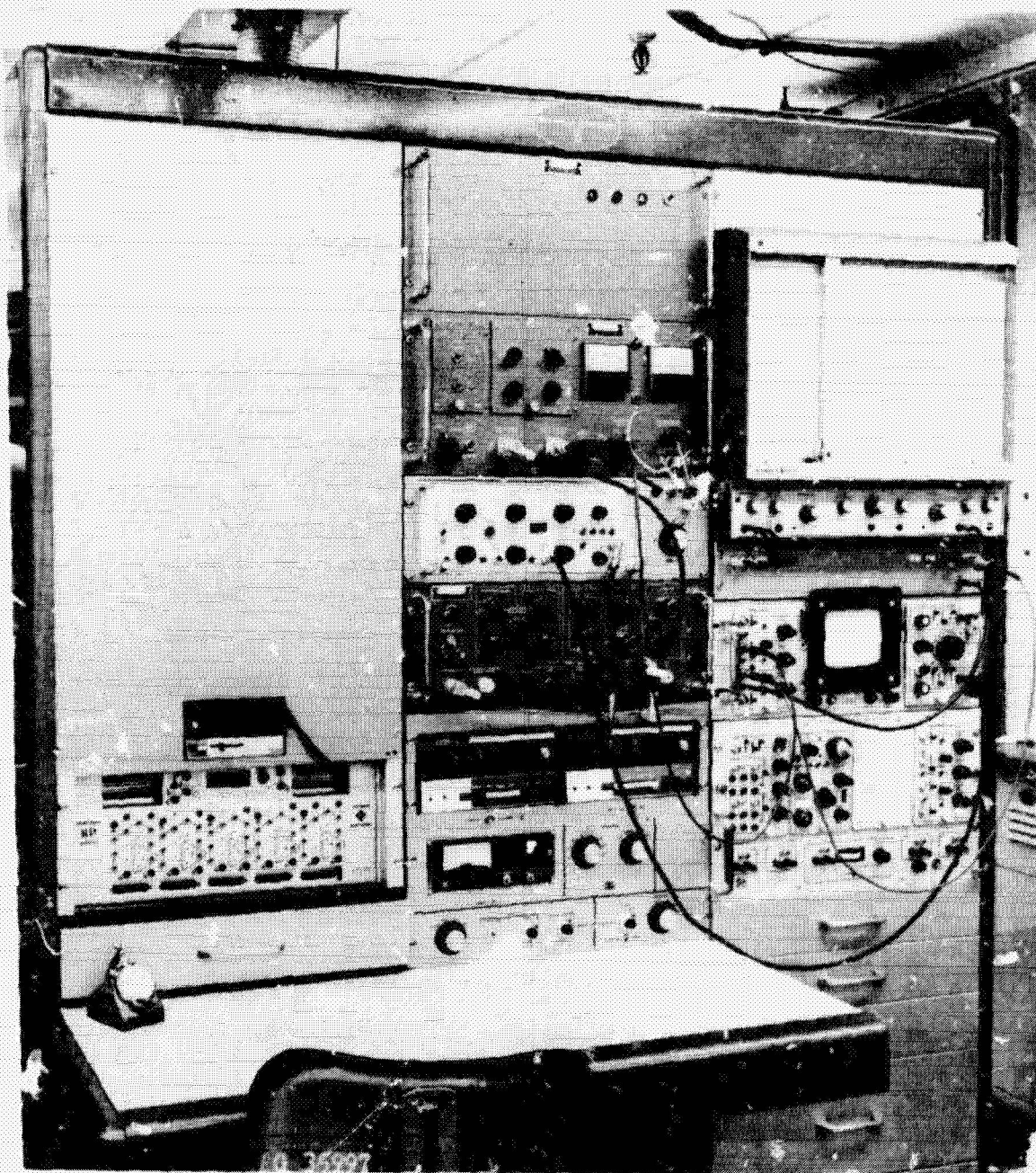
HDC ANALYTICAL TEST CELL

FIGURE 1



HDC ANALYTICAL TEST UNIT RIG

FIGURE 2



OPERATING CONSOLE FOR HDC ANALYTICAL TEST CELL

FIGURE 3

A-35

INSTRUMENTATION	
<u>Read-Outs</u>	<u>Calculations</u>
Inlet Air Temperature	Inlet Air P_{CO_2}
Inlet Air Dewpoint	CO_2 Removed
Inlet CO_2 Lira	Current Efficiency
Outlet Air Temperature	Power
Air Flow ΔP Across Cell	Air Flow Vel.
H_2 Inflow meter	Current Density
H_2 Inlet Press.	H_2 inflow
H_2 Inlet Temperature	ΔP Across Matrix
$H_2 + CO_2$ Outlet Flow	
CO_2 in H_2 Outlet (Lira)	
Cell Voltage	
Cell Current	
O_2 Concentration	
<u>Special Readings</u>	
pH at Anode	
pH at Cathode	
Activation Overvoltage at Anode	
Activation Overvoltage at Cathode	
Concentration Overvoltage	
IR Drop	

TABLE I

TEST	DEW POINT (°F)				PCO ₂ (mmHg)				AIR FLOW RATE (FT/SEC)				MATRIX THICKNESS			CURRENT DENSITY (asf)		
	40	50	60		0.25	1	4		5	10	20		.020	.040		6	12	24
Matrix Thickness & Base Line		X				X		X						X			X	
Current		X	X			X		X								X		X
CO ₂		X	X			X											X	
Mass Transport in Air		X				X				X							X	
PCO ₂ & DP	X				X				X								X	
	X					X				X							X	
	X								X								X	
Test Electrolyte			X														X	
Catalyst for CO ₂		X				X			X									X
NH ₃		X				X			X								X	
Trace Impurities CO		X				X			X								X	
H ₂ S		X				X			X								X	
H ₂ Flow and Backpressure		X				X			X								X	

Hy flow rates and backpressure will be determined from tests of Series III for cell design correlation.

TABLE II

SECTION VI

TRACE IMPURITIES

TEST PLAN

(NBS 3.5)

TEST NO. VI

HAMILTON STANDARD

PAGE 1 OF _____

PLAN OF TEST

JOB: Trace Impurities (WBS 3.5) PLAN PREPARED BY: J. R. Aylward

PROJECT & ORDER: NASA Contract NAS 9-12920 APPROVED BY: _____

INSTRUCTION: _____ TEST ENGINEER: _____

TIME PERIOD: _____ TO _____

1. WHAT IS ITEM BEING TESTED?
2. WHY IS TEST BEING RUN? WHAT WILL RESULTS SHOW OR BE USED FOR?
3. DESCRIBE TEST SET UP INCLUDING INSTRUMENTATION. ATTACH SKETCH OF INSTALLATION.
4. ITEMIZE RUNS TO BE MADE GIVING LENGTH OF EACH AND READINGS TO BE TAKEN.
5. SPECIAL INSTRUCTIONS: SAFETY PRECAUTIONS OR OPERATORS AND HANDLING EQUIPMENT. OBSERVATIONS BY SIGHT, FEEL, OR HEARING. LIST POINTS OF OBSERVATION WHICH MIGHT CONTRIBUTE TO ANALYSIS OF (A) PERFORMANCE OF UNITS, (B) INCIPIENT TROUBLE BEFORE IT OCCURS, AND (C) CAUSE OF FAILURE.
6. HOW WILL DATA BE USED OR FINALLY PRESENTED? GIVE SAMPLE PLOT, CURVE, OR TABULATION AS IT WILL BE FINALLY PRESENTED.

NUMBER ENTRY AS LISTED ABOVE AND DESCRIBE BELOW

1. Test Item: Trace impurities CO, H ₂ S, NH ₃ , Freon.
2. Purpose of Test: Determine if the above trace impurities and their oxidation or reduction products have any adverse affects on the HDC cell and investigate possible methods of recovering from any such affects.
3. Test Procedure: Particular procedure to be worked out for each impurity. In general potentiostatic sweeps will be made to determine adsorption characteristics, electrochemical reactivity and main reaction products, as a function of electrode potential and pH. Floating electrode tests will be used to determine poisoning effects, and if necessary small cell tests will be conducted when the above results are not conclusive. The cathode studies will use CS ₂ CO ₃ electrolyte (pH = 12) and the anode CsHCO ₃ (pH = 8).
4. Number of Runs: As required.
5. Special Instructions: None.
6. Test Results: The test results will be presented in table form, showing the amount of decrease in H ₂ and O ₂ absorbtion.

SECTION VII

Cs₂CO₃ ELECTROLYTE ANALYTICAL TEST CELL

TEST PLAN

(NBS 3.6)

TEST NO. VII

HAMILTON STANDARD

PAGE 1 OF _____

PLAN OF TEST

JOB: CS₂CO₂ Analytical Cell Tests (WBS 3.6)

PLAN PREPARED BY: J. R. Aylward

PROJECT & ORDER: NASA Contract NAS 9-12920

APPROVED BY: _____

INSTRUCTION: _____

TEST ENGINEER: _____

TIME PERIOD: _____ TO _____

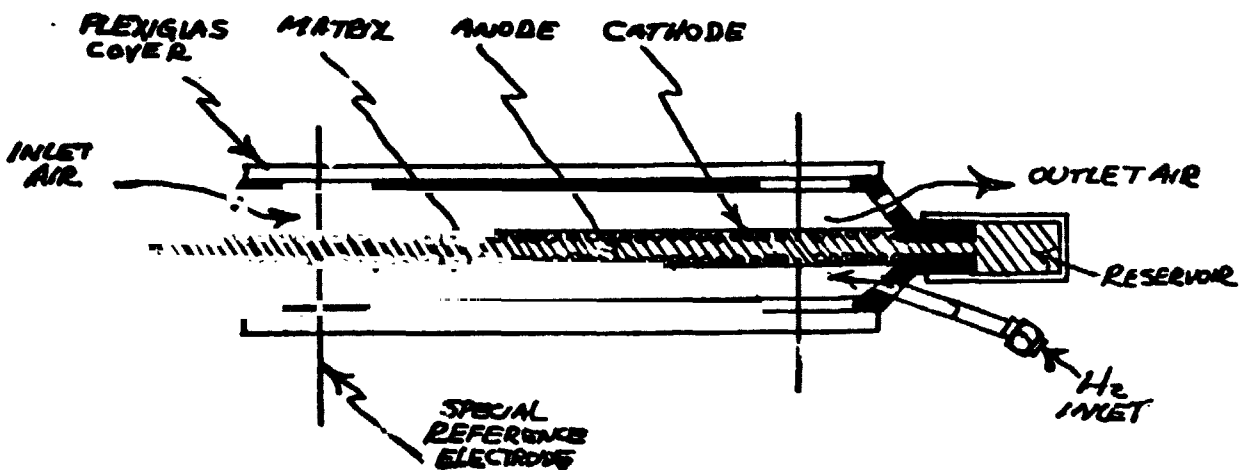
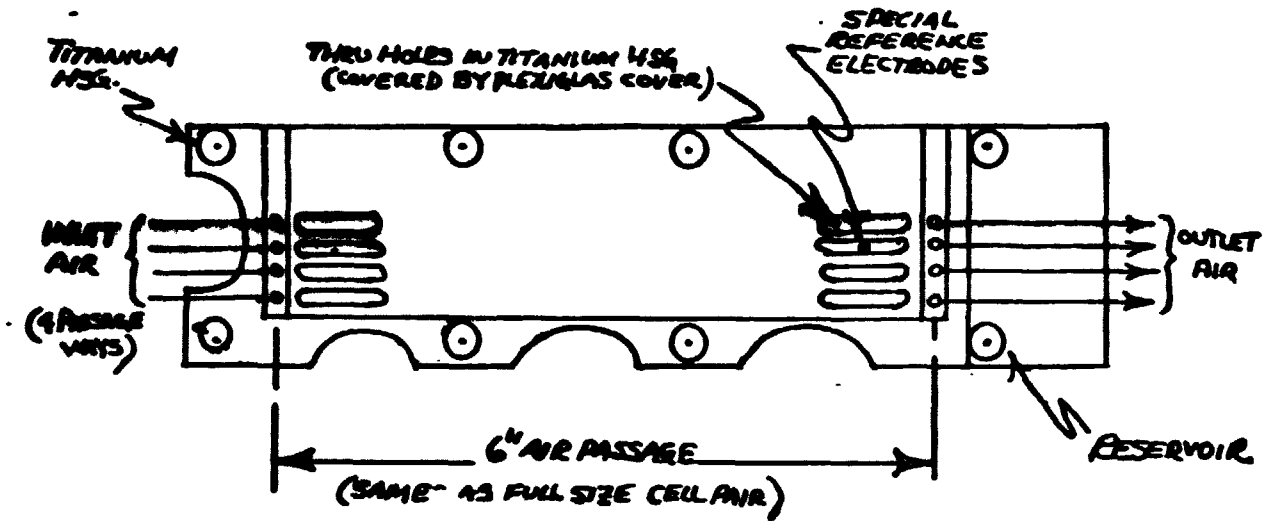
1. WHAT IS ITEM BEING TESTED?
2. WHY IS TEST BEING RUN? WHAT WILL RESULTS SHOW OR BE USED FOR?
3. DESCRIBE TEST SET UP INCLUDING INSTRUMENTATION. ATTACH SKETCH OF INSTALLATION.
4. ITEMIZE RUNS TO BE MADE GIVING LENGTH OF EACH AND READINGS TO BE TAKEN.
5. SPECIAL INSTRUCTIONS: SAFETY PRECAUTIONS FOR OPERATORS AND HANDLING EQUIPMENT. OBSERVATIONS BY SIGHT, FEEL, OR HEARING. LIST POINTS OF OBSERVATION WHICH MIGHT CONTRIBUTE TO ANALYSIS OF (A) PERFORMANCE OF UNITS, (B) INCIPIENT TROUBLE BEFORE IT OCCURS, AND (C) CAUSE OF FAILURE.
6. HOW WILL DATA BE USED OR FINALLY PRESENTED? GIVE SAMPLE PLOT, CURVE, OR TABULATION AS IT WILL BE FINALLY PRESENTED.

NUMBER ENTRY AS LISTED ABOVE AND DESCRIBE BELOW

1. Test Item: Analytical HDC Test Cell using Cs ₂ CO ₂ Electrolyte Reference figure 1).
2. Purpose of Test: To determine effective CO ₂ gas-phase mass transport coefficient and correlate with theoretical equation. Also to determine anolyte and catholyte pH variations over a range of operating conditions.
3. Test Procedure: The analytical test cell will be operated in an environment provided by the test rig as illustrated in figure 2. The electrical operation of the cell will be controlled and monitored by a potentiostat console pictured in figure 3. Each test condition will be run for approximately two days with at least three data readings taken each day. The data and calculations which will be made during each test condition are listed in Table I.
4. Itemized Runs: Mass transport; P _{CO₂} (0.25, 0.5, 1.0 mmHg) air velocity (5, 10, 20 ft/sec). Electrolyte pH; current density (12 ASF, 24 ASF). P _{CO₂} (0.25, 1, 4 mmHg), air dew point (6.). One test at nominal conditions, except for P _{CO₂} 3 mmHg, current density 5 ASF and air flow of 7 ft/sec.
5. Special Instructions: None. A-41

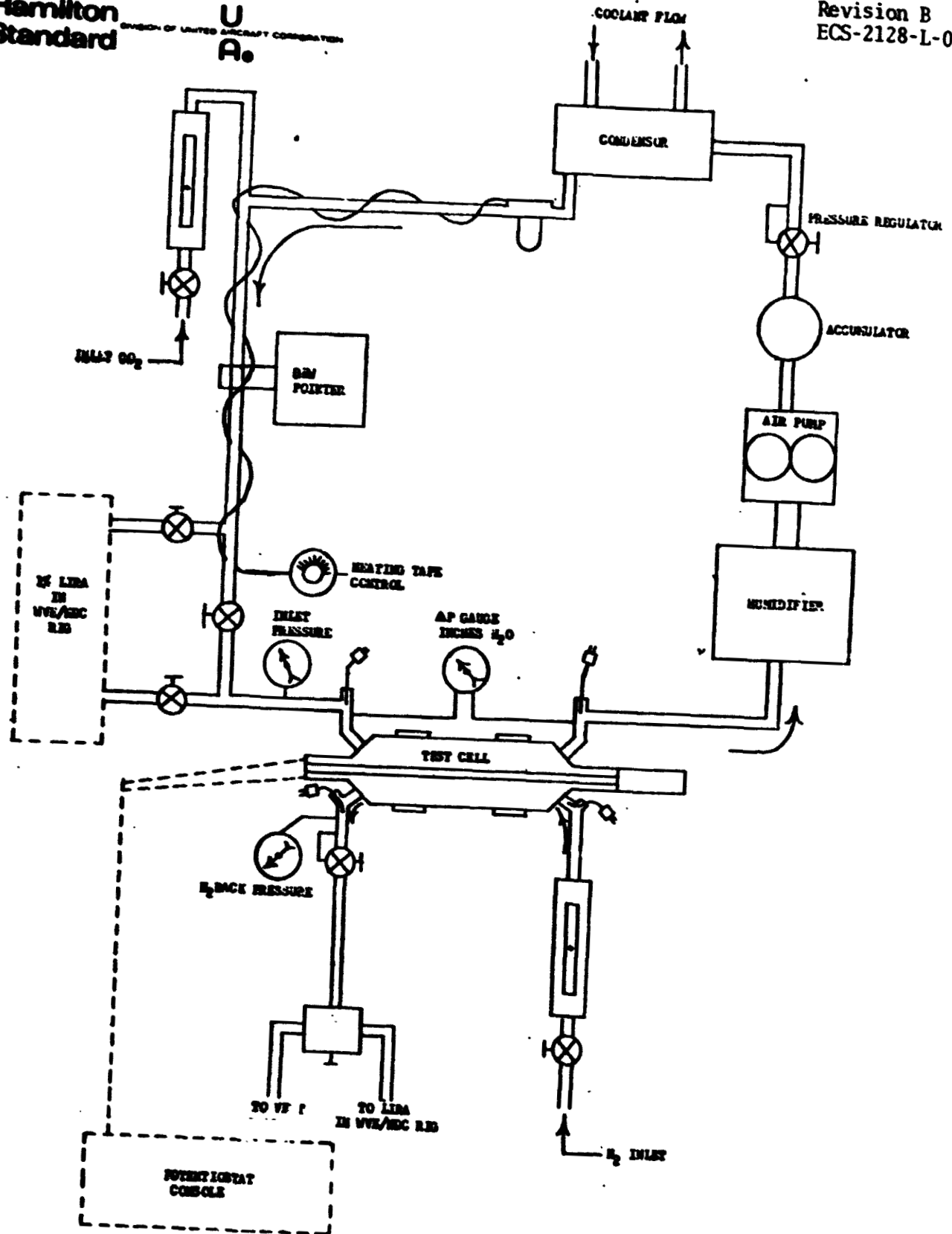
CS₂CO₃ Analytical Cell Tests (WBS 3.6) (Continued)

6. Test Results: Test data will be presented in tabular form as follows:
 - a. Mass transport coefficient for the various combinations of air velocity and CO₂ partial pressures.
 - b. pH values of the cesium carbonate at the cathode and anode for various combinations of current density, CO₂ partial pressures and inlet air dew points.



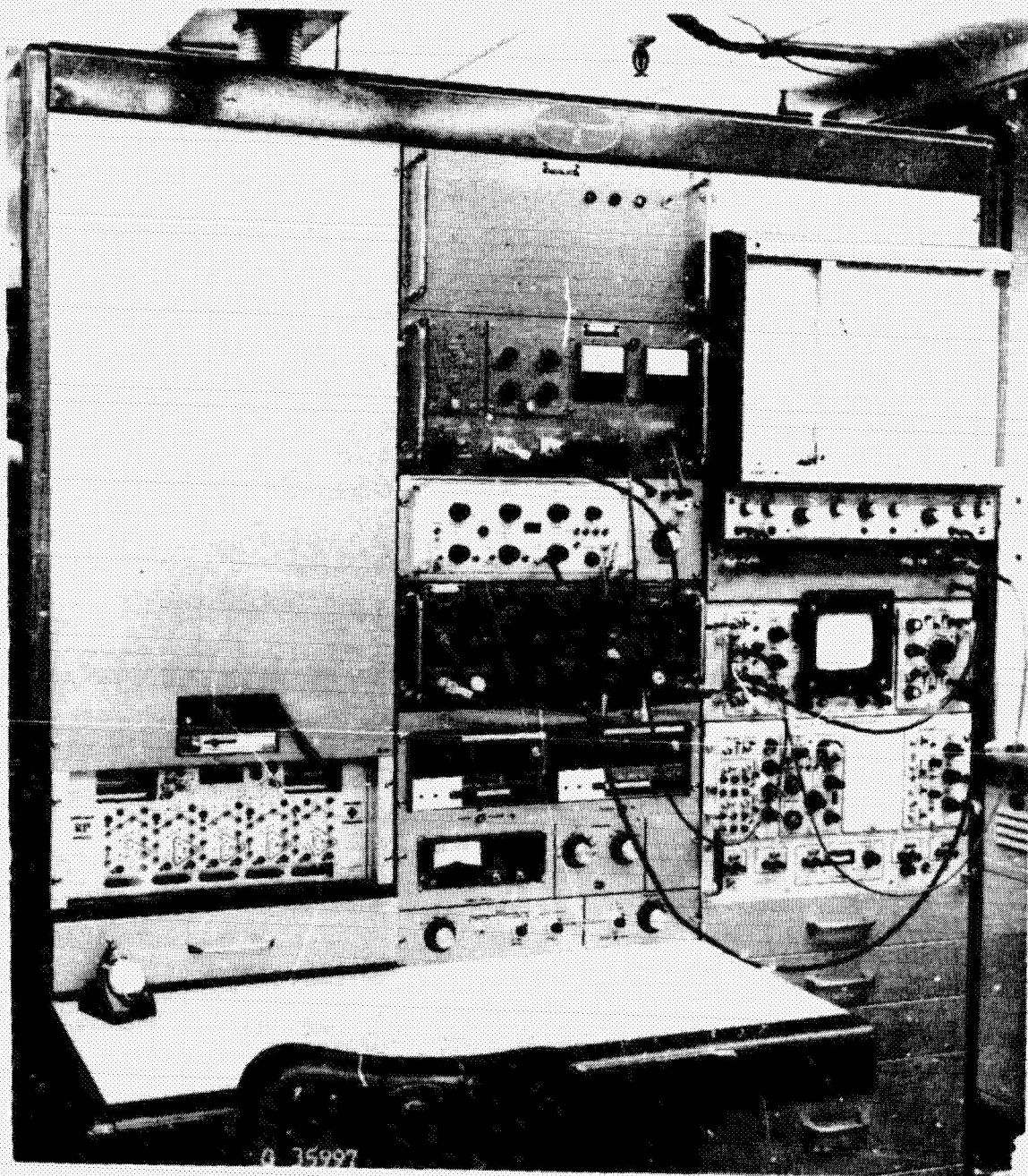
HDC ANALYTICAL TEST CELL

FIGURE 1



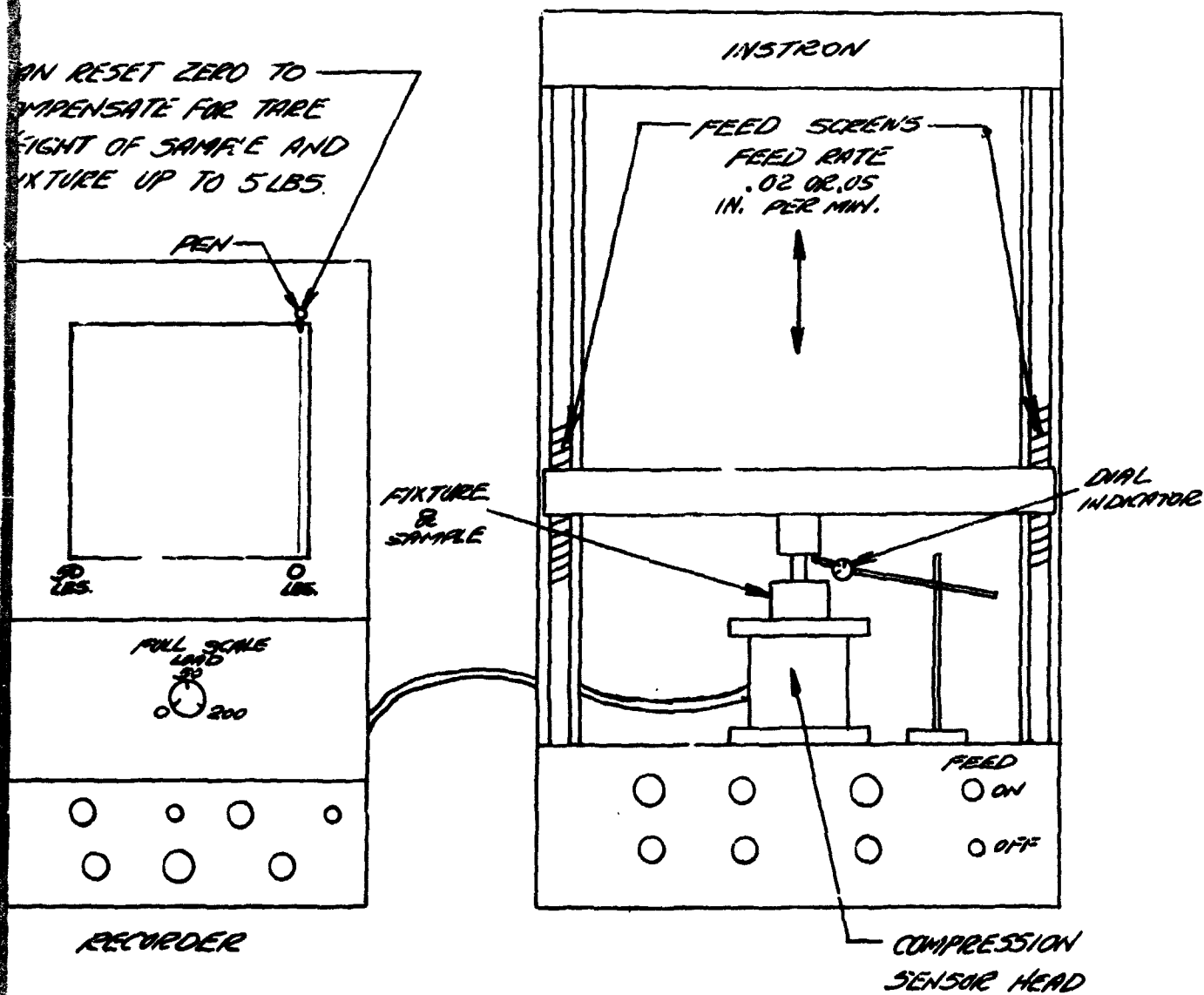
HDC ANALYTICAL TEST UNIT RIG

FIGURE 2



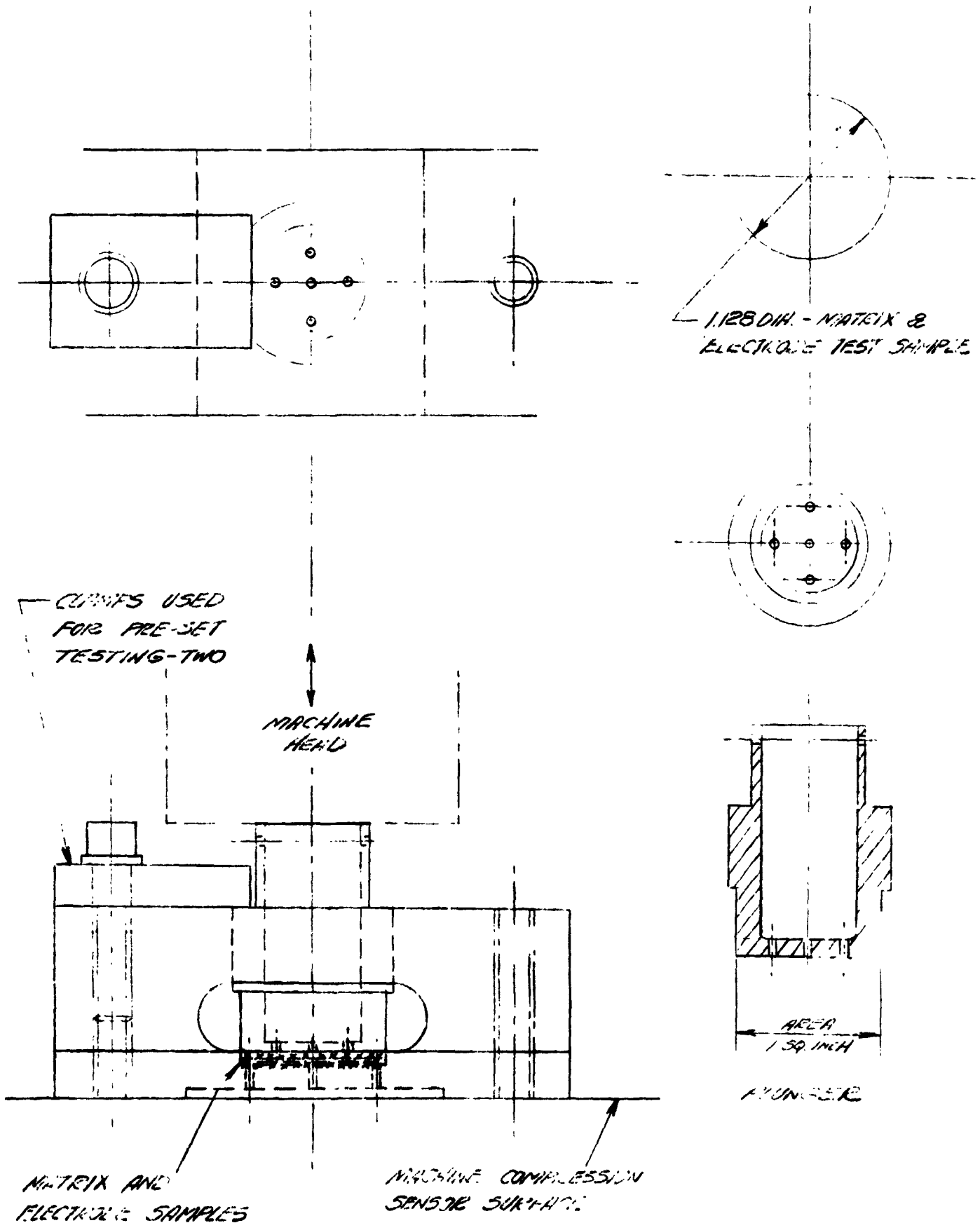
OPERATING CONSOLE FOR HDC ANALYTICAL TEST CELL

FIGURE 5



TEST SETUP

FIGURE 1



TEST FIXTURE

FIGURE 2

4. Test Runs:

Dynamic Tests

- A. Buildup - 2 asbestos and 2 electrode test samples wet with water.
Matrix compression - from .040 to solid height (steep slope on recorder) - feed .02 or .05 inches/min.
Instrumentation - recorder, force versus deflection indicator - distance traveled.
No. of tests - 2; change samples for each test.
- B. Buildup - 3 asbestos and 2 electrode test samples wet with water.
Matrix compression - .060 to solid/height (steep slope on recorder) - feed same as 4A.
Instrumentation - same as 4A.
No. of Tests - 2; change samples for each test.
- C. Buildup - 2 asbestos and 2 electrode test samples wet with water.
Matrix compression - first run .040 inches to solid height (steep slope on recorder) - feed same as 4A.
second to fifth run .040 inches to solid/height (steep slope on recorder) - same feed as 4A.
Instrumentation - same as 4A.
No. of tests - 5; same test samples.
- D. Buildup - 2 asbestos and 2 electrode test samples wet with water.
Matrix compression - .040 inches to .022 inches (matrix thickness) - feed same as 4A.
Hold at .022 inches for \approx 2 hours.
Repeat run .022 to solid height (steep slope on recorder).
Instrumentation - same as 4A except record reading on recorder every 15 minutes during the two hour hold period.
No. of tests - 1.

5. Pre-Set Tests

- A. Buildup - 2 asbestos and 2 electrode test samples wet with Cs_2CO_3 .
Matrix compression - .040 inches to .022 inches (matrix thickness) - feed same as 4A.
Hold (clamp) at .022 inches for one week (seven days) in chamber at 45°F dew point and 52°F dry bulb - mount so weight of plunger is not acting on compressed matrix.
After seven days hold time, make run from .022 inches to solid height (steep slope on recorder).
Instrumentation same as 4A.
No. of test - 1.
- B. Same as 5A except hold time is fourteen days.
- C. Same as 5A except hold time is forty-two days.

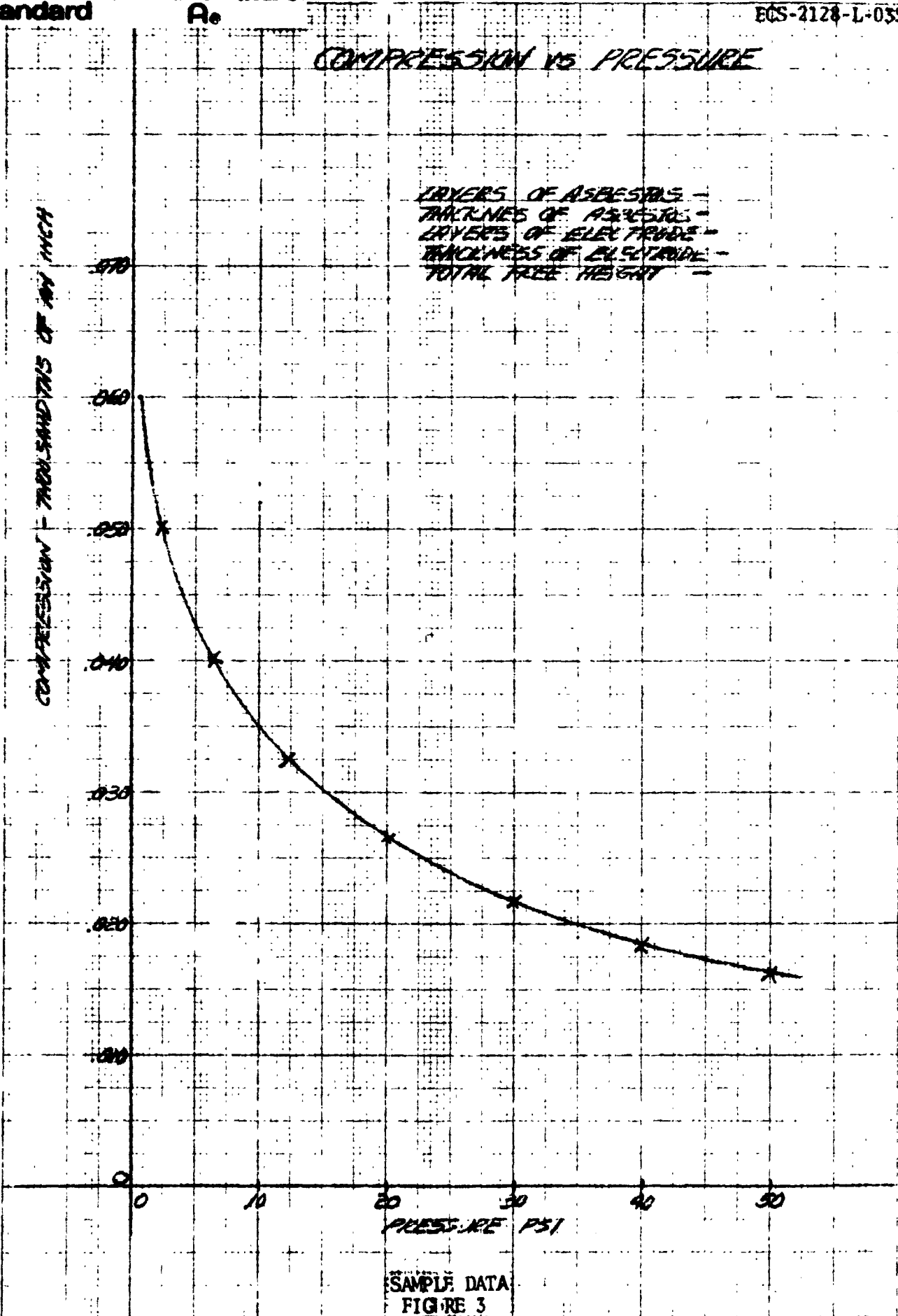
- D. Same as 5A except hold time is one hundred five days.
- E. Same as 5A except hold time is one hundred eighty days.

6. Instructions

Note - Instron machine will be run by a materials lab. technician.

- A. Mount compression sensor head on machine bed.
 - B. Place samples in test fixture and carefully lower plunger in place (see figure 2).
 - C. Place test fixture on compression sensor head flat surface, centering with machine spindle (see figure 1).
 - D. Lower center spindle until it just touches spindle, use shims.
 - E. Mount indicator so it touches spindle bottom surface, set indicator to zero.
 - F. Zero recorder, compensate for weight of fixture, samples and plunger.
 - G. Set full scale load knob to 50 lbs. - adjust lower or higher after observing initial test results.
 - H. Set machine feed (.02 or .05 inches/min.) and recorder paper speed.
 - I. Start machine and recorder - watch movement of recorder pen. When solid height is approached, slope of recorder curve becomes very steep. Shut off machine.
 - J. Take indicator reading to determine the number of thousandths travel.
 - K. Reverse feed to raise machine.
 - L. Repeat A through K for each test run.
7. Data will be plotted and presented as shown in figure 3.

For dynamic test 4D and pre-set tests show family of curves to show any changes with time.



23

PLAN OF TEST

JOB: HDC Analytical Cell Tests (WBS 9A.)

PLAN PREPARED BY: J. Huddleston

PROJECT & ORDER: NAS 9-12920

APPROVED BY: _____

INSTRUCTION: _____

TEST ENGINEER: _____

TIME PERIOD: _____ TO _____

1. WHAT IS ITEM BEING TESTED?
2. WHY IS TEST BEING RUN? WHAT WILL RESULTS SHOW OR BE USED FOR?
3. DESCRIBE TEST SET UP INCLUDING INSTRUMENTATION. ATTACH SKETCH OF INSTALLATION.
4. ITEMIZE RUNS TO BE MADE GIVING LENGTH OF EACH AND READINGS TO BE TAKEN.
5. SPECIAL INSTRUCTIONS: SAFETY PRECAUTIONS FOR OPERATORS AND HANDLING EQUIPMENT. OBSERVATIONS BY SIGHT, FEEL, OR HEARING. LIST POINTS OF OBSERVATION WHICH MIGHT CONTRIBUTE TO ANALYSIS OF (A) PERFORMANCE OF UNITS, (B) INCIPIENT TROUBLE BEFORE IT OCCURS, AND (C) CAUSE OF FAILURE.
6. HOW WILL DATA BE USED OR FINALLY PRESENTED? GIVE SAMPLE PLOT, CURVE, OR TABULATION AS IT WILL BE FINALLY PRESENTED.

NUMBER ENTRY AS LISTED ABOVE AND DESCRIBE BELOW

1. Item Being Tested: HDC Analytical Cell, Reference figure 1, of various configurations as noted in Table I.
2. Purpose of Test: To evaluate various cell modifications which are proposed (electrodes, matrix thickness, CO ₂ catalyst), that will reduce the power decay and improve the CO ₂ removal rate. This evaluation will be done on the analytical test cell instead of a full size cell pair.
3. Test Procedure: Testing of the analytical cell per the configurations and parameters of Table I will be performed on the Analytical Test Rig as as presented in Sections V and VII of the Master Test Plan.
4. Test Runs: There will be four basic tests as outlined in Table I. #1 Test - one test for a week duration. #2 Test - four tests (minimum of 4 electrodes to be screened) of approximately 2 days each. #3 Test - two tests (2 best electrodes) of approximately one week each. #4 Test - two tests (minimum and maximum matrix thickness) of approximately one week each.
5. Special Instructions: None.
6. Presentation of Data: The performance of the cell will be compared to that of previous Analytical Cell tests (Section VII) and to that of a full size cell pair.
A-52

PARAMETER	#1 - CO ₂ Catalyst Test	#2 - Electrode Screening (4) Tests	#3 - New Electrode (2) Tests	#4 - Matrix Thickness (2) Test
Cell Configuration Deviation from Std Cell*	Additive to Electrolyte of Carbonic Anhydrase	No. Reference Electrodes New Electrode Configurations	New Electrode Configuration	New Electrode Configuration One Layer of Matrix Four Layers of Matrix No Reference Electrodes
<u>SET CONDITIONS:</u>				
Inlet Air Temp. (°F)	70	70	70	70
Inlet Air Dew Point (°F)	63	63	63	63
Inlet Air P _{CO₂} (mmHg)	2.5	2.5	2.5	2.5
Inlet Air O ₂ Concen. (%)	21 - 22	21 - 22	21 - 22	21 - 22
Air Flow (ft/sec)	7	7	7	7
ΔP Across Matrix (psi)	None	None	None	None
H ₂ Flow (cc/min)	650	650	650	650
Current Density (asf)	12 & TBD	TBD	12 & TBD	TBD
<u>Monitored Parameters:</u>				
All Set Conditions	X	X	X	X
H ₂ + CO ₂ Outlet Flow	X	X	X	X
↳ CO ₂ in H ₂ + CO ₂ Flow	X	X	X	X
H ₂ Temp.	X	X	X	X
Outlet Air Temp.	X	X	X	X
Cell Voltage	X	X	X	X
Reference Voltages (5)	X	X	X	X
Anode & Cathode pH	X	X	X	X
IR of Cell	X	X	X	X
<u>Calculated Data:</u>				
Power	X	X	X	X
CO ₂ Removal Rate	X	X	X	X
CO ₂ Removal Efficiency	X	X	X	X

* Standard Cell Configuration - 1/24 full size cell pair, Cs₂CO₃ Electrolyte, P & NA Asbestos Matrix - 2 sheets of .020 compressed to .022, 4 reference electrodes, reservoir and modified housing to allow checking of pH at anode and cathode.

TEST CONDITIONS

TABLE I

- the lira which monitors the CO₂ in the outlet H₂+CO₂ gas flow will have its end points checked twice/week.

Changes in Operation - any change in the operating parameters of the cell pairs will be cleared through NASA/MSR prior to change. In emergencies where changes must be made to protect the test item, corrective action will be made without prior NASA/MSR review. However, a full review of the incident will be made within twenty-four hours (except on weekends).

6. Presentation of Data: The performance of the cell pair will be graphically presented versus time, i.e., power, CO₂ removal rate, current efficiency and voltage.

TABLE I
TEST CONDITIONS

● SET TEST CONDITIONS	Cs ₂ CO ₃ CELL PAIR					TMC CELL PAIR						
	CONDITIONING	PARAMETRIC TEST INITIAL & END			ENDURANCE	CONDITIONING	PARAMETRIC TEST INITIAL & END			ENDURANCE	PARAMETRIC TEST INITIAL & END	
INLET AIR TEMPERATURE (°F)	52				→	52				→	Room (74°F)	
INLET AIR DEW POINT (°F)	49	45			→	49	45			→	Room (60°F)	
INLET AIR P _{CO₂} (mm Hg)	3.0				→	3.0				→	1/4	3.0
INLET AIR O ₂ CONCENTRATION (%)	20-21				→	20-21						
AIR FLOW THROUGH CELL PAIR (SCFM)	10				→	10						
ΔP ACROSS CELL MATRIX (min) (PSI)	1				→	1						
H ₂ INFLOW TO CELL PAIR (cc/min)	900				→	900				→	②	②
CURRENT DENSITY (asf)	18	18	14	22	18	18	18	14	22	18	18	10
MIN. DURATION ON CONDITION (hours)	120	24	24	24	①	120	24	24	24	①	48	48

① TOTAL TIME OF ALL TESTING OF 2000 HRS AS A GOAL

② ADJUST H₂ FLOW TO OBTAIN GOOD H₂/CO₂ LIRA READING

● MONITORED PARAMETERS

All Set Conditions
H₂ + CO₂ Outlet Flow
% CO₂ in H₂ + CO₂ Outlet Flow
Cell Voltage
H₂ Temp.

● CALCULATED DATA

Power
CO₂ Removal Rate
Current Efficiency

● TEST DATA WILL BE TAKEN ONCE/DAY WITH THE EXCEPTION OF WEEKENDS